

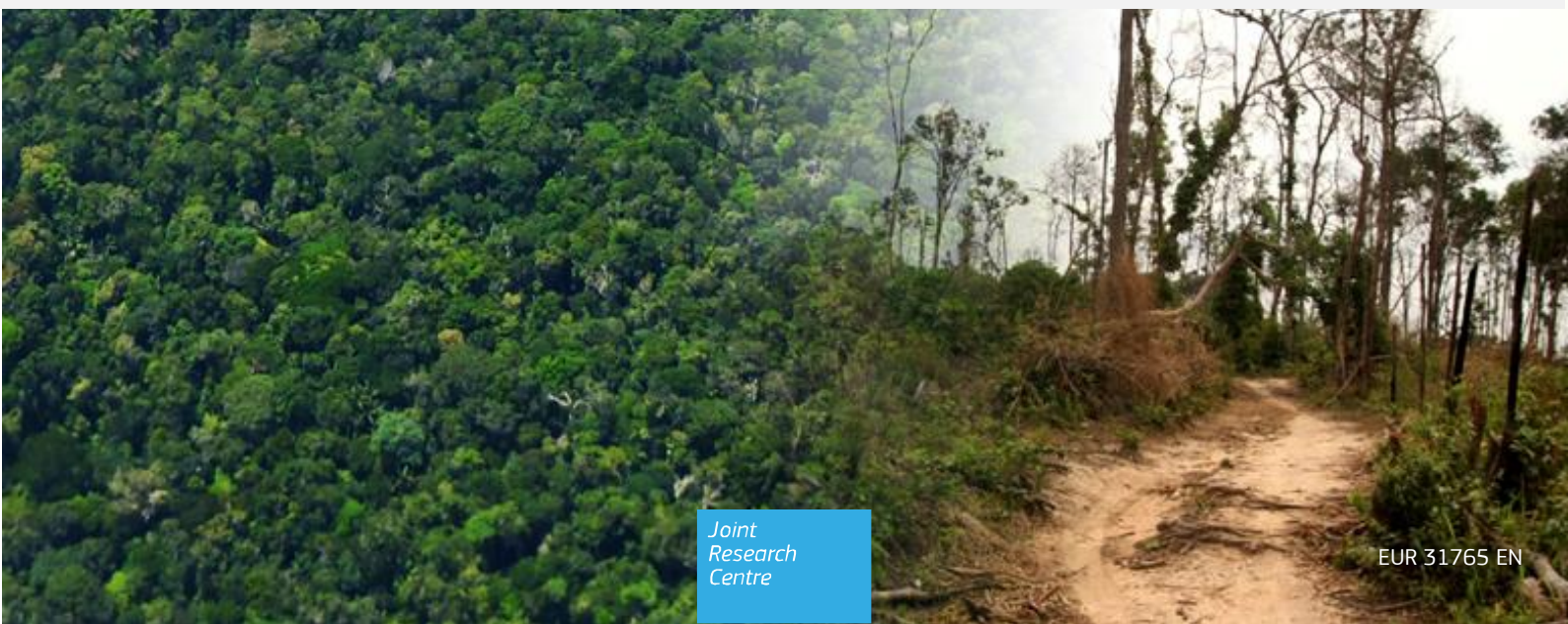


JRC SCIENCE FOR POLICY REPORT

Deforestation and forest degradation in the Amazon - Update for year 2022 and link to soy trade

Beuchle, R., Bourgoïn, C., Crepin, L., Achard, F.,
Migliavacca, M., Vancutsem, C.

2023



This publication is a Science for Policy report by the Joint Research Centre (JRC), the European Commission's science and knowledge service. It aims to provide evidence-based scientific support to the European policymaking process. The contents of this publication do not necessarily reflect the position or opinion of the European Commission. Neither the European Commission nor any person acting on behalf of the Commission is responsible for the use that might be made of this publication. For information on the methodology and quality underlying the data used in this publication for which the source is neither Eurostat nor other Commission services, users should contact the referenced source. The designations employed and the presentation of material on the maps do not imply the expression of any opinion whatsoever on the part of the European Union concerning the legal status of any country, territory, city or area or of its authorities, or concerning the delimitation of its frontiers or boundaries.

Contact information

Name: René Beuchle

Email: rene.beuchle@ec.europa.eu

EU Science Hub

<https://joint-research-centre.ec.europa.eu>

JRC134995

EUR 31765 EN

PDF ISBN 978-92-68-10002-8 ISSN 1831-9424 doi:10.2760/211763 KJ-NA-31-765-EN-N

Luxembourg: Publications Office of the European Union, 2023

© European Union, 2023



The reuse policy of the European Commission documents is implemented by the Commission Decision 2011/833/EU of 12 December 2011 on the reuse of Commission documents (OJ L 330, 14.12.2011, p. 39). Unless otherwise noted, the reuse of this document is authorised under the Creative Commons Attribution 4.0 International (CC BY 4.0) licence (<https://creativecommons.org/licenses/by/4.0/>). This means that reuse is allowed provided appropriate credit is given and any changes are indicated.

For any use or reproduction of photos or other material that is not owned by the European Union permission must be sought directly from the copyright holders.

How to cite this report: Beuchle, R., Bourgoïn, C., Crepin, L., Achard, F., Migliavacca, M. and Vancutsem, C., *Deforestation and forest degradation in the Amazon - Update for year 2022 and link to soy trade*, Publications Office of the European Union, Luxembourg, 2023, doi:10.2760/211763, JRC134995.

Contents

- Abstract1
- Foreword2
- Acknowledgements3
- Executive Summary4
- About this report5
- 1 Introduction7
- 2 Deforestation and forest degradation in the Pan-Amazon between 2000 and 2022 - estimates from the JRC-TMF dataset9
 - 2.1 Pan-Amazon10
 - 2.2 Bolivia17
 - 2.3 Brazil18
 - 2.4 Colombia19
 - 2.5 Ecuador20
 - 2.6 Guiana Shield (Guyana, Suriname and French Guiana)21
 - 2.7 Peru22
 - 2.8 Venezuela23
 - 2.9 Comparison of JRC-TMF and INPE-PRODES deforestation estimates for the Brazilian Legal Amazon24
- 3 Monitoring deforestation and forest degradation in the Brazilian Legal Amazon: estimates from Brazilian National Space Research Institute (INPE) for 2022/2326
 - 3.1 INPE-PRODES deforestation statistics26
 - 3.2 INPE-DETER deforestation and forest degradation alerts27
 - 3.2.1 INPE-DETER deforestation alerts 202227
 - 3.2.2 INPE-DETER forest degradation alerts 202229
 - 3.2.3 INPE-DETER deforestation and forest degradation alerts 2023 (January-October)29
 - 3.3 INPE-DETER deforestation alerts vs. IMAZON-SAD deforestation alerts 2022 and 2023 (January-October)31
- 4 Deforestation and soy trade in the Brazilian Amazon33
 - 4.1 Introduction33
 - 4.2 Background information33
 - 4.2.1 The emergence of soy in the Brazilian Amazon33
 - 4.2.2 The exposure of the EU to deforestation risk in the Brazilian Amazon through the soybean trade34
 - 4.3 Regional patterns of expansion36
 - 4.3.1 Methods36
 - 4.3.2 Results36

4.4	The complex task of attributing deforestation to soy production and exports	39
4.4.1	From deforestation to soybean: a potentially long pathway	39
4.4.2	Location of soy-driven deforestation and time lags	40
4.4.3	Indirect land use change.....	42
4.4.4	Infrastructure and land speculation	43
4.1	Towards sustainable soybean supply chains between the Brazilian Amazon and Europe	44
5	Government Policy in Brazil, related to deforestation and forest degradation in the Amazon (status end of 2022 / mid-2023)	45
6	Conclusions and Outlook.....	52
7	Annex 1: Impacts of using enhanced satellite imagery for year 2022 in TMF results .	53
7.1	Addition of imagery of the new Landsat-9 satellite for year 2022 in the JRC-TMF processing chain.....	53
7.2	Using 'Collection-2' rather than 'Collection-1' Landsat imagery	54
7.3	Combined use of Landsat and Sentinel-2 satellite data to create a hybrid map of forest disturbances for 2022 at 10 m spatial resolution.....	55
8	Annex 2: New research on forests, deforestation, forest degradation and regrowth in the Amazon (status July 2023).....	58
8.1.1	Forest	58
8.1.2	Forest and Climate Change	63
8.1.3	Deforestation	67
8.1.4	Forest degradation	86
8.1.5	Forest edge effects	93
8.1.6	Forest fires	95
8.1.7	Selective logging	104
8.1.8	Mining	113
8.1.9	Hunting	122
8.1.10	Protected Areas	127
8.1.11	Forest biomass and carbon	134
8.1.12	Forest regrowth and restoration.....	137
	References	145
	List of abbreviations and definitions	161
	List of figures	163

Abstract

Tropical forests are fundamental for the mitigation of global warming and for containing immense biodiversity, thus the knowledge about where, how, and why they change is of crucial importance in order to find countermeasures that can protect the remaining forests for all countries of the Amazon region.

This report aims to give an overview of the recent forest cover changes in the Amazon region, and furthermore, for Brazil, the country with the largest share of the Amazon to put these changes into a political and institutional perspective.

Consistent data specifically for monitoring forest degradation of the Amazon, caused mainly by forest fires and selective logging is scarce. Based on the JRC cloud-computed, large-scale tropical forest monitoring approach, estimates and maps on forest degradation are provided in this report, together with a thorough interpretation of recent forest cover change dynamics, and a view on forest cover changes in the region from 1990 to date.

Foreword

The Amazon forest is the Earth's largest rain forest, and is not only home to 10% of all known species worldwide, but also to a population of 47 million people, thereof 2 million of indigenous origin. The Amazon forest has undergone immense changes since the mid-1970s, when the first roads were built to penetrate the woods in order to develop the region. Currently, it is estimated that the Amazon has lost already 17% of its forest, mostly due to the expansion of agricultural areas. The area of degradation of the Amazon forest is thought to be approximately on the same scale, with fire, timber extraction and edge effects being the main causes.

As a carbon sink and climate stabilizer from local to global scale, as container of an immense floral and faunal biodiversity, as provider of forest products for the local population, of water for the Amazon river system as well as of water vapor for the 'flying rivers' that deposit rain in other regions, the services of the Amazon forest are indispensable. For the protection of the remaining forest, precise information about the forest's history, its status and dynamics is necessary in order to understand where measures have to be taken to prevent further clear-cutting or degradation of the Amazon. At the same time, reliable spatial information on forests can give directions for deciding on the "where, when and how" for an effective forest recovery strategy.

Over the past three decades, the JRC has been looking at changes in tropical forest cover; from the early 1990s onwards, JRC researchers used satellite imagery to assess the status of tropical forests and quantify their losses and gains, using multi-source satellite imagery and cloud computing. As a result, the JRC dataset, called the Tropical Moist Forest provides detailed information on forest cover change dynamics, including, information on the year of a forest's first of potential multiple disturbances, the duration of forest disturbances until a forest grow-back can be detected, the age of forest edges and of secondary forest, to name a few. This dataset maps for the first time on global tropical scale deforestation and forest degradation, the latter delivering crucial information, given the growing threat of forest degradation for indigenous people, biodiversity, and forests as carbon sinks.

In this report, forest cover change statistics for the Amazon region in year 2022 are shown with trends for the different Amazon countries, and statistics putting the 2022 situation into perspective with past forest cover change rates. For Brazil, also statistics of deforestation and forest degradation for the first half of 2023 are provided. In addition, the report looks at the link between deforestation and soy trade in the Brazilian Amazon region. It is part of the information delivered by the newly established EU Forest Observatory on deforestation, forest degradation, changes in the world's forest cover, and associated drivers. The goal of the Observatory is to provide global, transparent and easily accessible forest-related information.



Director Alessandra Zampieri
Directorate Sustainable Resources
Joint Research Centre

Acknowledgements

The contribution of Clément Bourgoïn was supported by the Directorate-General for Climate Action of the European Commission (DG-CLIMA) through the Lot 2 ('TroFoMo' - Tropical moist Forest Monitoring) of the ForMonPol Administrative Arrangement (Forest Monitoring for Policies) and by the Amazonia+ Administrative Arrangement (DG-INTPA) in the context of the TEI Amazon. Léa Crepin led chapter 4 on deforestation and soy trade in the Brazilian Amazon.

Thanks to Dario Simonetti, Silvia Carboni, René Colditz, Baudouin Desclée, Andrea Marelli, Paula Verónica Figueiredo Vilar Pires Correia, Iban Amezttoy and Astrid Verhegghen from JRC-D1 for their support.

The authors thank Thomas Kemper (JRC-E1) for the JRC internal review and Claire M. Wheatley for text corrections.

Cover photos by Thais Almeida Lima and René Beuchle

Authors

René Beuchle (JRC-D1)

Clément Bourgoïn (JRC-D1)

Léa Crepin (University of Paris-Saclay)

Frédéric Achard (JRC-D1)

Mirco Migliavacca (JRC-D1)

Christelle Vancutsem (JRC-D6)

Executive Summary

During year 2022, the JRC-TMF dataset on **Tropical Moist Forests** reports a 14.9% increase in forest disturbances in the Pan-Amazon region compared to year 2021 (35,480 km² of new disturbances in 2022 vs. 30,089 km² in 2021) - disturbances including both deforestation and forest degradation). The Amazon countries show different trends in forest cover change. Forest disturbances in Ecuador, the Guiana Shield countries (Guyana, Suriname and French Guiana) and in Bolivia increased significantly in 2022 compared to 2021 (by + 172.9%, 87.6% and 38.5% respectively). While forest disturbances in all moist forests of Brazil stayed roughly on the same level between 2022 and 2021 (1.8% increase), they increased by 9.3% in the Brazilian Legal Amazon (BLA). Forest disturbances decreased in Colombia, Venezuela and Peru by 16.2%, 14.9% and 7.0%, respectively.

The overall annual new disturbed forest area in the BLA increased from 21,632 km² in 2021 to 23,647 km² in 2022, according to JRC-TMF. The reported increase was supported by statistics from DETER, the near-real-time deforestation detection system from the Brazilian National Space Research Institute (INPE), that also showed an increase trend of forest disturbances of 63.7%, from 17,373 km² in 2021 to 28,438 km² in 2022 (yearly accumulated deforestation and forest degradation alerts).

This report provides also an overview regarding forest disturbances in the Brazilian Amazon for the first ten months in 2023, as reported by the INPE-DETER alert system. This alert system shows decreases of 49.7% and 32.6% between 2022 and 2023 (January-October period) for deforestation and forest degradation (by selective logging and forest fires), respectively. A second, independent deforestation alert system for the Brazilian Amazon, AMAZON-SAD, reports a 60.7% decrease between 2022 and 2023 for the same period.

Deforestation in the Amazon region is mostly driven by agricultural expansion for commodities such as cattle, soy and (indirectly) maize. Forest degradation is partially driven by selective logging of wood (the other main driver being fires). Soy and soy-derived products are included, amongst other commodities, in the EU regulation on deforestation-free products (EUDR). In this report, we discuss the relationship between soy production and recent deforestation patterns observed in the Amazon region. Soy exports from Brazil into the EU have been relatively stable at a high level over the period 2015-2020 with around 4 Mt per year. The soy production started around the years 2000 in the southern Amazon, while growing in area significantly since then.

Considering that pasture (for cattle) is the usual first agricultural usage after the removal of the forest, fast transformation of deforested areas to soy fields (i.e. within 5 years after deforestation) reached a peak in the early 2000s. The time lag between deforestation and plantation of soy increased significantly after 2006, often up to 15 years, especially in newly established areas of soy production north and east of the core initial area. New transport infrastructure in the Amazon region is planned to be ready in the next decade and may provide new incentives for the increase of soy production in the Amazon, with potential consequences on the forest cover and indigenous people in the region.

The political changes in Brazil at the beginning of 2023 seem to lead to a re-strengthening of the federal institutions in charge of environmental protection. However, for some pending issues, such as the development of infrastructure in the Amazon region, the re-empowering of law enforcement institutions and the permanence of the protection of indigenous areas from illegal mining, logging or land grabbing the stance and the assertiveness of the government in the current complex political picture needs to be considered on a longer term.

About this report

This report is published in the context of the newly established EU Forest Observatory on Deforestation and Forest Degradation, which is managed by the Joint Research Centre. One of the aims of the Observatory is to support the implementation of the new Regulation (EU) 2023/115 of the European Parliament and of the Council of the EU¹ on the making available on the Union Market and on the export from the Union of certain commodities and products associated with deforestation and forest degradation (hereafter referred as "Deforestation-free supply chains"). This Regulation aims to prevent that the Union's consumption and production of commodities causes deforestation and forest degradation within or outside the EU.

As in the previous reports, a specific focus is given to Brazil (in particular in sections 3 to 5), the country in the region with the largest share of Amazon rainforest and the largest country of the South American Mercosur region.

After the introduction (Section 1), Section 2 presents the JRC-TMF statistics updated up to year 2022 for all countries of the Amazon region and the comparison with data from INPE's Deforestation Monitoring Project (PRODES)² for the Brazilian Amazon. Furthermore, the latest available statistics of the INPE-DETER³ alert system (January to October 2023), regarding deforestation and forest degradation in the Brazilian Amazon, are presented in Section 3, including a comparison to the statistics from the deforestation alert system SAD⁴, run by the Brazilian NGO Instituto do Homem e Meio Ambiente (IMAIZON)⁵.

Section 4 reports a new analysis on the relationship between deforestation, soy production and international trade in the Brazilian Amazon. Soy is one of the seven 'relevant' commodities - besides oil palm, wood, cocoa, coffee, cattle and rubber - mentioned in the EU Regulation.

Section 5 deals with current Brazilian policies in a period of political change from the Bolsonaro government to the one of Luiz Ignácio Lula da Silva (Lula), which came into place at the beginning of 2023 after winning the federal election at the end of October 2022. The governmental changes corresponding to the set up of the new Lula government are described in relation to socio-environmental issues, e.g. the re-empowering of Brazilian law enforcement in the Amazon, the first ever creation of a Ministry of Indigenous Peoples and the new vision regarding transport infrastructure (roads, train lines, ports) to be developed in the Amazon region, to name a few.

Annex 1 describes the impacts of using a re-processed historical collection of Landsat Satellite imagery and new Landsat 9 imagery for year 2022 on the JRC-TMF results. Year 2022 has seen two major improvements related to the Landsat satellite imagery that is used to create the JRC-TMF dataset: the insertion of imagery from the new Landsat 9 satellite (in addition to Landsat 7 and 8 satellites) and the availability of a reprocessed 'Landsat Collection 2' archive (made available by the United States Geological Survey - USGS) with improved quality compared to 'Collection 1'). Furthermore, the JRC-TMF dataset is now including, as starting from year 2022, a new hybrid map of deforestation and forest degradation at 10 m resolution based on the combination of Landsat and Sentinel-2 imagery. The implications of this new approach for the detection of tropical forest disturbance are also discussed in Annex 1.

Annex 2 reports new scientific findings that have been published between the second half of 2022 and the first half of 2023, and which have not been cited in the main text. The findings deal with many aspects related to forest, deforestation, forest degradation and forest regrowth in the Amazon region. The focus in this report is on the scientific findings

¹ <https://eur-lex.europa.eu/legal-content/EN/TXT/HTML/?uri=CELEX:32023R1115>

² http://terrabrasilis.dpi.inpe.br/app/dashboard/deforestation/biomes/legal_amazon/rates

³ <http://terrabrasilis.dpi.inpe.br/app/dashboard/alerts/legal/amazon/aggregated/>

⁴ <https://imazon.org.br/en/imprensa/understanding-the-imazon-monitoring-system/>

⁵ <https://imazon.org.br/en/>

concerning forest cover changes in the Brazilian Amazon in a local, regional or global context.

1 Introduction

Tropical forests play an essential role in mitigation of climate change and its socio-economic consequences. Between 1990 and 2022, the Pan-Amazon forest has lost more than 20% of the original forest cover to deforestation or forest degradation, according to JRC-TMF data. While deforestation implies a permanent change from native forest to another land use (e.g. cropland), a degraded forest (e.g. through fire or selective logging) remains a forest, but suffers a substantial decline in forest structure or function over time [3], including a potential loss of carbon and biodiversity. Tropical forest degradation is often a precursor of deforestation [4]. Thomas E. Lovejoy and Carlos Nobre, two leading scientists on the Amazon forest, claimed in 2018 that a tipping point would be reached if parts of the Amazon, specifically in southern and eastern Amazonia, would reach 20-25% deforestation, turning these parts into a savanna type of landscape. They pointed at strict Amazon forest protection and at intensive forest restoration in order to maintain the most important pan-Amazon hydrological cycle, being critical for human well-being in Brazil as well as for South America [5,6]. According to recent research, Amazonia has become hotter and drier in the course of the past decades [7–10], while parts of the Amazon forest have already turned from a carbon sink to a carbon source, due to deforestation and climate change [11].

The nine countries sharing the Amazon forest have different forest cover change dynamics. Deforestation in the Amazon region is mainly triggered by expansion of pasture and cropland and by land grabbing [12–16]. Brazil and Bolivia have seen large forest areas affected by fire in the past 20 years, while other countries (like e.g. Ecuador) have been hit by large forest fires only rarely, due to specific climatic circumstances [17]. Small-scale and medium-scale gold mining (often illegal) increased in Ecuador, Peru, Brazil as well as in the Guyana Shield countries (Guyana, Suriname and French Guiana) over the past 15 years, with all potential negative consequences for environment and human population in the area [18–24]. Illegal (and/or unsustainable) selective logging is pervasive in many areas in the Amazon [25–29]. The estimates on illegality of selective logging operations in the region are high [30], ranging from 40%⁶ to “50% or more” [29], to 60%⁷ and up to 90%^{8,9}.

Amazonia has seen a surge of violence, i.e. human, environmental and convergent, in the past decade, along with an increase of illicit crops production and drug trafficking¹⁰. On national level, both cannabis and cocaine seizures have increased in Colombia (2014-2021), Peru (2016-2021), and the Brazilian Amazon (2012-2021), while there is apparently no clear trend in Bolivia for the period of 2012-2021. Many of the international drug trafficking routes go through the Amazon region, which has an extensive drug-related transport infrastructure like airstrips (often clandestine, within or outside conservation units), a vast river network and (legal and illegal) roads. The Amazon region is currently at the intersection of multiple forms of organized crime that are accelerating environmental devastation, with severe implications for the security, health, livelihoods and well-being of the population across the region [31–33].

After years of increasing deforestation on the continent, important changes have recently brought some change to the South American political scene. In Chile, Colombia and Brazil, presidents have been elected in 2022 that expressed their view that an increase of efforts related to environmental issues was necessary. The political changes could already been seen at the Conference of Parties (COP), when the then Brazilian President Elect Luiz

⁶<https://imazon.org.br/en/imprensa/almost-40-of-logging-in-the-amazon-is-illegal-shows-an-unprecedented-study/>

⁷<https://news.mongabay.com/2021/09/illegal-logging-reaches-amazons-untouched-core-terrifying-research-shows/>

⁸<https://www.nature.com/immersive/d41586-023-02599-1/index.html>

⁹<https://amazoniareal.com.br/amazonia-em-chamas-90-da-madeira-exportada-sao-ilegais-diz-policia-federal/>

¹⁰<https://foreignpolicy.com/2023/08/06/amazon-drugs-coca-cocaine-deforestation-environment-biodiversity-climate-change-criminal-brazil-peru-colombia-bolivia-lula-logging/>

Ignácio Lula da Silva (Lula) promised zero deforestation and forest degradation in the Brazilian Amazon until year 2030. The Colombian newly elected president Gustavo Petro promised to halt the high rates of deforestation in the Colombian Amazon, while Chile's new president Gabriel Boric pledged to take strong stance on climate change and environmental regulation. In a national referendum in Ecuador in August 2023, the population voted to halt oil drilling in the Yasuní National Park in the Amazon region¹¹.

In the Brazilian Amazon, in 2023, the first effects of the promised intensification of environmental protection have been observed. According to the INPE-DETER deforestation alert system, deforestation in the Brazilian Amazon in the first ten months of 2023 went down by 49.7%¹², while the Brazilian Institute for Environment and Renewable Natural Resources (IBAMA), responsible for the law enforcement related to environmental crime, intensified the action against illegal miners and loggers¹³ since the beginning of 2023¹⁴.

The question is how the new Brazilian president will be able to push through his environmental agenda against the conservative National Congress [34], and to which extent he will pursue his plans for the large-scale reform of the Amazon transport infrastructure, i.e. the construction of new or better roads, trains and waterways, which could, without ensured environmental and social impact assessments and law enforcement, trigger deforestation, land grabbing, forest fires, illegal selective logging and hunting in many areas of intact forest.

In this context, it is important to keep monitoring Amazon forest cover changes and get updated information on the forest dynamics in the region from the inter-comparison between different tropical forest monitoring efforts, and to improve our understanding of the main drivers of deforestation and forest degradation.

This report provides updated statistics of deforestation and forest degradation up to year 2022 for the humid forests of the Amazon region, based on the JRC Tropical Moist Forest (JRC-TMF) dataset¹⁵. It builds on previous reports on 'Deforestation and Forest Degradation in the Amazon' released in 2021 and 2022 [1,2]^{16,17}, which reported on forest disturbances until years 2020 and 2021, respectively.

¹¹<https://www.theguardian.com/world/2023/aug/21/ecuador-votes-to-halt-oil-drilling-in-amazonian-biodiversity-hotspot>

¹² <https://www.bbc.com/news/world-latin-america-66129200>

¹³ <https://www.gov.br/mma/pt-br/alertas-de-desmatamento-na-amazonia-caem-34-no-semester>

¹⁴ <https://www.gov.br/mma/pt-br/alertas-de-desmatamento-na-amazonia-caem-34-no-semester>

¹⁵ <https://forobs.jrc.ec.europa.eu/TMF/>

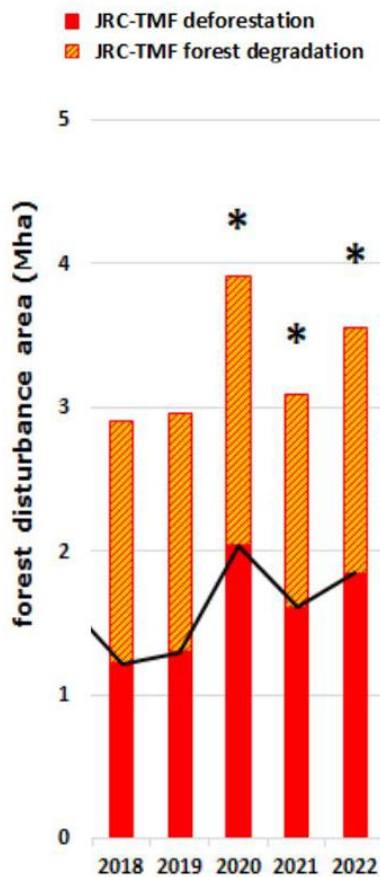
¹⁶ <https://publications.jrc.ec.europa.eu/repository/handle/JRC124955>

¹⁷ <https://publications.jrc.ec.europa.eu/repository/handle/JRC130081>

2 Deforestation and forest degradation in the Pan-Amazon between 2000 and 2022 - estimates from the JRC-TMF dataset

We report here the trends in national deforestation and forest degradation rates for the six countries in the Pan-Amazon region (Brazil, Colombia, Venezuela, Peru, Bolivia and Ecuador) and the countries of the Guiana Shield (Guyana, Suriname and French Guiana) from year 2000 up to year 2022. The two regions are defined by 'Amazonia *sensu stricto*' and 'Guiana', according to Eva and Huber (2005) [35]¹⁸.

Figure 1. Subset of JRC-TMF humid forest disturbances statistics for the Pan-Amazon for the past five years. The stars (2020-2022) indicate that the distribution of the two classes within the yearly overall forest disturbances is an "educated guess"



The JRC-TMF classification process starts out by mapping disturbances in the forest canopy on a yearly basis (Jan-Dec), regardless of their permanence. The distinction between deforestation and forest degradation is made three years after the disturbance occurred by measuring the permanence of the forest disturbance over time. If the forest canopy is disturbed permanently, i.e. shows no signs of forest regrowth over the three years following the disturbance, the 'forest disturbance' pixel falls into the deforestation class. If a 'forest disturbance' pixel shows clear signs of forest regrowth within the three years following the disturbance, it is classified as forest degradation.

In consequence, the distribution of yearly deforestation and forest degradation areas within the detected yearly overall disturbed forest areas are consolidated until 2019, but are estimated by applying a 20-year average (2000-2019), indicated by stars in Figure 1, for the years 2020-2022.

All statistics are based on the JRC-TMF dataset [4]^{19,20}. Figures 12-18 report on forest cover changes of the moist forest in Amazon countries, thus the statistics do not include the changes in e.g. the seasonal or dry forests and savannas of Venezuela, Colombia, Peru and Ecuador, in the Brazilian Caatinga and Cerrado biomes and in the Bolivian Chaco. For comparison, the corresponding statistics of "tree cover loss" from the Global Forest Change

¹⁸ <https://forobs.jrc.ec.europa.eu/amazon>

¹⁹ <https://forobs.jrc.ec.europa.eu/TMF/>

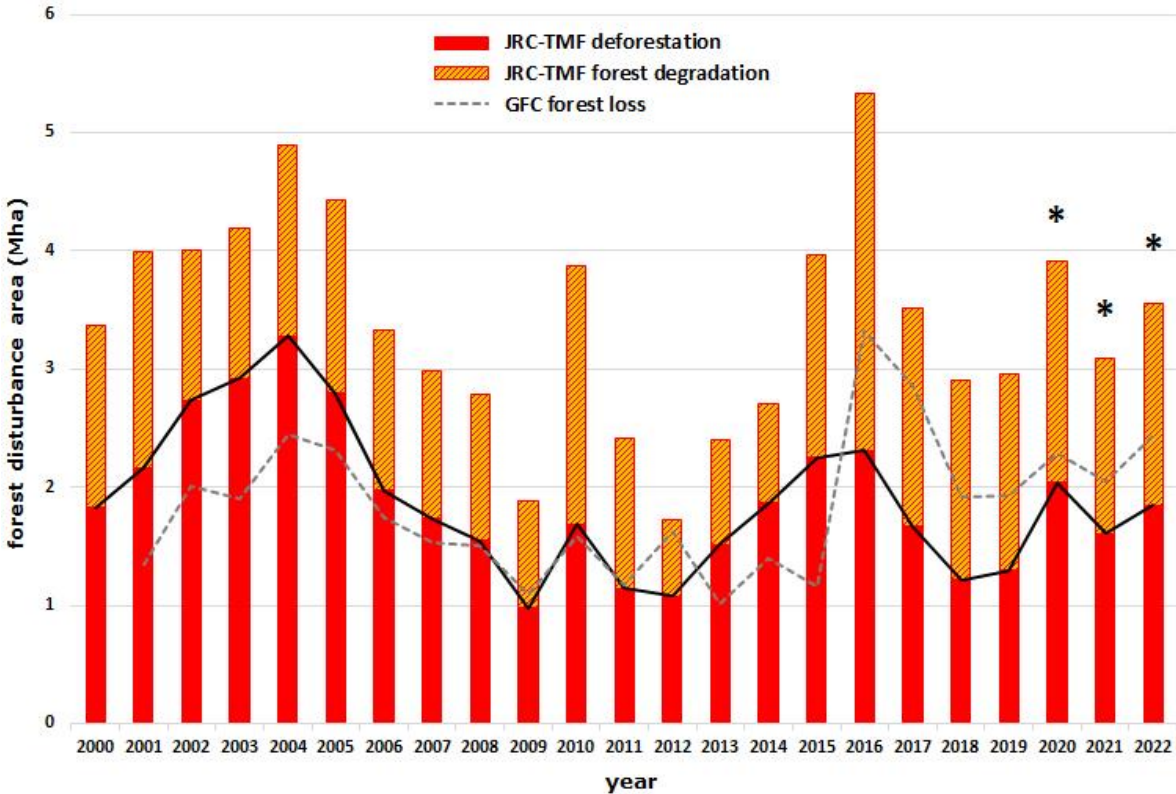
²⁰ <https://forobs.jrc.ec.europa.eu/TMF/data#stats>

(GFC)²¹ dataset are displayed in the mentioned figures as a grey dashed line. We extracted both JRC-TMF data and GFC data for the Pan-Amazon and the Brazilian Legal Amazon (BLA), based on the area definitions of Eva and Huber (2005) [35] and PRODES, respectively. For country statistics comparison, we extracted both JRC-TMF and GFC data based on the GAUL Level 0 country borders²² and the year 2000 JRC-TMF humid tropical forest extent as reference layer. For the three datasets JRC-TMF, PRODES and GFC data for the Brazilian Legal Amazon, the INPE-PRODES forest mask defining the humid forest within the BLA has been used additionally to ensure maximum comparability.

2.1 Pan-Amazon

Brazil drives the trend of forest cover change over the past 20 years in the Pan-Amazon, as it covers the largest part of the Amazon forest within the Pan-Amazon region and is the major contributor of deforestation and forest degradation area in the region.

Figure 2. Forest disturbances in the Pan-Amazon humid forest from 2000-2022. The geographic basis are the areas of “Amazonia sensu stricto” and “Guiana”, according to Eva and Huber [35]. GFC statistics appear as grey dashed line.

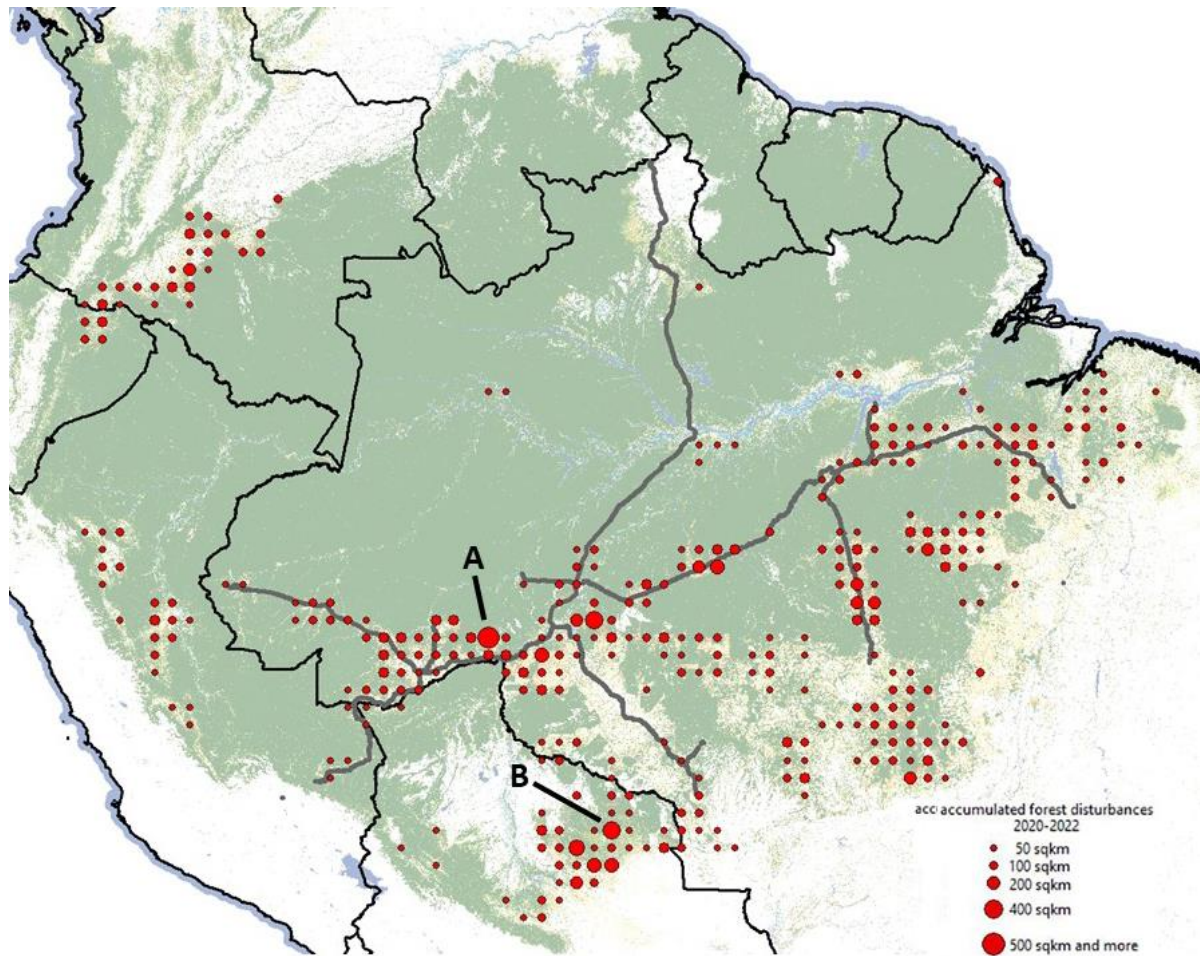


Altogether, 35,480 km² of forest were either deforested or degraded in the Pan-Amazon in 2022, constituting an increase of 14.9% with respect to 2021. In the past 22 years, the Pan-Amazon has lost 12.6% of its intact humid forest of 1999 (542.5 Mha), either by deforestation (8.0%, or 43.5 Mha) or forest degradation (4.6%, or 24.7 Mha).

²¹ <https://glad.earthengine.app/view/global-forest-change#bl=off;old=off;dl=1;lon=20;lat=10;zoom=3>
²² https://developers.google.com/earth-engine/datasets/catalog/FAO_GAUL_2015_level0

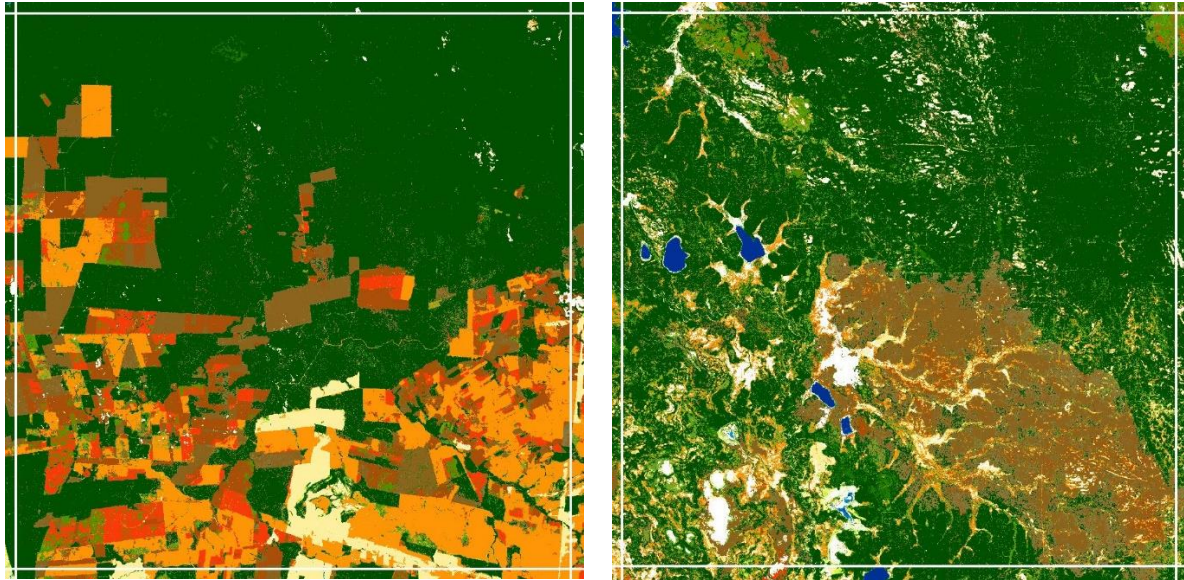
The deforestation and forest degradation areas of the single countries do not add up to the Pan-Amazon statistics, as for the country statistics also humid forest areas outside the Amazon region are considered by JRC-TMF data, as e.g. the Choco Forest on the Colombian Pacific coast or the Mata Atlântica in Brazil.

Figure 3. Distribution of accumulated JRC-TMF forest disturbances during period 2020-2022, i.e. the sum of deforestation and forest degradation (above an area of 30 km²) within 50 km X 50 km grid cells in the Pan-Amazon humid forest (red circles). The Country borders are shown as black lines, major roads as grey lines. Background: TMF forest cover change map, status 1990. Image width ca. 4,000 km



For the countries other than Brazil, the forest disturbances mostly occur close to the borders of the Amazon biome, e.g. showing the deforestation hot spot at the Northern border of the Colombian Amazon and some forest cover change activities on the western Amazon borders in Peru and Ecuador (Figure 3). Specifically in Brazil and Peru, new deforestation frontiers are created along the mayor highways cutting through the Amazon forest (e.g. the BR-319, BR-230, BR-163 and BR-364 in Brazil, and the 30C in Peru), i.e. forest disturbances often occur along these transport corridors. In the Southern and Eastern Amazon multiple access routes to the forest exist, thus the forest disturbance areas are more widespread rather than being concentrated along single major roads. Examples of the Amazon forest disturbances in the past three years are shown in Figure 4 (A and B, both with more than 500 km² of forest disturbances).

Figure 4. Examples of accumulated (2020-2022) JRC-TMF forest disturbances within two 50km X 50km grid cells in the Pan-Amazon humid forest. The borders of the 50 km X 50 km grid cells are shown in white. Left: new deforestation frontier in Southern Amazonas State (near the Rondônia State border) – all red and brown areas were deforested between 2020 and 2022. Right: Bolivian forest destroyed by a large fire in 2022 (brown area)



The Amazon country statistics regarding the forest disturbance areas show that Brazil was driving the overall absolute values, which is not surprising given the country’s large share of the Amazon forest and current forest disturbance dynamics (Figure 5). However, if the areas of forest disturbances are related to the country areas of remaining intact humid forest, according to the JRC-TMF data, Bolivia has the highest scores in both years 2021 and 2022, while e.g. Ecuador rises from the 4th place in 2021 to the 2nd in 2022 (Figure 6). The country statistics only cover the countries’ rainforests but include humid forest outside the Amazon region.

Figure 5. Disturbed humid forest area (deforestation and forest degradation) during years 2020, 2021 and 2022 for Amazon countries, according to JRC-TMF data

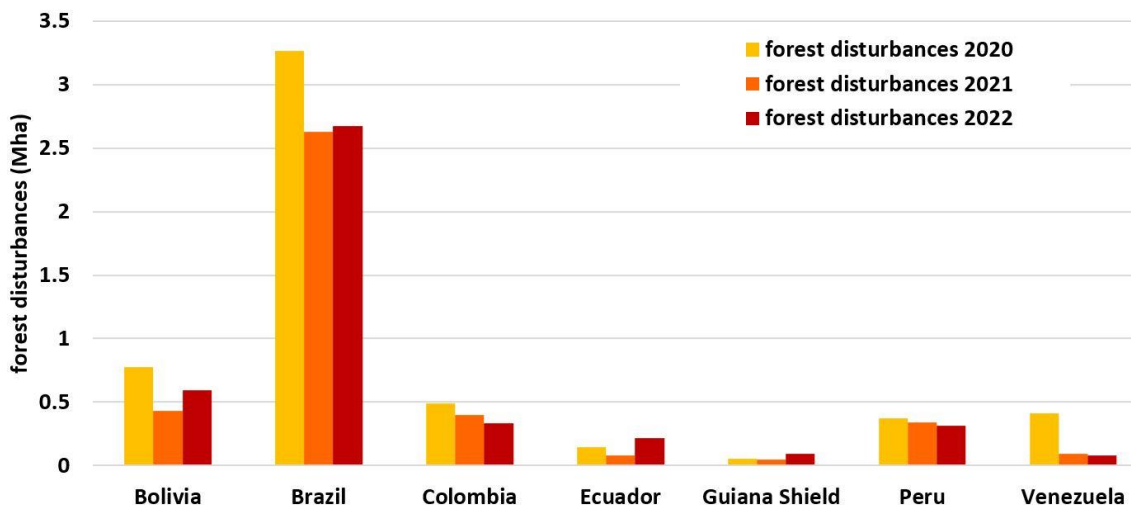


Figure 6. Percentage of disturbed forest area (deforestation and forest degradation) during years 2020, 2021 and 2022 in relation to remaining intact moist forests for Amazon countries, according to JRC-TMF data

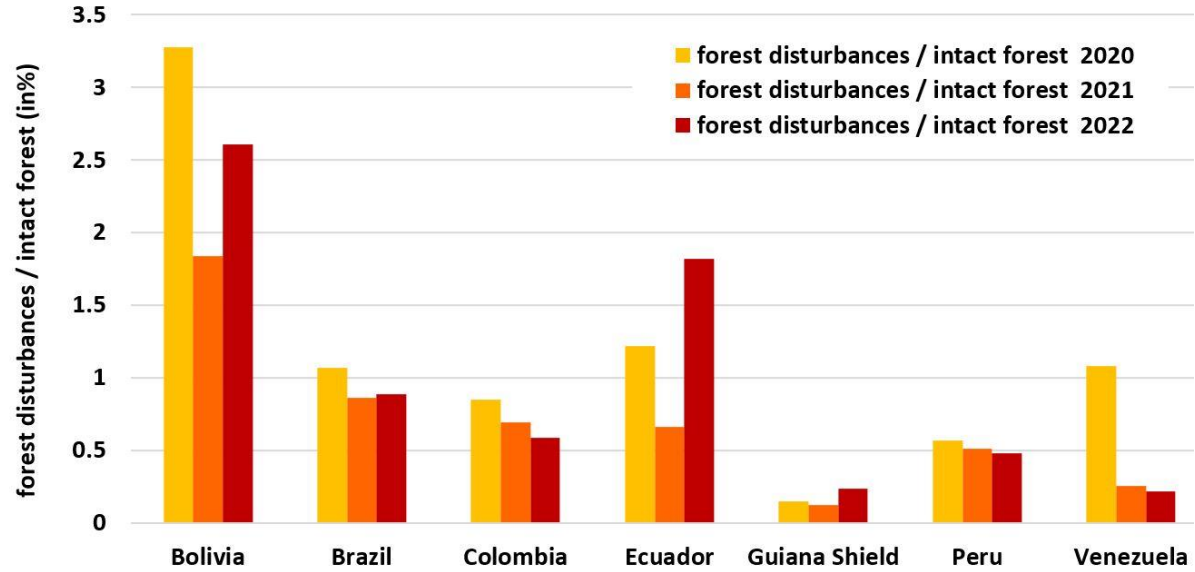
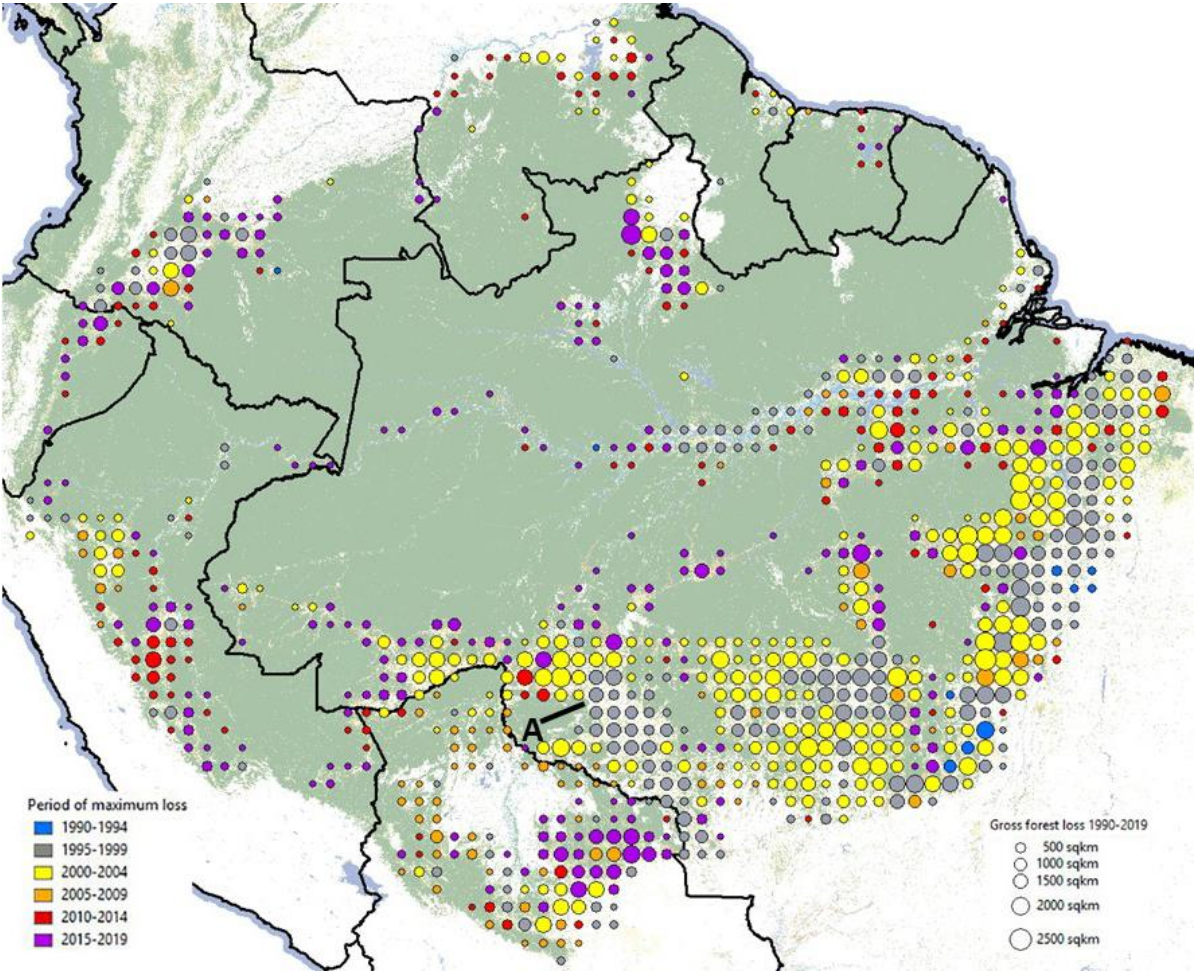


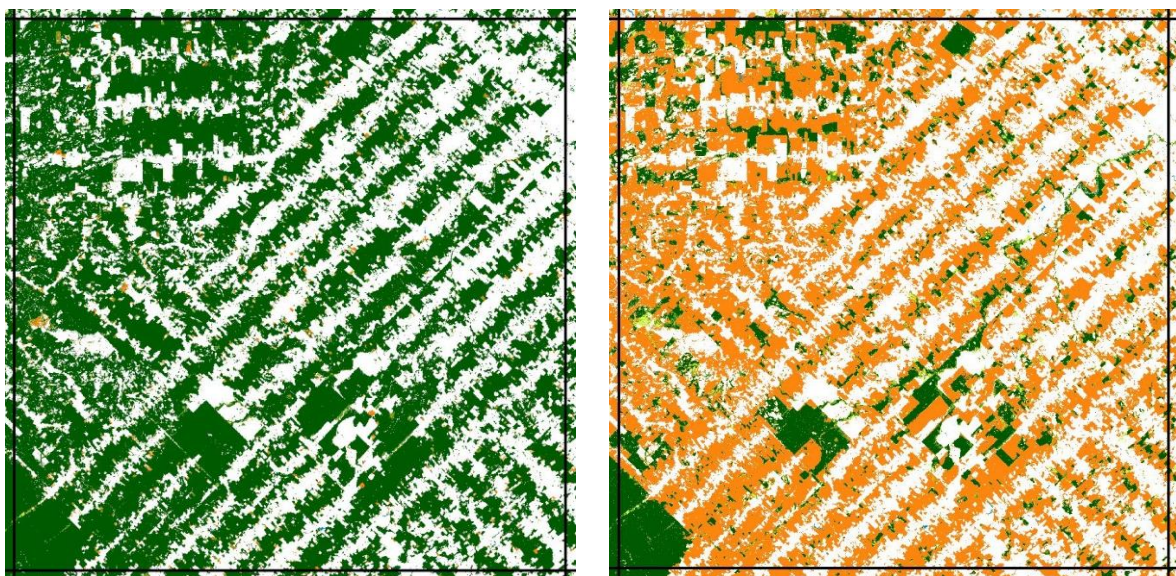
Figure 7. Deforested area between 1990 and 2019 in the Amazon region (i.e. Amazonia *sensu stricto* and Guiana, according to Eva & Huber, 2005) within 50 km X 50 km grid cells, with colours indicating the 5-year period of peak deforestation. Deforestation areas lower than 200 km² within a single grid cell are not displayed.



The historical perspective (Figure 7) shows distinct patterns of the deforestation front dynamics in the Amazon region. Specifically in the Southern and Eastern Brazilian Amazon the two periods of 1995-1999 and 2000-2004 stand out as periods of highest deforestation intensity in the region, while in the other regions (Colombia, Bolivia etc.) the periods of highest deforestation are more diverse. The period of lowest overall deforestation in Brazil is 2010-2014, and, in consequence, shows up in Figure 7 only in very few areas, while the rising deforestation in 2015-2019 is present mainly in the new deforestation frontiers of Roraima, Northern Rondônia / Southern Amazonas State, and along the highways in the interior of Amazonas State. Bolivia shows high, late deforestation, largely due to the expansion of soy²³.

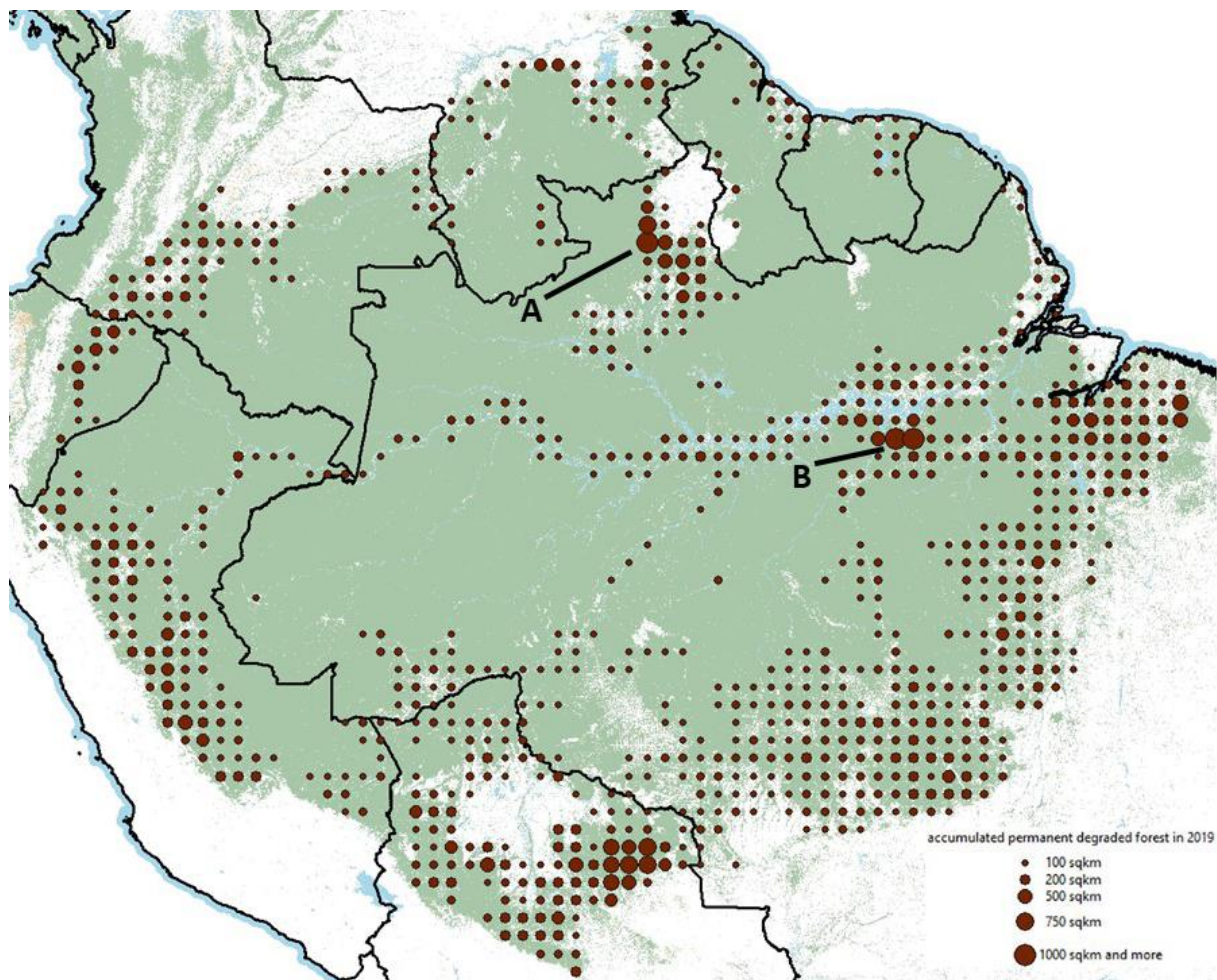
However, many of the areas, specifically at the southern and eastern Amazon border were partly deforested before 1990. In consequence, with a remaining limited forest area in grid cells that were deforested before year 1990, the circles are smaller compared to regions with full forest cover 1990 with undergoing deforestation at a later stage (see example A: Figure 8).

Figure 8. 50 km X 50 km grid cell with JRC-TMF data in Central Rondônia, with 67% forest cover in 1990 (left panel, with deforested areas before 1990 in white) due to 'early deforestation' in the 1970s and 1980s. By 2019, a further 83% of the forest standing in 1990 were deforested (right panel, with deforested areas during period 1990-2019 in orange).



²³<https://news.mongabay.com/2023/02/bolivia-has-a-soy-deforestation-problem-its-worse-than-previously-thought/>

Figure 9. Accumulated forest degradation (not followed by deforestation) during period 1990-2019, caused by selective logging, fire or natural events with subsequent forest recovery, areas per 50 km X 50 km grid cell (see Figure 11 for examples A and B)



The regions of largest degraded forest areas are in Bolivia and the Brazilian States of Rondônia and Pará. Specifically, forest fires constitute a large part of forest degradation areas in JRC-TMF data, while selective logging areas are generally smaller. However, the JRC-TMF dataset (as other pixel-based approaches) generally tend to underestimate forest areas affected by selective logging, due to the fact that some selective logging features, like smaller logging gaps, narrow skid trails and logging roads which are partly under the forest canopy cannot be detected by Landsat imagery [36-38].

Figure 10. Two examples of accumulated degraded forest over period 1990-2019, i.e. areas that are still forests in 2019 after a disturbance in the previous three decades. Left panel: Large burned forest area (989 km²) in Rondônia State, where forest fires happened near 'fishbone-type' secondary roads. Right panel: 1000 km² of burned forest near the city of Santarém (Pará State). Map width: 50 km, grid cell borders in white.

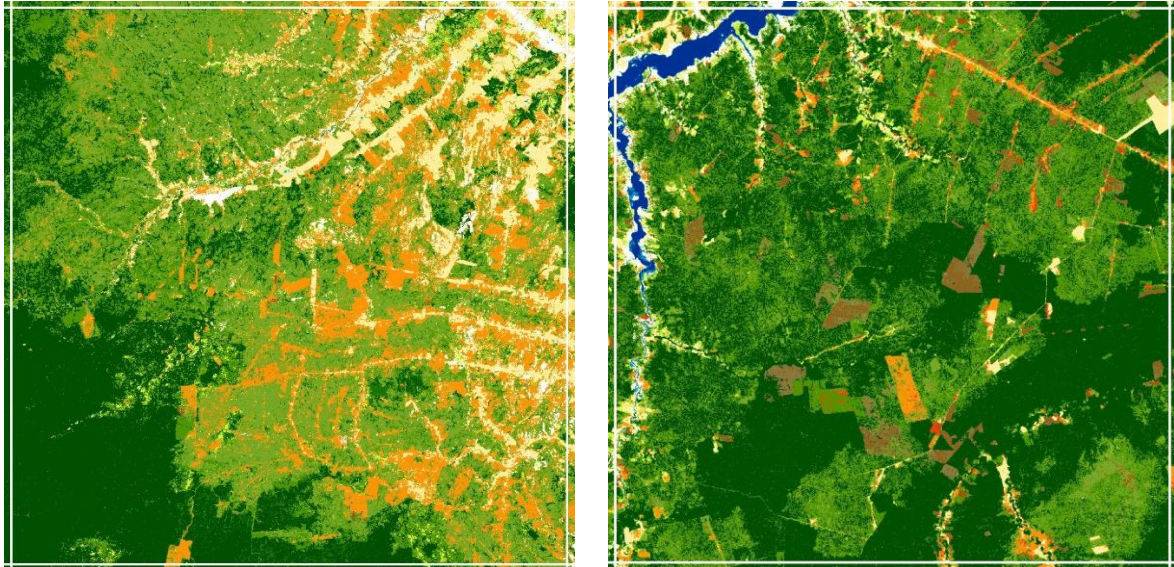
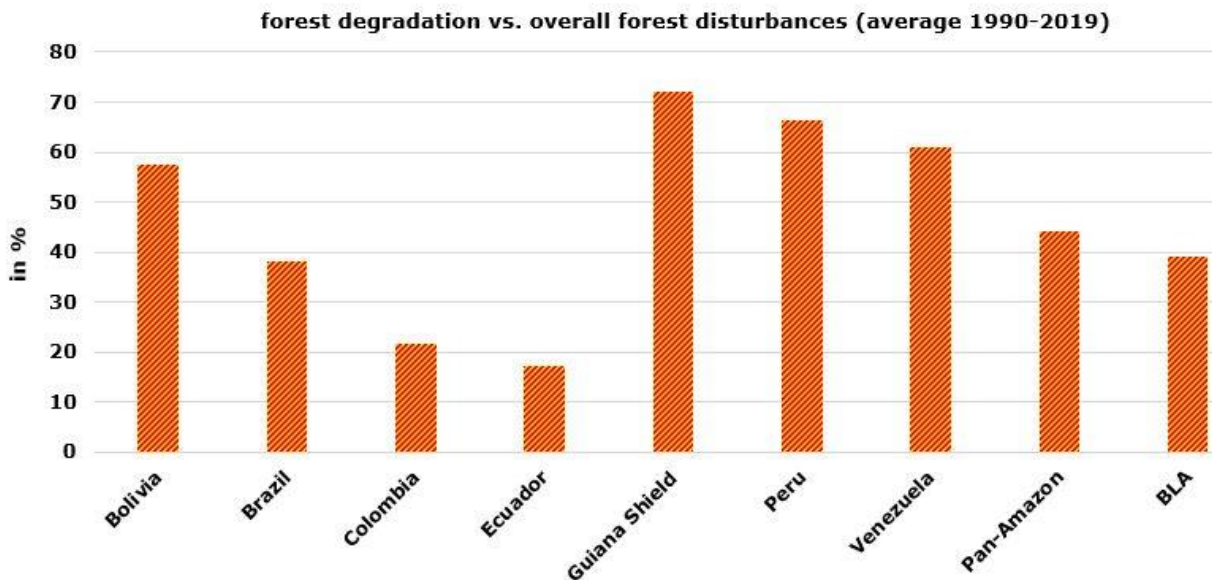


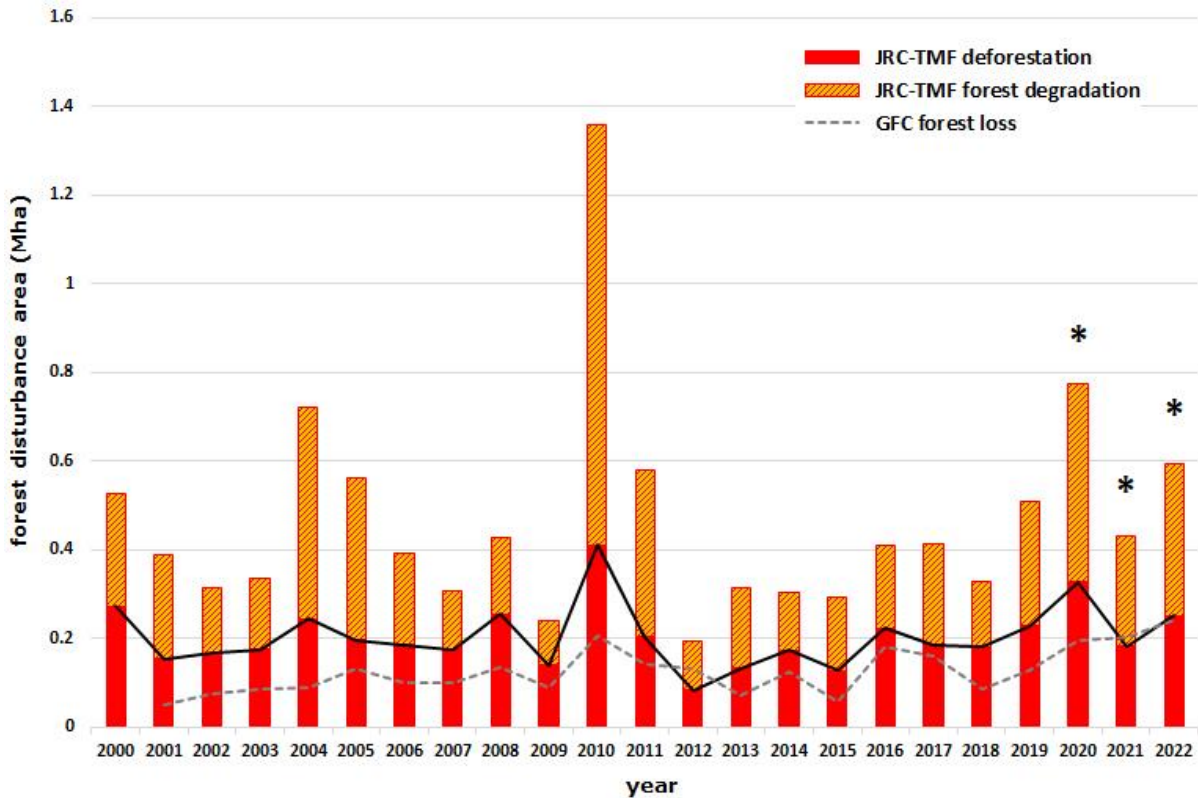
Figure 11. Percentage of average yearly forest degradation areas (i.e. mainly selective logging, forest fires and natural events) versus area of average yearly forest disturbances (i.e. deforestation and forest degradation) for Amazon countries and regions



In Bolivia as well as in Venezuela, the Guiana Shield countries and Peru, the yearly area of forest degradation is larger than the deforested area with 57%, 72%, 66% and 61%, respectively. In the Pan-Amazon, comprising all Amazon countries, the yearly average forest degradation consists in ca. 44% of the overall forest disturbances; in consequence, the yearly average deforestation area in the Pan-Amazon comprises ca. 56%. The yearly forest degradation statistics comprise areas that are deforested at a later stage (ca. 45% of all forest degradation areas, according to [4]).

2.2 Bolivia

Figure 12. Forest disturbances in the Bolivian humid forest from 2000 to 2022, according to JRC-TMF. Tree cover loss estimates from GFC appear as grey dashed line.



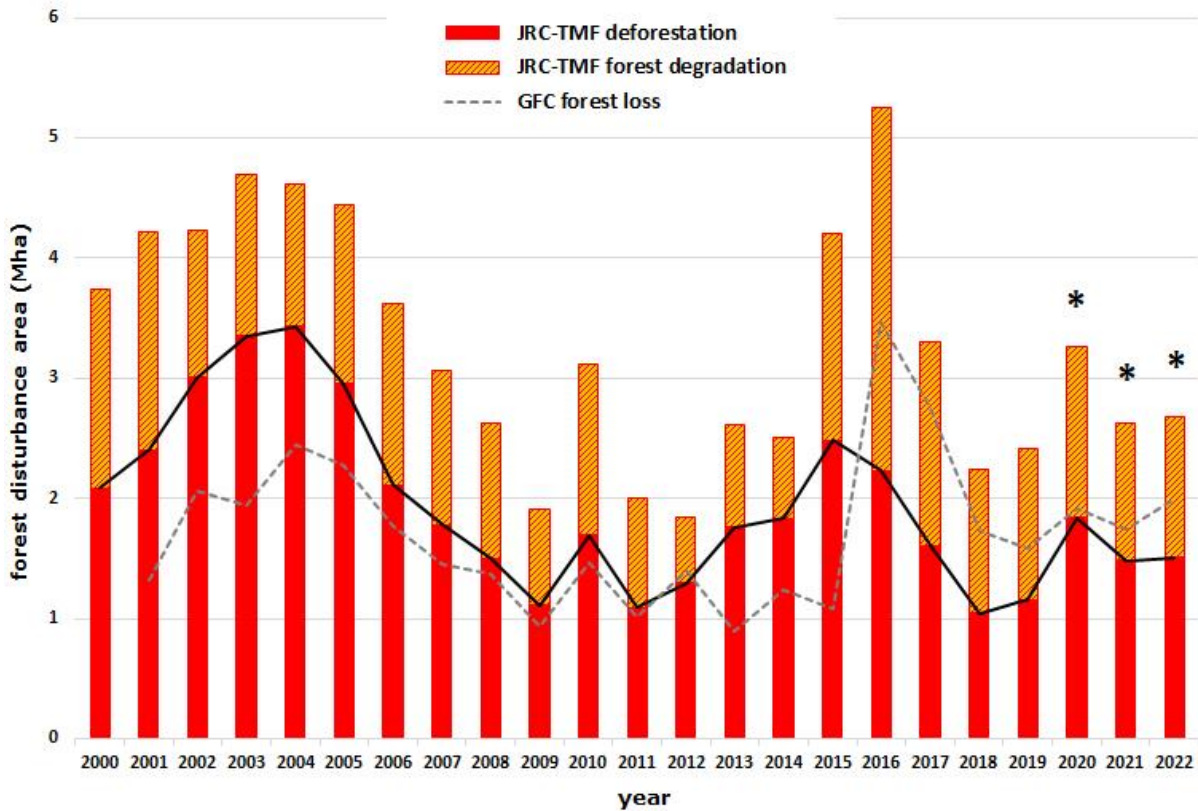
The forest disturbances for Bolivian humid forests in the last 20 years show the highest peaks for years of severe forest fires, as for the year 2010. At the time, the national Government announced a national emergency as a consequence of having more than 15,000 km² of land burned²⁴. In 2022, altogether 4,299 km² of humid forest were either deforested or degraded, which constitutes an increase of 38.5% compared to 2021.

In the past 22 years Bolivia has lost 29.5% of its intact humid forest of 1999 (31.0 Mha), either by deforestation (15.1%, or 4.7 Mha) or forest degradation (14.3%, or 4.4 Mha). GFC estimates are mostly lower than JRC-TMF but follow a similar yearly trend. For year 2022 TMF deforestation and GFC tree cover loss estimates are almost identical.

²⁴ <https://www.bbc.com/news/world-latin-america-11033521>

2.3 Brazil

Figure 13. Forest disturbances in the Brazilian humid forest from 2000 to 2022, according to JRC-TMF. Tree cover loss estimates from GFC appear as grey dashed line.



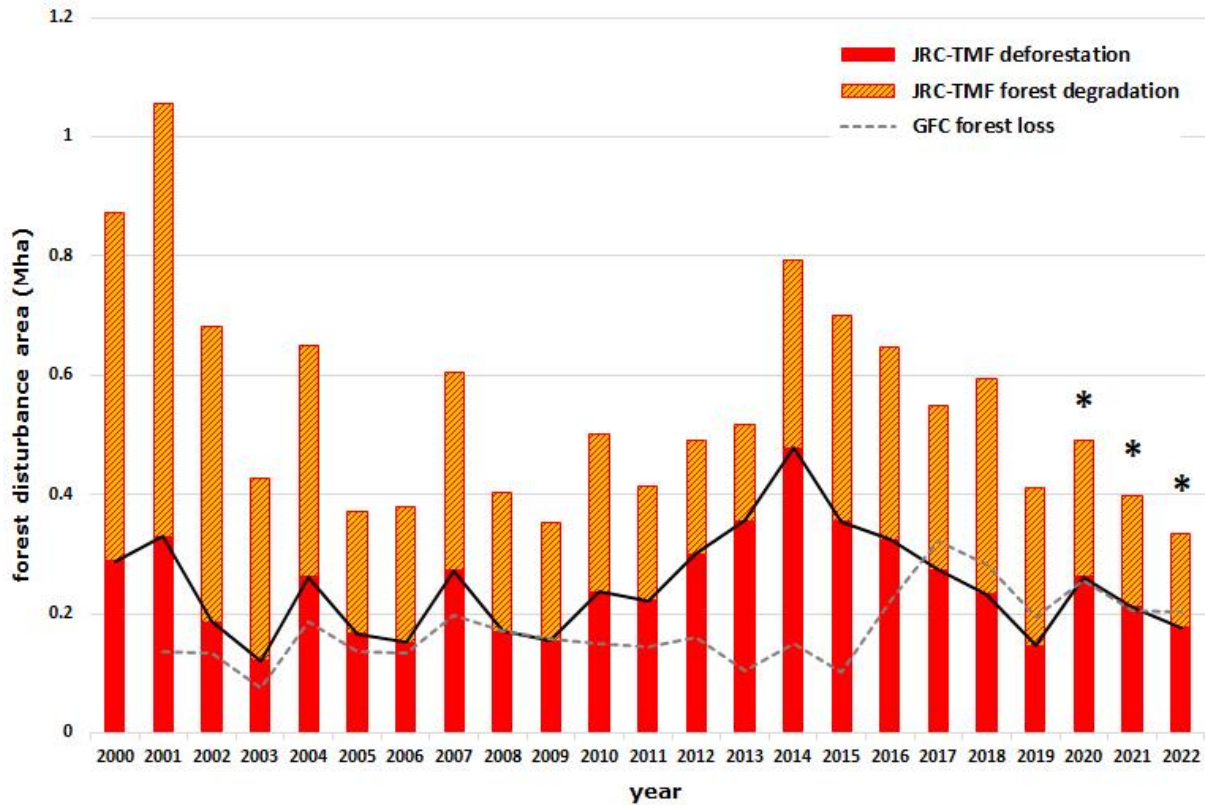
The Amazon being the Brazilian region undergoing most changes in humid forest cover, its forest dynamics clearly drive the overall Brazilian humid forest cover change statistics reported by JRC-TMF data. The decrease of the Amazon deforestation after 2004 and the peaks in forest degradation, mostly due to forest fires in 2010 and 2015-2017, are visible in the Brazilian Legal Amazon and the Brazilian statistics from JRC-TMF. Forest fires were responsible for a large part of the Brazilian forest degradation in 2022, while it had diminished considerably in 2021 due to the intensive rains in the region throughout the year. In this context, INPE-DETER reported a decrease in forest fire alerts of 79% for the Brazilian Legal Amazon from 2020 to 2021, while the alerts increased again in 2022 by 280% compared to 2021.

According to JRC-TMF statistics, 26,750 km² of forest were either deforested or degraded in 2022 in the Brazilian humid forest (i.e. Amazon forest and Atlantic forest), constituting an increase of 1.8% compared to 2021.

In the past 22 years Brazil has lost 18.2% of its intact humid forest of 1999 (359.9 Mha), either by deforestation (12.4%, or 44.7 Mha) or forest degradation (5.8%, or 20.9 Mha).

2.4 Colombia

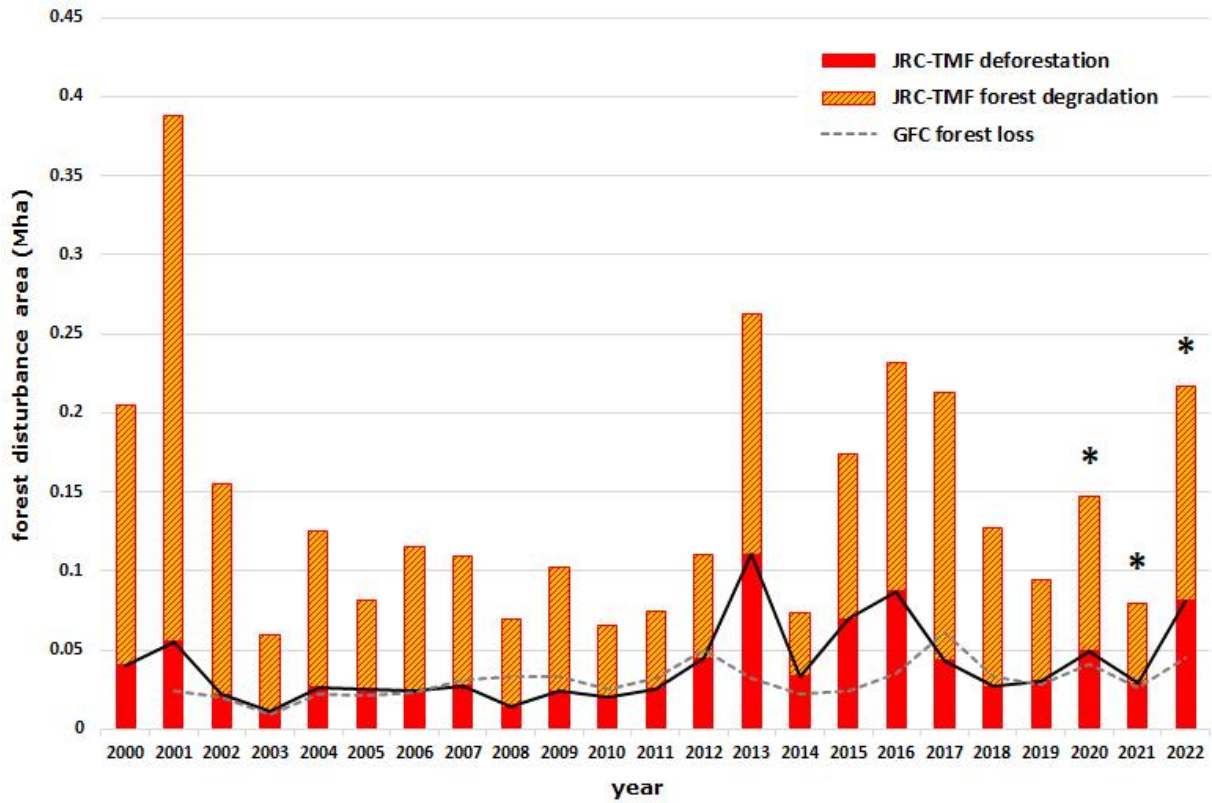
Figure 14. Forest disturbances in Colombian humid forest from 2000 to 2022, according to JRC-TMF. Tree cover loss estimates from GFC appear as grey dashed line.



The forest disturbance trends for Colombian humid forests in the last 23 years show increases and decreases staying on a level between ca. 4,000 km² and 8,000 km². The forest disturbance area of 2022 is 3,335 km², which constitutes a decrease of 16% in comparison with 2021. The overall forest disturbance area is the lowest since year 2000. In the past 22 years Colombia has lost 15.9% of its intact humid forest of 1999 (66.8 Mha), either by deforestation (8.5%, or 5.67 Mha) or forest degradation (7.4%, or 4.95 Mha).

2.5 Ecuador

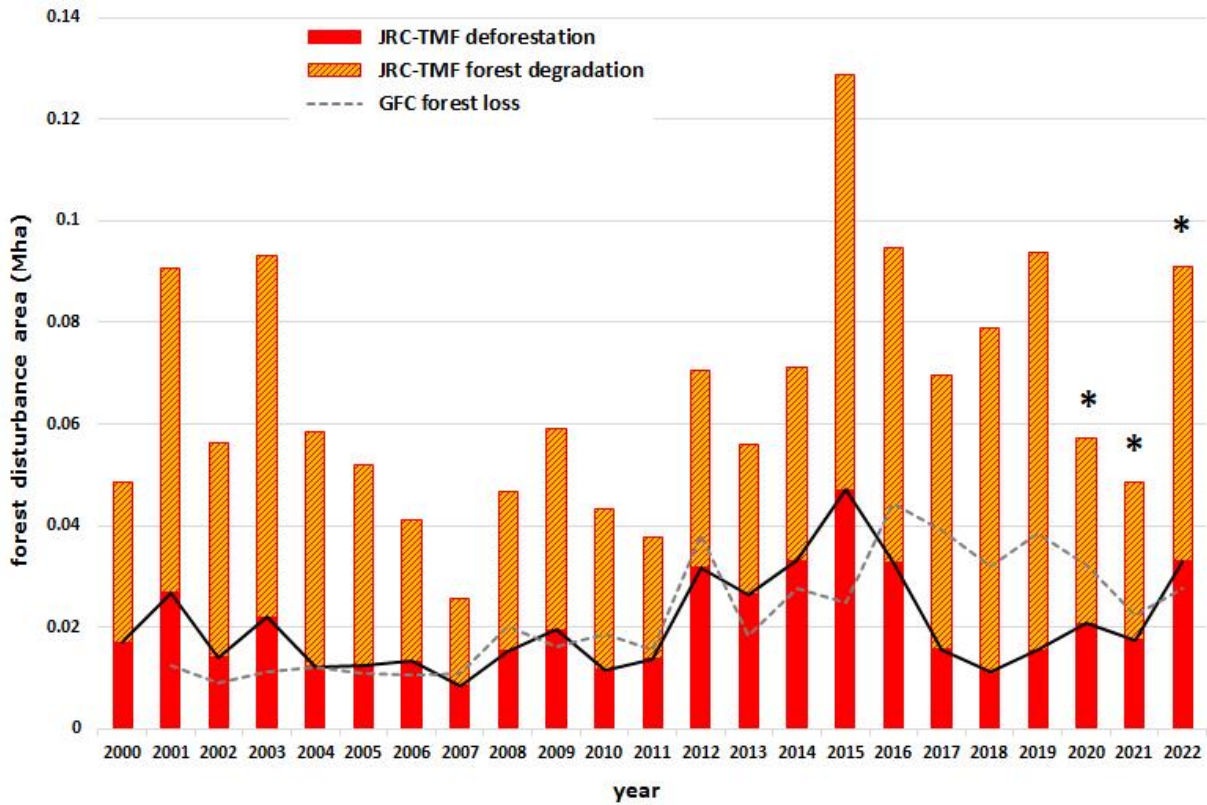
Figure 15. Forest disturbances in Ecuadorian humid forest from 2000 to 2022, according to JRC-TMF. Tree cover loss estimates from GFC appear as grey dashed line.



The Ecuadorian forest disturbance area in 2022 shows an increase of 172.9% compared to the previous year. Altogether, 2,165 km² of forest have been either deforested or degraded, which is the fourth largest area since year 2000, after years 2001 (3,874 km²), 2013 (2,623 km²) and 2016 (2,321 km²). In the past 22 years Ecuador has lost 18.8% of its intact humid forest of 1999 (14.6 Mha), either by deforestation (6.3%, or 0.92 Mha) or forest degradation (12.5%, or 1.82 Mha).

2.6 Guiana Shield (Guyana, Suriname and French Guiana)

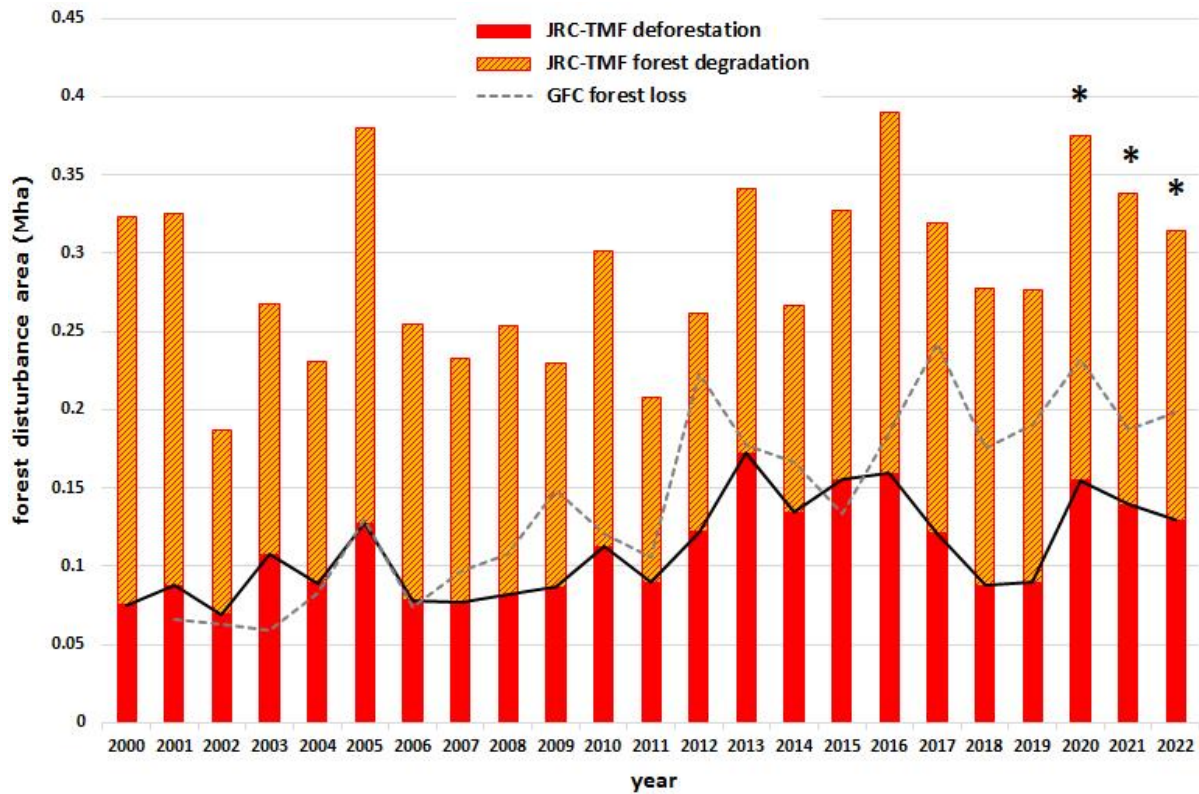
Figure 16. Forest disturbances in the Guiana Shield’s humid forest from 2000 to 2022, according to JRC-TMF. Tree cover loss estimates from GFC appear as grey dashed line.



In 2022, forest disturbances in the Guiana Shield (Guyana, Suriname and French Guiana) show an increase of 87.6%, compared to 2021, adding up to 910 km². In the past 22 years the Guiana Shield countries have lost 3.4% of its intact humid forest of 1999 (40.2 Mha), either by deforestation (1.2%, or 0.47 Mha) or forest degradation (2.2%, or 0.9 Mha).

2.7 Peru

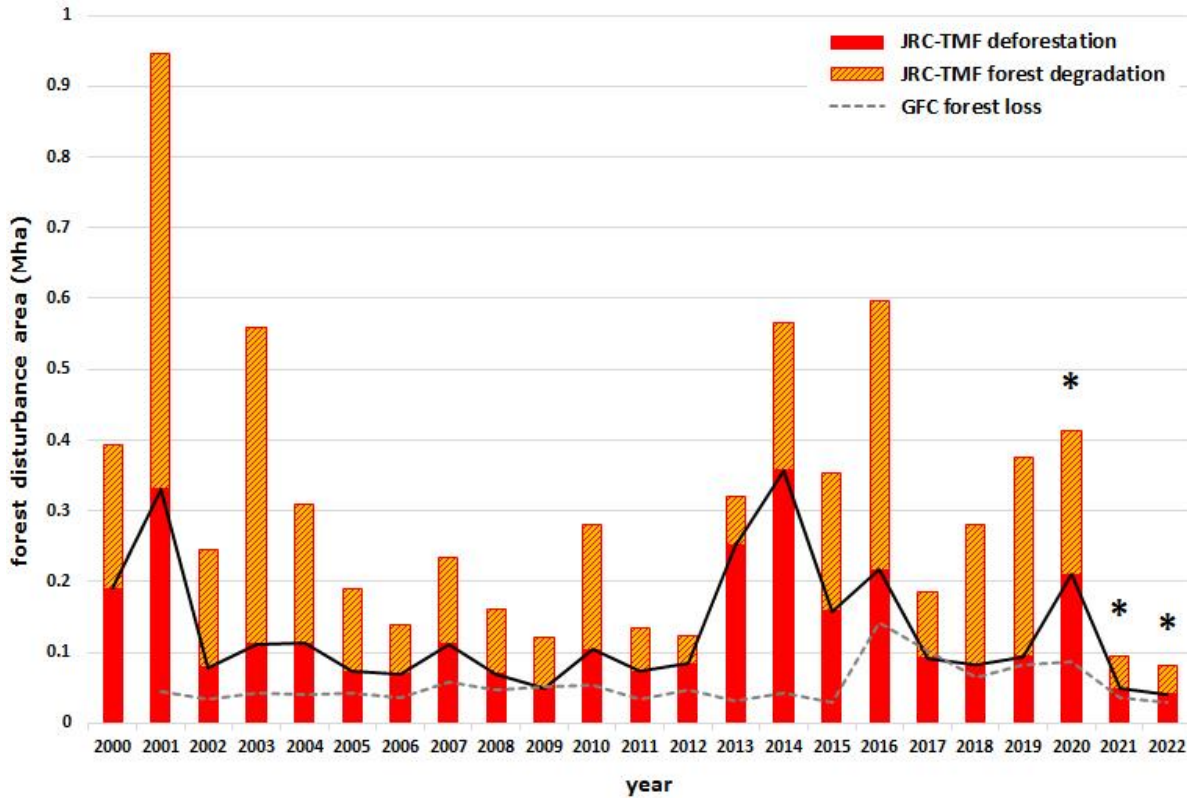
Figure 17. Forest disturbances in Peruvian humid forest from 2000 to 2022, according to JRC-TMF. Tree cover loss estimates from GFC appear as grey dashed line.



The trend for Peruvian humid forest disturbances in the last 20 years shows that, with 2,792 km², year 2022 is higher than average level. The decrease of the 2022 forest disturbance area, compared to 2021, is ca. 7%. In the past 22 years Peru has lost nearly 8.3% of its intact humid forest of 1999 (71.2 Mha), either by deforestation (3.6%, or 2.55 Mha) or forest degradation (4.7%, or 3.3 Mha)

2.8 Venezuela

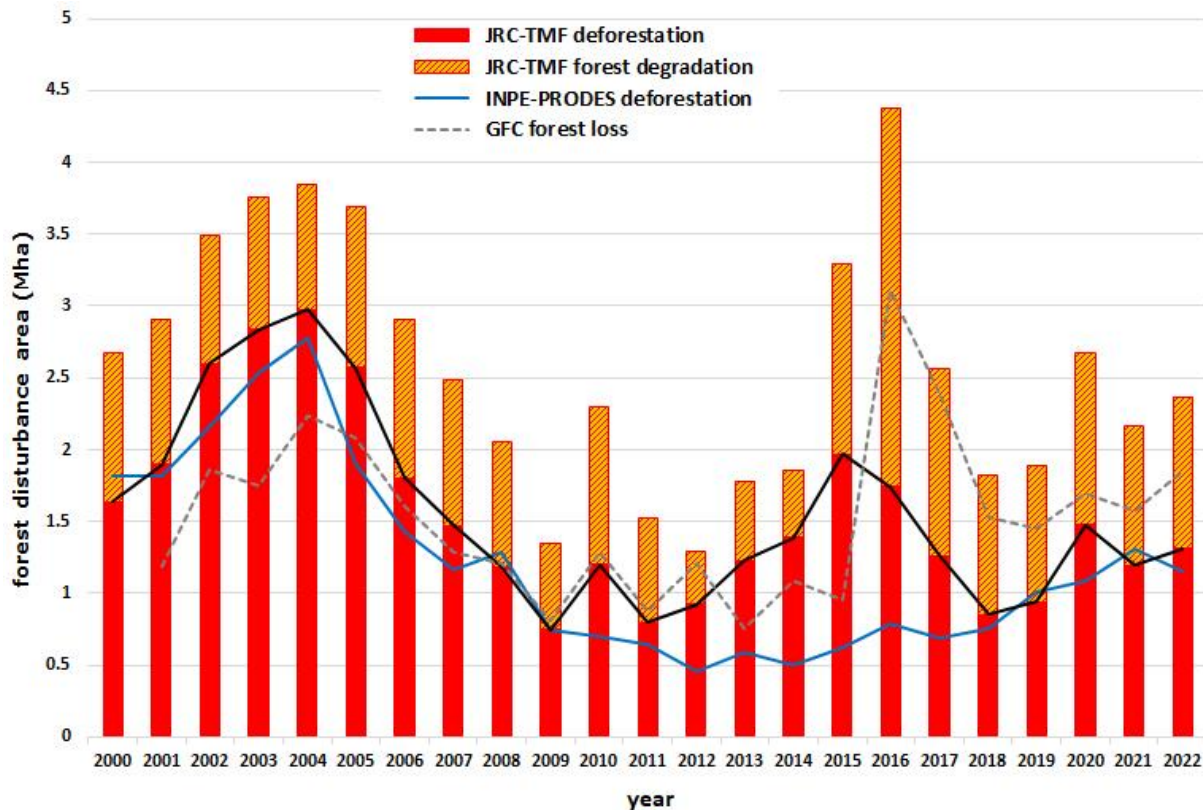
Figure 18. Forest disturbances in Venezuelan humid forest from 2000 to 2022, according to JRC-TMF. Tree cover loss estimates from GFC appear as grey dashed line.



Venezuela showed relatively few areas of forest disturbances in 2022, when 813 km² of humid forest have been either deforested or degraded. Compared to 2021, forest disturbances decreased by 15% in 2022. In the past 22 years Venezuela has lost 13.7% of its intact humid forest of 1999 (43.5 Mha), either by deforestation (6.9%, or 3.0 Mha) or forest degradation (6.8%, or 2.9 Mha)

2.9 Comparison of JRC-TMF and INPE-PRODES deforestation estimates for the Brazilian Legal Amazon

Figure 19. Annual deforestation and forest degradation in the BLA from 2000 to 2022, according to JRC-TMF data. Deforestation appears in red, forest degradation appears in orange. For comparison, INPE-PRODES and GFC deforestation estimates appear as blue and grey dashed lines, respectively.



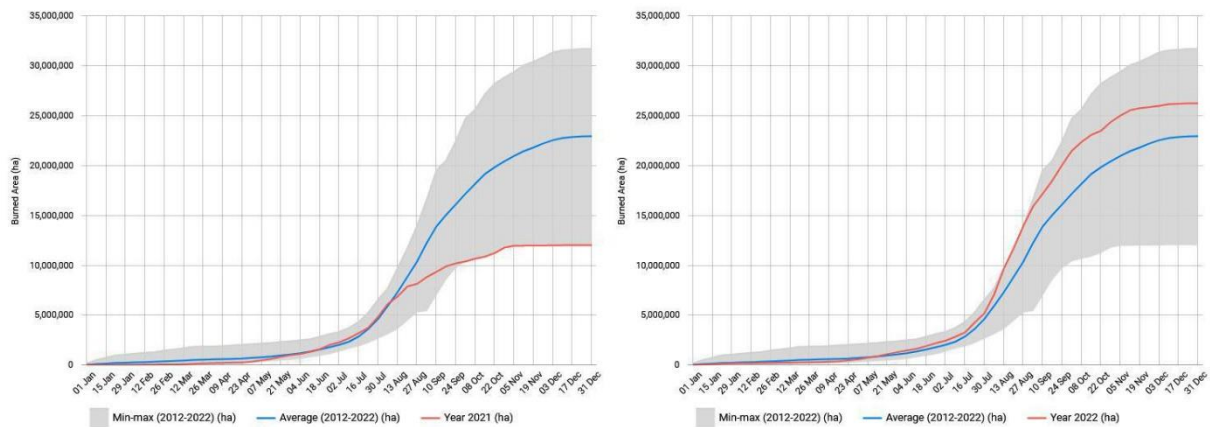
The overall annual new disturbed forest area in the BLA increased by 9.3% from 21,632 km² in 2021 to 23,647 km² in 2022. After the year 2021 with relatively high precipitation (according to CHIRPS precipitation data²⁵) during the fire season (i.e. July-November), 2022 showed an amount of rainfall, specifically in the Brazilian Arc of Deforestation [39], which was below average. In consequence, the area of burned forest increased in 2022 compared to 2021. This increase in forest fires in 2022 is reflected in the INPE-DETER forest degradation estimates, which show a forest fire increase of 280%²⁶. The Global Wildfire Information Network (GWIS) reported an increase of 118%% of burned areas (including forest fires and non-forest fires) for the Brazilian Legal Amazon in 2022 in comparison with 2021²⁷.

²⁵ <https://www.chc.ucsb.edu/data/chirps>

²⁶ <http://terrabrasilis.dpi.inpe.br/app/dashboard/alerts/legal/amazon/aggregated/>

²⁷ <https://gwis.jrc.ec.europa.eu/apps/gwis.statistics/seasonaltrend>

Figure 20. GWIS weekly cumulative burnt areas for the Brazilian Legal Amazon for year 2021 (left panel) and 2022 (right panel)



As mentioned before, the distinction between forest degradation and deforestation events for 2022 can only be done in three years from now, once a potential forest regrowth can be assessed and confirmed from satellite imagery. At the beginning of 2023, the consolidated attribution between the two classes was made for year 2019 for the first time. The relative class distribution within the overall disturbed forest areas for years 2020 to 2022 (red + orange bars in figure 19) is based on a 20-year historical average.

In the past 22 years the Brazilian Legal Amazon has lost 17.1% of its intact humid forest of 1999 (332.9 Mha), either by deforestation (10.8%, or 36.0 Mha) or forest degradation (6.3%, or 20.9 Mha)

3 Monitoring deforestation and forest degradation in the Brazilian Legal Amazon: estimates from Brazilian National Space Research Institute (INPE) for 2022/23

3.1 INPE-PRODES deforestation statistics

INPE carries out two parallel projects related to deforestation (Amazon and Cerrado biomes) and forest degradation monitoring (Amazon biome), called PRODES and DETER. PRODES produces consolidated statistics on deforestation once a year (usually at the end of November) for the period of August of the previous year until July of the current year (i.e. year of statistics publication), based mainly on Landsat imagery with 30 m spatial resolution²⁸. Recently, the geographical coverage of PRODES has been expanded to all Brazilian biomes. DETER produces daily, accumulated monthly and yearly deforestation and forest degradation alerts based on CBERS imagery with lower spatial, but higher temporal resolution (for more detail see chapter 3.3).

The PRODES consolidated statistics on the deforestation of humid forest in the Brazilian Legal Amazon (BLA) showed 9,001 km² for the period of August 2022 until July 2023²⁹, which constitutes a decrease of 22.4% in comparison with the corresponding period in 2021/22 (Figure 21). For the Cerrado biome, statistics for Aug '22 – July '23 were not available yet, the deforestation area given by INPE-PRODES for the precedent year was 10,689 km², constituting an increase of 25.3% compared to 2020/21³⁰ (Figure 22).

Figure 21. Yearly consolidated deforestation estimates ('reference years', i.e. August to July) for the Brazilian Legal Amazon reported by INPE-PRODES

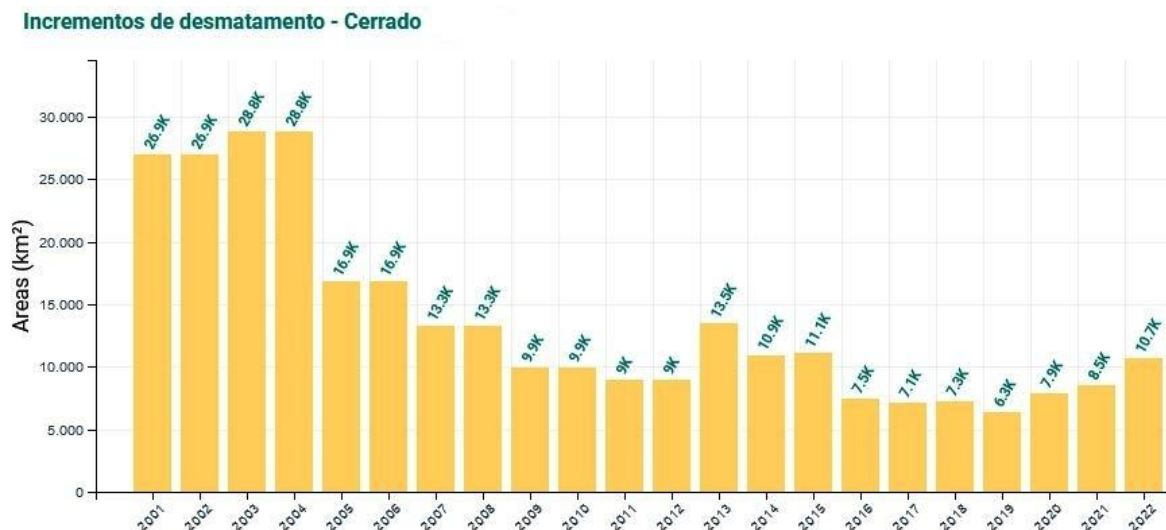


²⁸ <http://terrabrasilis.dpi.inpe.br/en/faq-2/>

²⁹ http://terrabrasilis.dpi.inpe.br/app/dashboard/deforestation/biomes/legal_amazon/rates

³⁰ <http://terrabrasilis.dpi.inpe.br/app/dashboard/deforestation/biomes/cerrado/increments>

Figure 22. Yearly consolidated deforestation estimates ('reference years', i.e. August to July) for the Brazilian Cerrado biome reported by INPE-PRODES



3.2 INPE-DETER deforestation and forest degradation alerts

3.2.1 INPE-DETER deforestation alerts 2022

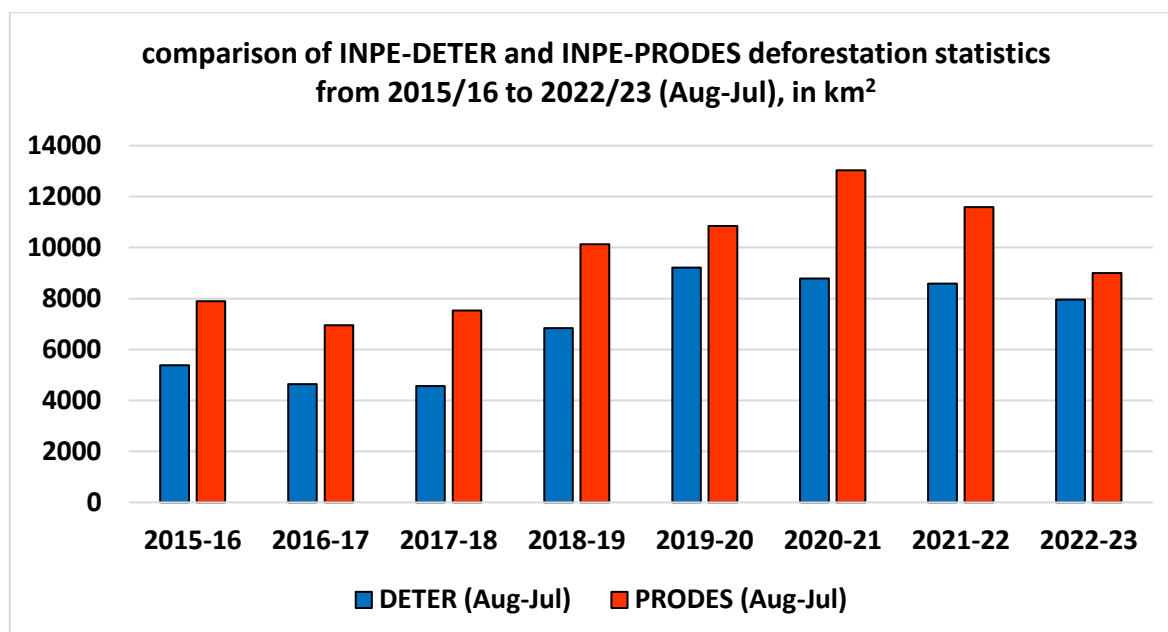
The INPE-DETER near-real-time system produces deforestation alerts (for the BLA and the Cerrado biome separately) and forest degradation alerts (BLA only), based on daily low-resolution satellite imagery. The system's 'daily warnings'³¹ provide substantial input to the Brazilian Institute of Environment and Renewable Natural Resources (IBAMA), responsible for the surveillance and control of deforestation and forest degradation in the Amazon and the Cerrado [40]. At the same time, the system's monthly aggregated data³² provide longer-term trends of forest cover change in the two regions.

The trends derived from the monthly INPE-DETER deforestation alerts aggregated over annual periods are usually consistent with INPE-PRODES figures reported (once a year) for the BLA as official consolidated annual deforestation areas. The comparison between 12 months of DETER accumulated monthly near-real-time deforestation alerts (August-July period) and official PRODES deforestation statistics from 2015/2016 to 2022/2023 periods shows significant differences, but overall consistent trends (Figure 23). DETER deforestation alert areas in 2022/2023 represent 88.3% of the PRODES consolidated Amazon deforestation areas for the same period. Over an 8-year period, DETER yearly statistics range from 60.7% (2017/18) to 88.3% (2022/23) compared to PRODES, with an average of 72.2%. For the Cerrado biome the DETER deforestation alerts capture in average (over a 5-year period) 61.9% of the PRODES consolidated deforestation estimates.

³¹ <http://terrabrasilis.dpi.inpe.br/app/dashboard/alerts/legal/amazon/daily/>

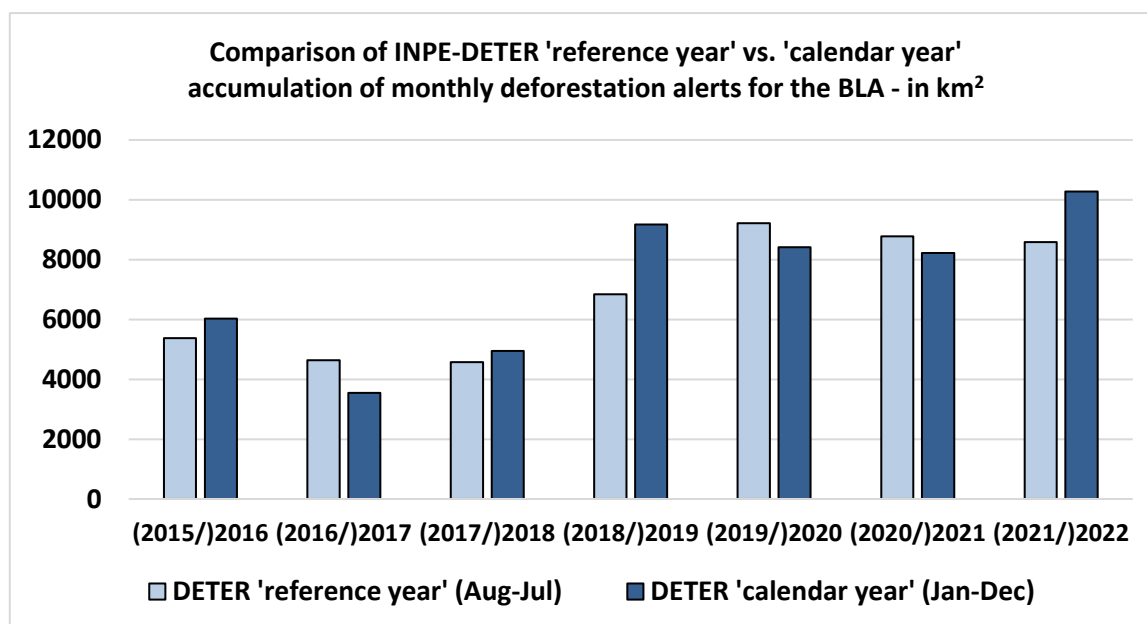
³² <http://terrabrasilis.dpi.inpe.br/app/dashboard/alerts/legal/amazon/aggregated/>

Figure 23. INPE-DETER yearly aggregation of deforestation near-real-time alerts (blue bars) and INPE-PRODES official consolidated deforestation estimates (red bars) from 2015/16 – 2022/23 (August-July) for the BLA



In 2022 (“calendar year”, i.e. Jan-Dec) INPE-DETER deforestation alerts for the Brazilian Legal Amazon³³ recorded an area of 10,278 km², which constitutes an increase of 19.6% compared to 2021. If the DETER “reference yearly period” (August-July, as used by PRODES) is taken into account, the estimates show a decrease from August 2021 – July 2022 of 2.2%, compared to the previous reference year period (Figure 24).

Figure 24. Difference between ‘reference year’ (August-July) and ‘calendar year’ (January-December) accumulation of INPE-DETER monthly deforestation alerts.



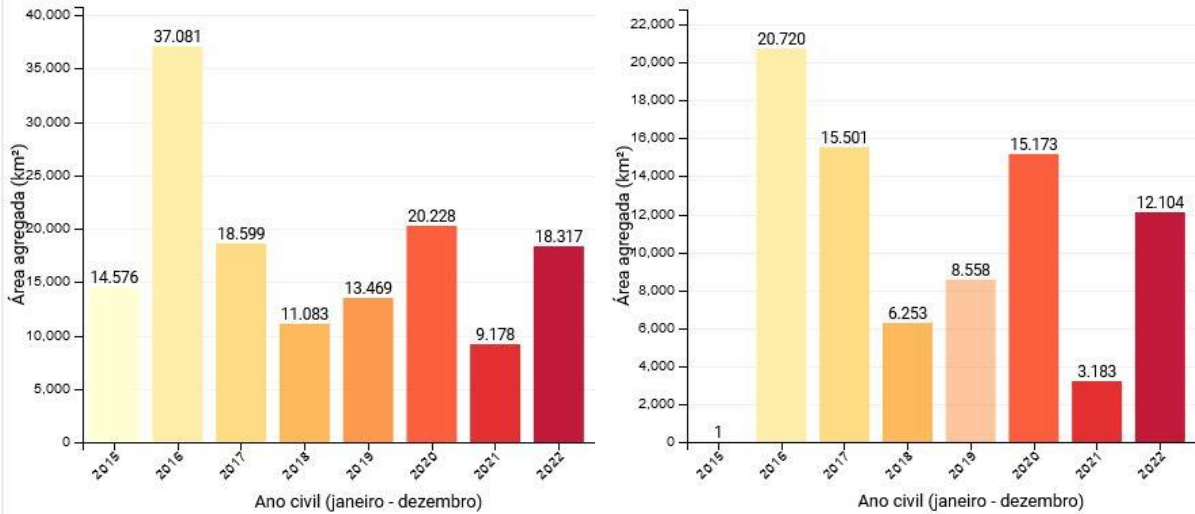
As the calendar year 2023 (January – December 2023) was not complete yet at the time of the report publication, Figure 24 could not be updated.

³³ <http://terrabrasilis.dpi.inpe.br/app/dashboard/alerts/legal/amazon/aggregated/>

3.2.2 INPE-DETER forest degradation alerts 2022

The INPE-DETER alerts on forest degradation areas comprise the classes 'selective logging', 'forest fires' and 'unspecified forest degradation'. The statistics for 2022 show an increase of overall BLA forest degradation of 99.6% (Figure 25), with forest fires alone increasing by 280% between 2021 and 2022 (Jan-Dec)³⁴. The overall increase of forest degradation is clearly driven by the increase of forest fires in 2022. The alerts of selective logging decreased in 2022 by 5.3% while 'unspecified forest degradation' increased by 22.9%.

Figure 25. left: INPE-DETER forest degradation alerts for the BLA, right: INPE-DETER forest fire alerts for the BLA (forest fire being a sub-class of the forest degradation alerts)

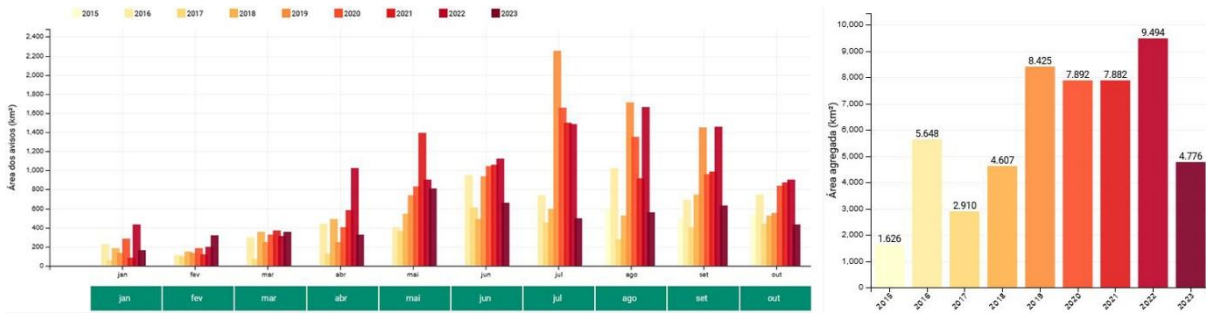


3.2.3 INPE-DETER deforestation and forest degradation alerts 2023 (January-October)

In the first ten months of 2023, the areas of deforestation in the Brazilian Legal Amazon decreased by 49.7% (Figure 26) compared to the same period in 2022 (9,494 km² in 2022 vs. 4,776 km² in 2023), while the area of forest degradation decreased by 32.6% (17,037 km² in 2022 vs. 11,491 km² in 2023), according to the INPE-DETER alert system. In this context, it is important to note that monthly alert estimates have a high uncertainty in particular due to persisting cloud cover that can limit the detection of forest cover changes during specific months (rainy season) and attribute such changes later during following drier months. In consequence, comparing monthly figures has limited meaningfulness, while observing trends in accumulated figures over yearly periods gives estimates that are more robust.

³⁴ <http://terrabrasilis.dpi.inpe.br/app/dashboard/alerts/legal/amazon/aggregated/>

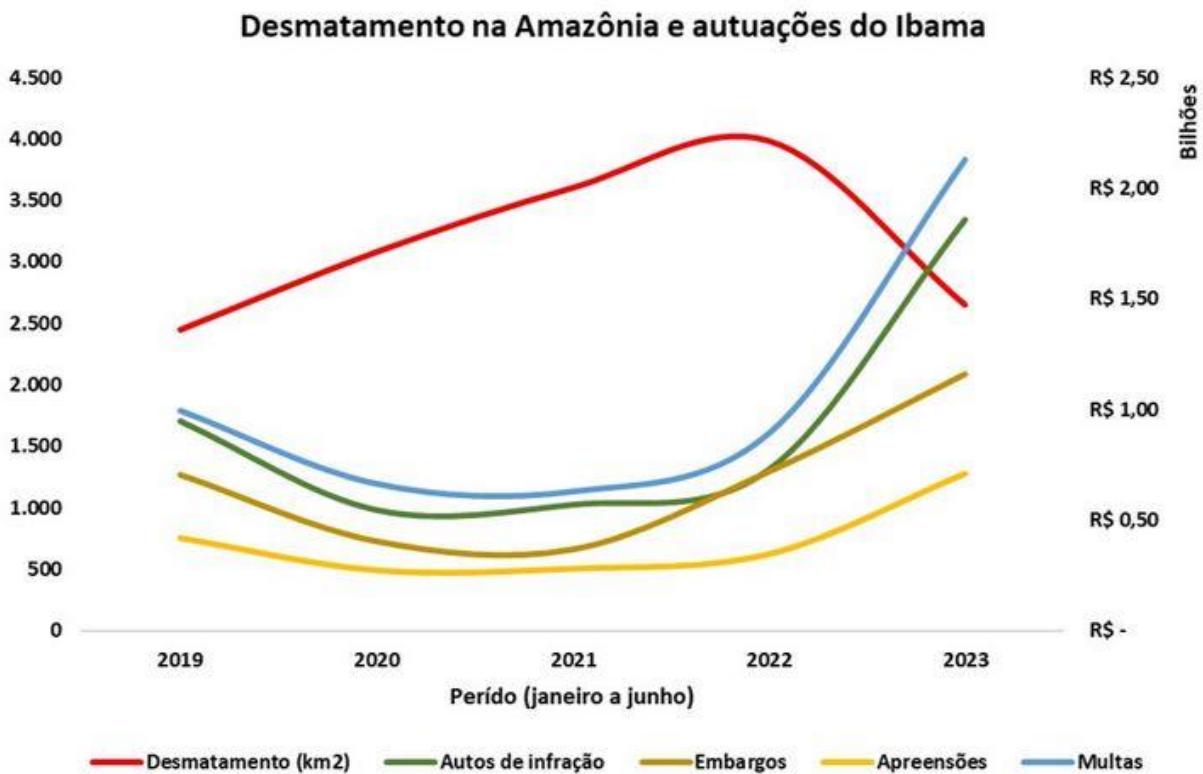
Figure 26. left: monthly statistics of INPE-DETER deforestation alerts 2023 for the BLA (January – October), right: INPE-DETER accumulated deforestation alerts for the BLA (January – October)³⁵



For the Cerrado biome, an increase of 34.1% in deforestation area is recorded by INPE-DETER for the first ten months of 2023, compared to the same period in the previous year³⁶.

The Brazilian Government officially published the data in a conference at the beginning of June 2023, led by the Minister of the Environment and Climate Change, Marina Silva. In this context, she pointed out that the decrease of deforestation alerts for the Legal Amazon needs to be seen as a consequence of the increase of deforestation law enforcement action by IBAMA together with an uptake of juridical files, embargoes, confiscations and fines³⁷.

Figure 27. DETER deforestation alerts for the Brazilian Legal Amazon (red line) of the January-June period, and the increase of law enforcement and legal action of IBAMA in 2023³⁸.



³⁵ <http://terrabrasilis.dpi.inpe.br/app/dashboard/alerts/legal/amazon/aggregated/>

³⁶ <http://terrabrasilis.dpi.inpe.br/app/dashboard/alerts/biomes/cerrado-nb/aggregated/>

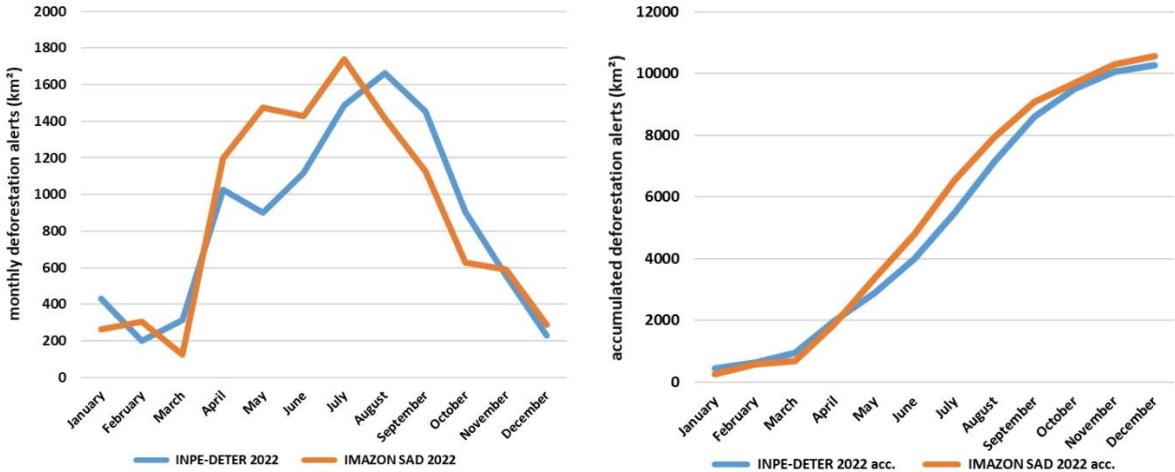
³⁷ <https://www.gov.br/mma/pt-br/alertas-de-desmatamento-na-amazonia-caem-34-no-semester>

³⁸ <https://www.gov.br/mma/pt-br/alertas-de-desmatamento-na-amazonia-caem-34-no-semester>

3.3 INPE-DETER deforestation alerts vs. AMAZON-SAD deforestation alerts 2022 and 2023 (January-October)

While INPE is a governmental agency, AMAZON, as an NGO, tracks deforestation independently of the Brazilian Government. Their deforestation tracking system has a similar scope and area of interest as INPE-DETER, but uses different data and image analyses techniques. INPE uses optical imagery with a spatial resolution of 64 m from the WFI sensor on board of the CBERS-4A satellite with a 3-day repetition rate³⁹ to detect newly deforested areas in near-real time. AMAZON uses different optical and radar satellite data (Landsat 8, Sentinel-1 and Sentinel-2)⁴⁰. Both systems report deforestation alerts on a monthly basis, while only DETER has the mandate to provide deforestation detections on a daily basis to law enforcement entities like IBAMA. For 2022, both systems report similar accumulated deforestation alert area for the Brazilian Amazon (Figure 28), as well as an acceleration of deforestation in April, which is the month where precipitation starts to get less towards the end of the rainy season. The accumulated deforested area 2022 reaches 10,278 km² according to INPE-DETER and 10,573 km² according to AMAZON-SAD. These figures constitute an increase of deforestation alert area in 2022 of 25.1% and 2.0%, respectively, compared to 2021 (Figure 28).

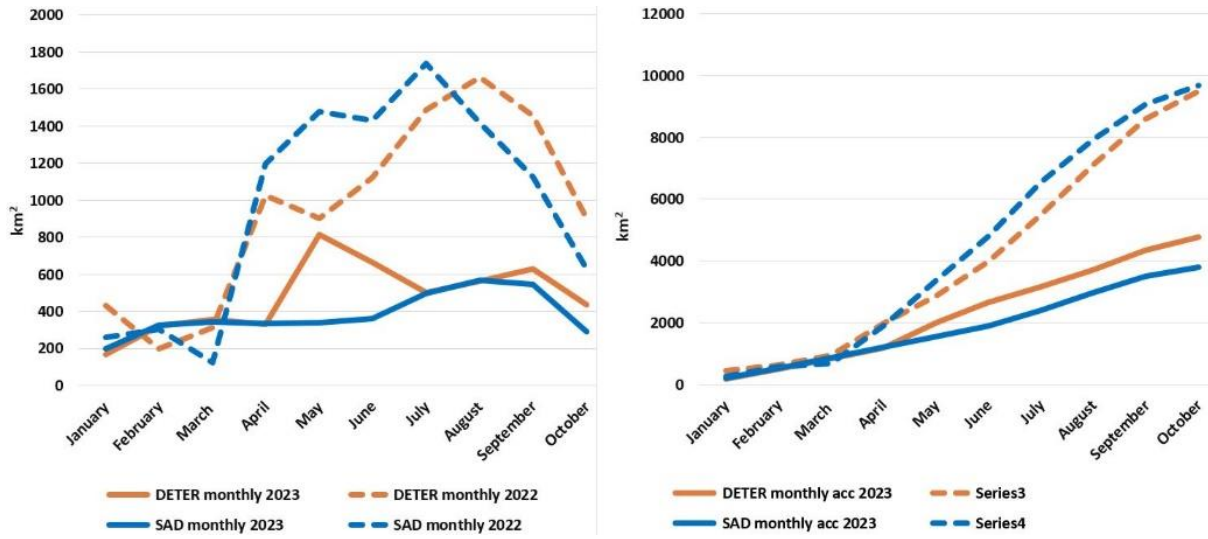
Figure 28. Monthly deforestation alerts from January – December 2022 (left), according to INPE-DETER and AMAZON-SAD, with accumulated monthly deforestation alerts of both systems (right)



Both deforestation alert systems show a deforestation decrease in the first ten months of 2023, compared to the same period of 2022 (Figure 29). While DETER reports a decrease of 49.5% (9,696 km² in 2022 vs. 4,776 km² in 2023), the SAD system shows an even more significant decrease of 60.7% (9,069 km² in 2022 vs. 3,806 km² in 2023).

³⁹ www.obt.inpe.br/OBT/assuntos/programas/amazonia/prodes/pdfs/Metodologia_Prodes_Deter_revisada.pdf
⁴⁰ <https://amazon.org.br/publicacoes/faq-sad/>

Figure 29. Monthly deforestation alerts (left) from the period January – October for year 2022 and 2023, according to INPE-DETER and IMAZON-SAD, with monthly accumulated deforestation alerts of both systems for the same period (right).



4 Deforestation and soy trade in the Brazilian Amazon

4.1 Introduction

Brazil became, in 2019, the largest soy producer in the world, ahead of the United States [41,42]. Soy is a sector of major importance for Brazil [43], accounting for 13.5% of all of its exports in 2021 [44]. This was achieved through a vast and fast expansion of the soy area in the last two decades, coupled with numerous environmental and social concerns [45]. Following the Greenpeace report "Eating up the Amazon" [46], soybean was exposed as one of the major drivers of deforestation in the Amazon. The area of soy production represented 0.2% of the Brazilian Amazon region in 1990; by 2021, the soybean area had increased to 1.9%.

This expansion has been fuelled by the soaring global demand for soy over the years. The EU is the second largest importer of soy and embedded tropical deforestation after China [47], outsourcing the environmental impact of its food consumption. Tropical deforestation is estimated to account for one sixth of the carbon footprint of a European citizen's diet [48].

In response to the concerns about deforestation, many governance arrangements directly targeting soy have been implemented, including the Amazon Soy Moratorium, private commitments, and certifications. However, deforestation in the Amazon due to soybean expansion persists [49,50].

On May, 31, 2023, the European Union adopted the new Regulation on "deforestation-free products" (Regulation (EU) 2023/1115), which covers seven commodities (soy, cattle, palm oil, cocoa, coffee, rubber and wood) and their derived products, such as leather, chocolate, tyres, or furniture. Under the regulation, the actors in the supply chain (e.g., operators or traders) must demonstrate that the products placed on the European market do not originate from recently deforested or degraded land. This is an important attempt to reconcile trade and sustainable modes of production and achieve more sustainable soy supply chains.

In this context, it is essential to understand the dynamics of soybean trade and deforestation in the high-value Amazon ecosystem, which is the objective of this chapter.

As in the rest of the report, the focus here is on the Amazon biome, although the expansion of soy is also damaging other biomes and vegetation types - for example, soybean production is recognized as a driver of deforestation and of the conversion of grasslands and rangelands in the Gran Chaco region in Argentina [51] and Paraguay [52].

It should also be noted that, although there are many countries producing soy in the Amazon, we present here data for Brazil only for reasons of data availability that are limited to this country. Brazil accounts for 60% of the Amazon biome, which also covers (partly) eight other countries, including Bolivia, where the recent expansion of soy has mainly been at the expense of forests, and this new deforestation hotspot should not be overlooked [53] ^{41,42,43}.

4.2 Background information

4.2.1 The emergence of soy in the Brazilian Amazon

Soybean was first domesticated in China 3000 years ago. For centuries it was produced and consumed mainly in China and Eastern Asia [41]. Today, the Americas dominate its

⁴¹ <https://www.globalforestwatch.org/blog/commodities/soy-production-forests-south-america/>

⁴² <https://insights.trase.earth/insights/soy-expansion-drives-deforestation-in-bolivia/>

⁴³ <https://www.theguardian.com/global-development/2023/oct/12/deforestation-in-bolivia-has-jumped-by-32-in-a-year-what-is-going-on>

production, and soy has become a global commodity, primarily processed into soybean meal to feed livestock worldwide.

Since its colonisation, Brazil's economic history has been punctuated by sugar, rubber, and coffee cycles, responding to periodic foreign demands for commodities and each linked to cycles of deforestation. Nevertheless, the current agricultural expansion exceeds anything the country has experienced before [54]. The production of Brazilian soy first occurred in the city of Santa Rosa in the state of Rio Grande do Sul, in 1914. Research began during the 1930's with the following objectives: to increase productivity and plant height, and to develop an appropriate pod height to facilitate agricultural mechanisation; to develop resistance to lodging and pest, and to increase seed quality with high oil yield and protein [55].

In the 1970s, rising soy prices incentivised more public research with the scope to increase soybean production in Brazil, especially with the creation of the EMBRAPA, the Brazilian Corporation for Agricultural and Livestock Research, and its dedicated soybean division⁴⁴. New varieties better suitable for tropical climate were developed. Until the 1970s, production was mainly concentrated in the southern states of the country (mainly Rio Grande do Sul and Paraná states). Developments of genetically modified soy and soil fertilisation allowed the expansion into central Brazil in the 1980s and 1990s [41,55]. In parallel with the expansion of the agribusiness into the Cerrado biome, the military dictatorship brought smallholders from other parts of the country to the Amazon without adequate public planning, which may have been at the root of many of the deforestation problems that have plagued the region since then [54]. The integration of the Amazon region into Brazil and its development was initially achieved through livestock farming in the 1970s. Soy, which also played a major role in deforestation, only arrived in the mid-1990s in the Amazon biome (Mato Grosso state). The production in this region intensified after the year 2000. Today, soybean from the Brazilian Amazon is still mainly produced in the state of Mato Grosso, but also in the states of Pará, Rondônia, Tocantins, Roraima and Maranhão.

4.2.2 The exposure of the EU to deforestation risk in the Brazilian Amazon through the soybean trade

The soybean development has been in response to growing international demand (80% of Brazil's production was exported in 2020⁴⁵). The publication of the TRASE database has revealed countries' exposure to the risk of deforestation for certain commodities, including soy. This database has the great advantage of being able to map the deforestation risk of countries and traders at the level of production municipalities, which is made possible by tracking supply chains. The TRASE data shows that, although the level of EU soy imports from the Brazilian Amazon has been stable (lines in Figure 30), exposure to deforestation risks from the Amazon, but also from other biomes, is declining (bars in Figure 30). Alongside the Cerrado biome, the Amazon basin is highly exposed to deforestation risks. Compared to other regions of the world, the EU's contribution to soy-related deforestation remains significant (figure 31). At the same time, China's exposure to deforestation has risen sharply, especially in 2018, when trade tensions between the US and China escalated.

In recent years an increase of the production of beef meat from the Brazilian Amazon was reported in the literature: Brazil is the second largest producer of beef meat and the largest exporter worldwide [56]. The EU is exposed to risks associated with the production of other commodities, notably livestock originating from the Amazon. In a recent study, zu Ermgassen et al. (2020) identified 73,000 to 74,700 ha/year of deforestation risk related to the export of cattle. Overall, approximately 480,000 to 520,000 ha/year of cattle-associated deforestation risk was identified [56]. Of the deforestation linked to cattle

⁴⁴ <https://www.embrapa.br/soja>

⁴⁵ <https://www.trase.earth/>

exports, between 55.0 to 56.6% came from municipalities in the Amazon; 40.7 to 43.0% in the Cerrado, and 0.1 to 0.2% in the Atlantic Forest. It should be noted that part of this deforested might be converted after a few years into soybean fields. Land is typically cleared and temporarily devoted to lower productivity uses, such as cattle rearing. In these cases, as the clearing directly benefited both the livestock and soy supply chain actors, deforestation could be attributed to both commodities. This is the approach adopted in the TRASE database.

Figure 30. Soy exports from Brazil and the Brazilian Amazon towards the EU and deforestation exposure (calculation based on TRASE data)

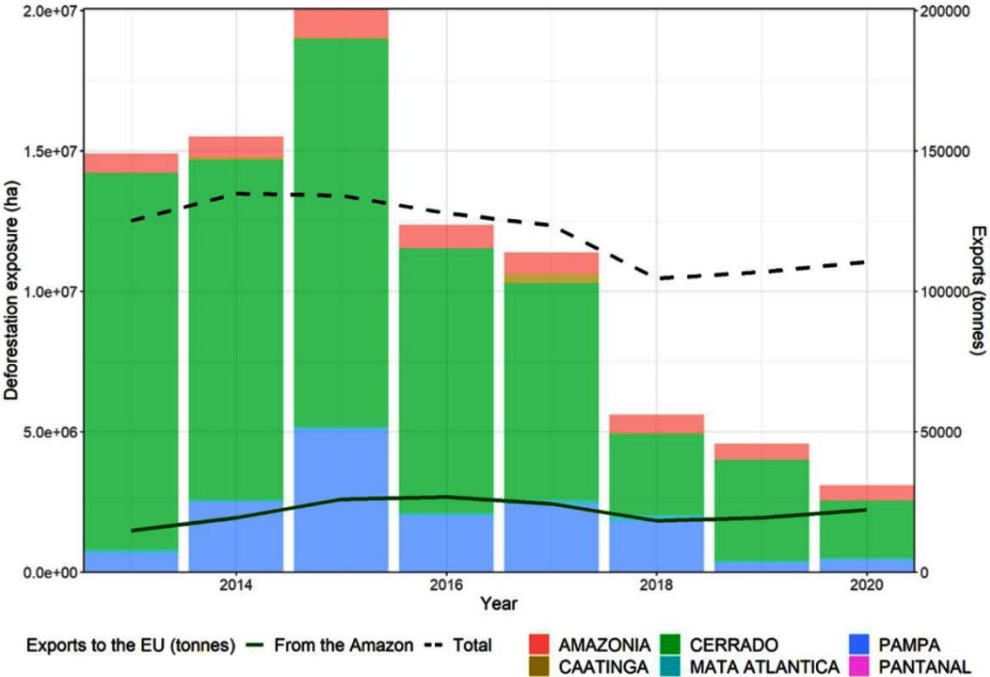
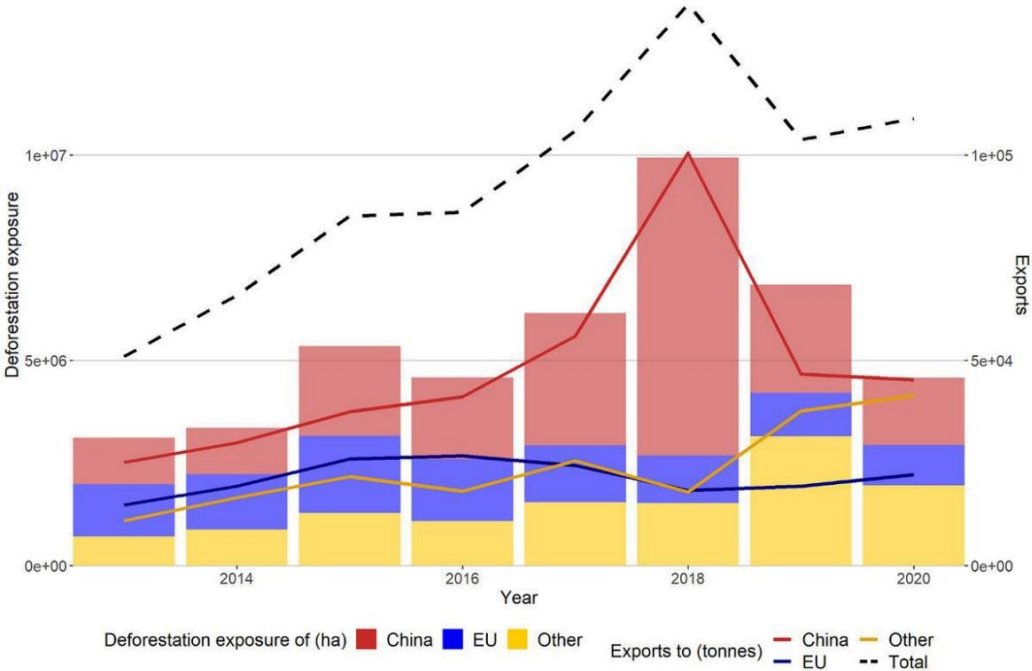


Figure 31. Soy exports and deforestation exposure in the Brazilian Amazon. Calculation based on (calculation based on TRASE data). "Other" does not include domestic consumption.



4.3 Regional patterns of expansion

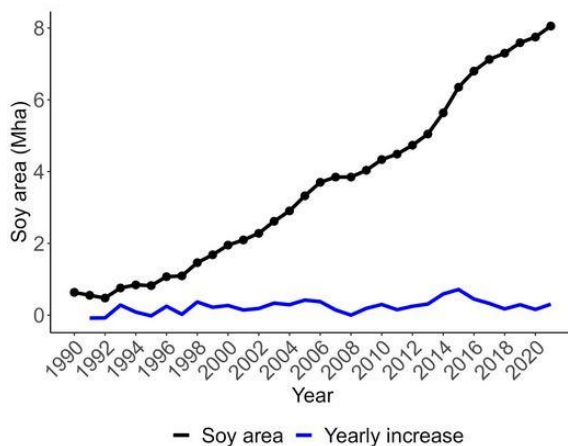
4.3.1 Methods

To analyse the dynamics of soybean expansion and deforestation in the tropical moist forest domain, annual time series (1985-2021) of soybean and pasture maps from MapBiomas [57] ⁴⁶ were combined with the JRC-TMF dataset [4] on forest cover change during period 1990-2021. Other data sources for the soybean area extent exist, including from the GLAD project [58] ⁴⁷, that uses yields consistent results. We analysed deforestation to soybean pathways (from JRC-TMF), including direct forest conversion to soybean and forest conversion to pasture followed by soybean expansion. It allows to investigate both the extent of the soybean-related deforestation in the Brazilian Amazon and its links with pasture expansion between 1990 and 2021.

4.3.2 Results

Between 1990 and 2021, the soybean area increased 11-fold in the Brazilian Amazon, reaching 85,575 km² (Figure 32), or more than twice the area of Belgium. About 53% of the soybean area comes from deforested primary forests after 1990 (calculations based on JRC-TMF and MapBiomas data).

Figure 32. Increase of the soy production area in the Brazilian Amazon



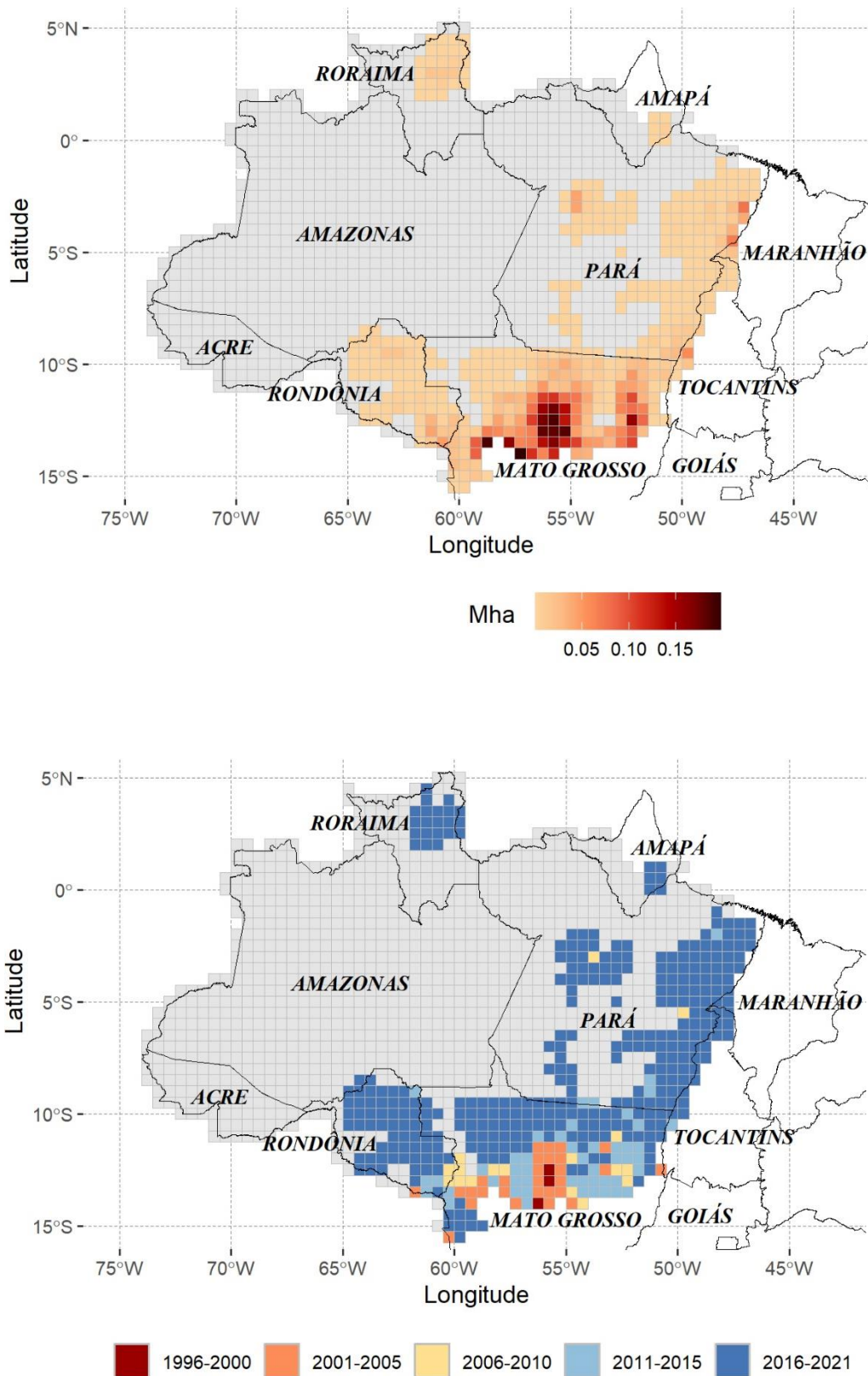
The first region for soy production is the Mato Grosso state, which accounts for 86% of the soy-cultivated lands. The second state is Para, accounting for 6.8% of the production area. The municipality of Sorriso in the North of Mato Grosso State is the largest soy producer, with 569,000 hectares of soy. Production is in fact concentrated in a few municipalities: 34 out of the 408 municipalities in the Brazilian Amazon produce 80% of the soy in the region. The location of soy-planted areas and yields depends on the development of the supply chain. These are regions with high cooperative membership and credit levels, and where cheap credit sources are more accessible [59]

The state of Mato Grosso experienced the largest increase in its area under soy, mainly in the early 2000s (see Figure 33). More recently, soybean has expanded further north into the state of Para, including along the road BR-163. Recent soy expansion has also taken place in the Roraima (RR) and Amapá (AP) states. These states have lower forest conversion costs due to a more 'savannah-like' natural vegetation, more favourable soy prices due to the shift in the growing season, and lower freight costs [60]. These regions are indeed located relatively close to the northern ports of Manaus (AM) and the port of Santana (AP).

⁴⁶ <https://amazonia.mapbiomas.org/en>

⁴⁷ <https://glad.earthengine.app/view/south-america-soybean#lon=-60;lat=-20;zoom=5>

Figure 33. Soy expansion in the Brazilian Amazon biome (*Amazonia sensu stricto* by Eva et al., 2005), soy production area (top panel) and period of maximum expansion (bottom panel) for 50 km X 50 km grid cells, based on JRC-TMF and MapBiomas data



The rapid expansion of soybean is the result of high market prices and indirect government subsidies (investments in infrastructures [61], including the complete asphaltting of the BR-163, the expansion of the Santarém port for soybeans exports, and the planned railway line for soy transport, called Ferrogrão. The pedo-climatic conditions and topography, which are crucial for mechanised agriculture, limit the expansion of soybean in some areas. Droughts, excessive rainfall, extreme temperatures, and low light affect the yields and thus determine the potential for soybean cultivation in a region [62]. However, large forest areas are still suitable for soy in the Amazon biome. It is estimated that around 46% of primary native vegetation (in 2015) is suitable for soy expansion [60]. More than half of this land is located within conservation units, settlements, indigenous lands or quilombos. The legal expansion on these lands is also limited by environmental measures such as the Soy Moratorium, the Forest code, which establishes a Legal Reserve of 80% in private properties, and by the inaccessibility of most areas. In the current soy farms of the Amazon biome, it has been estimated that only 1% (or 49,273 ha) of the soy farms have soy-suitable, forested areas that could be legally cleared [63].

The region most threatened by soy expansion is currently the MATOPIBA region (covering parts of the Brazilian States of Maranhão, Tocantins, Piauí and Bahia) in the north-eastern Cerrado [62], where there are fewer legal restrictions on deforestation. Moreover the EU regulation on "deforestation-free products" (Regulation (EU) 2023/1115) considers only forests and not other vegetation types such as other wooded land or savannah vegetation, which are the predominant vegetation types in the Cerrado biome. According to Aragão et al. (2022), it is expected that more stringent expected future regulations, e.g. the potential inclusion of other wooded land in the EU Regulation after its first review, will drive pre-emptive deforestation in the Cerrado [64].

Brazil is projected to increase its soybean production area by 12.4 million hectares by 2050, with 10.8 million hectares in the Cerrado biome [65]. However, in case of a lack of law enforcement, the deforestation risk (direct or delayed) could increase also in the Amazon region, potentially triggered by incentives like the reduction of transports costs due to new grain transport infrastructure - this on the background that large parts of the Amazon biome have potential for soy cultivation [60,63,66].

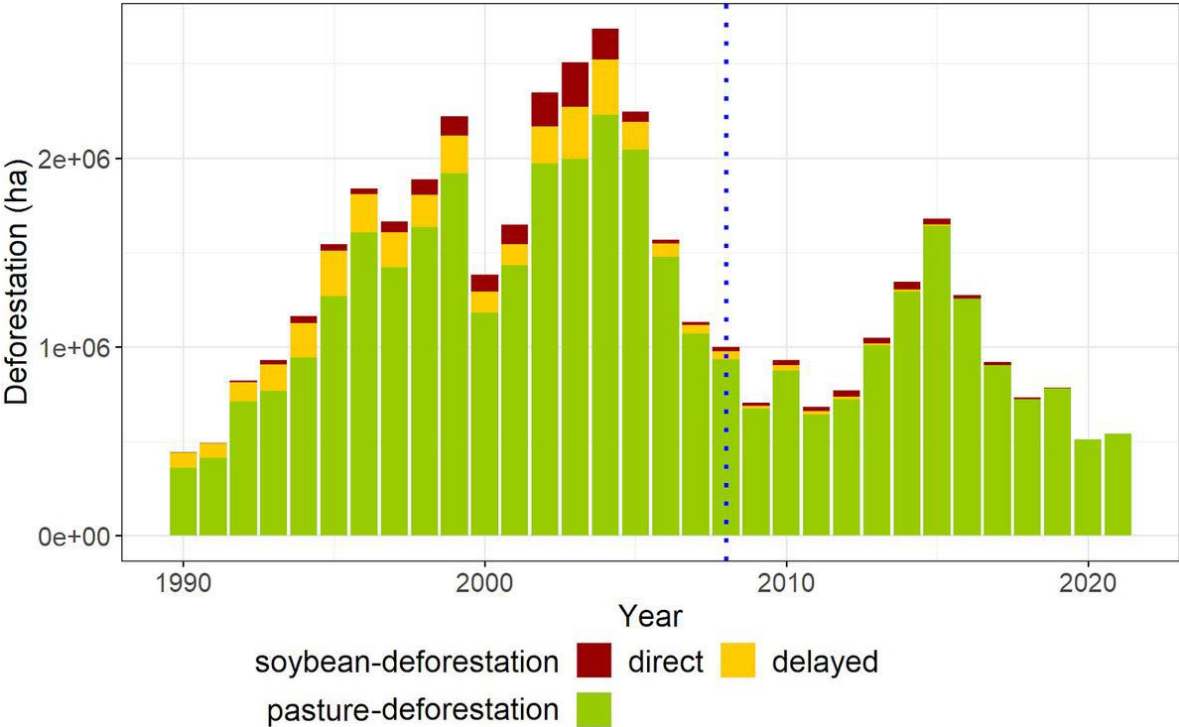
4.4 The complex task of attributing deforestation to soy production and exports

4.4.1 From deforestation to soybean: a potentially long pathway

Soybean contributed to the ongoing deforestation of the Amazon as second driver after expansion of pastureland (Figure 34). However, it is challenging to quantify precisely the contribution of the expansion of soy crop in the deforestation process. Indeed, soy is often not planted immediately after the deforestation event, but after a first period of pasture ('direct' soy deforestation versus 'delayed' soy deforestation in Figure 34), thus making it difficult to attribute with precision the cause of deforestation to pasture or soy expansion. The time lag between the deforestation event and the first year of soybean planting varies considerably across locations (Figure 35), giving geographic indication of the deforestation dynamics in the region [58].

There are several explanations for the different patterns in the time lags. Firstly, the soil may require some preparation before it is suitable for soybean plantations⁴⁸. More importantly, deforested land may be used first for livestock rearing or to secure land cleared for speculation purposes. In Song et al. (2021), the time lag between the deforestation event and the first soy plantation is used to differentiate between soy as a "direct" or "latent" driver of deforestation, using a threshold of three years to distinguish these two categories. In contrast, the TRASE database, which attributes the deforestation exposure to trading companies and exporters, chooses a time lag of five years [67]. A similar approach is used by Pendrill et al. (2019) [48].

Figure 34. Deforestation in the Brazilian Amazon from 1990 to 2021 due to soy plantation within five years (red bars), soy plantation at least five years after the deforestation event (yellow bars), and permanent pasture (green bars). The dotted blue line marks the cut-off date of the Soy Moratorium. The chart is based on JRC-TMF and MapBiomass data.



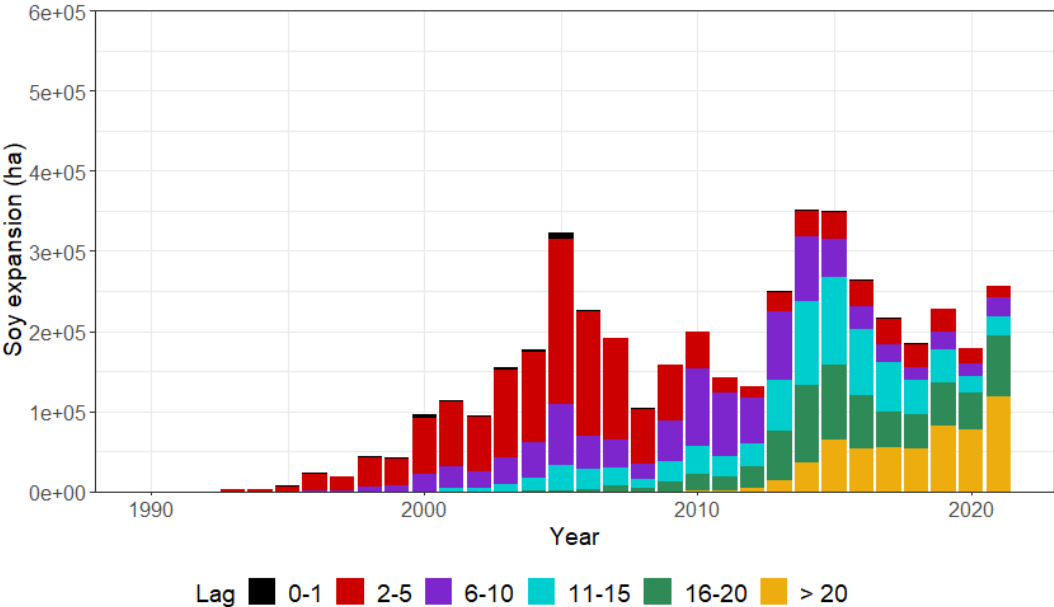
⁴⁸ <https://www.maaproject.org/2022/soy-brazilian-amazon/>

We observe that the amount of deforestation directly induced by soy increased in the beginning of the 2000s, then decreased, suggesting decoupling of deforestation for soy (directly or delayed) from deforestation to pasture (Figure 34). The accentuated expansion of soy cultivation on already cleared land, rather than on forest, from the late 2000s onwards has been interpreted as a success of environmental measures taken by the Brazilian government and the soy sector [68]. The measures include the Soy Moratorium, a sectoral agreement under which traders agree not to purchase soybean originating from land deforested after 24th July 2006 (reference date then postponed to 22nd July 2008).

The most recent five years (2018-2022) cannot be interpreted in a robust manner since we have yet to observe whether the new deforestation during this period leads to soy cultivation. For the same reason, it is difficult to draw any conclusion from soy as a latent driver. We can only observe direct transition from forest to soy up to 2021, possibly with pasture as the first land use after deforestation; longer time lags can only be detected in the future. However, soy is a quantitatively important land use that follows deforestation, even if it is much smaller than pasture. Soy can therefore be considered a main driver of deforestation in the Brazilian Amazon.

There is a variety of dynamics underlying soybean expansion (Figure 35). Some areas are converted to soy more than 20 years after deforestation, while others are converted in the year of the deforestation event. Figure 35, which represents new soybean areas broken down according to the time between deforestation and soy plantation, shows two things: 1. Despite significant inter-annual variations, high levels of land keep being converted to soy in the Brazilian Amazon. 2. Recently, the new land converted to soy has remained pasture for quite a long time. Areas deforested more than 10 years ago have contributed significantly to soybean expansion over the past decade. It supports the view that soybean expansion trajectories are decoupling from deforestation. Nevertheless, direct conversion to soy continues, in violation of the soy moratorium [49].

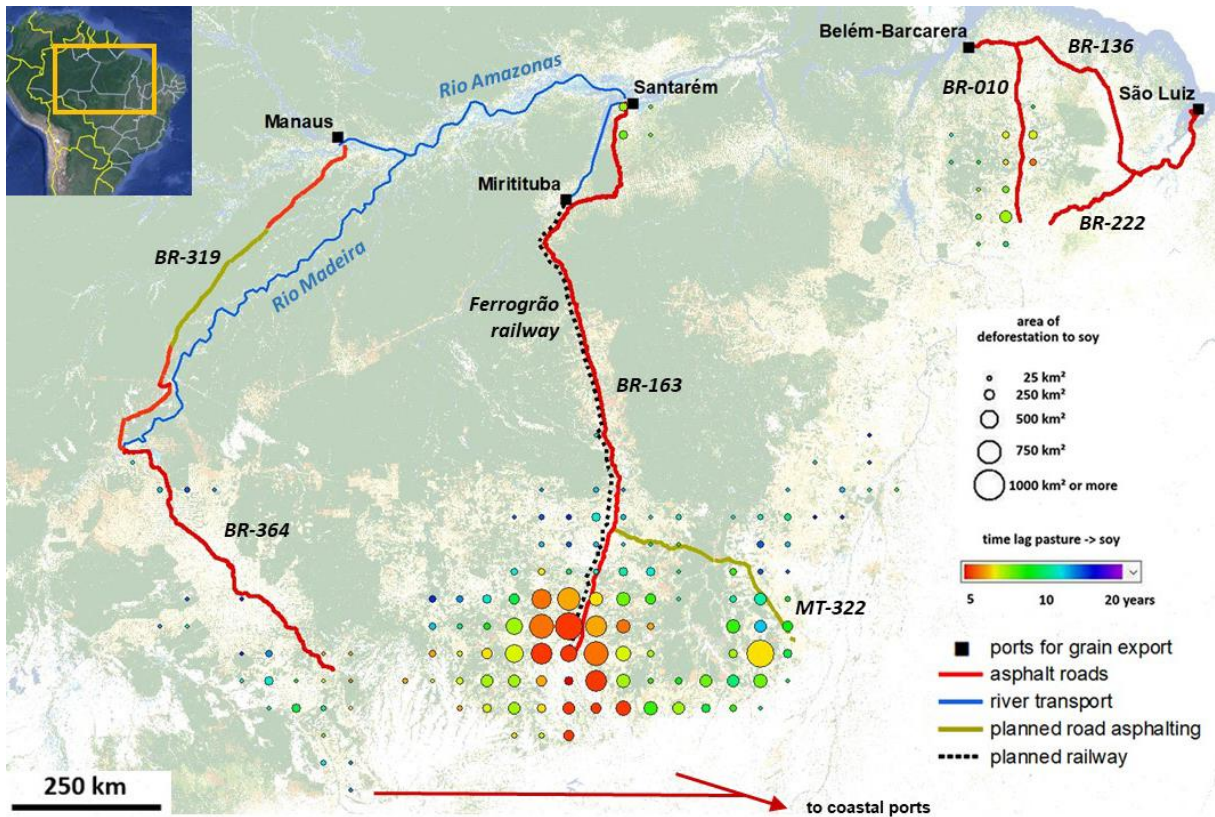
Figure 35. Soybean expansion in the Brazilian Amazon categorised in terms of time lag between the forest conversion and soybean plantation.



4.4.2 Location of soy-driven deforestation and time lags

Figure 36 shows the location and extent of deforestation between 1990 and 2020, differentiated by the average time lag between deforestation and soy plantation. The main extent of soy-driven deforestation can be observed in the south of Mato Grosso, where soy areas expanded both on recently deforested land and on old deforestation patches.

Figure 36. Relationship between the areas converted to soybean and average time lags between deforestation and soy planting within 50 km X 50 km size grid cells. Main existing grain transport network to the ports of international trade and new infrastructure projects (roads, train lines) are overlaid (road lines taken from <https://www.openstreetmap.org/>).



The average area-weighted time lags between deforestation and soy plantation, calculated within 50 km X 50 km grid cells, are shorter (four to six years) in areas of large soy fields than in areas where soy production is at smaller scale (often 10 years and more) (Figures 36 and 37). This conceals a significant heterogeneity at the landscape level, as shown in Figure 38: within the same region, old and more recent pastures are converted to soy.

Figure 37. Area of deforestation leading to soy fields vs average time lag between deforestation and soybean expansion within 50 km X 50 km grid cells (with trend line)

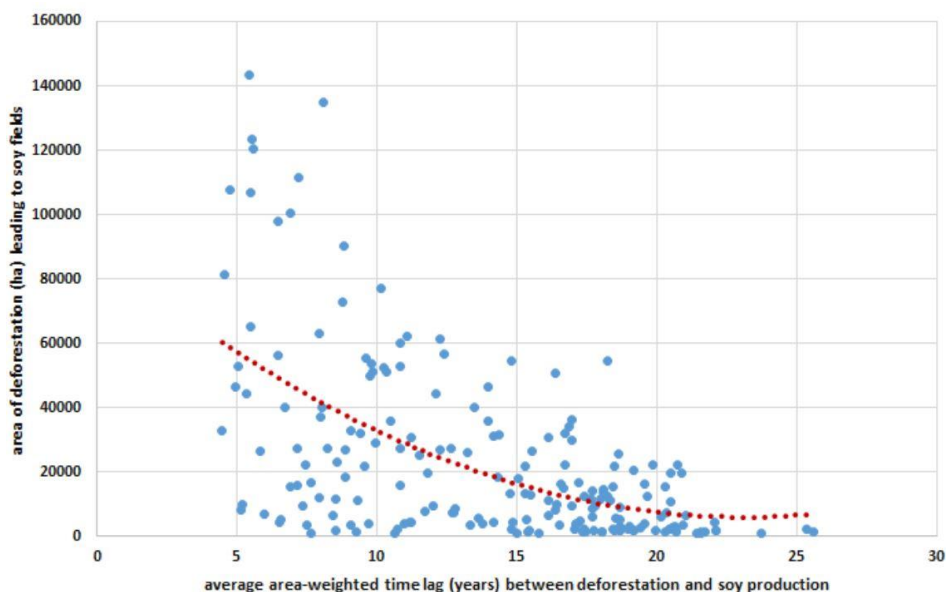
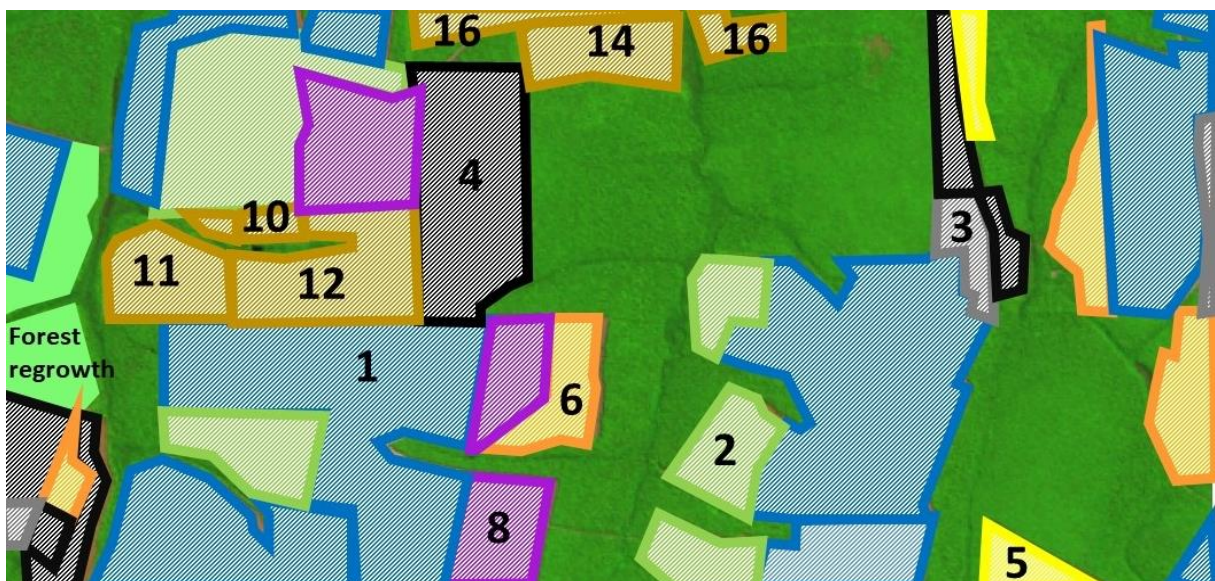


Figure 38. Top Panel: Landsat image from 2010, bottom panel: time lags (years) between deforestation and soybean expansion at the landscape-level (lon: -56.4 / lat: -12). Since 2010, the land cover patterns are unchanged, image width ca. 16 km



4.4.3 Indirect land use change

While it is clear that soybean encroaches on forests, the literature on land use change has demonstrated the existence of another effect, the indirect land use change (iLUC): mechanised agriculture encroaches on existing pastures, displacing them elsewhere to the forest frontier. Richards et al. (2014) show that in the Brazilian Amazon, between 2003 and 2008, the iLUC was large and significant [69]. They estimate that a 10% reduction in soy cultivation in former grazing areas would have reduced deforestation by 40%. The expansion of soy into grazing areas in Mato Grosso has shifted beef production to Pará, contributing to deforestation in that region [56].

4.4.4 Infrastructure and land speculation

The expansion of pastureland and soy in Latin America is closely linked to land speculation. The impact of soybean on deforestation could go beyond the direct or delayed changes in land use. Indeed, agriculture-driven deforestation goes beyond the direct expansion of commodity production into forests [70]. Forestland prices embed a speculative part related to the conversion to alternative land use [71], and the expectation of a future increase in land value is a motivation to clear forest, even though soybean is planted years after. Richards et al. (2014) state that the soybean's sector ability to influence the speculative demand for rural land is a key mechanism explaining forest loss in the Amazon [69]. Moreover, Pendrill et al. (2022) demonstrate that, globally, 90 to 99% of deforestation occurs in landscapes where agriculture is the main driver of forest cover loss, but only 45 to 65% of deforestation can be attributed to the expansion of actively managed cropland, pasture, or tree crops [70].

Land speculation and soybean expansion are also connected to infrastructure development. Agribusiness carries a significant political weight in Brazil. It prompts the government to build massive infrastructure development (railways, highways, waterways, ports), to transport crops and fertilisers. The public expenditures on projects then stimulate private investments, including land speculation, especially since a large part of the land is suitable for soybean cultivation (see section 3.2.).

In this context, the current plans to modernise transport infrastructure in the Brazilian Amazon sparked opposition among environmentalists. To overcome the poor quality of its transport infrastructure, Brazil has announced a mid-term plan to build railways for reducing transportation costs (until 2035). Within this plan, the Ferrogrão railroad (shown in Figure 6), is particularly controversial because of its potential impact on deforestation. This 1,000 km line, which will connect Sinop (Mato Grosso) to Itaituba (Pará) along the BR-163 road axis, is part of a long-standing strategy to integrate the Amazon region. The project is expected to generate major economic benefits for the region's grain producers and to increase their competitiveness. Studies [72–74] show that the new infrastructure has the potential to significantly reduce transport costs to soy-producing municipalities (by between 1% and 52%, according to [73]). At the same time, this cost reduction, as well as the synergistic and cumulative impacts generated by the changes in flows at the regional level, should have adverse effects on land use changes, by encouraging farmers and ranchers to extend their agricultural land by deforestation. The municipalities benefiting from the project will have a net deficit of native vegetation (1.3 million hectares), indicating a significant risk of further forest loss [73]. Bragança et al. (2020) estimate that the increase in deforestation should amount to 2,043 km² (conservative estimate) [74].

Another example would be the expected incentives for soy expansion in the region of Rondônia and Southern Amazonas State. While not being yet on the level of Mato Grosso soy production, Rondônia has tripled his soybean area from 2009-2019 with potentially further expansion in the future. The town of Humaitá in the South of Amazonas State (bordering Northern Rondônia) is expected to be a future big agricultural hub for the transport of soy from Rondônia to the port of Manaus, specifically after the complete paving of the BR-319 highway. This road consolidation would make transport of grain and other commodities to Manaus cheaper and more reliable than river transport or transport on an unpaved highway. The consolidated road could trigger the increase of soy production in Rondônia as well as land speculation and illegal selective logging along the highway, potentially leading to an increase of deforestation, forest degradation and violation of indigenous rights in the region [75–77]. The effects would be comparable to the road consolidation (asphalting) of the Cuiabá-Santarém Highway (BR-163) in Mato Grosso and Pará some years before [78]. These examples illustrate that infrastructure has a major role in the evolution of soy-related deforestation risk.

4.1 Towards sustainable soybean supply chains between the Brazilian Amazon and Europe

A mosaic of sustainability governance arrangements and mechanisms have been developed to reduce the pressure of soy on deforestation. These include the Amazon Soy Moratorium, voluntary certification schemes for sustainable soy, and private commitments. While it is difficult to say whether private commitments (very heterogeneous) and certifications (low adoption) have had any effect so far on soybean-driven deforestation [79], the literature is more positive about the impact of the Amazon Soy Moratorium [63,80,81]. The Amazon Soy Moratorium was successful over a decade, although it is suspected that it has been partially offset by leakages (across less regulated biomes like the Cerrado and on-properties towards other commodities) [82–84]. However in recent years, shifts in environmental political rhetoric have led to setbacks for the Amazon and other biomes [85], also for soy as there are increasing soy areas not in compliance with the Amazon Soy Moratorium [49].

The new EU legislation aims at tackling deforestation and forest degradation by ensuring that soy and beef products placed on the EU market are not generated in areas deforested after the cut-off date. By institutionalising standards, the EU regulation is expected to be a strong driver for deforestation-free supply chains, as soy producers in Brazil face demands to produce soy responsibly [54]. To effectively reduce deforestation, interventions should address the interdependencies between the expansion of different commodities [70] and between landscapes (e.g. Amazon and Cerrado biomes in the case of soy).

5 Government Policy in Brazil, related to deforestation and forest degradation in the Amazon (status end of 2022 / mid-2023)

After some years of growing international political isolation during the previous presidency, the new government has put back Brazil in a prominent role in global politics^{49,50,51}. At the same time, signs have been set for more Brazilian involvement in regional and global environmental issues⁵².

The new Brazilian president, as one of his first actions, reactivated the Amazon Fund⁵³ as a strategically important tool in order to quickly rebuild and strengthen efforts against deforestation and creating sustainable development in the Amazon region [86]. The Fund, hosted by the Brazilian Development Bank BNDS, will "significantly increase its fundamental role in supporting strategic actions necessary for the transition to a sustainable economy, with solutions based on nature and the promotion of socio-diversity and bioeconomy" [87]. The Fund had been paralysed by the previous Brazilian president, and main donors withdrew their support⁵⁴. It currently contains more than 600 million Euro, donated by Norway, Germany, and other countries⁵⁵.

Federal Environmental Institutions

The Brazilian federal institutes involved in forest monitoring, environmental protection and indigenous people's rights, namely the Brazilian National Space Research Institute (INPE), the Brazilian Institute for Environment and Renewable Natural Energy (IBAMA) and the National Foundation of Indigenous People (FUNAI) have been weakened and dismantled during the Bolsonaro presidency [88–98]^{56,57,58}, which came to an end in December 2022.

INPE is responsible *inter alia* for national forest cover change monitoring (PRODES and DETER projects). In the past eight years, INPE lost 28% of its positions for officials⁵⁹. During the Bolsonaro presidency, INPE's director, the renowned Brazilian scientist Ricardo Galvão, had been exonerated⁶⁰. In the first year of the Bolsonaro presidency, 2019, the main institution responsible for law enforcement in the Brazilian Amazon, IBAMA, lost 24% of its Inspection and Control Program budget [99]. After heavy criticism by members of the Bolsonaro government, IBAMA's Director, Suely de Araujo, resigned in the same year⁶¹. Many IBAMA state superintendents resigned or were replaced between 2019 and 2022^{62,63}.

⁴⁹<https://www.eurac.edu/en/blogs/mobile-people-and-diverse-societies/lula-s-migration-and-foreign-policy-agendas-and-the-future-of-south-american-regi>

⁵⁰<https://www.almendron.com/tribuna/the-restoration-of-brazilian-foreign-policy/>

⁵¹<https://www.dw.com/en/lula-has-high-hopes-for-post-bolsonaro-brazils-international-role/a-64661092>

⁵²<https://www.foreignaffairs.com/south-america/restoration-brazilian-foreign-policy>

⁵³<https://www.euronews.com/green/2023/01/03/lula-tells-cop27-brazil-is-back-as-he-vows-to-end-deforestation-in-the-amazon>

⁵⁴<https://www.theguardian.com/world/2022/nov/04/brazil-supreme-court-ruling-to-reactivate-amazon-fund-gives-hope-in-fight-to-save-rainforest>

⁵⁵<https://www.amazonfund.gov.br/en/home/>

⁵⁶<https://news.mongabay.com/2019/06/brazil-guts-environmental-agencies-clears-way-for-unchecked-deforestation/>

⁵⁷<https://www.science.org/content/article/brazilian-institute-head-fired-after-clashing-nation-s-president-over-deforestation>

⁵⁸<https://brazilreports.com/the-future-of-funai-part-1-brazils-indigenous-protectors-denounce-the-dismantling-of-their-institution-during-bolsonaro-government/3322/>

⁵⁹<https://g1.globo.com/sp/vale-do-paraiba-regiao/noticia/2023/02/11/inpe-tem-o-menor-quadro-de-funcionarios-em-oito-anos.ghtml>

⁶⁰<https://www.science.org/content/article/brazilian-institute-head-fired-after-clashing-nation-s-president-over-deforestation>

⁶¹<https://www.dw.com/pt-br/presidente-do-ibama-pede-exonera%C3%A7%C3%A3o/a-46988770>

⁶²<https://www.climatepolicyinitiative.org/publication/an-analysis-of-the-new-legal-framework-for-ibamas-administrative-sanctioning-procedure-and-its-effects-on-combating-deforestation-in-the-amazon/>

⁶³<https://exame.com/brasil/ministro-ricardo-salles-demite-4-superintendentes-do-ibama-no-mesmo-dia/>

The overall area of DETER deforestation alerts in the BLA more than doubled in the years 2019–2022 (36,092 km²)⁶⁴, compared to the years 2015–2018 (16,729 km²). At the same time, the number of infraction notices issued by IBAMA more than halved from almost 9,500 in 2016 to 3,500 in 2020. Despite increasing deforestation rates from 2016 to 2020, the number of administrative judgements related to environmental crime collapsed from ca. 10,000 in 2016 to almost 0 (zero) in 2020 [100].

An important step for the re-empowering of the federal institutions in 2023 was the change of the top management under the new presidency. IBAMA had been weakened during the previous government, but according to IBAMA's new president (since the beginning of 2023), Rodrigo Agostinho, "IBAMA has started to move again, after having been 'cut in half' over the past years". In the context of re-empowering IBAMA, Agostinho is not only counting on federal funds, but also on international sources like the Amazon Fund, the Inter-American Development Bank and the Global Fund for Environment, all of which have already contacted IBAMA⁶⁵. In May 2023, IBAMA has rejected the controversial request by the Brazilian state oil company Petrobras to drill for oil at the mouth of the Amazon River⁶⁶, a decision being intensely discussed in the Brazilian political circles⁶⁸.

Indigenous People

In the first days of the Lula presidency, a Ministry of Indigenous Peoples was created, with Sônia Guajajara being the first Indigenous woman to become a minister⁶⁹. Joênia Wapichana became the first indigenous president of FUNAI^{70,71,72}. At the same time, INPE's former president, Ricardo Galvão, has been appointed as head of the prestigious National Council of Scientific and Technological Development (CNPq)⁷³. However, in May 2023 the progressive policy of the new president has come under attack by the conservative-dominated Congress, which moved to severely weaken the Ministries of Environment and Indigenous Peoples. The congress approved a draft legislation that would strip the Environment Ministry of the control of the Rural Environmental Registry, a key tool in the fight against illegal deforestation, land grabbing, and water resources. The rule change would also reassign the responsibility for delimiting Indigenous Territories from the Ministry for Indigenous Peoples to the Ministry of Justice⁷⁴.

The Yanomami people in the Northern Brazilian Amazon suffer malnutrition, diseases, mercury contamination and violence [101]⁷⁵, all of which were triggered by illegal gold mining on their territory [102]⁷⁶. Taking into consideration this current and potential other, humanitarian crises caused by illegal gold mining operations, the re-vitalisation of IBAMA, as the main law enforcement organ in the Brazilian Amazon, is crucial. More than 20,000

⁶⁴ <http://terrabrasil.dpi.inpe.br/app/dashboard/alerts/legal/amazon/aggregated/>

⁶⁵ <https://www.dgabc.com.br/Noticia/3950071/ibama-quer-reduzir-desmatamento-pela-metade-no-primeiro-ano-do-governo-lula>

⁶⁶ <https://www.reuters.com/business/environment/brazil-environment-agency-rejects-petrobras-request-drill-amazon-2023-05-18/>

⁶⁷ <https://abcnews.go.com/Business/wireStory/oil-drilling-project-mouth-amazon-river-rejected-brazils-99416743>

⁶⁸ <https://www.camara.leg.br/noticias/965838-comissao-de-meio-ambiente-vai-discutir-intencao-da-petrobras-de-explorar-petroleo-na-foz-do-rio-amazonas/>

⁶⁹ <https://rwi.lu.se/news/sonia-guajajara-first-indigenous-woman-to-become-a-minister-in-brazil/>

⁷⁰ <https://www.terra.com.br/noticias/brasil/politica/rui-costa-exonera-coordenadora-da-funai-que-atuou-na-gestao-bolsonaro-e-rezou-com-padre-kelmon,452d162dfb85cc02f60484cd1c60a6f5byirhza1.html>

⁷¹ <https://www.pressenza.com/2023/02/brazil-joenia-wapichana-first-indigenous-woman-to-chair-funai-takes-office-on-friday-3/>

⁷² <https://aamazonia.com.br/servers-and-indigenous-peoples-celebrate-the-resumption-of-funai-with-joenia-wapichana-as-president/?lang=en>

⁷³ <https://g1.globo.com/ciencia/noticia/2023/01/16/demitido-do-inpe-por-bolsonaro-ricardo-galvao-e-o-novo-presidente-do-cnpq.ghtml>

⁷⁴ <https://www.theguardian.com/world/2023/may/25/brazil-congress-environment-indigenous-ministry-powers>

⁷⁵ <https://www.dw.com/pt-br/merc%C3%BArio-do-garimpo-contamina-a-natureza-por-tempo-indeterminado/a-64688777>

⁷⁶ <https://theworld.org/stories/2023-02-15/lula-declares-humanitarian-crisis-brazils-yanomami-territory-cracks-down-illegal>

illegal gold miners had been working on Yanomami Land by the end of 2022 without governmental intervention, despite various official complaints from the indigenous people. For 2023, IBAMA and FUNAI plan a joint permanent presence in the Yanomami and other indigenous areas⁷⁷. Related to the Yanomami humanitarian crisis, the former Brazilian Government is under investigation for genocide by the Brazilian Federal Court⁷⁸. However, the Yanomami are only one of many indigenous people to be affected by illegal trespassing of their lands; invaders seizing control of large areas in indigenous lands has been a common issue in the past years⁷⁹.

The bill on the time frame ('marco temporal'⁸⁰) for the demarcation of Indigenous Areas (**PL 490/2007**) is still under discussion at the Brazilian Federal Supreme Court (STF) and the National Congress. Brazil has gone back to officially approving Indigenous Areas in 2023, a practice that had been completely abandoned under the former government. With the creation of a Ministry for Indigenous People in early 2023, the PL 490/2007 is expected to lose momentum, while with the foreseen official approval (homologation) of 13 already outlined TIs ('Terras Indígenas' = Indigenous Lands), Brazil goes back to fulfil its obligation in the Federal Constitution and according to the Brazilian Law⁸¹. The homologation of TIs is a practice that had been completely abandoned under the former government. In the first five months of 2023, six TIs have been officially approved, with maximum rights for the indigenous population being granted under the Constitution^{82,83}. The first TI homologated under the new presidency was the TI Avá-Canoeiro in the State of Goiás. This particular TI had been demarcated already in 1996, but had never been officially approved since. In general, formal property rights to indigenous lands have as direct impact a decrease of violence, a positive impact on environmental and territorial protection and on other factors of indigenous welfare [103,104]. On 30th May 2023, the Brazilian Chamber of Deputies (Lower House of the National Congress) has endorsed the controversial 'marco temporal' bill^{84,85}. However, the Supreme Federal Court declared the proposed law as anti-constitutional on 20 September 2023⁸⁶.

Environmental Laws

In 2022, the Bolsonaro presidency brought forward many initiatives that were opposed to the protection of the Amazon forest, or incentives to weaken the forest's protection status through Proposed Laws (PLs) or Proposed Constitutional Amendments (PECs). For instance, it was foreseen to prohibit the creation of new Protected Areas in Mato Grosso State (**PEC 12/2022**)⁸⁷, the exclusion of the State of Mato Grosso from the Legal Amazon (**PL 337/2022**) [105]⁸⁸, or a bill that should legalize mining in indigenous lands (**PL 191/2020**). The latter, the so-called "mining bill", has been declared unconstitutional by

⁷⁷<https://www.dgabc.com.br/Noticia/3950071/ibama-quer-reduzir-desmatamento-pela-metade-no-primeiro-ano-do-governo-lula>

⁷⁸<https://www.dw.com/pt-br/stf-manda-investigar-governo-bolsonaro-por-suspeita-de-genoc%C3%ADdio/a-64565191>

⁷⁹<https://news.mongabay.com/2022/07/under-bolsonaro-policy-invaders-seize-control-of-250000-hectares-of-indigenous-lands/>

⁸⁰ <https://verfassungsblog.de/indigenous-rights-and-the-marco-temporal/>

⁸¹<https://www.jornalopcao.com.br/reportagens/brasil-volta-a-demarcar-terras-indigenas-e-da-esperancas-aos-ava-canoeiro-em-goias-469107/>

⁸²<https://www.nexojornal.com.br/grafico/2023/05/10/A-homologa%C3%A7%C3%A3o-de-terras-ind%C3%ADgenas-no-Brasil-por-governo?posicao=5>

⁸³<https://apnews.com/article/brazil-amazon-indigenous-climate-lula-95ad8bb0c9b43007470a20897001af81>

⁸⁴<https://www.camara.leg.br/noticias/967344-camara-aprova-projeto-do-marco-temporal-de-demarcacao-das-terras-indigenas>

⁸⁵<https://www.reuters.com/world/americas/indigenous-groups-protest-brazil-bill-limiting-recognition-tribal-lands-2023-05-30/>

⁸⁶<https://www.france24.com/en/americas/20230922-brazil-s-indigenous-peoples-celebrate-massive-land-rights-victory>

⁸⁷<https://www.olhardireto.com.br/noticias/exibir.asp?id=514333&edt=33¬icia=petista-apresenta-emenda-para-retirar-de-pec-a-proibicao-de-criar-novas-unidades-de-conservacao&edicao=1>

⁸⁸<https://www.olhardireto.com.br/noticias/exibir.asp?id=514369¬icia=juarez-quer-retomar-discussao-sobre-proposta-para-excluir-mato-grosso-da-amazonia-legal&edicao=2>

the Brazilian Commission of Environmental Rights on 30th January 2023^{89,90}; yet, the political discussion about the proposed law is ongoing [106]⁹¹.

The bills on 'Land Grabbing' ('PL da grilagem'), **PL 2633/2020 and PL 510/2021**, would legalise land claims in areas of 'undesigned public forest' (UPF), which contain more than half of the deforested areas in Brazilian Amazonia⁹². Passing the bills would legalise future deforestation in UPFs, in addition to a probable 'amnesty' for already illegally cleared forest. [34,107–109]. The proposed law 2633/2020 is awaiting approval in the Brazilian National Congress [34].

PL 337/2022: The proposed new law, which foresees the exclusion of Mato Grosso State from the Brazilian Legal Amazon - thus avoiding the relatively strict forest protection laws applied in the region - has not been ratified during the past presidency. However, the law proposal is still on the table and currently been discussed in the Brazilian parliament. The acceptance of the proposal appears unlikely, because the government of Mato Grosso State and the new federal government have expressed their opposition⁹³.

PEC 12/2022: The PEC foresees, amongst other issues, the prohibition of the creation of new conservation areas in Mato Grosso, proposed by the Mato Grosso State Government in 2022. However, members of the new federal government propose a change of the Amendment with the effect of suppressing the prohibition of new protected areas, including a request for a public hearing on the case^{94,95}.

PL 3729/2004 (Environmental Licensing General Law): The proposed law had been accepted by the Brazilian Chamber of Deputies in 2021 and currently awaits the adoption by the Brazilian Senate. The law would facilitate the environmental licensing with flexibilities for infrastructural works like train lines, pipelines and other types of infrastructures. While the PL's supporters see an opportunity to promote economic growth, the adversaries fear that the PL would reduce the influence of environmental institutions in the control of the works and reduce the responsibilities of the enterprises that are involved in projects that are potentially harmful to the environment^{96,97}. The proposed law is pending⁹⁸.

PL 6299/2002 ("Poison Bill"): The proposed law is awaiting the adoption by the Brazilian Senate. It foresees the approval of new pesticides by only one institution, the Ministry of Agriculture, Livestock and Food Supply, excluding thus IBAMA and the Brazilian National Health Regulatory Agency (ANVISA) from the process. ANVISA has already expressed their concern about the PL⁹⁹, which would mean that new agrochemicals are not (any more) evaluated for potential health risks. In some Brazilian regions, e.g. in Mato Grosso, contamination of population and ecosystems with pesticides is common, while monitoring,

⁸⁹ <http://genjuridico.com.br/2023/02/06/parecer-projeto-de-lei-no-191-2020/>

⁹⁰ <https://www.iabnacional.org.br/noticias/projeto-de-lei-que-permite-exploracao-de-terras-indigenas-e-rejeitado-pelo-iab>

⁹¹ <https://congressoemfoco.uol.com.br/area/congresso-nacional/deputados-ignoram-yanomami-e-articulam-por-mineracao-na-amazonia/>

⁹² <https://ipam.org.br/registre-de-desmatamento-na-amazonia-esta-ligado-a-grilagem-de-terras-publicas/>

⁹³ <https://www.olhardireto.com.br/noticias/exibir.asp?id=514369¬icia=juarez-quer-retomar-discussao-sobre-proposta-para-excluir-mato-grosso-da-amazonia-legal&edicao=2>

⁹⁴ <https://www.olhardireto.com.br/noticias/exibir.asp?id=514333&edt=33¬icia=petista-apresenta-emenda-para-retirar-de-pec-a-proibicao-de-criar-novas-unidades-de-conservacao&edicao=1>

⁹⁵ <https://www25.senado.leg.br/web/atividade/materias/-/materia/153068>

⁹⁶ <https://www.sigalei.com.br/blog/meio-ambiente-na-agenda-do-congresso-nacional>

⁹⁷ https://diariopopular.com.br/opiniao/o_resgate_ambiental_do_estado_brasileiro__428004

⁹⁸ <https://www.camara.leg.br/proposicoesWeb/fichadetramitacao?idProposicao=257161>

⁹⁹ <https://www.gov.br/anvisa/pt-br/assuntos/noticias-anvisa/2018/agrotoxicos-anvisa-e-contraria-ao-pl-6299-02>

assessment of impacts on people and environment and countermeasures are scarce [91,110,111]^{100,101,102,103}. The proposed law is pending¹⁰⁴.

MP 1154/2023 The Provisional Measure (MP) hinders Brazil's ability to control deforestation and increase threats to indigenous lands. Once implemented, it removes power from federal agencies. This affects the Ministry of Environment by moving the responsibility of the Rural Environmental Registry (CAR) and the National Water and Basic Sanitation Agency to other ministries, which are under more influence from 'ruralists' and landowners. Moreover, the Ministry of Indigenous Peoples is stripped of its power to designate new Indigenous lands. In addition, the Brazilian Institute of the Environment and Renewable Natural Resources (IBAMA) no longer has veto power over the licensing of large infrastructure projects [112]. The Chamber of Deputies approved the MP on 31 May 2023.

Infrastructure

While the Bolsonaro government had promoted (and carried out) Amazon infrastructure projects without hesitation and without thorough consideration of socio-environmental issues¹⁰⁵, the new government's position on the topics of Amazon forest protection and infrastructure is ambiguous. In a statement in late 2022, concerning e.g. the complete asphalted the BR-319 Highway from Porto Velho to Manaus, the newly elected president said that the Highway "was important for the economies of Amazonas and Rondônia States and that the consolidation (i.e. asphalted) should be finalised if the federal, state and municipal governments would commit to environmental protection of the area"¹⁰⁶, i.e. would see to the law enforcement to avoid deforestation and forest degradation in the region of the BR-319¹⁰⁷. However, it was not specified how the mentioned law enforcement should be secured – now, but also by future potentially changing governments, and if the (up to now) missing compulsory consultation of the impacted indigenous population [112]^{108,109} would take place. According to the new president of IBAMA, Rodrigo Agostinho, the concession for asphalted the BR-319 is currently under review¹¹⁰. According to Botelho et al. (2022), 41% of the Amazon forest lies within a 10 km distance of a road, while at least 86% of the extent of these roads are unofficial, i.e. are "built by loggers, goldminers, and unauthorized land settlements, starting from existing official roads." [113]¹¹¹. The widely discussed planned construction of a bridge across the Xingu River (within the Xingu Indigenous Land) [114], as part of the MT-322 Highway, has moved forward with the auctioning of the bridge construction¹¹².

¹⁰⁰https://amazonianativa.org.br/wp-content/uploads/2022/12/OPAN_RT_Monocultura-algodao-MT-versao-PT-v2.pdf

¹⁰¹ <https://contraosagrototoxicos.org/alunos-de-escola-rural-sao-intoxicados-com-agrotoxico-em-sinop/>

¹⁰²https://inhabitants-tv.org/oct2018_colonialismomolecular/E-book_Atlas_Agrot%C3%B3xico_2017_Larissa_Bombardi.pdf

¹⁰³<https://www.pan-europe.info/press-releases/2019/05/pesticide-intoxication-brazil-and-eus-double-standards>

¹⁰⁴ <https://www.camara.leg.br/proposicoesWeb/fichadetramitacao?idProposicao=46249>

¹⁰⁵<https://news.mongabay.com/2023/07/the-human-modified-landscapes-hml-and-the-brazilian-highway-network/>

¹⁰⁶ <https://amazoniareal.com.br/lula-e-a-rodovia-br-319/>

¹⁰⁷<https://amazoniareal.com.br/br-319-o-caminho-para-o-colapso-da-amazonia-e-a-violacao-dos-direitos-indigenas/>

¹⁰⁸<https://www1.folha.uol.com.br/ambiente/2022/08/indigenas-dizem-que-nao-foram-ouvidos-sobre-obras-da-br-319-que-corta-amazonia.shtml>

¹⁰⁹<https://www.theguardian.com/environment/2023/jun/05/amazon-road-ruin-highway-threatens-heart-rainforest>

¹¹⁰<https://www1.folha.uol.com.br/ambiente/2023/03/licenca-para-br-319-depende-de-estudos-diz-novo-presidente-do-ibama.shtml>

¹¹¹<https://news.mongabay.com/2022/09/road-network-spreads-arteries-of-destruction-across-41-of-brazilian-amazon/>

¹¹²<https://folha360.com.br/mato-grosso/governo-licita-projetos-para-construcao-de-129-pontes-de-concreto-em-mato-grosso/>

Figure 39. End of the asphalt (in 2019) of the BR-319 highway Manaus – Porto Velho, ca. 200 km southwest of Manaus (picture by Google Street View)



The EF-170 Ferrogrão infrastructure project, which should connect the towns of Sinop (Mato Grosso) and Miritituba (Pará) for facilitating the transport of soy across almost 1000 km northwards via train to the port of Santarém on the Amazon river, had been stopped in 2021 due to potential negative socio-environmental impacts. It was feared that the high risk of deforestation would specifically increase in areas where the new railway would significantly lower the grain transport costs to the ports of exportation on the Amazon river [73]¹¹³. In addition, the impact the train line on nearby indigenous communities and protected areas had not been evaluated throughout. Moreover, the new train line could have triggered direct and indirect deforestation by the rail construction itself and by an expected growth of the population in the settlements and towns along the line [115]. The project has reappeared on the political agenda recently, but was suspended, for the time being, by the Brazilian Supreme Federal Court (STF)¹¹⁴, which nevertheless permitted new environmental impact studies related to the project to be elaborated.

In the year 2000, the “Initiative to Integrate the Regional Infrastructure of South America” (IIRSA) was adopted by various South American countries to coordinate their infrastructure projects [116]. The projects comprise a number of roads leading to and through the mostly intact Western Amazon forest^{115,116} with little attempt to assess their cumulative impacts [117]. It needs to be seen how the different national governments in the Amazon region follow up these road projects.

Drugs, crimes and violence

Illicit drug trafficking is exacerbating and amplifying an array of other criminal economies in the Amazon Basin, including illegal land occupation, illegal logging, illegal mining, trafficking in wildlife and other crimes that affect the natural ecosystems and communities [118]. Specifically the Amazon regions of Bolivia Brazil, Colombia and Peru at the intersection of multiple forms of organized crime that are accelerating environmental devastation, with severe implications for the security, health, livelihoods and well-being of

¹¹³<https://www.climatepolicyinitiative.org/dataviz/governance-area-of-influence-and-environmental-risks-of-transport-infrastructure-investments-case-studies-in-the-state-of-para/>

¹¹⁴<https://www.reuters.com/business/environment/brazil-court-upholds-suspension-forest-reduction-ferrograo-grain-railway-2023-06-01/>

¹¹⁵ <https://maaproject.org/2022/amazon-roads/>

¹¹⁶ <https://education.nationalgeographic.org/resource/amazonian-road-decision/>

the population across the region [31,119]. The weakening of federal institutions dealing with law enforcement, environmental protection and indigenous peoples' rights in the Amazon [120] caused an expansion of criminal action. In consequence, major cities in the Brazilian Amazon recorded violence related to drug trade from 2017 onwards. Of the 30 most violent cities in Brazil, thirteen are in the Legal Amazon [121].

Activists defending the environment live a dangerous life throughout the Amazon region^{117,118}. A report published in 2021 found the highest rates of violence in municipalities with high pressure of deforestation and in highly deforested municipalities¹¹⁹. In July 2022, after the killing of the journalist Dom Philips and the indigenist Bruno Pereira, the European Parliament published a resolution related to the situation of Brazilian indigenous and environmental defenders, strongly condemning "the increasing violence, attacks and harassment against human rights and environmental defenders, indigenous peoples, minorities and journalists"¹²⁰.

¹¹⁷<https://www1.folha.uol.com.br/internacional/en/scienceandhealth/2022/09/brazil-is-the-deadliest-country-for-land-and-environment-defenders.shtml>

¹¹⁸<https://www.land-links.org/wp-content/uploads/2022/09/Environmental-Defenders-Under-Threat-Global-Lessons-from-the-Amazon-Final.pdf>

¹¹⁹ <https://forumseguranca.org.br/wp-content/uploads/2022/03/violencia-amazonica-relatorio-final-web.pdf>

¹²⁰ <https://eur-lex.europa.eu/legal-content/EN/TXT/PDF/?uri=CELEX:52022IP0292>

6 Conclusions and Outlook

In the presidential elections of October 2022, Brazil elected Luiz Ignácio Lula da Silva (Lula), who took over from Jair Bolsonaro on 1st January 2023. There was a notable increase in deforestation and forest degradation in the Amazon in Bolsonaro's last year in power.

Forest disturbances (deforestation and forest degradation) in the Pan-Amazon increased in 2022 by 14.9%, compared to 2021. However, the national statistics for moist tropical forest range from an increase of 172.9% in Ecuador to a decrease of 16.2% in Colombia, depending on factors like temperature, precipitation, but, most important, on the political will to fight deforestation, forest fires, land grabbing, illegal mining and selective logging.

The impact of the political setting related to deforestation rates can be observed at present in Brazil, where deforestation alerts, according to the Brazilian INPE-DETER system, have dropped by 49.7% in the first ten months of 2023, compared to the same period in the previous year. The newly elected Brazilian president has started to act according to his promise to reinforce environmental protection, made at the COP 27 in Egypt at the end of 2022. However, deforestation in the Cerrado biome has increased by 34.1% in the same period, while selective logging in the Brazilian Amazon, as a main driver of forest degradation, is on the highest level in 2023 since the start of the DETER system in 2016 (increase of 27.3% compared to the first ten months of 2022). This shows that the institutional re-strengthening still needs time to be fully achieved, after a longer period of dismantling of federal institutes dealing with environmental law enforcement. Open posts need to be filled, the internal structure reorganised, effective environmental laws need to be applied (rather than disregarded) or (re-) established [120,121]¹²¹.

Regarding his expressed goal towards zero deforestation by 2030^{122,123} the current Brazilian president has to deal with various obstacles. He faces a National Congress dominated by a conservative (anti-environmental) majority and the hostility towards environmental measures from the population in the most-heavily deforested parts in Amazonia [34,124].

However, there are areas on Lula's agenda, which are seen by many as at least 'problematic' regarding Amazon environmental protection¹²⁴. The Brazilian president has expressed his support for the complete asphaltting of the BR-319 highway Porto Velho – Manaus, facilitating road transport of commodities like soy, cattle and wood, as well as for the planned Ferrogrão railway, running from the soy fields of Mato Grosso to the ports on the Amazon River (see chapters 4 and 5). Road asphaltting in the Amazon can facilitate the migration of actors and processes from Brazil's notorious 'arc of deforestation' to most of what remains of intact Brazil's Amazon forest [125], especially if law enforcement is not secured. The Ferrogrão railway could give incentives for further expansion of soy cultivation (potentially causing direct or delayed deforestation), due to more competitive grain transport prices at international level [126]. The new Brazilian President supports gas and oil extraction in the western Brazilian Amazon and at the estuary of the Amazon River [125,127]¹²⁵, in addition, he is in favour of building a large number of hydropower dams in the Amazon region [125]. Both types of infrastructure can bring economic incentives for the region, but they will potentially have irreversible negative impacts on forests, the aquatic environment and indigenous people [128–132].

¹²¹<https://www.brasildefato.com.br/2023/02/25/o-ibama-voltou-a-trabalhar-diz-rodriago-agostinho-novo-presidente-do-orgao>

¹²²<https://www.politico.com/news/2023/06/06/brazils-lula-lays-out-plan-to-halt-amazon-deforestation-00100342>

¹²³<https://www.newscientist.com/article/2347429-cop27-brazils-lula-promises-zero-deforestation-in-the-amazon-by-2030/>

¹²⁴<https://english.elpais.com/international/2023-05-07/brazils-amazon-megaprojects-threaten-lulas-green-ambitions.html>

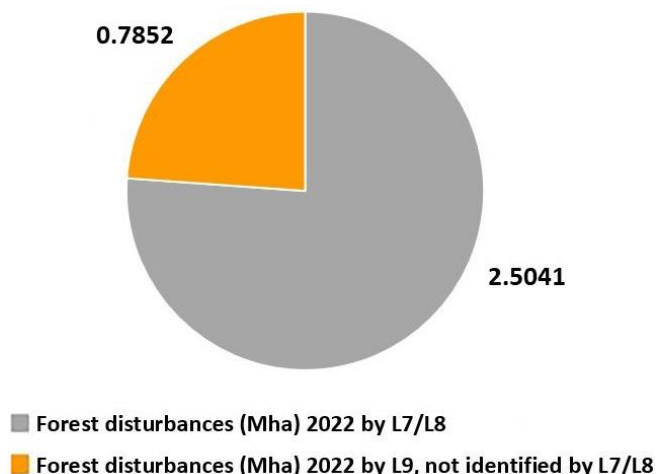
¹²⁵<https://www.gov.br/ibama/pt-br/assuntos/noticias/2023/ibama-nega-licenca-de-perfuracao-na-bacia-da-foz-do-amazonas/parecer-coexp-fza-59.pdf>

7 Annex 1: Impacts of using enhanced satellite imagery for year 2022 in TMF results

7.1 Addition of imagery of the new Landsat-9 satellite for year 2022 in the JRC-TMF processing chain

On 27 September 2021, the Landsat 9 satellite was launched to ensure the continuity of the Landsat mission [133]¹²⁶. The first Landsat 9 images from October 31st were made available by USGS in November 2021¹²⁷. In consequence, imagery of three Landsat satellites were available for the JRC-TMF 2022 analysis, rather than, as for the previous years, only from Landsat 7 and 8. Each Landsat satellite acquires 22 images per year (16-day repeat cycles). In consequence, the usage of data from three satellites add 50% of observations to a Landsat 7/8 combination. The increase in imagery allows observations at higher temporal resolution, which, especially in the humid tropics, increases the chance to get imagery with reduced or no cloud cover.

Figure 40: Comparison of mapped forest disturbance area 2022 (Pan-Amazon) with Landsat 9 and Landsat7/8 imagery



We tested the effect of adding new Landsat 9 data to the JRC-TMF processing chain over the Pan-Amazon region for the year 2022 through a comparison with the processing of year 2022 without the new sensor's imagery. Using all three sensors in the processing chain resulted in an increase of the overall forest disturbance area (i.e. both deforestation and forest degradation) of 0.79 Mha (or 31.4%) compared to the use of Landsat 7 and 8 only (see Figure 40). This underlines the importance to use the complementarity of the two datasets (i.e. Landsat 7/8 and Landsat 9) for mapping tropical moist forest disturbances in a more exhaustive manner.

According to a preliminary analysis of JRC-TMF results for 2022, the additional forest disturbances mapped through addition of Landsat 9 imagery in the processing chain concerns mostly forest degradation rather than deforestation (with a proportion of 91.5%).

The addition of Landsat 9 data should thus not have a significant effect on the detection of deforestation, whereas for the trend in forest degradation between 2021 and 2022 this additional detection effect should be considered.

¹²⁶ <https://www.usgs.gov/landsat-missions/landsat-9>

¹²⁷ <https://www.nasa.gov/press-release/nasa-usgs-release-first-landsat-9-images>

7.2 Using 'Collection-2' rather than 'Collection-1' Landsat imagery

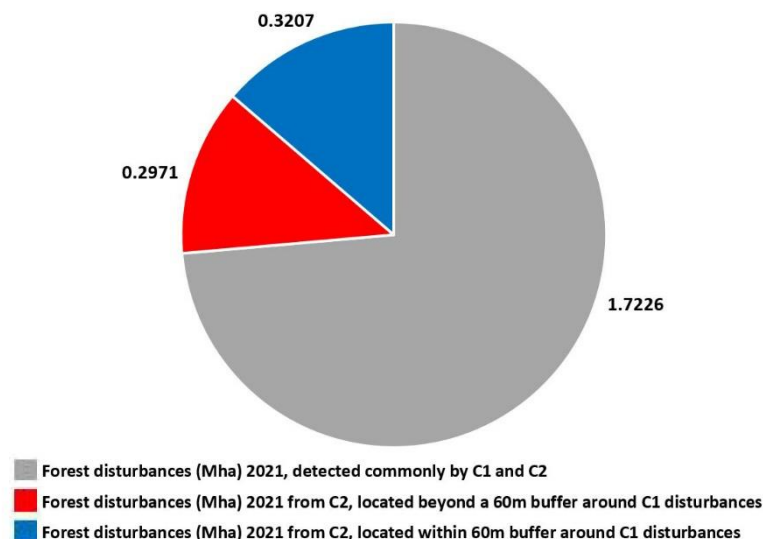
According to the United States Geological Survey (USGS), the initial Landsat Collection ('Collection-1') from 1984 – 2022 underwent in the past months "the second major reprocessing effort on the Landsat archive", resulting in 'Collection-2' imagery¹²⁸. This work was designed, amongst other issues, to improve the geometric accuracy of the imagery, to improve the digital elevation modelling, to improve the radiometric calibration and to deliver the data in optimised file format for cloud processing. While many satellite scenes had been excluded from the 'workable archive' (i.e. in Landsat Collection-1) by USGS due to their low quality, a fair number of them have now been added to the Collection-2 imagery. For the Pan-Amazon region, this resulted in a 20% increase of 'valid observations' for the analysis of 2021 imagery.

JRC-TMF processing of year 2022 was already made with Landsat Collection-2 (C2) imagery, however, the TMF statistics of the years before (2021 and before) had been based on Landsat Collection-1 (C1). Consequently, the concern is a potential bias, until the TMF data is fully reprocessed with historical C2 data (1990-2021). The reprocessing and integration of the resulting yearly forest cover change maps into the TMF dataset will be achieved by the end of 2023.

To evaluate the impact of using the C2 archive instead of C1, we processed JRC-TMF data for year 2021 separately from C1 and C2 imagery. For year 2021 and at the pan-tropical level, we quantified an increase of 13% in the detection of forest disturbances (new degradation or deforestation) from C2, compared to C1. Moreover, 66% of forest disturbances detected from C2 are also detected by C1, while 18% are within 60m (~ 2 Landsat size pixels) from forest disturbances detected by C1, most probably due to the increased geometric accuracy in C2 data. Finally, 16% of C2 forest disturbances are located beyond this buffer areas, most probably due to the increased number of Landsat observations.

For the Pan-Amazon, the increase (ca. 0.297 Mha) of mapped forest disturbances (i.e. deforestation and forest degradation) using the Landsat C2 collection is 6.9% (i.e. lower than the 13% at pan-tropical level). The increase of mapped forest disturbances in C2 imagery within a 60 m buffer of the C1 disturbances (ca. 0.321 Mha) are explained by poor image geometry of C1 (shifted pixels), are thus considered as artefacts from the use of C2 and hence not counted as 'real increase'.

Figure 41: Comparison of forest disturbance mapping with Landsat Collection-1 vs. Collection-2, based on the JRC-TMF forest cover change mapping during year 2021 for the Pan-Amazon

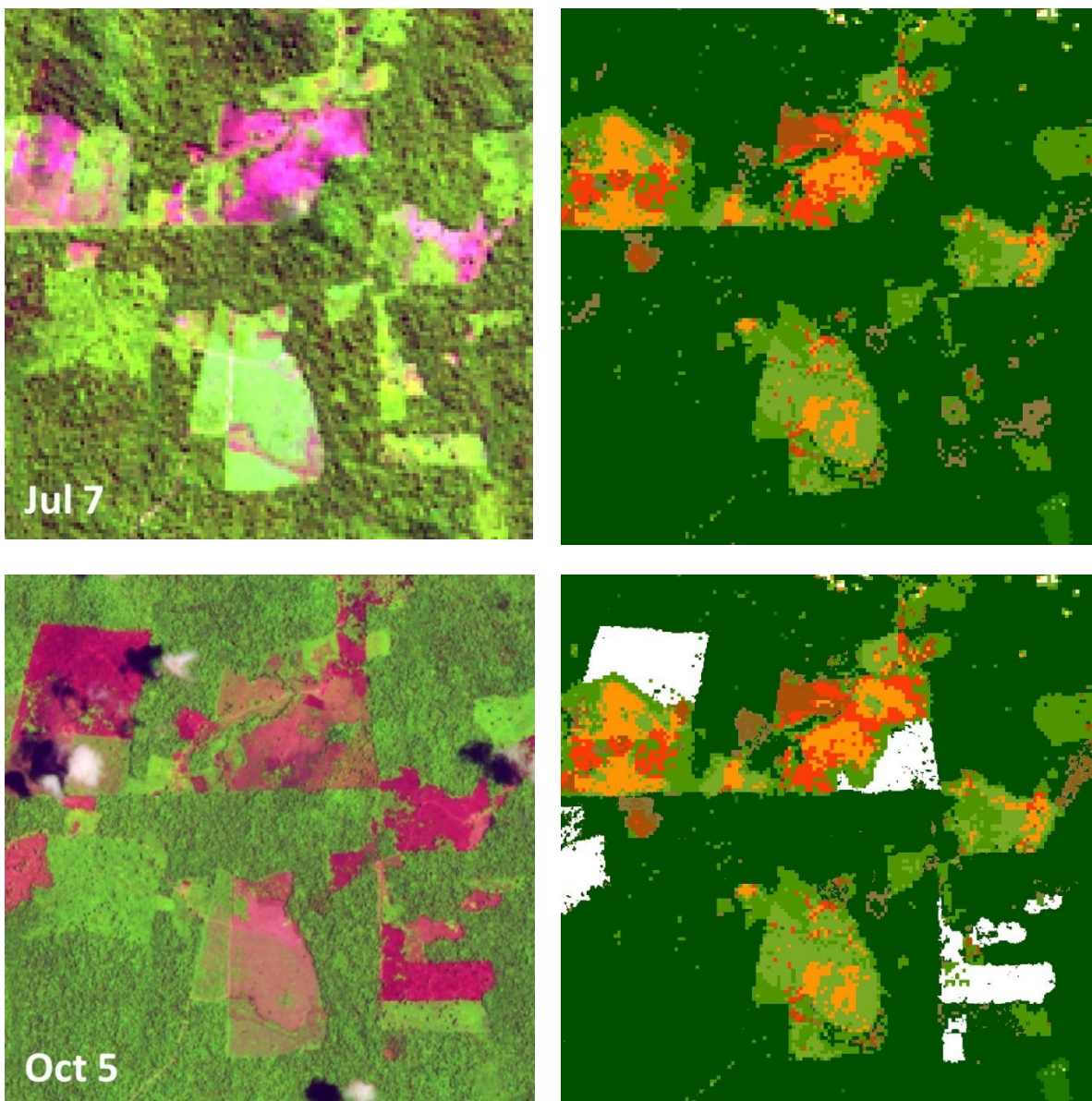


¹²⁸ <https://www.usgs.gov/landsat-missions/landsat-collection-2>

7.3 Combined use of Landsat and Sentinel-2 satellite data to create a hybrid map of forest disturbances for 2022 at 10 m spatial resolution

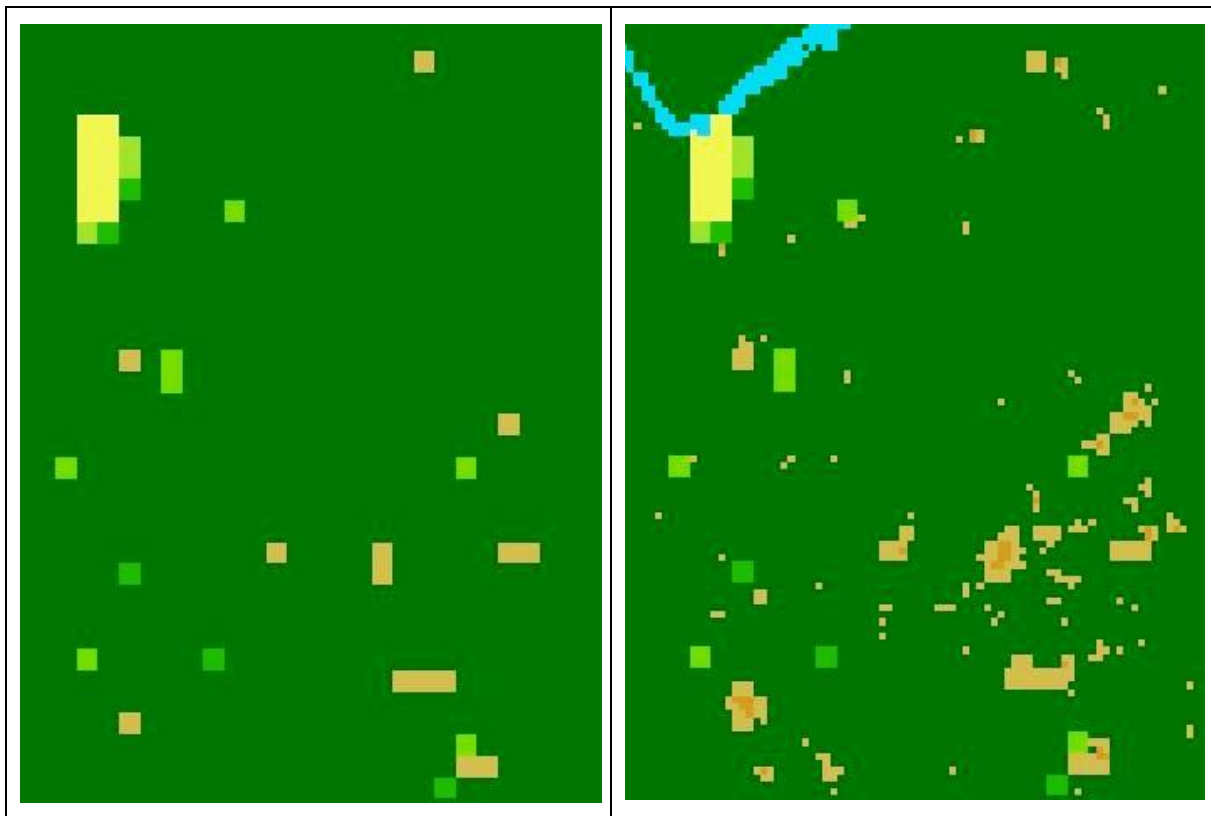
The hybrid transition map combines the updated transition map derived from Landsat images at 30m spatial resolution for the period 1990-2022, with the detections of forest disturbances by Sentinel-2 at 10m for the year 2022. It captures the sequential dynamics of forest disturbances from the first year of the monitoring period to the end of 2022 at 30 m spatial resolution from Landsat imagery. The integration of Sentinel-2 data allows a better identification of degraded forests at 10 m spatial resolution, and a refinement of the disturbance edges and linear disturbances, such as logging roads and small rivers within the forest (Figure 43). In addition, it allows for a more timely detection of deforestation areas, specifically at the beginning of the Amazon rainy season (October-November for the Southern Amazon), due to the overall increase of observations (Figure 42).

Figure 42: Comparison between Landsat-based TMF map (top right panel) and new hybrid Landsat - Sentinel-2 map (bottom right panel), with additional deforestation area mapped (displayed in white) due to additional availability of cloud-free Sentinel-2 imagery. Dates of last cloud-free observation 2022 of Landsat 8 (top left panel) and S2 (bottom left panel) are indicated on satellite images. Image width: ca. 5 km



The hybrid JRC-TMF transition map is still in a prototype phase, it will be consolidated once the back-processing of the whole Sentinel-2 archive (2016-2021), notably the improvement of the geometric accuracy, will be completed by the European Space Agency (ESA) – expected by end of year 2023.

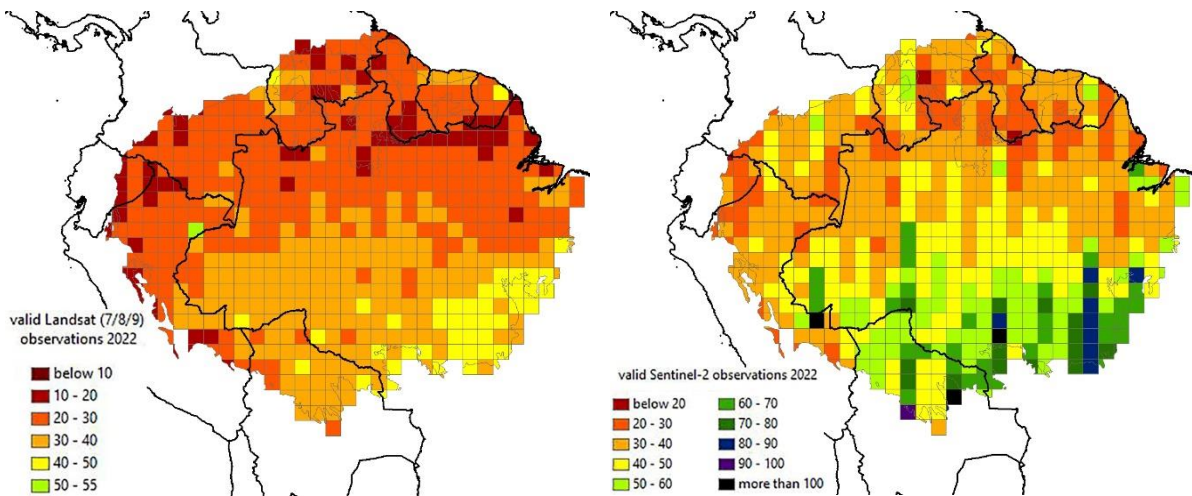
Figure 43: Comparison between Landsat-based TMF map (left panel) and the hybrid Landsat – Sentinel-2 map (right panel), with more detection of selective logging (light brown) and smaller rivers (blue) due to higher spatial resolution of Sentinel-2 imagery. Image width: ca. 700 m



In average, Landsat imagery (i.e. all Landsat 7/8/9 sensors combined) had 28.7 valid observations (VOs), i.e. without clouds, haze, sensor artifacts and geolocation issues, for each pixel in the Pan-Amazon in 2022. Sentinel-2 imagery provided an average of 42.3 valid observations per pixel in the same year, adding up to an overall number of (average) hybrid VOs per pixel of 71 (increase of 147.4% of VOs by adding Sentinel-2 into the TMF process).

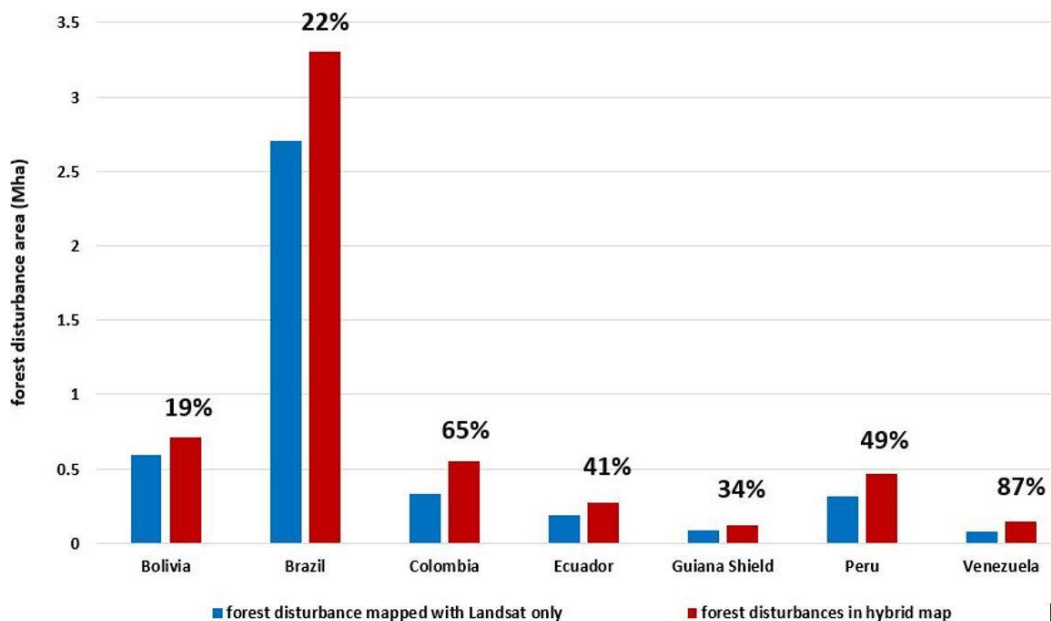
The average VOs per grid cell of both satellites are not equally distributed [134,135]. Landsat data as well as Sentinel-2 imagery show a gradient from North to South (/Southeast) with higher numbers of VOs the further South (/Southeast) the grid cells are located. This is due to higher cloud cover in the North and West of the Amazon and the clearly defined dry season in the Southeastern Amazon, roughly lasting from May/June to September/October.

Figure 44: Average number of valid observations (VOs) per pixel for 250 km x 250 km grid cells in the Amazon region. Left: Landsat 7/8/9, right: Sentinel-2



Higher spatial resolution and the availability of more imagery (with large regional differences) increase the possibility of forest disturbance detection from satellite. In total, forest disturbances 2022 in the Pan-Amazon in the hybrid map are ca. 22.7% above the areas of forest disturbance only mapped with Landsat imagery. Figure 45 shows the country-specific increase of forest disturbance detection in the hybrid map.

Figure 45: Moist forest disturbances 2022 mapped with a hybrid approach (Landsat, Sentinel-2), compared to the mapped forest disturbances with Landsat only. Surplus of the hybrid map is indicated as percentage

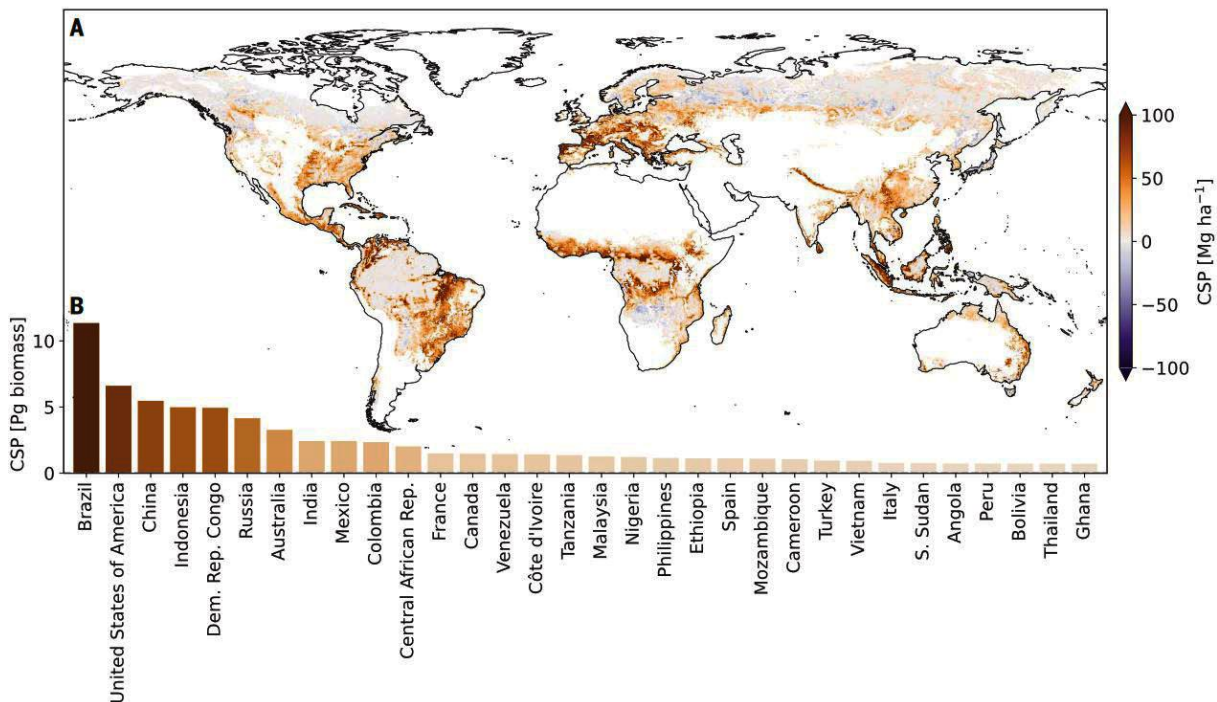


8 Annex 2: New research on forests, deforestation, forest degradation and regrowth in the Amazon (status July 2023)

8.1.1 Forest

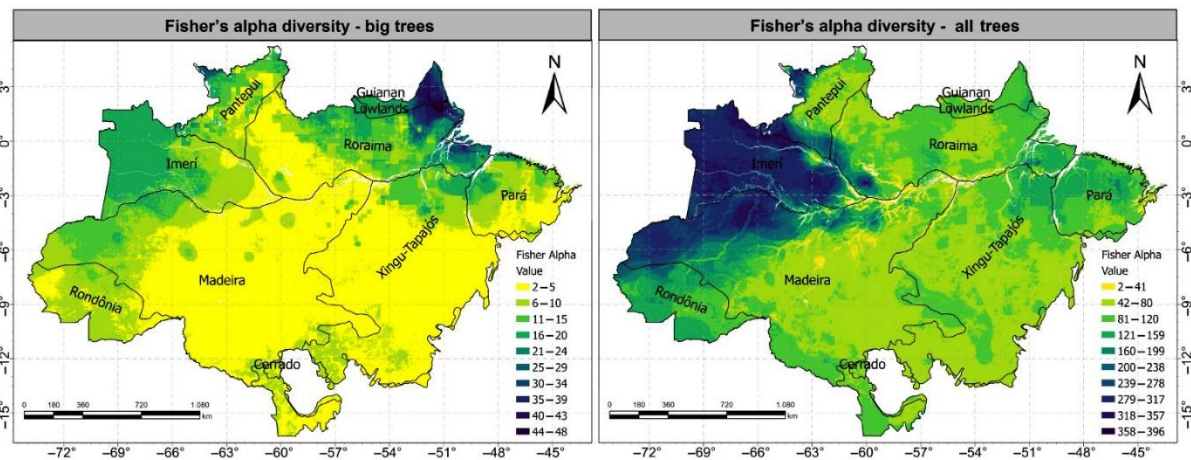
Roebroek et al. (2023) analyse how much carbon could be stored in global forests if they would be released from human management. The authors state that carbon storage in forests would be a cornerstone of policy-making to prevent global warming from exceeding 1.5°C. However, the global impact of management (for example, harvesting) on the carbon budget of forests remains poorly quantified. They integrated global maps of forest biomass and management with machine learning to show that by removing human intervention, under current climatic conditions and carbon dioxide (CO₂) concentration, existing global forests could increase their aboveground biomass by up to 44.1 (error range: 21.0 to 63.0) petagrams of carbon. This is an increase of 15 to 16% over current levels, equating to about 4 years of current anthropogenic CO₂ emissions. Therefore, without strong reductions in emissions, this strategy holds low mitigation potential, and the forest sink should be preserved to offset residual carbon emissions rather than to compensate for present emissions levels [136].

Figure 46: Additional carbon storage potential. (A) Additional carbon storage potential (CSP) in the hypothetical scenario in which all forests would resettle in their natural equilibrium if all direct human management was removed from them. The CSP is calculated from the difference between biomass carrying capacity and the expected biomass (the biomass that would occur under local conditions with the given natural disturbance regime and average intensity of human intervention). (B) National statistics of additional CSP for countries where absolute values exceed 0.7 Pg biomass [136].



De Lima et al. (2023) examine how environmental variation drive the diversity patterns of large trees in the Amazon. For more than three decades, major efforts in sampling and analyzing tree diversity in South America have focused almost exclusively on trees with stems of at least 10 and 2.5 cm diameter, showing highest species diversity in the wetter western and northern Amazon forests. By contrast, little attention has been paid to patterns and drivers of diversity in the largest canopy and emergent trees, which is surprising, given these have dominant ecological functions. The authors use a machine learning approach to quantify the importance of environmental factors and apply it to generate spatial predictions of the species diversity of all trees (dbh \geq 10 cm) and for very large trees (dbh \geq 70 cm) using data from 243 forest plots (108,450 trees and 2832 species) distributed across different forest types and biogeographic regions of the Brazilian Amazon. The diversity of large trees and of all trees was significantly associated with three environmental factors, but in contrasting ways across regions and forest types. Environmental variables associated with disturbances, for example, the lightning flash rate and wind speed, as well as the fraction of photosynthetically active radiation, tend to govern the diversity of large trees. Upland rainforests in the Guiana Shield and Roraima regions had a high diversity of large trees. By contrast, variables associated with resources tend to govern tree diversity in general. Places such as the province of Imeri and the northern portion of the province of Madeira stand out for their high diversity of species in general. Climatic and topographic stability and functional adaptation mechanisms promote ideal conditions for species diversity. Finally, we mapped general patterns of tree species diversity in the Brazilian Amazon, which differ substantially depending on size class [137].

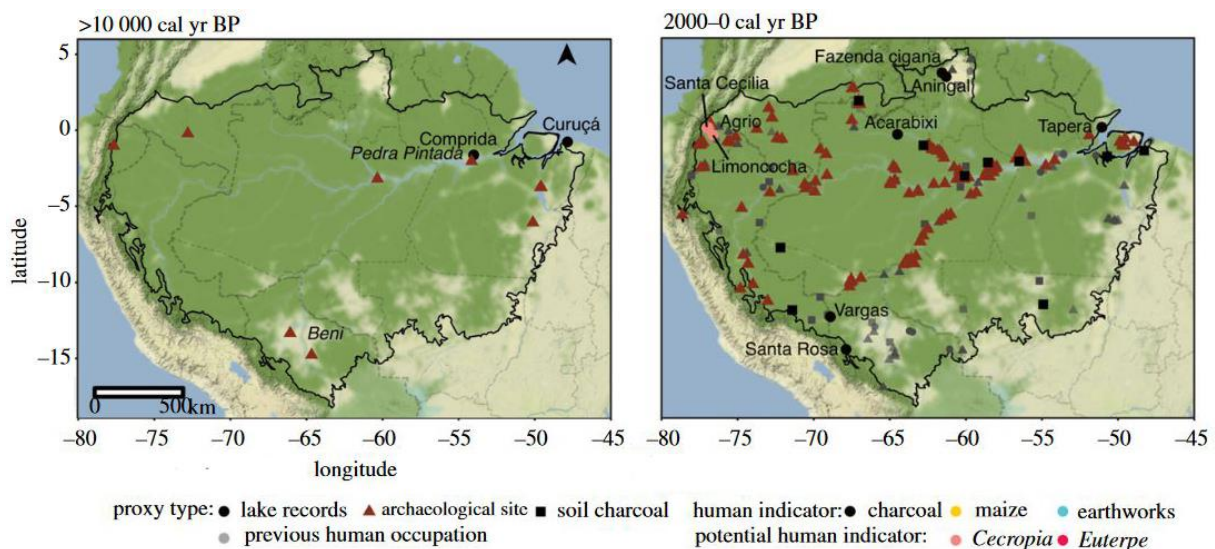
Figure 47: Fisher's alpha-diversity distribution for large trees (dbh \geq 70 cm) and diversity distribution considering all trees (dbh \geq 10 cm) estimated by the RF model for the Brazilian Amazon [137].



Nascimento et al. (2022) explore how human activity in the mid-Holocene exerted gradual influence on Amazonian forest vegetation. Humans have been present in Amazonia throughout the Holocene, with the earliest archaeological sites dating to 12 000 years ago. The earliest inhabitants began managing landscapes through fire and plant domestication, but the total extent of vegetation modification remains relatively unknown. The authors compile palaeoecological records from lake sediments containing charcoal and from pollen analyses to understand how human land-use affected vegetation during the early to mid-Holocene, and place their results in the context of previous archaeological work. They identified gradual, rather than abrupt changes in forest openness, disturbance and enrichment, with useful species at almost all sites. Early human occupations occurred in peripheral sites of Amazonia, where natural fires are part of the vegetation dynamics, so human-made fires did not exert a novel form of disturbance. Synchronicity between

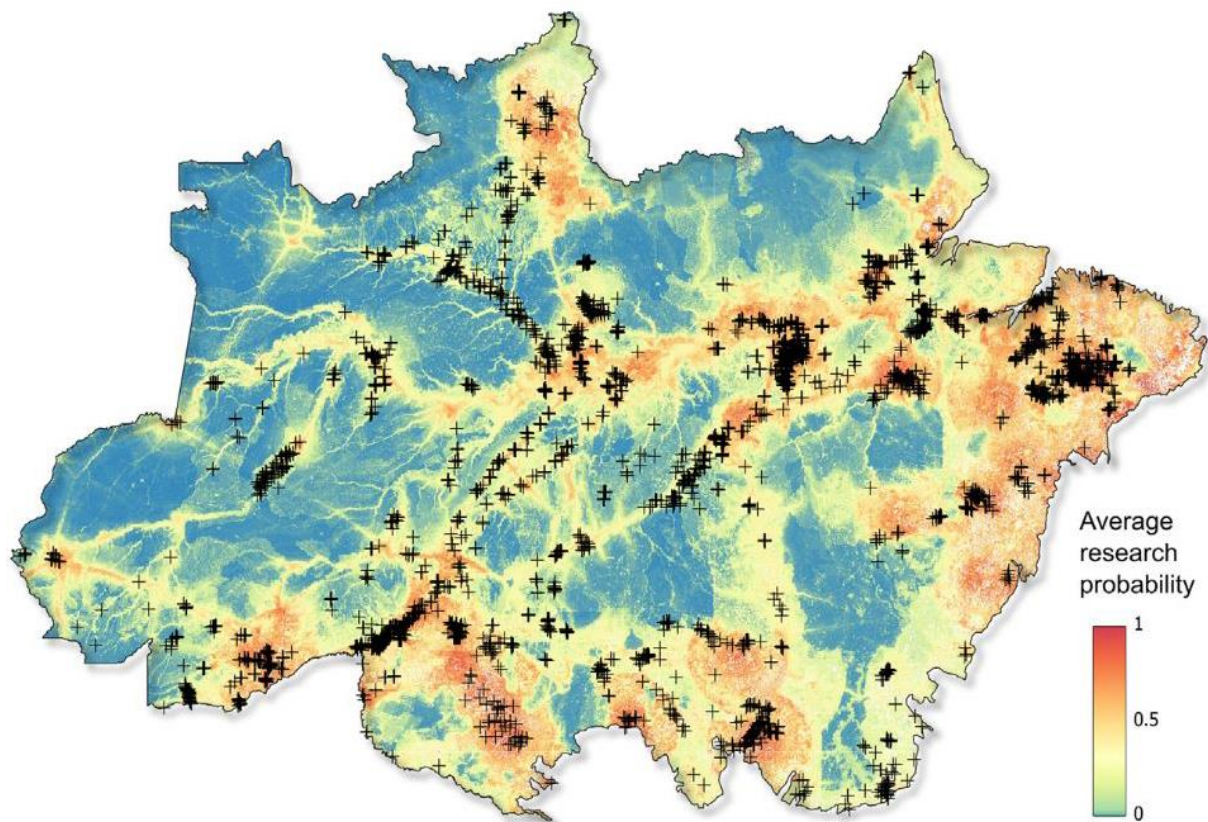
evidence of the onset of human occupation in lake records and archaeological sites was found for eastern Amazonia. For southwestern and western Amazonia and the Guiana Shield, the timing of the onset of human occupation differed by thousands of years between lake records and archaeological sites. Plant cultivation showed a different spatio-temporal pattern, appearing ca 2000 years earlier in western Amazonia than in other regions. Our findings highlight the spatial-temporal heterogeneity of Amazonia and indicate that the region cannot be treated as one entity when assessing ecological or cultural history [138].

Figure 48. Map of the distributions of the earliest dated evidence of human occupation (based on lake sediment (circles), soil charcoal (squares) and archaeological records (triangles) plotted in 2000-year time bins from before 10 000 cal yr BP until present (here only the earliest and most recent time bins are shown). Phytolith soil records from archaeological sites are shown as archaeological sites (triangles). Circle colours indicate the proxy used by the original author to indicate the onset of humans, and symbols in grey indicate sites where the earliest evidence of human occupation happened on an earlier panel. Black line represents the Amazonia *sensu stricto* boundary [138].



Carvalho et al. (2023) look at how accessibility and the proximity to research facilities influences Brazilian Amazon research probability. While the increasing availability of global databases on ecological communities has advanced our knowledge of biodiversity sensitivity to environmental changes, vast areas of the tropics remain understudied. In the American tropics, Amazonia stands out as the world's most diverse rainforest and the primary source of Neotropical biodiversity, but it remains among the least known forests in America and is often underrepresented in biodiversity databases. To worsen this situation, human-induced modifications may eliminate pieces of the Amazon's biodiversity puzzle before we can use them to understand how ecological communities are responding. To increase generalization and applicability of biodiversity knowledge, it is thus crucial to reduce biases in ecological research, particularly in regions projected to face the most pronounced environmental changes. The authors integrate ecological community metadata of 7,694 sampling sites for multiple organism groups in a machine learning model framework to map the research probability across the Brazilian Amazonia, while identifying the region's vulnerability to environmental change. 15%–18% of the most neglected areas in ecological research are expected to experience severe climate or land use changes by 2050. This means that unless we take immediate action, we will not be able to establish their current status, much less monitor how it is changing and what is being lost [139].

Figure 49 The map represents the average research probability across all organism groups and habitat types, i.e. aquatic, wetlands and uplands research probabilities [139].

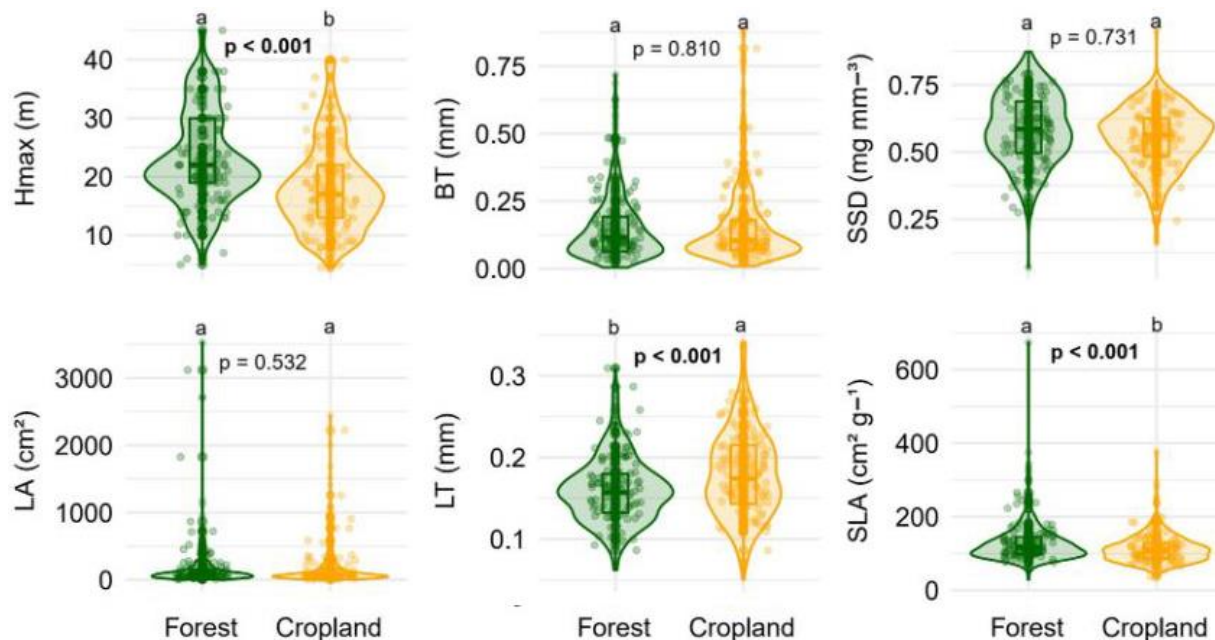


Delaroche et al. (2022) look at how different Brazilian vegetation maps, specifically on the Amazon–Cerrado border, result in an ambiguous forest protection status in areas of transition. The way vegetation is officially named, classified, and identified has critical implications for ecosystems and biodiversity conservation. Yet little attention is given to how such issues hinder the efficacy of laws mandating environmental conservation on private land. In the Brazilian Amazon, where half of the land is now already under private tenure or is available for future land-uses, differences in vegetation mapping and interpretation directly affect the level of protection in private rural properties, especially in transition areas where forest and savanna areas intermingle. Since Brazil’s Native Vegetation Protection Law (NVPL) attaches a higher percentage of protection to forest-located properties, landowners may be tempted to use conflicting mappings and different vegetation classifications to claim their properties are located in areas other than forests to reduce their conservation requirements. The authors compare three official vegetation databases and examine different law interpretation scenarios to assess the extent to which the level of private conservation may fluctuate. They found a difference of up to 430,000 km² of protected vegetation (an area the size of Iraq) according to the database and vegetation characteristics chosen. This technical ambiguity may lead to make additional deforestation legal or reduce sharply the amount of vegetation to be restored for these areas, if left unaddressed. Clarifying the database and criteria used to define forest is critical, especially as Brazilian states may make different choices in that regard, and cases in which loopholes are exploited occurred in the recent past. Given the importance of this region for global biodiversity conservation and climate, the authors highlight the urgent need to: (1) support additional research to clarify vegetation characteristics and location;

(2) agree on a harmonized methodology to determine forests for NVPL implementation, and (3) explore alternative criteria for defining forests when databases conflict [140].

Maracahipes-Santos et al. (2023) analyse the trees' responses to the surrounding land cover in riparian forest edges in Southern Amazonia. Tropical forest fragmentation from agricultural expansion alters the microclimatic conditions of the remaining forests, with effects on vegetation structure and function. However, little is known about how the functional trait variability within and among tree species in fragmented landscapes influence and facilitate species' persistence in these new environmental conditions. The authors assessed potential changes in tree species' functional traits in riparian forests within six riparian forests in cropland catchments (Cropland) and four riparian forests in forested catchments (Forest) in southern Amazonia. They sampled 12 common functional traits of 123 species across all sites: 64 common to both croplands and forests, 33 restricted to croplands, and 26 restricted to forests. They found that forest-restricted species had leaves that were thinner, larger, and with higher phosphorus (P) content, compared to cropland-restricted ones. Tree species common to both environments showed higher intraspecific variability in functional traits, with leaf thickness and leaf P concentration varying the most. Species turnover contributed more to differences between forest and cropland environments only for the stem-specific density trait. They conclude that the intraspecific variability of functional traits (leaf thickness, leaf P, and specific leaf area) facilitates species persistence in riparian forests occurring within catchments cleared for agricultural expansion in Amazonia [141].

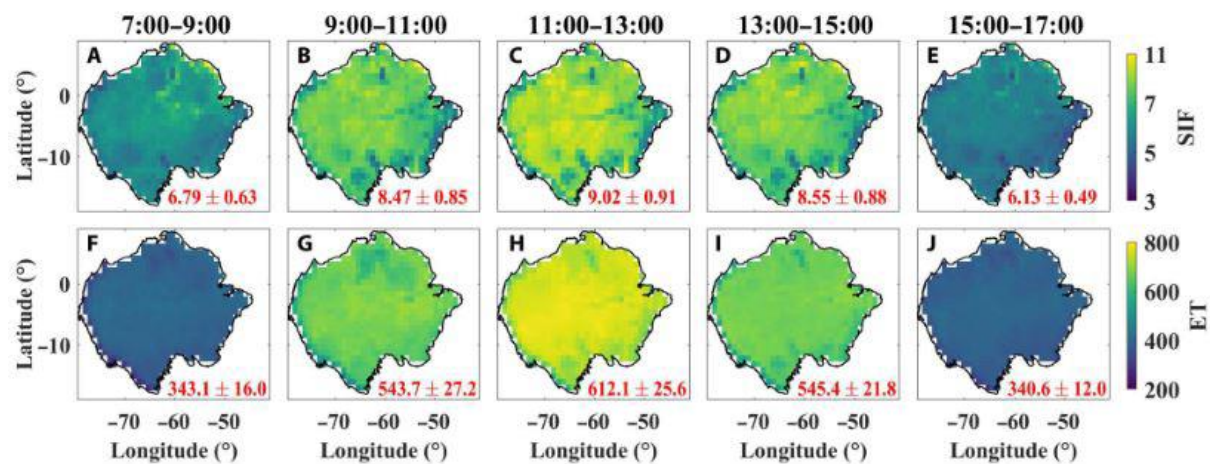
Figure 50: Mean functional traits of riparian forest tree communities in forested catchments (Forest) and cropland catchments (Cropland) in southern Amazonia, Querência-MT, Brazil. Hmax = maximum tree height; BT = bark thickness; SSD = stem-specific density; LA = leaf area; LT = leaf thickness, SLA = specific leaf area [141]



8.1.2 Forest and Climate Change

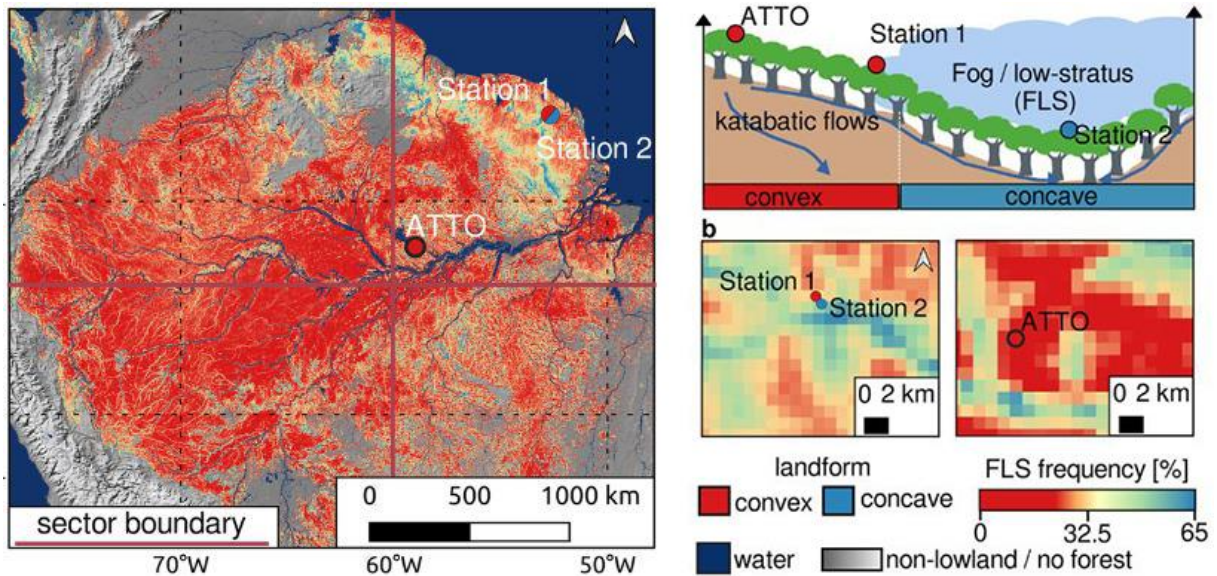
Zhang et al. (2023) examine at large diurnal compensatory effects that mitigate the response of Amazonian forests to atmospheric warming and drying. Photosynthesis and evapotranspiration in Amazonian forests are major contributors to the global carbon and water cycles. However, their diurnal patterns and responses to atmospheric warming and drying at regional scale remain unclear, hindering the understanding of global carbon and water cycles. The authors used proxies of photosynthesis and evapotranspiration from the International Space Station to reveal a strong depression of dry season afternoon photosynthesis (by $6.7 \pm 2.4\%$) and evapotranspiration (by $6.1 \pm 3.1\%$). Photosynthesis positively responds to vapor pressure deficit (VPD) in the morning, but negatively in the afternoon. Furthermore, they projected that the regionally depressed afternoon photosynthesis will be compensated by their increases in the morning in future dry seasons. These results shed new light on the complex interplay of climate with carbon and water fluxes in Amazonian forests and provide evidence on the emerging environmental constraints of primary productivity that may improve the robustness of future projections [142].

Figure 51: Diurnal patterns of solar-induced chlorophyll fluorescence (SIF, $\text{mW} \cdot \text{m}^{-2} \cdot \text{nm}^{-1}$) and evapotranspiration (ET, $\text{W} \cdot \text{m}^{-2}$) in Amazonian forests throughout 2015–2020 at 2-hour intervals: 7:00 to 9:00, 9:00 to 11:00, 11:00 to 13:00, 13:00 to 15:00, and 15:00 to 17:00. The mean and SD are shown in the bottom right of each panel. The spatial resolution is $1^\circ \times 1^\circ$ [142].



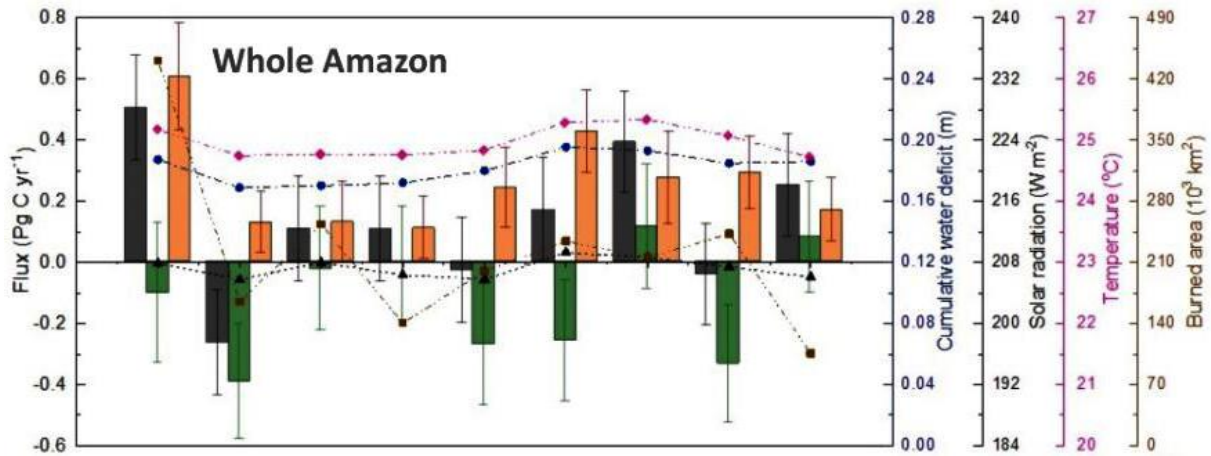
Pohl et al. (2023) find that valleys are a potential refuge for the Amazon lowland forest in the face of increased risk of drought. Despite the Amazon rainforest being home to an incredible variety of plant and animal species and playing a crucial role in regulating the Earth's climate, climate change and human activities are putting this important ecosystem at risk. In particular, increasing droughts are making it harder for certain organisms to survive. The authors analyze a satellite-based data set of fog/low-stratus (FLS) frequency and a spatio-temporal drought index. They show that vulnerable organisms may find refuge in river valleys where FLS provides a source of moisture. They find that these favourable microclimates exist throughout the Amazon basin, with the highest occurrence and stability in steep river valleys. They suggest that protecting these hygric climate change refugia could help preserve the biodiversity and functioning of the Amazon ecosystem in the face of future droughts. The authors state that this would also help stabilize atmospheric moisture recycling, making the region more resilient to climate change [143].

Figure 52: Left: Location of three typical sites with two convex and one concave landforms. Convex: Amazon Tall Tower Observatory ATTO with 13% long-term FLS-frequency and Station 1 with 32% long-term FLS-frequency, concave: Station 2 with 50% long-term FLS-frequency. Right: Idealised cross section illustrating at which topographic position the threshold between TLCF (tropical lowland cloud forests) and non-TLCF conditions is expected to be reached [143].



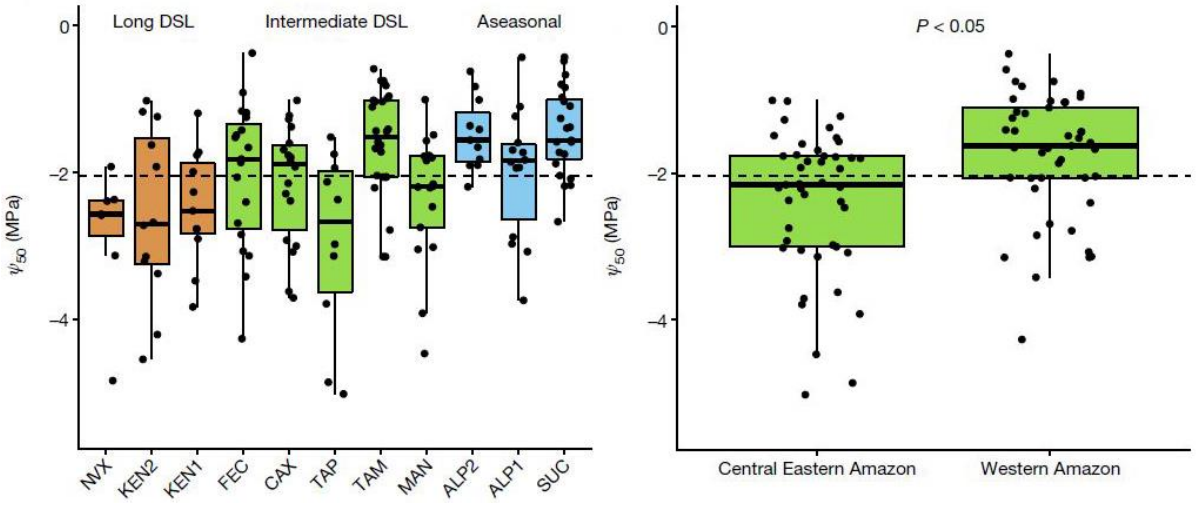
Basso et al. (2023) find the Amazon a minor carbon source caused by fire emissions by atmospheric CO₂ inversion analysis. Deforestation declined between 2005 and 2012 but more recently has again increased with similar rates as in 2007–2008. The resulting forest fragments are exposed to substantially elevated temperatures in an already warming world. These temperature and land cover changes are expected to affect the forests, and an important diagnostic of their health and sensitivity to climate variation is their carbon balance. In a recent study based on CO₂ atmospheric vertical profile observations between 2010 and 2018, and an air column budgeting technique used to estimate fluxes, the authors reported the Amazon region as a carbon source to the atmosphere, mainly due to fire emissions. Instead of an air column budgeting technique, they use an inverse of the global atmospheric transport model, TOMCAT, to assimilate CO₂ observations from Amazon vertical profiles and global flask measurements. They estimate inter- and intra-annual variability in the carbon fluxes, trends over time and controls for the period of 2010–2018. This is the longest period covered by a Bayesian inversion of these atmospheric CO₂ profile observations to date. The analyses indicate that the Amazon is a small net source of carbon to the atmosphere (mean 2010–2018 = 0.13 ± 0.17 Pg C yr⁻¹, where 0.17 is the 1 σ uncertainty), with the majority of the emissions coming from the eastern region (77 % of total Amazon emissions). Fire is the primary driver of the Amazonian source (0.26 ± 0.13 Pg C yr⁻¹), while forest carbon uptake removes around half of the fire emissions to the atmosphere (-0.13 ± 0.20 Pg C yr⁻¹). The largest net carbon sink was observed in the western-central Amazon region (72 % of the fire emissions). They find larger carbon emissions during the extreme drought years (such as 2010, 2015 and 2016), correlated with increases in temperature, cumulative water deficit and burned area. Despite the increase in total carbon emissions during drought years, they do not observe a significant trend over time in their carbon total, fire and net biome exchange estimates between 2010 and 2018. The analysis thus cannot provide clear evidence for a weakening of the carbon uptake by Amazonian tropical forests [144].

Figure 53: Annual mean carbon fluxes for the Amazon: : posterior total flux with the Amazon vertical profile observations in the inversion (black bars) and posterior fire fluxes using MOPITT carbon monoxide observations in the inversion (red bars). Annual cumulative water deficit (blue line), annual mean temperature (pink line), annual mean shortwave solar radiation downward flux (all sky; black line) and annual total burned area (brown line) [144]



Tavares et al (2023) evaluate variation in plant hydraulic properties across the Amazon. Although xylem embolism resistance thresholds (for example, ψ_{50}) and hydraulic safety margins (for example, HSM_{50}) are important predictors of drought-induced mortality risk, little is known about how these vary across Earth's largest tropical forest. The authors present a pan-Amazon, fully standardized hydraulic traits dataset and use it to assess regional variation in drought sensitivity and hydraulic trait ability to predict species distributions and long-term forest biomass accumulation. Parameters ψ_{50} and HSM_{50} vary markedly across the Amazon and are related to average long-term rainfall characteristics. Both ψ_{50} and HSM_{50} influence the biogeographical distribution of Amazon tree species. However, HSM_{50} was the only significant predictor of observed decadal-scale changes in forest biomass. Old-growth forests with wide HSM_{50} are gaining more biomass than are low HSM_{50} forests. They propose that this may be associated with a growth–mortality trade-off whereby trees in forests consisting of fast-growing species take greater hydraulic risks and face greater mortality risk. Moreover, in regions of more pronounced climatic change, They find evidence that forests are losing biomass, suggesting that species in these regions may be operating beyond their hydraulic limits. Continued climate change is likely to further reduce HSM_{50} in the Amazon, with strong implications for the Amazon carbon sink [145].

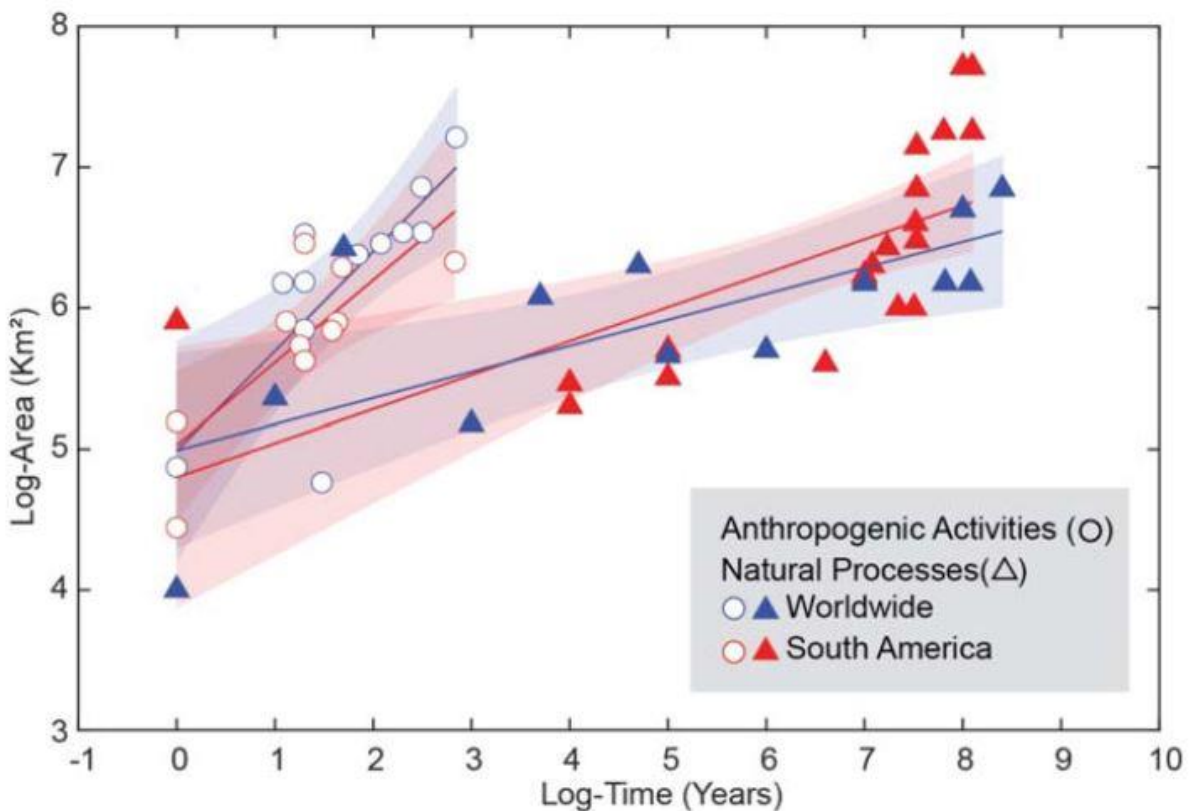
Figure 54: Hydraulic trait variation across and within Amazon forest sites, left: Xylem water potential at which 50% of the conductance is lost (ψ_{50}), right: hydraulic trait variation within forests with intermediate dry season length (DSL), subsetted according to Amazon region (central eastern Amazon: TAP, CAX and MAN; western Amazon: FEC and TAM). [145]



8.1.3 Deforestation

In their review, Albert et al. (2023) compare rates of anthropogenic and natural environmental changes in the Amazon and South America and in the larger Earth system. They focus on deforestation and carbon cycles because of their critical roles on the Amazon and Earth systems. They found that rates of anthropogenic processes that affect Amazonian ecosystems are up to hundreds to thousands of times faster than other natural climatic and geological phenomena. These anthropogenic changes reach the scale of millions of square kilometres within just decades to centuries, as compared with millions to tens of millions of years for evolutionary, climatic, and geological processes. The main drivers of Amazonian habitat destruction and degradation are land-use changes (such as land clearing, wildfires, and soil erosion), water-use changes (such as damming and fragmenting rivers and increased sedimentation from deforestation), and aridification from global climate change. Additional important threats come from overhunting and overfishing, introduction of invasive exotic species, and pollution from the mining of minerals and hydrocarbons [146].

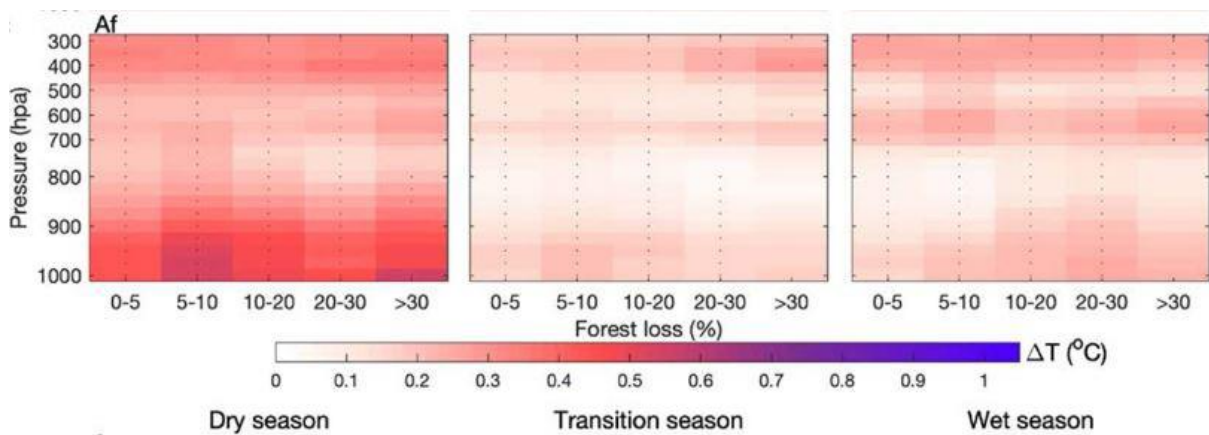
Figure 55: Temporal and spatial scales of anthropogenic and natural processes in the Earth system. Data for 55 cases, with references in Table 1. Circles and triangles indicate anthropogenic and natural processes, respectively; red and blue symbols indicate processes from South America and globally, respectively. All regressions are power functions represented as linear curves on a log-log plot [146].



Xu et al. (2022) demonstrate that 20 years deforestation has led to a warmer and dryer lower troposphere over the Amazon. As a result, the warmer and dryer lower troposphere enhanced updraft winds that impeded external water supplies from the tropical Atlantic

Ocean, which would otherwise moisten the lower atmosphere. The lower troposphere desiccation is the strongest during the dry and transition seasons in the monsoon and savanna climate zones, and is emerging in the rainforest climate zone and wet season in monsoon and savanna climate zones despite much greater and more evenly distributed rainfall. The observed atmospheric desiccation suppresses vegetation growth and may offset CO₂ fertilization effects at large spatial scales. The severe atmospheric desiccation in the southern and eastern Amazon cannot be compensated by enhanced water supplies from the Atlantic Ocean, indicating that the Amazon hydrological system is approaching an irreversible transition exacerbated by rapid deforestation. However, the incipient drying during the wet season and over the Amazon rainforest suggests that large-scale forest conservation and ecological restoration are still promising and offer the last opportunities for reversing the drying trend and preventing ecosystem collapse [147].

Figure 56: Lower atmosphere warmed as a function of forest loss. Temperature change (ΔT_a , °C) profiles from 1000 to 300 hpa during 2000–2019 in relative to 1980–1999 for tropical rainforest climate zones during the dry, transition and wet seasons. The blue '+' indicates the level below which forest loss positively contributed to the warming. Black dots indicate ΔT is statistically significant for the category of forest loss at a pressure level [147].



Duku and Hein (2023) examine the impacts of past and ongoing deforestation on the rainfall patterns in South America. Despite recent advances in modelling forest–rainfall relationships, the current understanding of changes in observed rainfall patterns resulting from historical deforestation remains limited. To address this knowledge gap, the authors analysed how 40 years of deforestation has altered rainfall patterns in South America as well as how current Amazonian forest cover sustains rainfall. First, they develop a spatiotemporal neural network model to simulate rainfall as a function of vegetation and climate inputs in South America; second, they assess the rainfall effects of observed deforestation in South America during the periods 1982–2020 and 2000–2020; third, they assess the potential rainfall changes in the Amazon biome under two deforestation scenarios. They find that, on average, cumulative deforestation in South America from 1982 to 2020 has reduced rainfall over the period 2016–2020 by 18% over deforested areas, and by 9% over non-deforested areas across South America. They also find that more recent deforestation, that is, from 2000 to 2020, has reduced rainfall over the period 2016–2020 by 10% over deforested areas and by 5% over non-deforested areas. Deforestation between 1982 and 2020 has led to a doubling in the area experiencing a minimum dry season of 4 months in the Amazon biome. Similarly, in the Cerrado region, there has been a corresponding doubling in the area with a minimum dry season of 7 months. These changes are compared to a hypothetical scenario where no deforestation occurred. Complete conversion of all Amazon forest land outside protected areas would reduce average annual rainfall in the Amazon by 36% and complete deforestation of all

forest cover including protected areas would reduce average annual rainfall in the Amazon by 68%. The findings emphasize the urgent need for effective conservation measures to safeguard both forest ecosystems and sustainable agricultural practices [6].

Figure 57: Relative changes (%) in rainfall magnitude as a result of the conversion of tree cover outside protected areas in the Amazon biome (green boundary) to pasture (left); and all tree cover in the biome to pasture (right) [6].

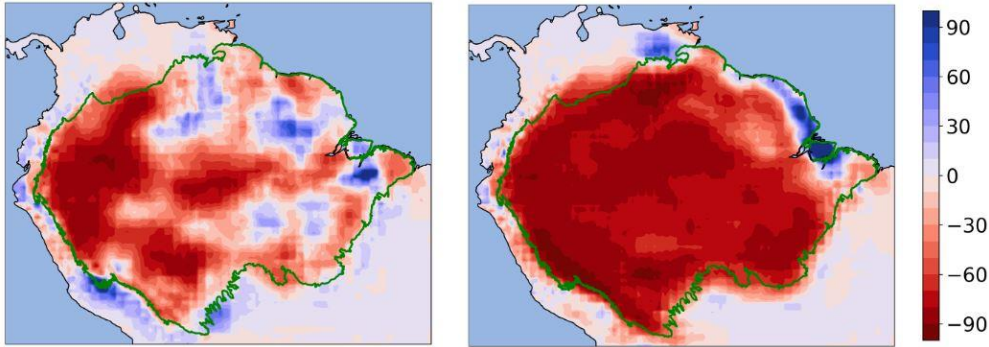
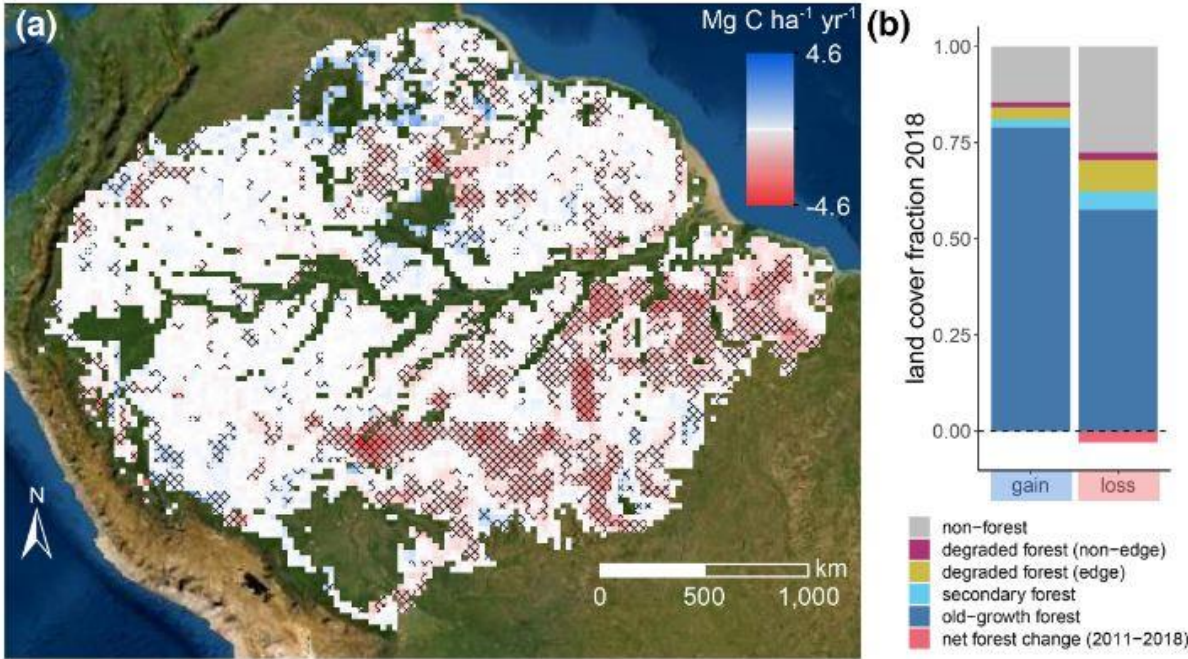


Figure 58: Trends in AGC and the associated forest cover fractions. (a) AGC trends (2011–2019) over the Amazon biome. Grid-cells where trends are significant are indicated with cross-hatches and cells where reliable data were not available are omitted (e.g. flooded areas and regional anomalies). (b) Mean land cover fractions in 2018 averaged over grid-cells showing significant positive (gain) and negative (loss) trends. Displayed are the proportions of old-growth, degraded (edge and non-edge), secondary forest and non-forest area. Edge degradation includes forest within 120 m distance from human-made forest edges. The net change in forest area fraction relative to 2011 is also indicated (~0 for gain cells, -0.03 or 4% reduction for loss cells) [148]

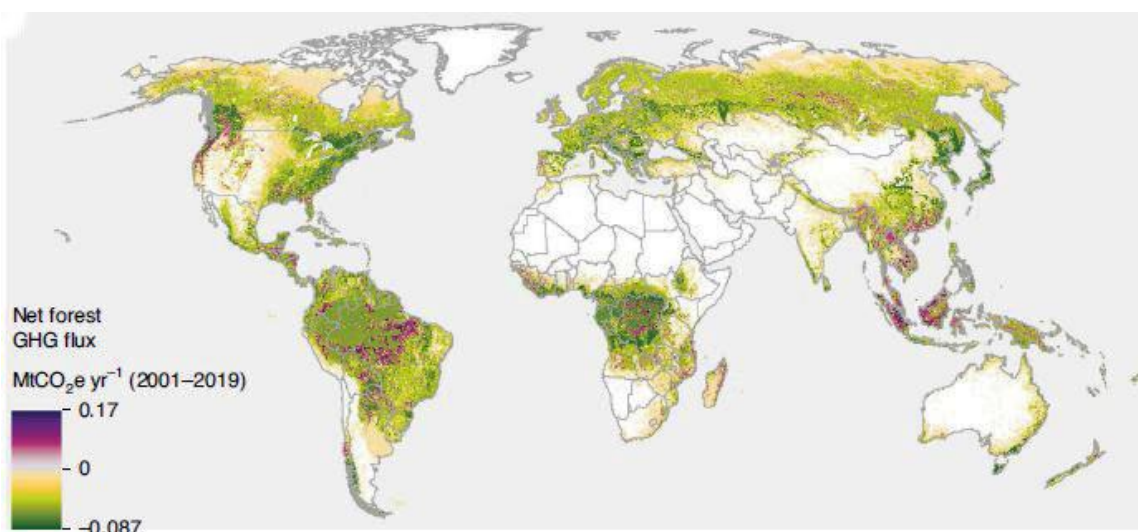


In the Amazon, deforestation and climate change lead to increased vulnerability to forest degradation, threatening its existing carbon stocks and its capacity as a carbon sink. Fawcett et al. (2023) use satellite L-Band Vegetation Optical Depth (L-VOD) data that

provide an integrated (top-down) estimate of biomass carbon to track changes over 2011–2019. The authors combined high-resolution annual maps of forest cover and disturbances with biomass maps to model carbon losses (bottom-up) from deforestation and degradation, and gains from regrowing secondary forests. An increase of deforestation and associated degradation losses since 2012, which greatly outweighs secondary forest gains. Degradation accounted for 40% of gross losses. After an increase in 2011, old-growth forests show a net loss of aboveground carbon between 2012 and 2019. The sum of component carbon fluxes in their model is consistent with the total biomass change from L-VOD of 1.3 PgC over 2012-2019. Across nine Amazon countries, it was found that while Brazil contains the majority of biomass stocks (64%), its losses from disturbances were disproportionately high (79% of gross losses). The multi-source analysis provides a pessimistic assessment of the Amazon carbon balance and highlights the urgent need to stop the recent rise of deforestation and degradation, particularly in the Brazilian Amazon [148].

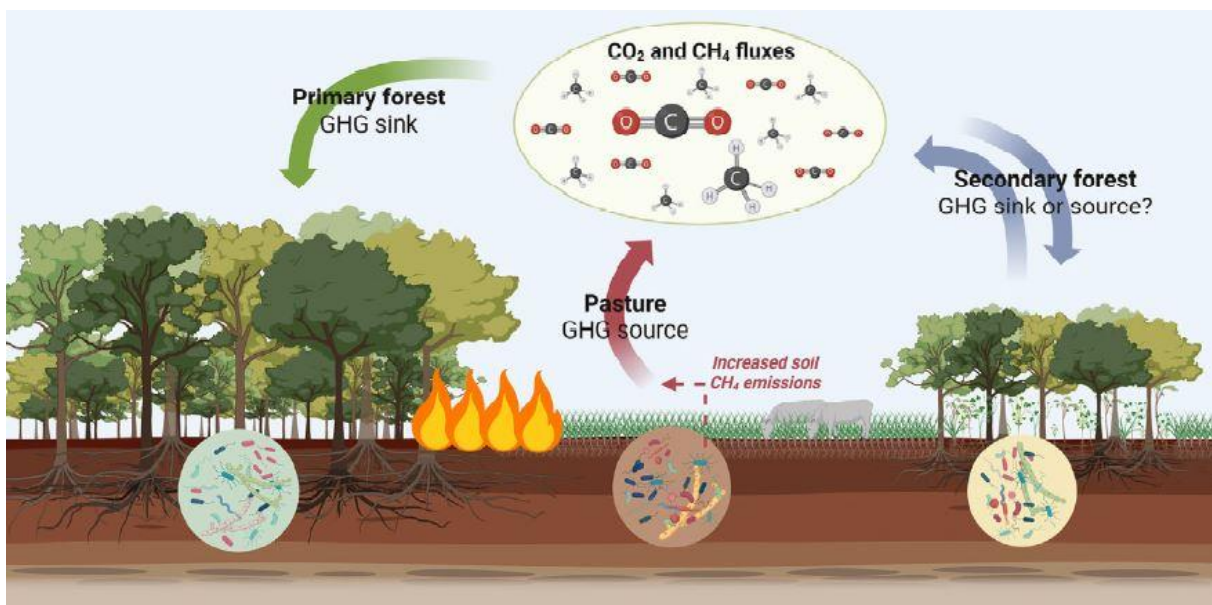
In the annual Hamburg Climate Futures Outlook, researchers from the Cluster of Excellence Climate, Climatic Change, and Society (CLICCS) make the first systematic attempt to assess which climate futures are plausible, by combining multidisciplinary assessments of plausibility. The 2023 Hamburg Climate Futures Outlook addresses the question: What affects the plausibility of attaining the Paris Agreement temperature goals? Among the many possible climatic futures, not all are plausible. The purpose of the second Hamburg Climate Futures Outlook is to systematically assess the plausibility of a climate future in which the Paris Agreement temperature goals are attained, namely holding global warming to well below 2°C and, if possible, to 1.5°C, relative to pre-industrial levels. Assessing plausible climate futures involves addressing a complex combination of social and physical dynamics. The authors establish the CLICCS Plausibility Assessment Framework to guide and integrate social and physical plausibility assessments. They analyse the dynamics of ten dominant social drivers of de-carbonization and of six select physical processes of public interest like e.g. the Polar Ice Shield Melt, the Permafrost Thaw, the Atlantic Meridional Overturning Circulation Instability and the Amazon Forest Dieback [149].

Figure 59: Net annual GhG flux. For display purposes, maps have been resampled from the 30-m observation scale to a 0.04° geographic grid. Values in the legend reflect the average annual GhG flux from all forest dynamics occurring within a grid cell, including emissions from all observed disturbances and removals from both forest regrowth after disturbance as well as removals occurring in undisturbed forests [150].



Harris et al. (2021) produce global maps of twenty-first century forest carbon fluxes. To date, several forest carbon monitoring systems have been developed for different regions using various data, methods and assumptions, making it difficult to evaluate mitigation performance consistently across scales. The authors integrate ground and Earth observation data to map annual forest-related greenhouse gas emissions and removals globally at a spatial resolution of 30 m over the years 2001–2019. They estimate that global forests were a net carbon sink of $-7.6 \pm 49 \text{ GtCO}_2\text{e yr}^{-1}$, reflecting a balance between gross carbon removals ($-15.6 \pm 49 \text{ GtCO}_2\text{e yr}^{-1}$) and gross emissions from deforestation and other disturbances ($8.1 \pm 2.5 \text{ GtCO}_2\text{e yr}^{-1}$). The geospatial monitoring framework introduced here supports climate policy development by promoting alignment and transparency in setting priorities and tracking collective progress towards forest-specific climate mitigation goals with both local detail and global consistency [150].

Figure 60: Impacts of forest-to-pasture conversion in the Brazilian Amazon: Three typical Amazonian upland landscapes (left to right): primary forest, pasture (the most common anthropogenic land use of the region), and secondary forest (originating from abandoned deforested areas). Pasture establishment (through vegetation clearing and burning) alters above-ground biodiversity and releases large emissions of greenhouse gases (GHGs), while primary forests are sinks of carbon dioxide (CO_2) and methane (CH_4). Secondary forests sequester carbon, but in the short term, total GHG emissions from deforestation cannot be entirely offset by secondary forest growth. For the situation below ground, these processes are even less well understood. Forest-to-pasture conversion impacts soil properties, microbial communities, and their ecosystem services, leading to a CH_4 sink-to-source shift from soils due to changes in the number of CH_4 -producing and -consuming microorganisms. However, it is still unclear whether soil microbial communities from secondary forests and their roles, including CH_4 regulation, can be completely recovered [151].

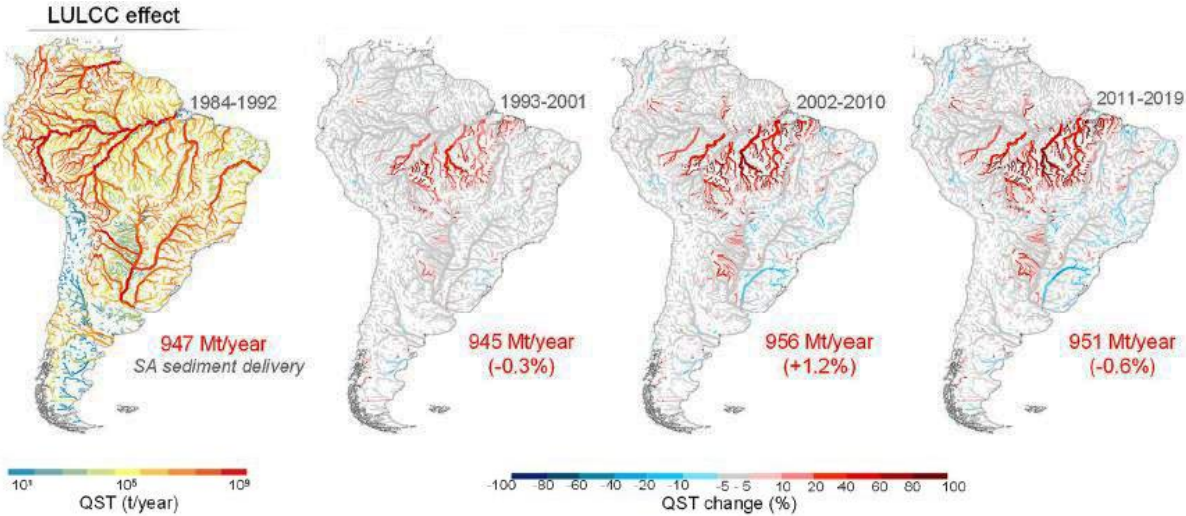


Venturini et al. (2023) look at the effects of Amazon deforestation on soil microbes. They state that Soil microorganisms are sensitive indicators of land-use and climate change in the Amazon, revealing shifts in important processes such as greenhouse gas (GHG) production, but they have been overlooked in conservation and management initiatives. Integrating soil biodiversity with other disciplines while expanding sampling efforts and targeted microbial groups is crucially needed. In the Amazon, agricultural and pasture lands are usually established through forest clearing and burning. This process alters the

natural characteristics of the soils, causing initial increases in soil pH, nutrient content and availability, and soil structure degradation. In the long run, converting rainforests to pastures may result in nutrient depletion and, not surprisingly, more than half (56%) of Amazonian pastures are now moderately or severely degraded. These impacts have negatively affected below-ground biodiversity, including microbes [151].

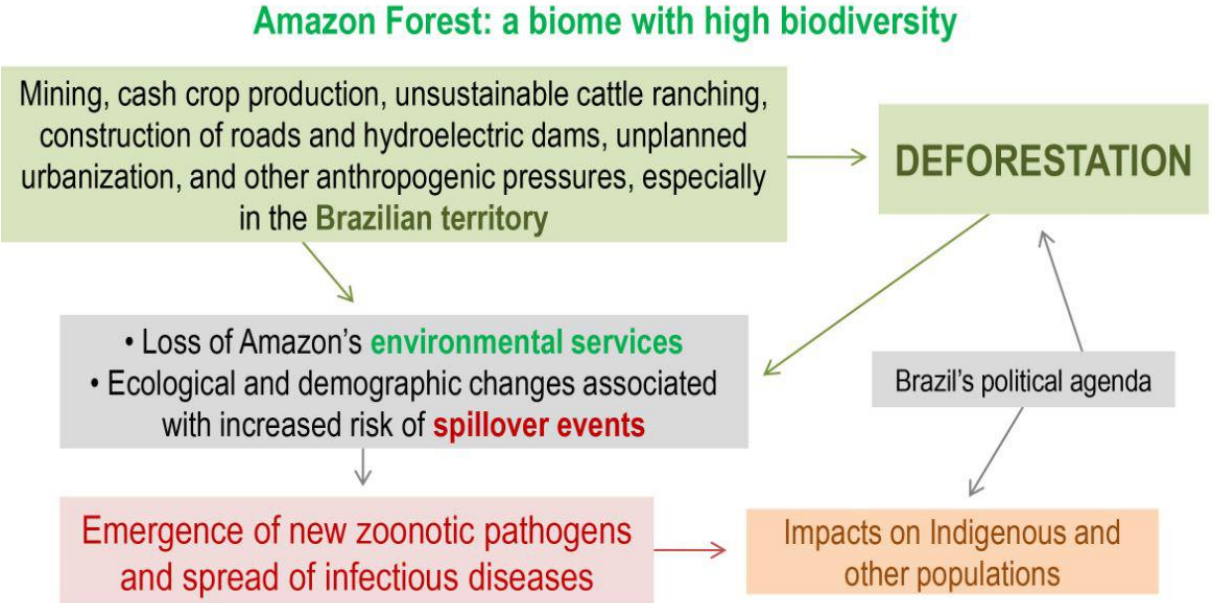
Fagundes et al. (2023) examine human-induced changes in South American river sediment fluxes from 1984 to 2019. River sediment fluxes have been impacted in South America (SA), one of the continents with the highest erosion and sediment transport rates globally. However, the magnitude and spatio-temporal distribution of the main drivers of changes have been poorly identified and explored. The authors performed simulations using a hydrological-hydrodynamic-sediment model to comprehensively estimate the spatial and temporal sediment changes and trends in SA from 1984 to 2019. They found that 51% of the main SA rivers experienced significant changes in simulated sediment transport (QST) over this period, with 36% due to Amazon deforestation and river damming and 15% due to precipitation changes. They estimated a 10% reduction in the average sediment delivery to the oceans. Deforestation was responsible for QST changes higher than 80% in some Amazon sites, and hydropower expansion led to a greater reduction of sediment flows (80%–100%) in the Tocantins, Uruguay, Upper Paraná, lower São Francisco, Desaguadero, and Negro rivers. In addition, the results suggest that reservoirs built in the Amazon region in the 2011–2019 period are also affecting sediment transport. The modeling outputs provide unprecedented information about the status of river sediment dynamics in SA, and a template to develop evidence-based strategies and transboundary policies related to continental-wide sediment dynamics and the conservation and restoration of ecosystems [152].

Figure 61: Temporal changes in sediment fluxes in South American rivers between 1984 and 2019. Maps show the QST and their changes (%) considering the isolated effect of land use and land cover changes (LULCC). The map on the left shows QST values for the baseline period (1984–1992). The other maps present the sediment flow changes compared with the baseline period. Numbers in red indicate the average sediment delivery from South America (SA) to the oceans in each period. Percentage values indicate the increase or decrease of sediment delivery compared with the previous period [152].



Ellwanger et al. (2022) make the connection between environmental disturbances and zoonotic spillover, with a specific view on the Amazon region. Zoonotic spillover is a phenomenon characterized by the transfer of pathogens between different animal species. Most human emerging infectious diseases originate from non-human animals, and human-related environmental disturbances are the driving forces of the emergence of new human pathogens. Synthesizing the sequence of basic events involved in the emergence of new human pathogens is important for guiding the understanding, identification, and description of key aspects of human activities that can be changed to prevent new outbreaks, epidemics, and pandemics. This review synthesizes the connections between environmental disturbances and increased risk of spillover events based on the One Health perspective. Anthropogenic disturbances in the environment (e.g., deforestation, habitat fragmentation, biodiversity loss, wildlife exploitation) lead to changes in ecological niches, reduction of the dilution effect, increased contact between humans and other animals, changes in the incidence and load of pathogens in animal populations, and alterations in the abiotic factors of landscapes. These phenomena can increase the risk of spillover events and, potentially, facilitate new infectious disease outbreaks. Using Brazil as a study model, this review brings a discussion concerning anthropogenic activities in the Amazon region and their potential impacts on spillover risk and spread of emerging diseases in this region. [153]

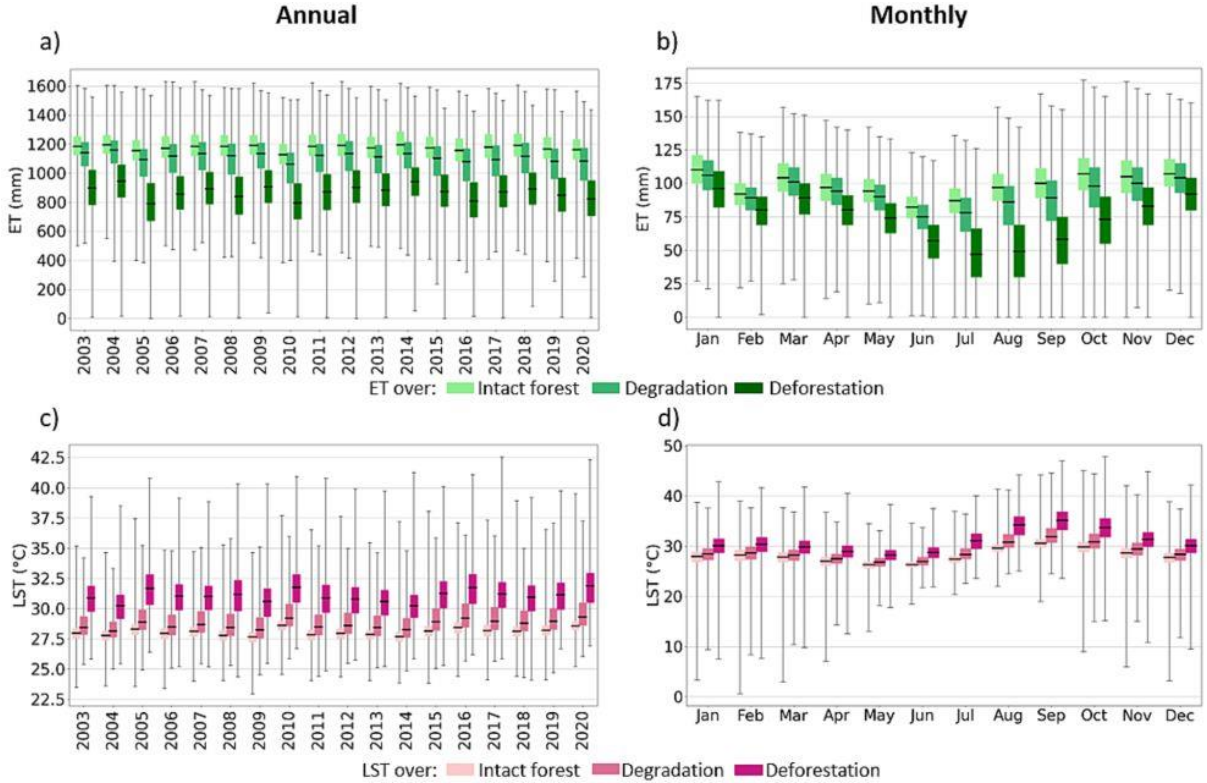
Figure 62: Deforestation and other anthropogenic pressures on Amazon Forest are closely connected activities. These pressures facilitate spillover events, the emergence of pathogens and the spread of infectious diseases, affecting populations living inside and outside the Amazon region [153].



Reygadas et al. (2023) talk about the Effects of deforestation and forest degradation on ecosystem service indicators across the Southwestern Amazon. According to the authors, the integrity of this region is threatened by global changes in climate and local to regional changes in land-use and land-cover. Unlike most Amazonia-land-change research which as focused primarily on deforestation, the authors evaluated the effects of both deforestation and forest degradation on three Ecosystem Service Indicators (ESIs) –

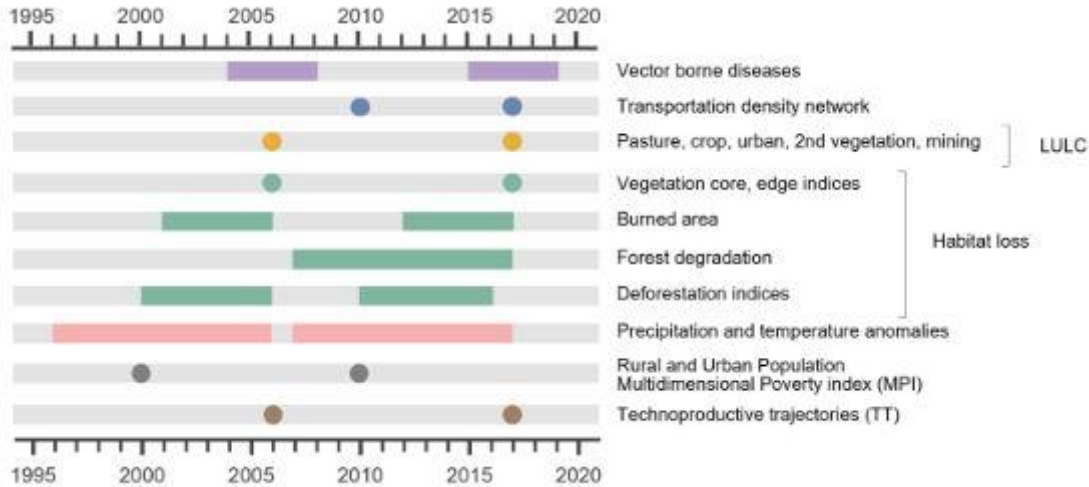
evapotranspiration (ET), land surface temperature (LST), and precipitation (P) – at the local and watershed scale across the SWA between 2003 and 2020. They computed annual and monthly ESI differences over distinct forest conditions and buffers around disturbed areas (degraded or deforested). They also determined the influence of forest disturbance trends on ESI trends at the pixel and watershed level through a Partial Mann-Kendall approach. The results show that ESI differences among different forest conditions are statistically-significant and more pronounced during the dry season. In comparison with intact forest, monthly P rates were up to 25 % lower over any type of disturbance; whereas ET rates were up to 15 % and 48 % lower, and LST rates up to 1.6 °C and 4.4 °C higher, over degraded and deforested areas, respectively. ET and LST edge effects were only significant within buffers around some of the most heavily disturbed areas. At the pixel scale, negative trends in ET and positive trends in both LST and P were more frequently explained by forest disturbances as these trends themselves become more pronounced. ET and LST trends determined by disturbances were generally located near roads, rivers, and human settlements; and surprisingly, they found that degradation more often influences these trends than deforestation, which they attribute to the practice of converting deforested areas into crops whose growing season ET and LST rates are similar to those in natural vegetation. At the watershed scale, the analysis suggested that the climate implications of degradation and deforestation have not scaled up to this level yet; however, literature has shown that even the local impacts we report here can have important implications for areas outside of the SWA, which emphasizes the importance of continuing to conserve this remote region [154].

Figure 63: Data distribution of a) the annual ET totals, b) the average of the monthly ET totals, c) the annual LST averages, d) the average of the monthly LST averages over areas classified as intact forest, degradation, and deforestation in the entire study area [154].



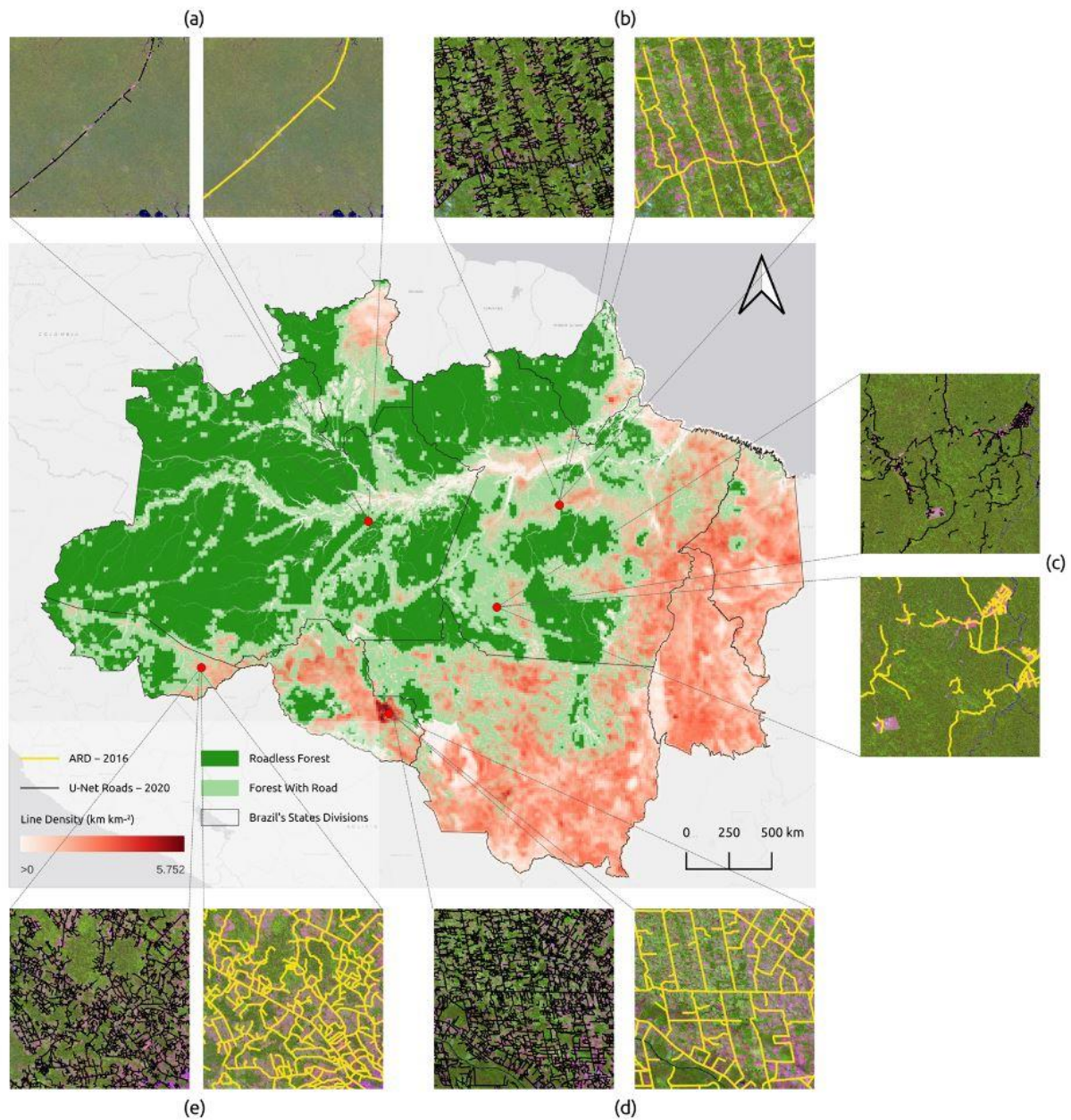
Rorato et al. (2023) describe a new collection of environmental, socio-economic and epidemiological indicators for all municipalities of the Brazilian Legal Amazon (BLA). The dataset is the result of a scientific synthesis research initiative conducted by scientists from several natural and social sciences fields, consolidating multidisciplinary indicators into a coherent dataset for integrated and interdisciplinary studies of the Brazilian Amazon. The dataset allows the investigation of the association between the Amazonian agrarian systems and their impacts on environmental and epidemiological changes, furthermore enhancing the possibilities for understanding, in a more integrated and consistent way, the scenarios that affect the Amazonian biome and its inhabitants [155].

Figure 64: The Trajetorias dataset indicators are computed for two periods for each municipality, as shown in the diagram. The reference point of each period is the date of agrarian census, from which the rural techno-productive trajectory is computed. The database harmonizes epidemiological, environmental and economic indicators [155]



Botelho et al (2022) present their efforts to automate the detection of unofficial roads (herein, roads) in the Brazilian Amazon using artificial intelligence (AI). In this region, roads are built by loggers, goldminers, and unauthorized land settlements from existing official roads, expanding over pristine forests and leading to new deforestation and fire hotspots. Previous research used visual interpretation, hand digitization, and vector editing techniques to create a thorough Amazon Road Dataset (ARD) from Landsat imagery. The authors found an astonishing footprint of roads in the Brazilian Legal Amazon, with 3.46 million km of roads mapped in 2020. Most roads are in private lands (~55%) and 25% are in open public lands under land grabbing pressure. The roads are also expanding over forested areas with 41% cut or within 10 km from the roads, leaving 59% of the 3.1 million km² of the remaining original forest roadless. The AI and post-AI models fully automated road detection in rural areas of the Brazilian Amazon make it possible to operationalize road monitoring. The AI road map is used to understand better rural roads' impact on new deforestation, fires, and landscape fragmentation and to support societal and policy applications for forest conservation and regional planning [113].

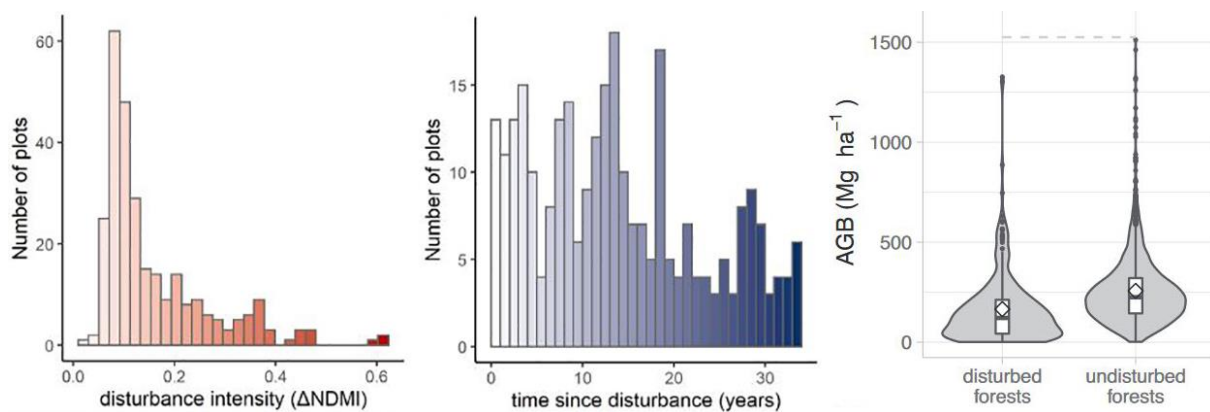
Figure 65: Road density obtained with the U-Net road model. A comparison of the U-Net model (2020) and the Amazon Road Dataset (ARD, 2016) is shown in the image panels: (a) the BR-319 highway with unconnected segments by the U-Net road model (black line) and ARD showing the full connected length; (b) the fishbone road pattern of the Trans-Amazonia highway main road (BR-230) and perpendicular ones; (c) a typical road pattern of selective logging; (d,e) a geometric road pattern in agriculture lands [113].



Requena Suarez et al. (2023) analyse forest disturbances and recovery in the Peruvian Amazon since 1984 by combining remote sensing and National Forest Inventory data. While Amazonian forests continuously experience disturbance, the effect that disturbances have on biomass and biodiversity over time has not yet been assessed at a large scale. The authors evaluate the degree of recent forest disturbance in Peruvian Amazonia and the effects that disturbance, environmental conditions and human use have on biomass and biodiversity in disturbed forests. They integrate tree level data on aboveground

biomass (AGB) and species richness from 1840 forest plots from Peru's National Forest Inventory with remotely sensed monitoring of forest change dynamics, based on disturbances detected from Landsat-derived Normalized Difference Moisture Index time series. The results show a clear negative effect of disturbance intensity on tree species richness. This effect was also observed on AGB and species richness recovery values towards undisturbed levels, as well as on the recovery of species composition towards undisturbed levels. Time since disturbance had a larger effect on AGB than on species richness. While time since disturbance has a positive effect on AGB, unexpectedly we found a small negative effect of time since disturbance on species richness. We estimate that roughly 15% of Peruvian Amazonian forests have experienced disturbance at least once since 1984, and that, following disturbance, have been increasing in AGB at a rate of 4.7 Mg ha⁻¹ year⁻¹ during the first 20 years. Furthermore, the positive effect of surrounding forest cover was evident for both AGB and its recovery towards undisturbed levels, as well as for species richness. There was a negative effect of forest accessibility on the recovery of species composition towards undisturbed levels. The authors recommend that forest-based climate change mitigation endeavours consider forest disturbance through the integration of forest inventory data with remote sensing methods [156].

Figure 66: Number of forest inventory plots per disturbance intensity Δ NDMI (left) and time since disturbance event (centre), aboveground biomass of disturbed and undisturbed forest (right) [156]



Butt et al. (2022) examine the connection between deforestation and fire in the Brazilian Amazon and the collateral gain of curbing deforestation for air quality and other public health benefits. In addition, they analyse the factors that lead to an increased fire activity in the region. According to the authors, climate, deforestation, and forest fires are closely coupled in the Amazon, but models of fire that include these interactions are lacking. The authors trained machine-learning models on temperature, rainfall, deforestation, land-use, and fire data to show that spatial and temporal patterns of fire in the Amazon are strongly modified by deforestation. Fire count across the Brazilian Amazon increases by 0.44 percentage points for each percentage point increase in deforestation rate. A model is used to predict that the increased deforestation rate in the Brazilian Amazon from 2013 to 2020 caused a 42% increase in fire counts in 2020. They predict that if Brazil had achieved the deforestation target under the National Policy on Climate Change, there would have been 32% fewer fire counts across the Brazilian Amazon in 2020. Using a regional chemistry-climate model and exposure-response associations, the estimate is that the improved air quality due to reduced smoke emission under this scenario would have resulted in 2,300 fewer deaths due to reduced exposure to fine particulate matter. According to the authors, the analysis demonstrates the air quality and public health benefits that would accrue from reducing deforestation in the Brazilian Amazon. At the

same time, they estimate that that warming over the Amazon over the past 40 years have already driven a 21%–25% increase in fire [157].

Figure 67: Permutation importance across all years (2003–2020) representing the importance of features for fire count prediction. Boxes show quartiles of the calculated permutation importance across individual years the median of which showing 50th percentile. Calculated permutation importance is taken as an average combination of neural network (NN) and XGBoost (XGB). Model (NN and XGB) prediction sensitivity showing annual change in total fires across the BAB as a function of incremental changes in surface temperature (+0.1 K to +1K), precipitation (–1% to –10%) and deforestation (+1% to +50%) calculated as an average across all years (2003–2020) [157].

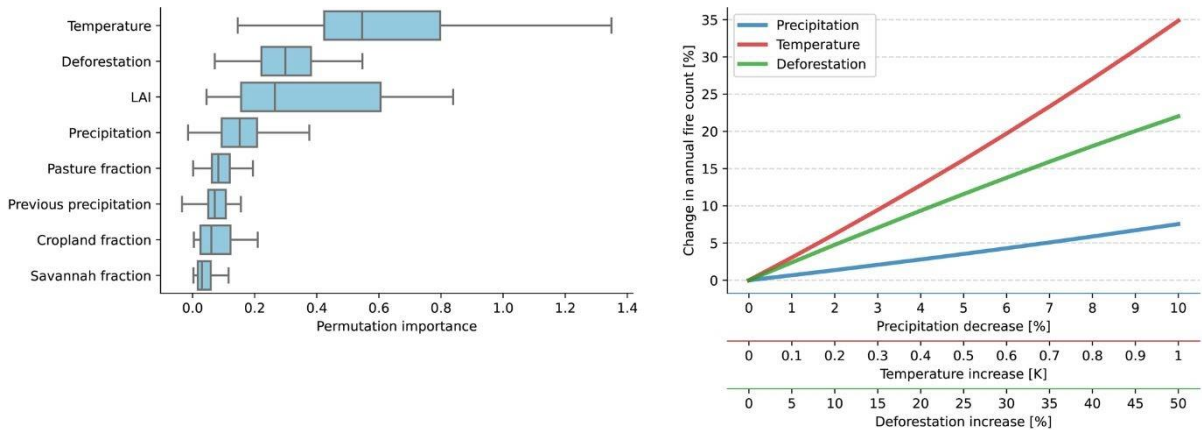
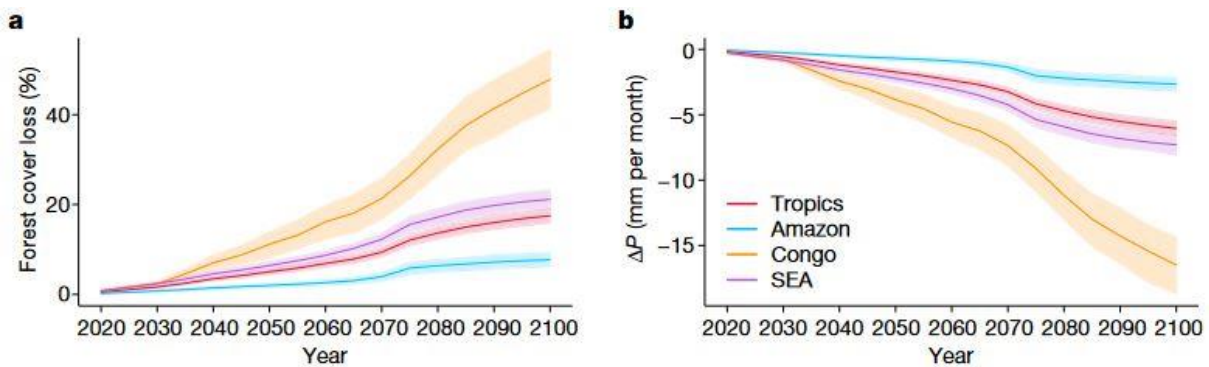


Figure 68: Impact of projected future forest loss on annual mean precipitation. Left: mean projected forest cover loss over 2015–2100 under Shared Socioeconomic Pathway 3–Representative Concentration Pathway 4.5 for the tropics, Amazon, Congo and SEA. Right: Impact of projected forest cover loss on precipitation (P ; ± 1 standard error from the mean) [158]



Smith et al. (2023) look at the consequences of tropical deforestation for changes in precipitation on a global scale. Tropical forests play a critical role in the hydrological cycle and can influence local and regional precipitation. Previous work has assessed the impacts of tropical deforestation on precipitation, but these efforts have been largely limited to case studies. A wider analysis of interactions between deforestation and precipitation - and especially how any such interactions might vary across spatial scales - is lacking. The authors show reduced precipitation over deforested regions across the tropics. Their results arise from a pan-tropical assessment of the impacts of 2003–2017 forest loss on precipitation using satellite, station-based and reanalysis datasets. The effect of deforestation on precipitation increased at larger scales, with satellite datasets showing

that forest loss caused robust reductions in precipitation at scales greater than 50 km. The greatest declines in precipitation occurred at 200 km, the largest scale we explored, for which one percentage point of forest loss reduced precipitation by 0.25 ± 0.1 mm per month. Reanalysis and station-based products disagree on the direction of precipitation responses to forest loss, which the authors attribute to sparse in situ tropical measurements. They estimate that future deforestation in the Congo will reduce local precipitation by 8–10% in 2100. Their findings provide a compelling argument for tropical forest conservation to support regional climate resilience [158].

Pacheco and Meyer (2022) look at the relation between Brazil’s deforestation and land tenure. Tropical forestlands are experiencing changes in land-tenure regimes, but how these changes may affect deforestation rates remains ambiguous. The authors use Brazil’s land-tenure and deforestation data and quasi-experimental methods to analyse how six land-tenure regimes (undesignated/untitled, private, strictly protected and sustainable-use protected areas, indigenous, and quilombola lands) affect deforestation across 49 spatio-temporal scales. They find that undesignated/untitled public regimes with poorly defined tenure rights increase deforestation relative to any alternative regime in most contexts. The privatization of these undesignated/untitled lands often reduces deforestation, particularly when private regimes are subject to strict environmental regulations such as the Forest Code in Amazonia. However, private regimes decrease deforestation less effectively and less reliably than alternative well-defined regimes, and directly privatizing either conservation regimes or indigenous lands would most likely increase deforestation. The study informs the ongoing political debate around land privatization/protection in tropical landscapes and can be used to envisage policy aligned with sustainable development goals [159].

Figure 69: Effects of alternative land-tenure regimes (here: private lands) on forest-to-agriculture conversion rates in Brazil. Circles indicate average effects sizes estimated using regression analysis (using matched parcels) at different spatial-temporal scales, compared to two alternative counterfactuals. Labelled effect sizes (larger circles) report effects across Brazil over the period 1985–2018. Effects to the left of the zero line indicate a decrease in average parcel-level deforestation rate (to the right: increase) [159].

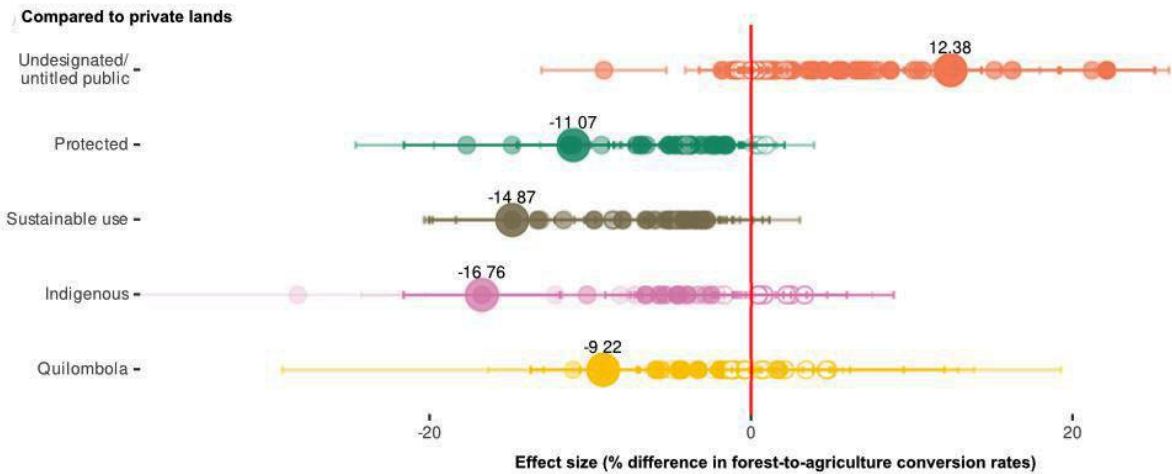
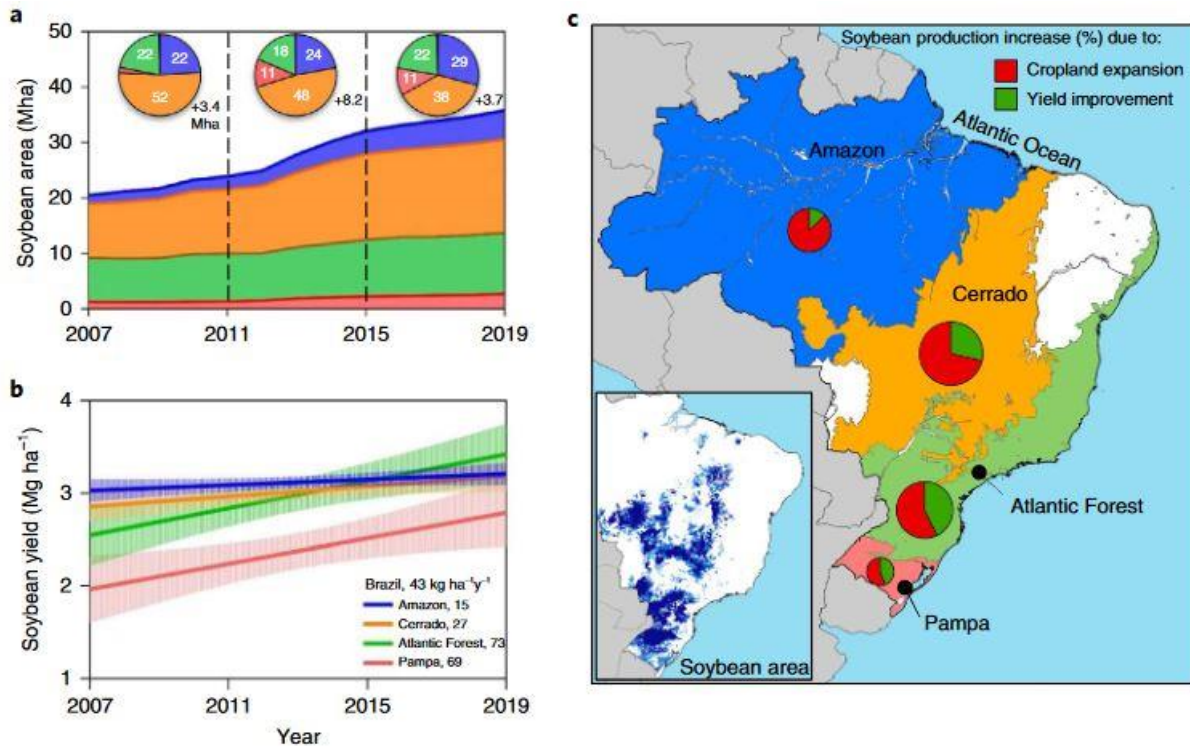


Figure 70: Trends in soybean area and yield in main producing areas in Brazil. A: percentage of soybean expansion occurring in each biome, while the total increase in soybean area in each period is shown next to the pie charts. B: annual rate of yield improvement for each region during 2007–2019, with shadow bands representing the 95% confidence intervals estimated for the fitted linear regression models. Values indicate the annual rate of yield improvement in each region and for Brazil. C: Contribution of cropland expansion and yield improvement to soybean production increase in each region. The size of the pie chart in each region is proportional to the share of national soybean production [160].



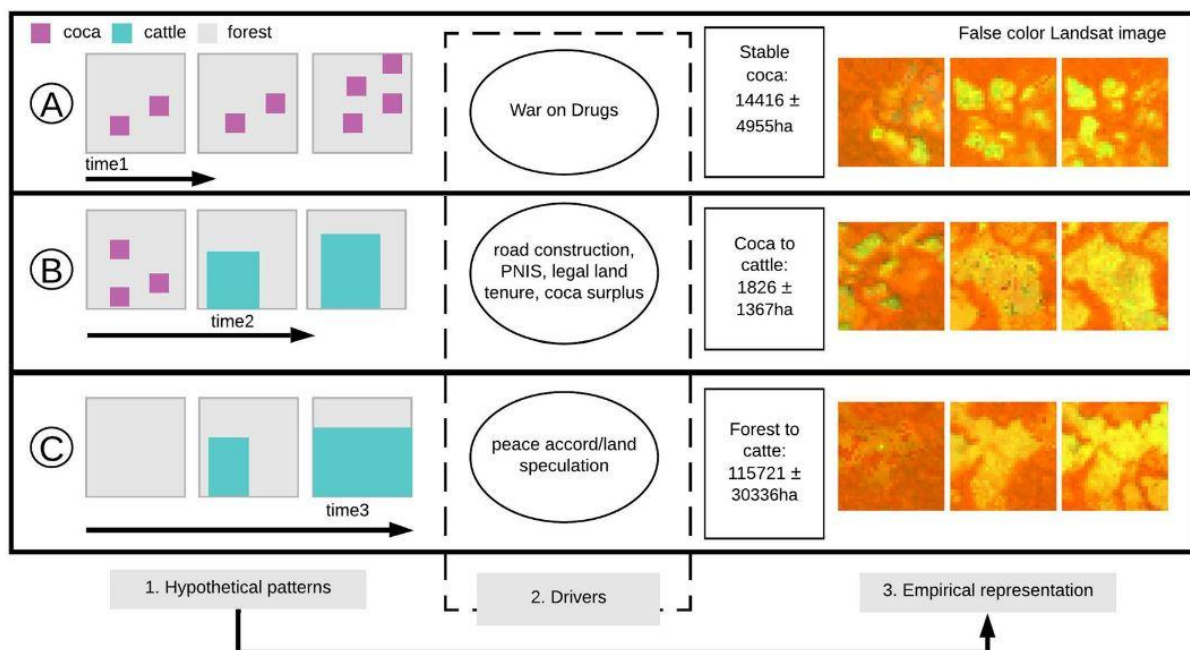
Marin et al. (2022) look at the question about how the Amazon forest can be protected by intensification of soy agriculture. The conversion of rainforest for soybean production raises concerns about how Brazil can reconcile production and environmental goals. The authors investigated the degree to which intensification could help Brazil produce more soybean without further encroachment on the Amazon forest. Their analysis shows that the continuation of current trends in soybean yield and area would lead to the conversion of an additional 5.7 Mha of forests and savannahs during the next 15 years, with an associated 1,955 Mt of CO₂ released into the atmosphere. In contrast, the acceleration of yield improvement, coupled with the expansion of soybean area only in areas currently used for livestock production, would allow Brazil to produce 162 Mt of soybean without deforestation and with 58% lower global climate warming relative to that derived from the continuation of current trends. The continuation of current trends in soybean area expansion (BAU scenario) would drive massive encroachment on the Amazon rainforest, biodiversity loss and increased global warming. Imposing restrictions on expanding soybean area, without an explicit effort to accelerate historical rates of yield gain and intensify the pasture-based livestock sector (NCE scenario), would lead to a substantial negative economic impact due to lower national crop production. However, an alternative pathway would balance out environmental and economic goals: Brazil can reverse current patterns of soybean expansion via a dual intensification of crop and livestock systems, coupled with land-use planning (INT scenario), without incurring substantial trade-offs between crop production and economic profit. To be effective, however, intensification

would require proper policy and enforcement to ensure that land savings derived from crop yield improvement led to land sparing for nature [160].

In the same context (soy and deforestation in Brazil), Gollnow et al. (2022) examine the effectiveness of zero-deforestation supply chain policies for soy. Corporate zero-deforestation supply chain commitments (ZDCs) have the potential to address deforestation, especially if strong state-led forest governance is absent. Yet, because ZDC adoption is limited to particular locations and supply chains, these commitments may fall short at reducing regional deforestation and protecting biodiverse ecosystems. The authors leverage time series of spatially explicit corporate commodity sourcing data and ZDCs to assess the current and potential effect of ZDCs within soybean supply chains on forest loss and biodiversity. We focus on the Brazilian Amazon, where the first ZDC (soy moratorium, SoyM) was implemented, and the Cerrado, where companies have adopted but not implemented ZDCs. They found that in the Amazon, SoyM signatories that controlled the market caused a 57% reduction in direct deforestation for soy from 2006 to 2015. In the Cerrado, if companies had implemented their ZDCs with the same relative effectiveness as in the Amazon, deforestation for soy could have been reduced by 46%. Thus, ZDC implementation in the Cerrado via stringent monitoring and enforcement could contribute substantially to forest and habitat conservation. Yet, incomplete ZDC adoption leaves >50% of soy-suitable forests and the biodiversity that they harbour outside the reach of ZDCs. To protect these forests, it is vital to incentivize more companies—including smaller, less publicly exposed traders—to make and implement ZDCs, while also promoting forest governance through public policy [161].

Murillo-Sandoval et al. (2023) examine the post-conflict expansion of coca farming and illicit cattle ranching in Colombia. Illicit cattle ranching and coca farming have serious negative consequences on the Colombian Amazon's land systems. The underlying causes of these land activities include historical processes of colonization, armed conflict, and narco-trafficking. The authors aim to examine how illicit cattle ranching and coca farming are driving forest cover change over the last 34 years (1985–2019). To achieve this aim, they combine two pixel-based approaches to differentiate between coca farming and cattle ranching using hypothetical observed patterns of illicit activities and a deep learning algorithm. They found evidence that cattle ranching, not coca, is the main driver of forest loss outside the legal agricultural frontier. There is evidence of a recent, explosive conversion of forests to cattle ranching outside the agricultural frontier and within protected areas since the negotiation phase of the peace agreement. In contrast, coca is remarkably persistent, suggesting that crop substitution programs have been ineffective at stopping the expansion of coca farming deeper into protected areas. Countering common narratives, the authors found very little evidence that coca farming precedes cattle ranching. The spatiotemporal dynamics of the expansion of illicit land uses reflect the cumulative outcome of agrarian policies, Colombia's War on Drugs, and the 2016 peace accord. The study enables the differentiation of illicit land activities, which can be transferred to other regions where these activities have been documented but poorly distinguished spatiotemporally. The authors provide an applied framework that could be used elsewhere to disentangle other illicit land uses, track their causes, and develop management options for forested land systems and people who depend on them [13].

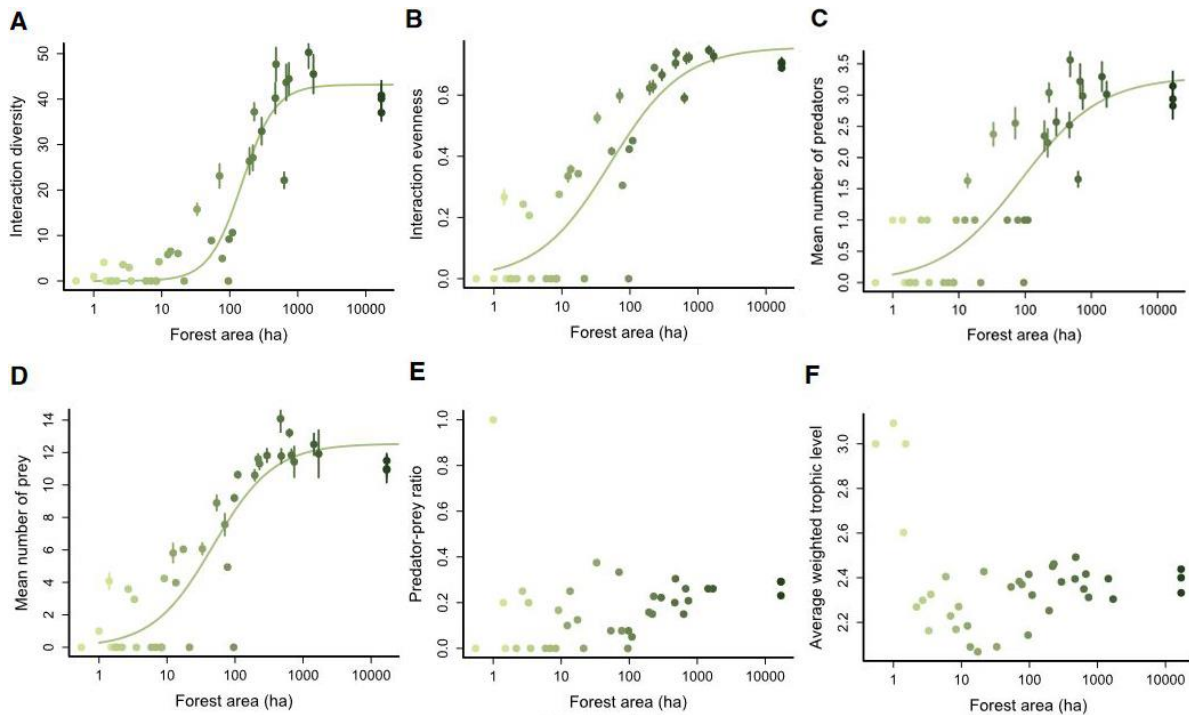
Figure 71: A conceptual framework describing hypothetical and empirical land change patterns arising from different drivers of illicit land use activities. (1) Hypothetical patterns depend on historical institutional processes: (A) The War on Drugs and perverse incentives for coca substitution promote coca stabilization within PAs; (B) agrarian policies, such as the Integrated National Program for the Substitution of Illicitly Used Crops (PNIS), that promote cattle as a strategy less "illicit" than coca farming promote conversion from coca to cattle; (C) peace accord policies that enhanced land speculation for cattle ranching. (2) While drivers are not mutually exclusive, places outside the agricultural frontier (PAs and deeper regions of the Amazon) provide incentives for illicit activities that lead to consolidating coca and cattle to obtain rent and guaranteed economic returns for small farmers. (3) Coca and cattle lands produce diverse land-use patterns in the observed Landsat time-series (NIR, SWIR1, Red—false color combination). The areas reported refer to the mean and standard deviation area of change during the 34-year study period in the Amazon [13].



Pires et al. (2023) examine the effects of habitat loss in Amazonian forests on food web complexity. The conversion of natural ecosystems into human-modified landscapes (HMLs) is the main driver of biodiversity loss in terrestrial ecosystems. Even when species persist within habitat remnants, populations may become so small, that ecological interactions are functionally lost, disrupting local interaction networks. To uncover the consequences of land use changes toward ecosystem functioning, there is a need to understand how changes in species richness and abundance in HMLs rearrange ecological networks. The authors used data from forest vertebrate surveys and combined modelling and network analysis to investigate how the structure of predator-prey networks was affected by habitat insularization induced by a hydroelectric reservoir in the Brazilian Amazonia. They found that network complexity, measured by interaction diversity, decayed non-linearly with decreasingly smaller forest area. Although on large forest islands (>100 ha) prey species were linked to 3–4 potential predators, they were linked to one or had no remaining predator on small islands. Using extinction simulations, the authors show that the variation in network structure cannot be explained by abundance-related extinction risk or prey availability. Their findings show that habitat loss may result in an abrupt disruption of terrestrial predator-prey networks, generating low-complexity ecosystems that may not retain functionality. Release from predation on some small islands may produce cascading effects over plants that accelerate forest degradation, whereas predator spillover on others

may result in overexploited prey populations. Our analyses highlight that in addition to maintaining diversity, protecting large continuous forests is required for the persistence of interaction networks and related ecosystem functions [162].

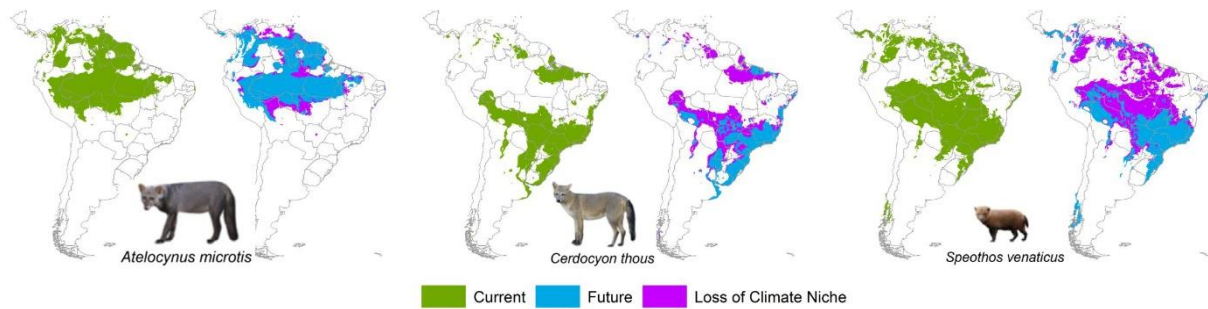
Figure 72: Structure of predator-prey networks (A–F) Variation in different structural descriptors of predator-prey networks as a function of forest area within surveyed forest sites. Circles represent the mean and error bars the standard deviation for the metrics computed for each of 100 potential networks generated per site. The colour gradient follows forest area, and the three darkest circles represent mainland forest sites. Curves represent the model with highest fit [162]



De Oliveira et al. (2023) look at the effect of climate change and deforestation on the habitat of three species of wild canids in the Amazon forest. Ecological traps occur when species choose to settle in lower-quality habitats, even if this reduces their survival or productivity. This happens in situations of drastic environmental changes, resulting from anthropogenic pressures. In the long term, this could mean the extinction of the species. The authors investigated the dynamics of occurrence and distribution of three canid species (*Atelocynus microtis*, *Cerdocyon thous*, and *Sphoerodes venaticus*) considering human threats to their habitats in the Amazon Rainforest. They analyzed the environmental thresholds for the occurrence of these species and related to the future projections of climatic niches for each one. All three species will be negatively affected by climate change in the future, with losses of up to 91% of the suitable area of occurrence in the Brazilian Amazon. *A. microtis* appear to be more forest-dependent and must rely on the goodwill of decision-makers to be maintained in the future. For *C. thous* and *S. venaticus*, climatic variables and those associated with anthropogenic disturbances that modulate their niches today may not act the same way in the future. Even though *C. thous* is least dependent on the Amazon Forest, this species may be affected in the future due to the ecological traps. *S. venaticus* can also undergo the same process, but perhaps more drastically due to the lower ecological plasticity of this species compared to *C. thous*. Their results suggest that the ecological traps may put these two species at risk in the future. Using the canid species as a model, the authors had the opportunity to investigate these ecological effects that can affect a large part of the Amazonian fauna in the current scenario. Considering

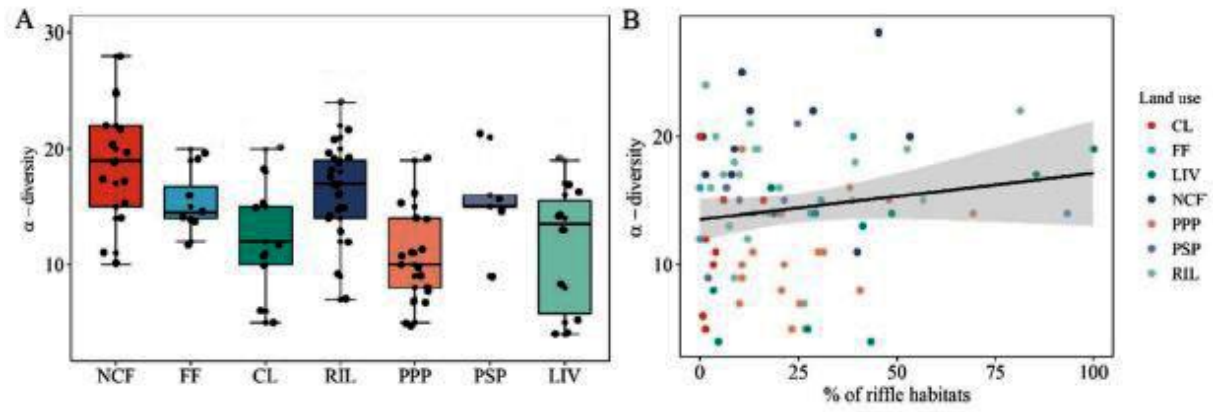
the high degree of environmental degradation and deforestation in the Amazon Rainforest, the theory of ecological traps must be discussed at the same level as habitat loss, considering the strategies for preserving the Amazon biodiversity [163].

Figure 73: Predictions of climatic niche distributions for the three species of wild Amazon canids (*Atelocynus microtis*, *Cerdocyon thous*, and *Speothos venaticus*) in South America, based on a mean ensemble considering the best Jaccard values for each modelling method. Current — Areas of occurrence considering the current climate suitability for the species; Future — Climate niche projections for 2060 for each species; Loss of Climate Niche—Areas that will lose climate suitability for the species in the future [163].



Faria et al. (2023) look at the effects of different land use types on environmental heterogeneity and aquatic insect diversity in Amazonian streams. The Amazon forests are under threat from multiple human land uses, but the effect of the different types of land uses on environmental heterogeneity and the α - and β -diversity of aquatic insects remains unclear. The authors studied how habitat features of streams and aquatic insect diversity in the orders Ephemeroptera, Plecoptera, and Trichoptera (EPT) responded to different land uses in the Brazilian Amazon. By sampling and analyzing EPT community data from 83 streams distributed in multiple land uses and land covers, they found that the impact of forest conversion was mixed. Despite contiguous and fragmented forest streams presenting similar environmental conditions, they differed in insect diversity metrics. α -diversity was highest in contiguous forest streams and EPT β -diversity was higher in streams surrounded by livestock farming and primary oil palm plantations. The association between land use and habitat degradation may not be so direct, mainly when streams are inserted into or surrounded by forest fragments. This has important implications because politicians and policymakers often regard forest fragments as degraded landscapes, to justify their conversion to other land uses. Our study shows that forest fragments must be protected and restored to reduce the risks of degrading the ecological condition of Amazonian streams [164].

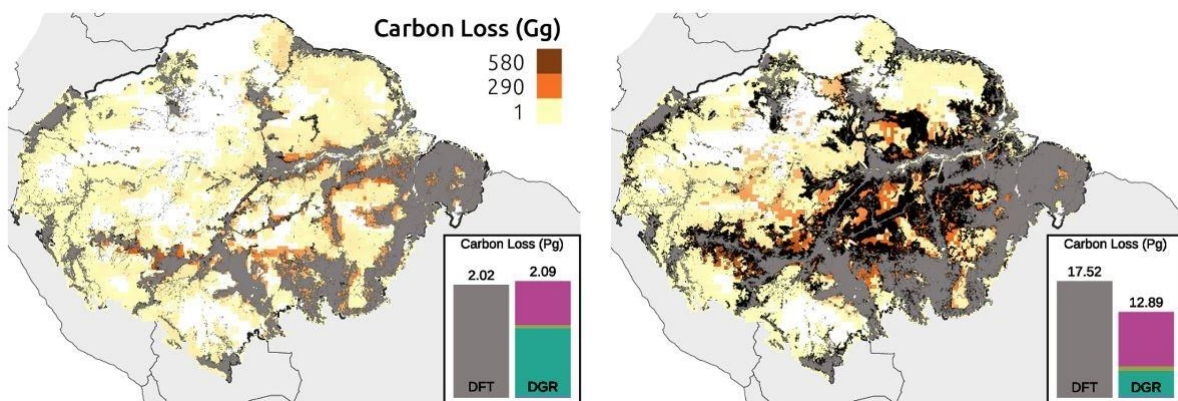
Figure 74: A: Box plot of the EPT α -diversity in the natural contiguous forest (NCF), forest fragment (FF), conventional logging (CL), reduced-impact logging (RIL), plantation of primary oil palm (PPP), plantation of secondary oil palm (PSP), and livestock farming (LIV). The horizontal line represents the median; the box represents the interquartile range (IQR), and the whiskers represent values up to $\pm 1.5 \times$ IQR from the 75th and 25th percentiles, respectively. B: Relationship between α -diversity and % of riffle habitats. The gray color represents the confidence interval of 0.95 for the linear model [164]



8.1.4 Forest degradation

Most analyses of land-use and land-cover change in the Amazon forest have focused on the causes and effects of deforestation. However, anthropogenic disturbances cause degradation of the remaining Amazon forest and threaten their future. Among such disturbances, the most important are edge effects (due to deforestation and the resulting habitat fragmentation), timber extraction, fire, and extreme droughts that have been intensified by human-induced climate change. Lapola et al. (2023) synthesize knowledge on these disturbances that lead to Amazon forest degradation, including their causes and impacts, possible future extents, and some of the interventions required to curb them. Analysis of existing data on the extent of fire, edge effects, and timber extraction between 2001 and 2018 reveals that $0.36 \times 10^6 \text{ km}^2$ (5.5%) of the Amazon forest is under some form of degradation, which corresponds to 112% of the total area deforested in that period. Adding data on extreme droughts increases the estimate of total degraded area to $2.5 \times 10^6 \text{ km}^2$, or 38% of the remaining Amazonian forests. Estimated carbon loss from these forest disturbances ranges from 0.05 to $0.20 \text{ Pg C year}^{-1}$ and is comparable to carbon loss from deforestation (0.06 to $0.21 \text{ Pg C year}^{-1}$). Disturbances can bring about as much biodiversity loss as deforestation itself, and forests degraded by fire and timber extraction can have a 2 to 34% reduction in dry-season evapotranspiration. The underlying drivers of disturbances (e.g. agricultural expansion or demand for timber) generate material benefits for a restricted group of regional and global actors, whereas the burdens permeate across a broad range of scales and social groups ranging from nearby forest dwellers to urban residents of Andean countries. First-order 2050 projections indicate that the four main disturbances will remain a major threat and source of carbon fluxes to the atmosphere, independent of deforestation trajectories [29].

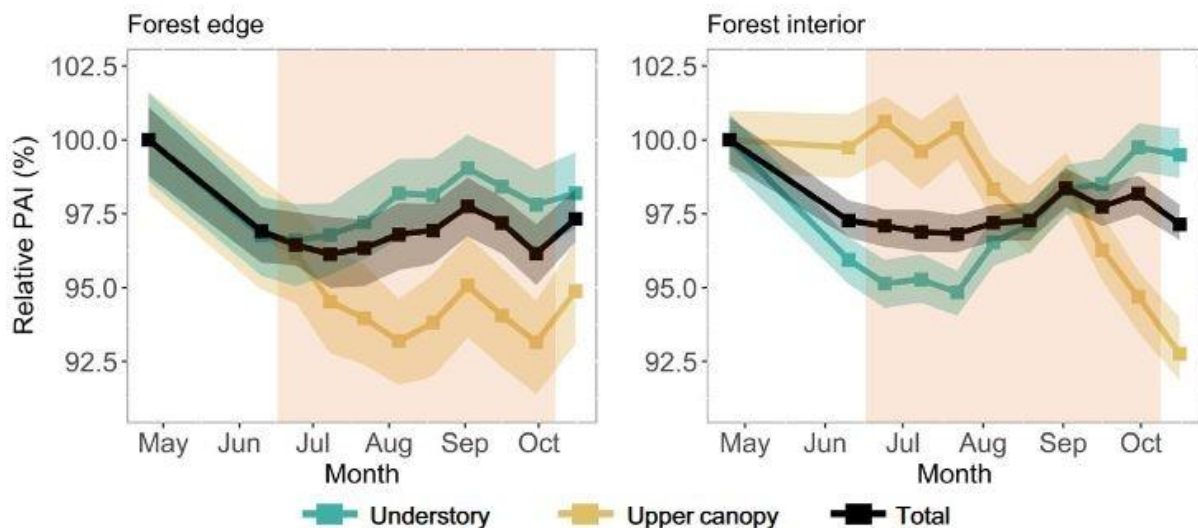
Figure 75: Projections of 2019–2050 resulting combined carbon losses of Amazon forest degradation concerning the main proximate drivers (extreme drought, edge effects, fire occurrence and timber extraction) under climate and deforestation governance (GOV), left and business-as-usual (BAU) scenarios, right. Inset charts show resulting carbon emissions in the 2019–2050 period resulting from deforestation (DFT) and degradation (DGR). The share of C emissions per driver is shown in the DGR bar (purple = edge effect, pink = drought, cyan = fire and green = logging). Black map areas denote deforestation in the 2019–2050 period, whereas gray areas depict deforestation prior to 2019 [29].



Nunes et al. (2022) use terrestrial LiDAR surveys every two weeks spanning wet and dry seasons in Central Amazonia to show that plant phenology varies strongly across vertical strata in old-growth forests, but is sensitive to disturbances arising from forest

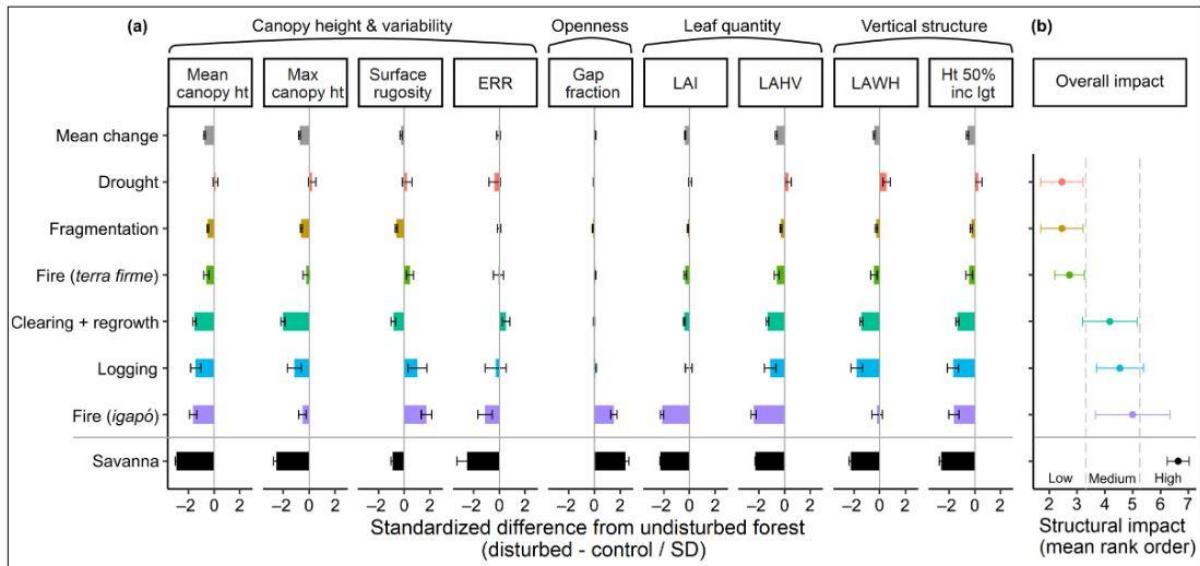
fragmentation. In combination with continuous microclimate measurements, they find that when maximum daily temperatures reached 35 °C in the latter part of the dry season, the upper canopy of large trees in undisturbed forests lost plant material. In contrast, the understory greened up with increased light availability driven by the upper canopy loss, alongside increases in solar radiation, even during periods of drier soil and atmospheric conditions. However, persistently high temperatures in forest edges exacerbated the upper canopy losses of large trees throughout the dry season, whereas the understory in these light-rich environments was less dependent on the altered upper canopy structure. Our findings reveal a strong influence of edge effects on phenological controls in wet forests of Central Amazonia [165].

Figure 76: Predicted relative Plant area index (PAI, %) time-series. Forest phenology acquired using a Terrestrial Laser Scanner (TLS) within the Biological Dynamics of Forest Fragments Project (BDFFP) was vertically stratified, with the understory (<15 m aboveground) and upper canopy (≥15 m aboveground) presenting different trajectories of growth during the dry season. However, the vegetation structure and phenology were both significantly altered by edge effects up to 40 m from the forest fragment margins. The shaded areas represent 95% confidence intervals based on uncertainty in those parameter estimates [165].



Smith et al. (2023) analysed the effects of a range of land-use and climate-change disturbances on fine-scale canopy structure using a large database of profiling canopy lidar collected from disturbed and mature Amazon forest plots. At most of the disturbed sites, surveys were conducted 10–30 years after disturbance, with many exhibiting signs of recovery. Structural impacts differed in magnitude more than in character among disturbance types, producing a gradient of impacts. Structural changes were highly coordinated in a manner consistent across disturbance types, indicating commonalities in regeneration pathways. At the most severely affected site burned *igapó* (seasonally flooded forest) – no signs of canopy regeneration were observed, indicating a sustained alteration of microclimates and consequently greater vulnerability to transitioning to a more open-canopy, savanna-like state. Notably, disturbances rarely shifted forests beyond the natural background of structural variation within mature plots, highlighting the similarities between anthropogenic and natural disturbance regimes, and indicating a degree of resilience among Amazon forests. Studying diverse disturbance types within an integrated analytical framework builds capacity to predict the risk of degradation-driven forest transitions [166].

Figure 77: Structural impact of different disturbance types on (a) key structural metrics that are (b) summarized as the mean rank order impact, from least impacted (drought and fragmentation) to most impacted (burned *igapó*), across all 11 focal metrics included in the HCPC. Structural impacts of burned *igapó* closely align with the structural differences between the savanna versus mature forest contrast (outgroup, black). In (a), impact is quantified as the difference in each structural metric relative to the control forest (disturbed minus control), standardized by the standard deviation (SD); bars show means of transect sections and error bars indicate 95% CIs; grey vertical lines at zero indicate no change relative to the control. Disturbance types are separated into forest type where the latter has an important effect (fire in *terra firme* versus *igapó* forests). Structural metrics are as follows: mean canopy height, maximum canopy height, surface rugosity, ERR, gap fraction, LAI, LAHV, LAWH, and height of 50% incident light [166].



Reducing deforestation underpins global biodiversity conservation efforts. However, this focus on retaining forest cover overlooks the multitude of anthropogenic pressures that can degrade forest quality and imperil biodiversity. Pillay et al. (2022) use remotely sensed indices of tropical rainforest structural condition and associated human pressures to quantify the relative importance of forest cover, structural condition and integrity (the cumulative effect of condition and pressures) on vertebrate species extinction risk and population trends across the global humid tropics. They found that tropical rainforests of high integrity (structurally intact and under low pressures) were associated with lower likelihood of species being threatened and having declining populations, compared with forest cover alone (without consideration of condition and pressures). Further, species were more likely to be threatened or have declining populations if their geographic ranges contained high proportions of degraded forest than if their ranges contained lower proportions of forest cover but of high quality. Our work suggests that biodiversity conservation policies to preserve forest integrity are now urgently required alongside ongoing efforts to halt deforestation in the hyper-diverse humid tropics [167].

Figure 78: The relative importance of forest integrity, structural condition and forest cover on the odds of mammals, birds, reptiles and amphibians being threatened and having declining population trends. Forest integrity tended to be associated with a beneficial effect on biodiversity (lower odds of species being threatened and having declining population trends), relative to forest cover [167].

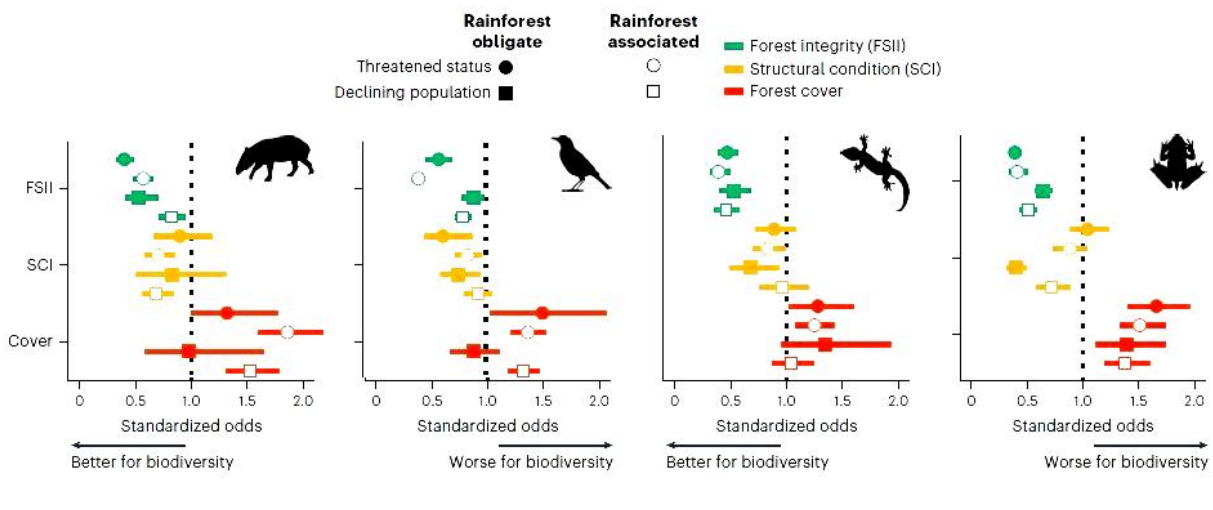
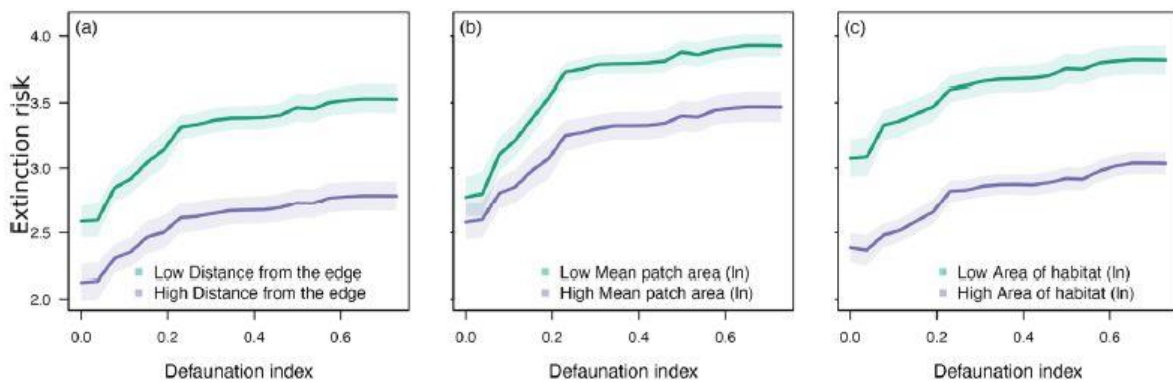


Figure 79: Interaction between area of habitat and threat variables. The plots show the response of one variable at two fixed values of the interacting variable, corresponding to its 5th percentile (green) and 95th percentile (purple). The shaded areas represent the 95% confidence intervals of the responses calculated across the responses of the ten imputed datasets. Different slopes in the two curves represent the interaction between the two variables [168].

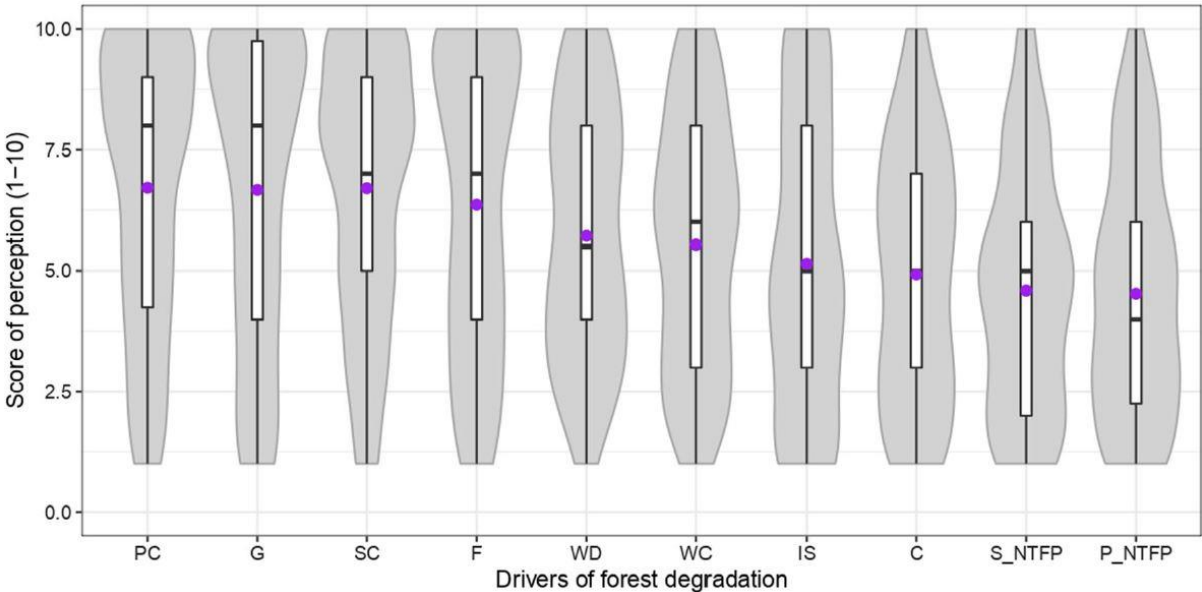


Mancini et al. (2023) examine the synergistic effects of habitat fragmentation and hunting on the extinction risk of neotropical primates. They state that habitat fragmentation and overexploitation of natural resources are the most prevalent and severe threats to biodiversity in tropical forests. Several studies have estimated the effect of these threats on species extinction risk, however the effect resulting from their interaction remains poorly understood. Here, we assess whether and how habitat area, fragmentation, and hunting can synergistically affect the extinction risk of neotropical primates (Platyrrhine). The authors use a Random Forest model to estimate the Red List extinction risk category of 147 primate species based on their biological traits and the environmental predictors they are exposed to. They find that environmental variables are better predictors of extinction risk than biological traits, and that hunting and fragmentation interact creating synergistic feedback that lead to higher extinction risk than when considered in isolation. They also show that the effect of environmental predictors is mediated by biological traits,

with large species being sensitive to habitat area and fragmentation, and frugivorous species more threatened by hunting. The results increase the understanding of potentially interactive effects between different threats, habitat area and species traits, supporting the idea that multiple threats can reinforce each other and should be thus addressed simultaneously in conservation agendas [168].

Armenteras et al. (2022) study the different stakeholders' perspectives of the drivers of forest degradation. They use Colombia as a case study for understanding synergies and trade-offs of the sustainable development goals (SDGs) and analysed what the most important causes are, to whom it matters, and their regional contribution. A common perception was identified, but miscommunication and misunderstandings occur between local- and national-level actors in terms of their views on responsibilities and rates of change. The results are a call for action. According to the authors, cross-scale governance is necessary to improve the design and implementation of policies for forest management at the subnational and local levels and to ensure that we move toward sustainable development without worsening existing inequalities. It is essential that countries provide the enabling conditions to develop a coherent governing framework [169].

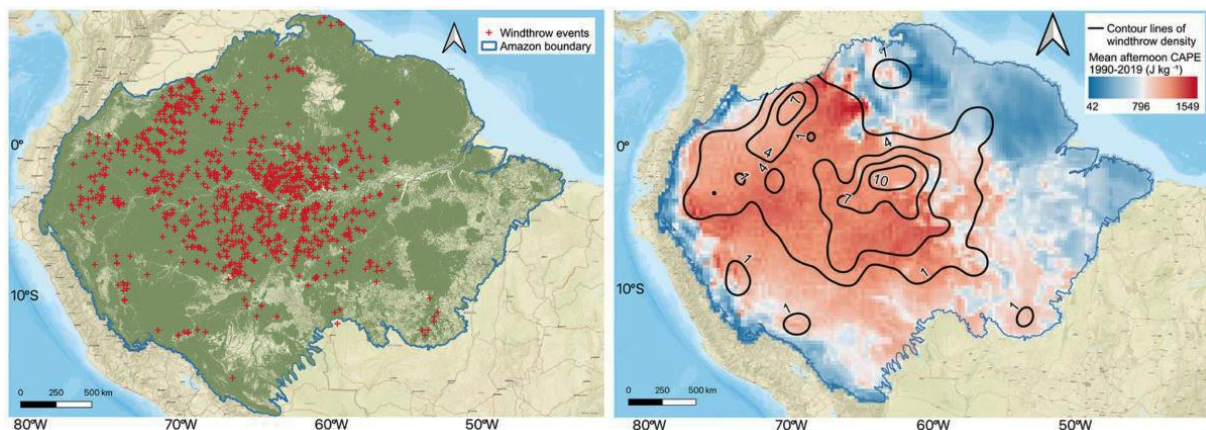
Figure 80: Mean values of stakeholders' perceptions of the importance of forest degradation. The purple dots correspond to the means. The central horizontal bars are the medians. The lower and upper limits of the box are the first and third quartiles. C-coal; F-fire; G-grazing; IS-invasive species; P_NTFFP-persistent extraction for domestic use of NTFP, PC-persistent cutting, S_NTFFP-selective extraction for domestic use of NTFP, SC-selective cutting, WC-wood for commercial use, WD-wood for domestic use [169].



Feng et al. (2023) analyse the interconnection between windthrow disturbances and storm frequency under global warming in the Amazon. Forest mortality caused by convective storms (windthrow) is a major disturbance in the Amazon. However, the linkage between windthrows at the surface and convective storms in the atmosphere remains unclear. In addition, the current Earth system models (ESMs) lack mechanistic links between convective wind events and tree mortality. They find an empirical relationship that maps convective available potential energy, which is well simulated by ESMs, to the spatial

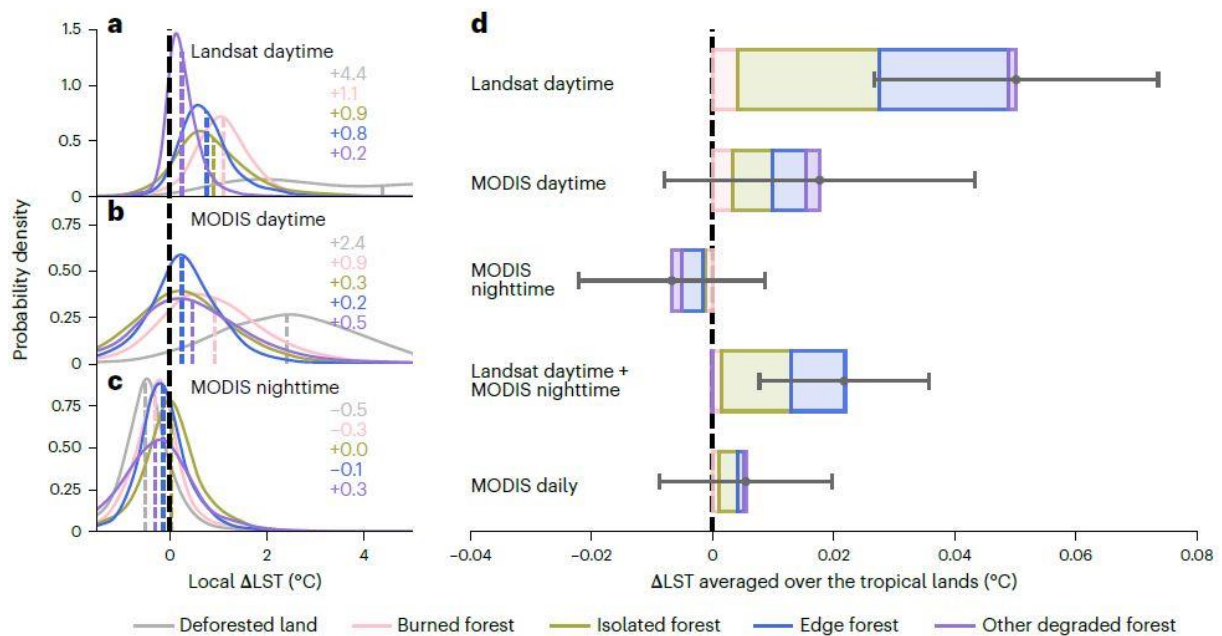
pattern of large windthrow events. This relationship builds connections between strong convective storms and forest dynamics in the Amazon. Based on the relationship, our model projects a $51 \pm 20\%$ increase in the area favourable to extreme storms, and a $43 \pm 17\%$ increase in windthrow density within the Amazon by the end of this century under the high-emission scenario (SSP 585). These results indicate significant changes in tropical forest composition and carbon cycle dynamics under climate change. Tree mortality plays important roles in determining forest carbon balance across Amazonia, and variable disturbance regimes increase uncertainty in the tropical forest carbon sink capacity over time. Extreme convective storms are important drivers of tree mortality in the Amazon region, and affect biomass patterns and function composition of Amazonian forests. In this study, the authors provide a framework for representing the coupling between forest mortality on the land surface and windstorms in the atmosphere. The relationship between extreme storms and tree mortality also implies that increasing frequency of convective storms may contribute to the observed increase in tree mortality and a weakening of the carbon sink across Amazonia [170].

Figure 81: The spatial pattern of windthrows and mean afternoon convective available potential energy (CAPE). Left: 1012 Windthrow events identified manually using Landsat 8 images; green colour in the background represents forested area. Right: Contour lines of windthrow density (counts per 10,000 km²) over the mean afternoon CAPE at 0.25° resolution [170]



Zhu et al. (2023) examine comparable biophysical and biogeochemical feedbacks on warming from tropical moist forest degradation. Degraded forests induce biophysical feedback on climate, as they sustain less cooling from evapotranspiration. The authors estimate the biophysical and biogeochemical temperature changes caused by tropical moist forest degradation using high-resolution remote sensing data from 2010. Degraded forests, including burned, isolated, edge and other degraded forests, account for 24.1% of the total tropical moist forest area. The land surface temperature of degraded tropical moist forests is higher than that of nearby intact forests, leading to a warming effect of $0.022 \pm 0.014^\circ\text{C}$ over the tropics. The cumulative carbon deficit of degraded forests reaches $6.1 \pm 2.0 \text{ PgC}$, equivalent to a biogeochemical warming effect of $0.026 \pm 0.013^\circ\text{C}$. Forest degradation caused by anthropogenic disturbances from 1990 to 2010 induces a daytime warming effect of $0.018 \pm 0.008^\circ\text{C}$ and a carbon deficit of $2.3 \pm 0.8 \text{ PgC}$. These values are of the same order of magnitude as those due to deforestation. Our results emphasize the importance of accounting for the combined biophysical and biogeochemical effects in mitigation pledges related to reducing forest degradation and the restoration of tropical forest [171].

Figure 82: Δ LST (Land Surface Temperature) of forest degradation estimated from different satellite data. Δ LST is calculated as the LST of each land cover type minus the LST of paired interior forests. a–c: Kernel density distributions of Δ LST for Landsat daytime (a), MODIS daytime (b) and MODIS nighttime (c). Coloured dashed lines and numbers show the weighted mean values. d: Biophysical Δ LST averaged over all tropical land areas from different satellite data. Dots and error bars represent the mean values and one standard deviation of all 0.25° grid cells in the tropics [171]



Hughes et al. (2023) look at global hotspots of wildlife trade with a focus on tropical species, and its consequences in the context of phylogenetic and functional diversity, while putting Brazilian wildlife trade into global perspective. Wildlife trade is a multibillion-dollar industry targeting a hyper-diversity of species and can contribute to major declines in abundance. A key question is understanding the global hotspots of wildlife trade for phylogenetic (PD) and functional (FD) diversity, which underpin the conservation of evolutionary history, ecological functions and ecosystem services benefiting humankind. Using a global dataset of traded bird and mammal species, the authors identify that the highest levels of traded PD and FD are from tropical regions, where high numbers of evolutionary distinct and globally endangered species in trade occur. The standardized effect size (ses) of traded PD and FD also shows strong tropical epicentres, with additional hotspots of mammalian ses.PD in the eastern United States and ses.FD in Europe. Large-bodied, frugivorous and canopy-dwelling birds and large-bodied mammals are more likely to be traded whereas insectivorous birds and diurnally foraging mammals are less likely. Where trade drives localized extinctions, the results suggest substantial losses of unique evolutionary lineages and functional traits, with possible cascading effects for communities and ecosystems. Avoiding unsustainable exploitation and lost community integrity requires targeted conservation efforts, especially in hotspots of traded phylogenetic and functional diversity [172].

8.1.5 Forest edge effects

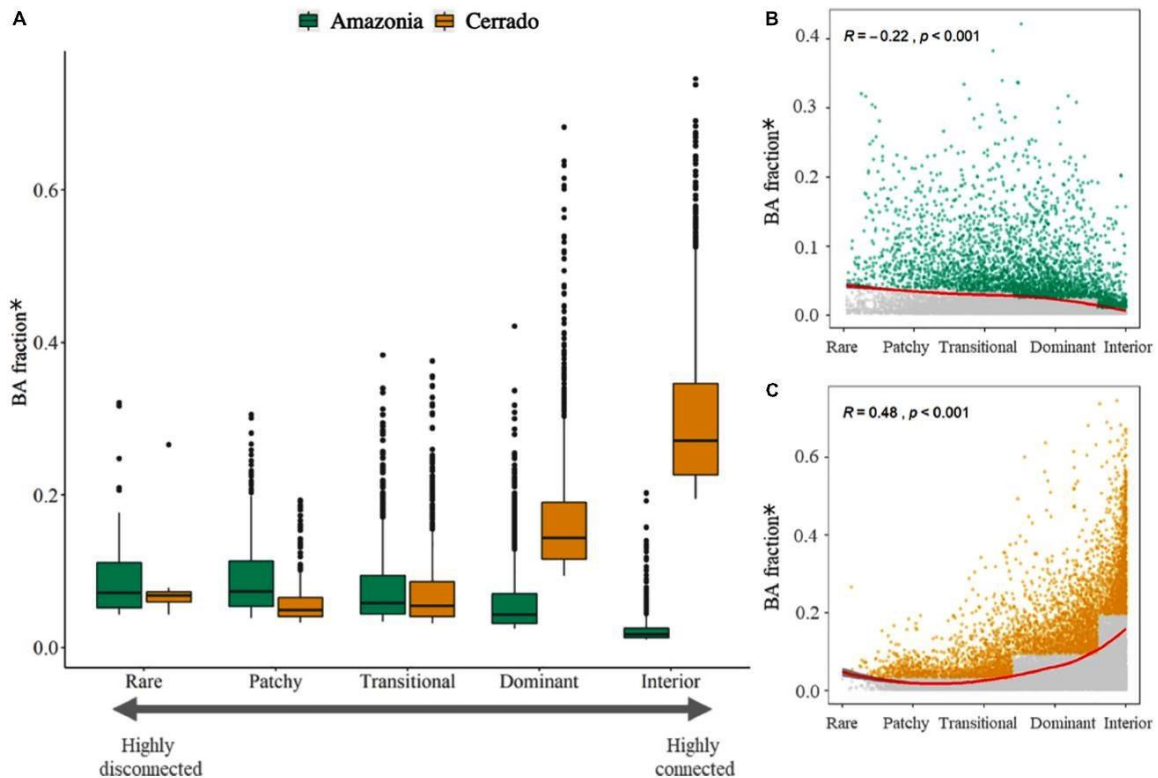
Almost all world's forest areas are predicted to be near edges by 2100, making the detection and prediction of biodiversity responses to edges an urgent need. Yet, idiosyncratic observations across studies have hampered general inferences on the main drivers of edge effects. Willmer et al. (2022) provide a global meta-analysis on 674 forest edge-interior comparisons of plant and animal communities, considering both global and local drivers as well as their interactions, to predict the direction and magnitude of edge effects on species richness. They found a clear latitudinal gradient in both the direction and magnitude of edge effects, with edges in temperate regions having more species than interior forests, while tropical communities generally had fewer species at edges. Unexpectedly, communities near high-contrast edges had higher richness at edges more frequently than near low-contrast edges. In addition, richness decreases at edges were weaker in regions subjected to historical disturbance than regions without historical disturbance. These patterns were modulated by distance from the edge and became clearer when comparing more distant sampling locations. The author's results provide possible explanations for the variable impacts of edge effects and forest fragmentation on biodiversity, showing that a combination of local and global predictors are able to partially predict variation in edge effects. Overall, edge effects tend to cause a decrease in species richness at tropical forest edges more frequently than in temperate communities. In addition, richness decreases at edges are stronger in regions not subjected to historical disturbance. Thus, environmental filters at different time scales mediate community responses to edges. Considering environmental contrasts, increases in species richness are more likely to occur adjacent to hard matrices. This suggests that mechanisms such as resource complementation might be more important than anticipated. The finding that edge effects contribute to both increases and decreases in species richness at forest edges, depending on the historical and ecological conditions of the study site, provides a possible explanation for the well-known heterogeneity in both edge and fragmentations effects on biodiversity. Given that both the direction and magnitude of edge effects vary according to local and global drivers, the authors reinforce the conclusion that tropical communities are more prone to local species loss due to edge proximity. Therefore, actions to reduce edge density may be especially needed in tropical landscapes. Finally, the study indicates that assuming a unique landscape design is ideal for biodiversity conservation globally may be inadequate, since edge impacts on species richness are clearly spatially heterogeneous [173].

Püttker et al. (2020) look at indirect effects of habitat loss via habitat fragmentation with a cross-taxa analysis of forest-dependent species in the Brazilian Atlantic Forest. Recent studies suggest that habitat amount is the main determinant of species richness, whereas habitat fragmentation has weak and mostly positive effects. The authors challenge these ideas using a multi-taxa database, including 2230 estimates of forest-dependent species richness from 1097 sampling sites across the Brazilian Atlantic Forest biodiversity hotspot. They used a structural equation modelling approach, accounting not only for direct effects of habitat loss, but also for its indirect effects (via habitat fragmentation), on the richness of forest-dependent species. The authors reveal that in addition to the effects of habitat loss, habitat fragmentation has negative impacts on animal species richness at intermediate (30-60%) levels of habitat amount, and on richness of plants at high (> 60%) levels of habitat amount, both of which are mediated by edge effects. Based on these results, they argue that dismissing habitat fragmentation as a powerful force driving species extinction in tropical forest landscapes is premature and unsafe. Since the magnitude of edge effects depend on the land use next to habitat, the study's results highlight that – besides increasing habitat amount – reducing total length of edges and/or edge contrast and thereby the extent of edge effects in intermediate to high-forested

landscapes may be a very effective tool in maximizing species retention. In addition, our results suggest that forest fragmentation should have detectable impacts on species even in highly forested landscapes. If the configuration of forest patches in such landscapes results in high edge density, biological, and especially plant communities, may lose a significant number of species, even at high total levels of habitat amount and connectivity [174].

8.1.6 Forest fires

Figure 83: Boxplot with the average (2002–2018) normalized burned area (BA) fraction by each FAD category for Amazonia and Cerrado biomes; (B) Scatterplot showing the relationship between the normalized BA fraction and FAD for Amazonia, points highlighted in green were used in the boxplot (>75th percentile) for each category, grey points are the lower 75th percentile and the red line shows the fitted loess regression considering all the grid-cells; (C) Scatterplot showing the relationship between the normalized BA fraction and FAD for Cerrado, points highlighted in orange were used in the boxplot (>75th percentile) for each category, grey points are values <75th percentile and the red line shows the fitted LOESS regression considering all the grid-cells [175].

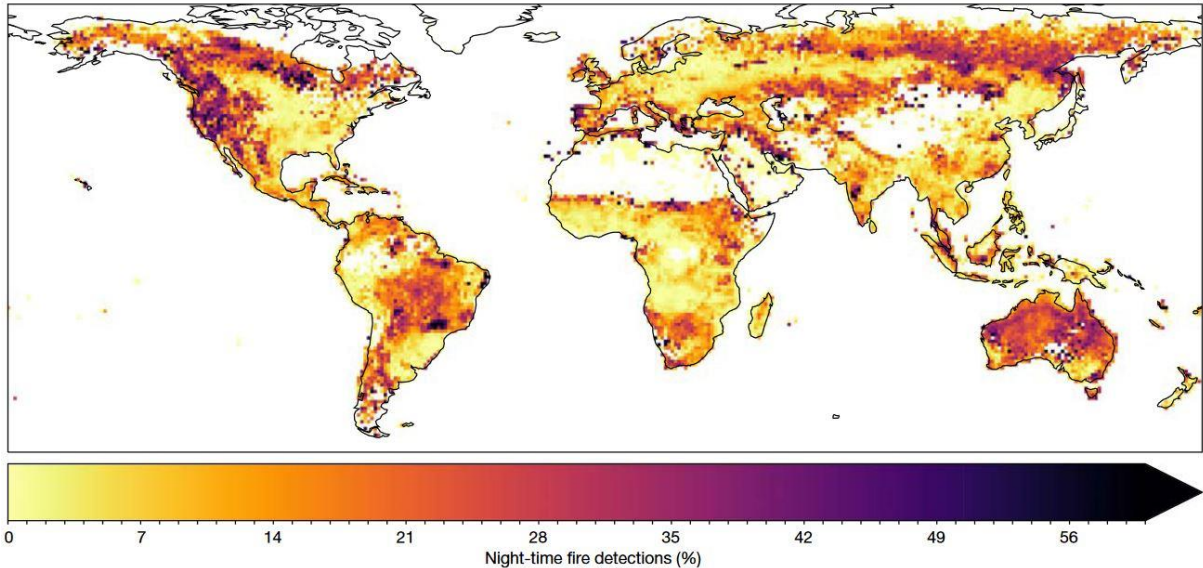


The two major Brazilian biomes, Amazonia and Cerrado (savanna), are increasingly exposed to fires. The Amazonian Forest is a fire sensitive ecosystem where fires are a typically rare disturbance while the Cerrado is naturally fire-dependent. Human activities, such as landscape fragmentation and land-use management, have modified the fire regime of the Cerrado and introduced fire into the Amazonian Forest. There is limited understanding of the role of landscape fragmentation on fire occurrence in the Amazonia and Cerrado biomes. Due to differences in vegetation structure, composition, and land use characteristics in each biome, Rosan et al. (2022) hypothesize that the emerging burned area (BA) patterns will result from biome-specific fire responses to fragmentation. The aim of this study was to test the general relationship between BA, landscape fragmentation, and agricultural land in the Amazonia and the Cerrado biomes. To estimate the trends and status of landscape fragmentation a Forest Area Density (FAD) index was calculated based on the MapBiomas land cover dataset for both biomes between 2002 and 2018. BA fraction was analysed within native vegetation against the FAD and agricultural land fraction. The results showed an increase in landscape fragmentation across 16% of Amazonia and 15% of Cerrado. They identified an opposite relationship between BA fraction, and landscape fragmentation and agricultural fraction contrasting the two biomes. For Amazonia, both landscape fragmentation and agricultural fraction increased BA fraction due to an increase of human ignition activities. For the Cerrado, on the other hand, an increase in landscape

fragmentation and agricultural fraction caused a decrease in BA fraction within the native vegetation. For both biomes, the authors found that during drought years BA increases whilst the divergent trends driven by fragmentation in the two contrasting global biomes are maintained. This understanding will be critical to informing the representation of fire dynamics in fire-enabled Dynamic Global Vegetation Models and Earth System Models for climate projection and future ecosystem service provision [175].

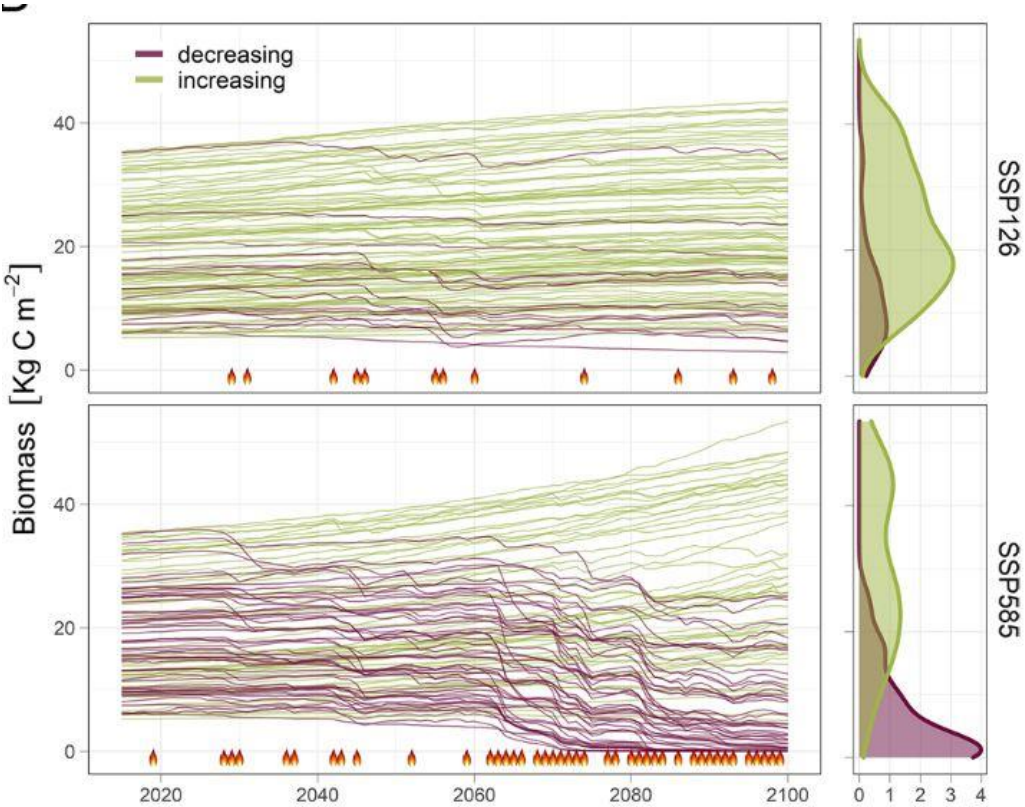
Balch et al. (2022) look at the effect of rising temperatures on the night-time barriers to global fire. Night-time provides a critical window for slowing or extinguishing fires owing to the lower temperature and the lower vapour pressure deficit (VPD). However, fire danger is most often assessed based on daytime conditions, capturing what promotes fire spread rather than what impedes fire. Although it is well appreciated that changing daytime weather conditions are exacerbating fire, potential changes in night-time conditions — and their associated role as fire reducers — are less understood. The authors show that night-time fire intensity has increased, which is linked to hotter and drier nights. Their findings are based on global satellite observations of daytime and night-time fire detections and corresponding hourly climate data, from which landcover-specific thresholds of VPD (VPDt) are determined, below which fire detections are very rare (less than 95 per cent modelled chance). Globally, daily minimum VPD increased by 25 per cent from 1979 to 2020. Across burnable lands, the annual number of flammable night-time hours—when VPD exceeds VPDt—increased by 110 hours, allowing five additional nights when flammability never ceases. Across nearly one-fifth of burnable lands, flammable nights increased by at least one week across this period. Globally, night fires have become 7.2 per cent more intense from 2003 to 2020, measured via a satellite record. These results reinforce the lack of night-time relief that wildfire suppression teams have experienced in recent years. The authors expect that continued night-time warming owing to anthropogenic climate change will promote more intense, longer-lasting and larger fires [176].

Figure 84: Large portions of the globe experience night-time fires. The map shows the percentage of 2003–2020 active fire detections (n = 80,190,449) that occurred at night, from MODIS Fire Information for Resource Management System (FIRMS) data aggregated to 1° resolution. The displayed pixel values are thresholded at 60% detection; less than 1% of the mapped land area had more than 60% of fire detections at night [176].



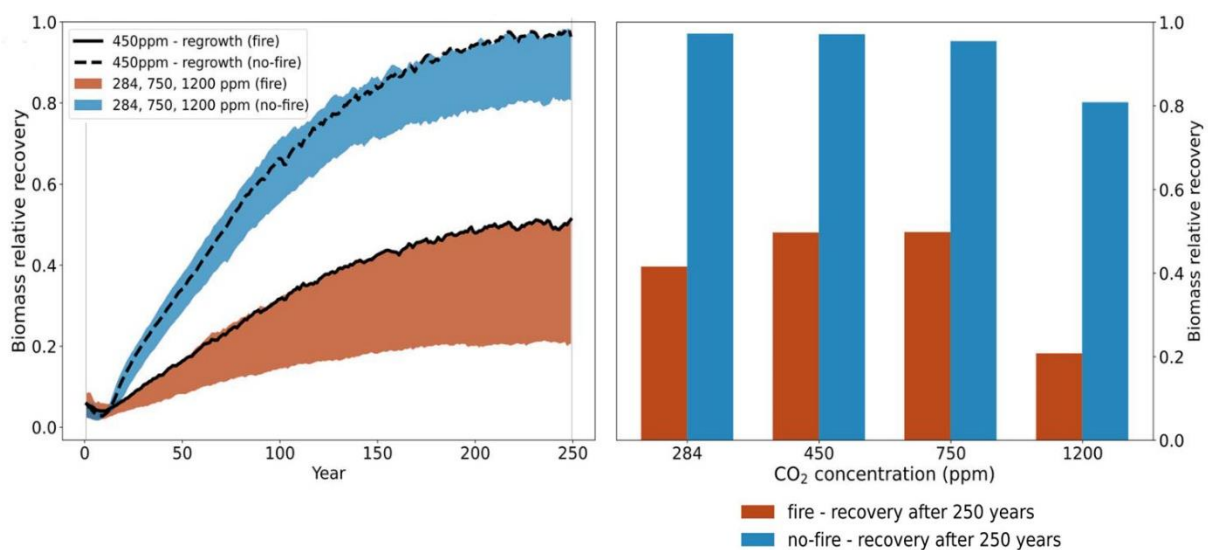
Tropical forests contribute a major sink for anthropogenic carbon emissions essential to slowing down the build-up of atmospheric CO₂ and buffering climate change impacts, according to Cano et al. (2022). However, the response of tropical forests to more frequent weather extremes and long-recovery disturbances like fires remains uncertain. Analyses of field data and ecological theory raise concerns about the possibility of the Amazon crossing a tipping point leading to catastrophic tropical forest loss. In contrast, climate models consistently project an enhanced tropical sink. The authors show a heterogeneous response of Amazonian carbon stocks in GFDL-ESM4.1, an Earth System Model (ESM) featuring dynamic disturbances and height-structured tree-grass competition. Enhanced productivity due to CO₂ fertilization promotes increases in forest biomass that, under low emission scenarios, last until the end of the century. Under high emissions, positive trends reverse after 2060, when simulated fires prompt forest loss that results in a 40% decline in tropical forest biomass by 2100. Projected fires occur under dry conditions associated with El Niño Southern Oscillation and the Atlantic Multi-decadal Oscillation, a response observed under current climate conditions, but exacerbated by an overall decline in precipitation. Following the initial disturbance, grassland dominance promotes recurrent fires and tree competitive exclusion, which prevents forest recovery. EC-Earth3-Veg, an ESM with a dynamic vegetation model of similar complexity, projected comparable wildfire forest loss under high emissions but faster post-fire recovery rates. The results reveal the importance of complex nonlinear responses to assessing climate change impacts and the urgent need to research post-fire recovery and its representation in ESMs [177].

Figure 85: Projected trends in total tree biomass in the Neo-tropics based on GFDL-ESM4.1 global simulations under CMIP6 emission scenarios SSP1-2.6 (optimistic future pathway) and SSP5-8.5 (pessimistic future pathway). Each line corresponds to the dynamics of natural tropical forests in an individual grid cell location (i.e., tiles that were unaffected by changes in land use). Trajectories showing a decrease in total biomass are highlighted with a purple hue. Flames along the abscissa indicate years with high carbon emissions due to fires. *Right:* Distribution (as probability density function) of tree biomass by the end of the simulation for grid cell locations showing increasing or decreasing trends [177].



Drüke et al. (2023) examine the impact of fire for the potential future Amazon forest recovery after large-scale deforestation. Previous research highlighted the role of fire in amplifying irreversible large-scale Amazon die-back. However, large-scale feedback analyses, which integrate the interplay of fire with climate and land-use change, are currently lacking. To address this gap, the authors applied the fire-enabled Potsdam Earth Model to examine these feedback mechanisms in the Amazon. By studying forest recovery after complete deforestation, we discovered that fire prevents regrowth across 56-82% of the potential natural forest area, contingent on atmospheric carbon dioxide levels. After a 250 years-long grassland phase, the model allowed trees to re-establish in the Amazon region in the final simulation phase of 250 years (recovery phase). Without fire, ca. 95% of the original biomass recovered in all scenarios tested except under the 1200 ppm scenario, which regained only ca. 80% of the corresponding control experiment. For the latter, extremely dry and hot conditions persisted in parts of the northern Amazon such that extreme heat stress on woody vegetation prevented forest recovery. The research emphasizes the significant contribution of fire to the irreversible transition, effectively locking the Amazon into a stable grassland state. Introducing fire dynamics into future assessments is vital for understanding climate and land-use impacts in the region [178].

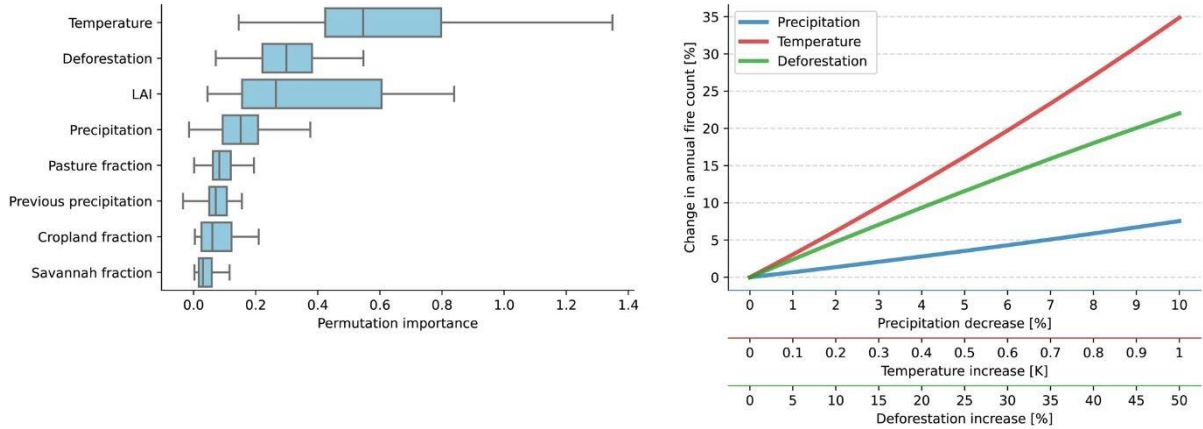
Figure 86: Left: Time series of biomass recovery. Without fire (dashed line for 450 ppm and blue area for other CO₂ concentrations), biomass nearly fully recovers under 284, 450, and 750 ppm, respectively, but only 80% under 1200 ppm. Fire (solid line for 450 ppm and red area for other CO₂ concentrations) inhibits full biomass recovery, with only 20% (at 1200 ppm), 40% (at 284 ppm), and 50% (at 450 ppm and 750 ppm) of biomass recovered after 250 years. Right: Bar plot showing final relative biomass under different atmospheric CO₂ concentration forcing (mean of the last 10 years of the recovery phase). Biomass is normalized to its corresponding control simulation experiment (same atmospheric CO₂ concentration) [178].



Butt et al. (2022) look at the relation between deforestation, fire and air quality in the Brazilian Amazon. Climate, deforestation, and forest fires are closely coupled in the Amazon, but models of fire that include these interactions are lacking. The authors trained machine-learning models on temperature, rainfall, deforestation, land-use, and fire data to show that spatial and temporal patterns of fire in the Amazon are strongly modified by deforestation. They find that fire count across the Brazilian Amazon increases by 0.44 percentage points for each percentage point increase in deforestation rate. Butt et al. used the model to predict that the increased deforestation rate in the Brazilian Amazon from 2013 to 2020 caused a 42% increase in fire counts in 2020. They predict that if Brazil had

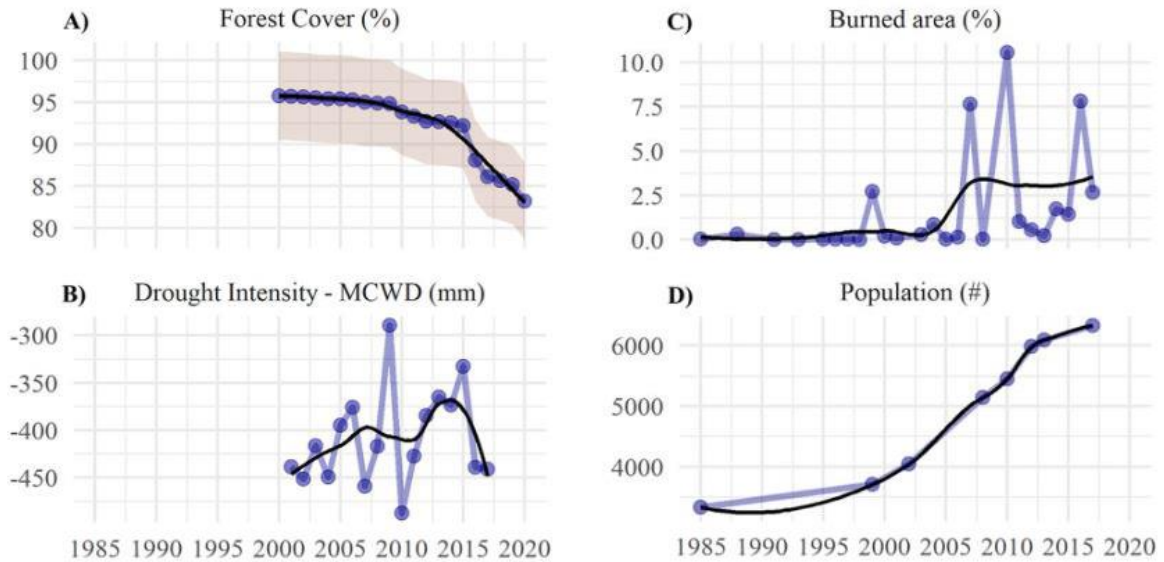
achieved the deforestation target under the National Policy on Climate Change, there would have been 32% fewer fire counts across the Brazilian Amazon in 2020. Using a regional chemistry-climate model and exposure-response associations, they estimate that the improved air quality due to reduced smoke emission under this scenario would have resulted in 2,300 fewer deaths due to reduced exposure to fine particulate matter. The analysis demonstrates the air quality and public health benefits that would accrue from reducing deforestation in the Brazilian Amazon [157].

Figure 87: Left: Permutation importance across all years (2003–2020) representing the importance of features for fire count prediction. Boxes show quartiles of the calculated permutation importance across individual years the median of which showing 50th percentile. Calculated permutation importance is taken as an average combination of neural network (NN) and XGBoost (XGB). Right: Model (NN and XGB) prediction sensitivity showing annual change in total fires across the BAB as a function of incremental changes in surface temperature (+0.1 K to +1K), precipitation (−1% to −10%) and deforestation (+1% to +50%) calculated as an average across all years (2003–2020) [157].



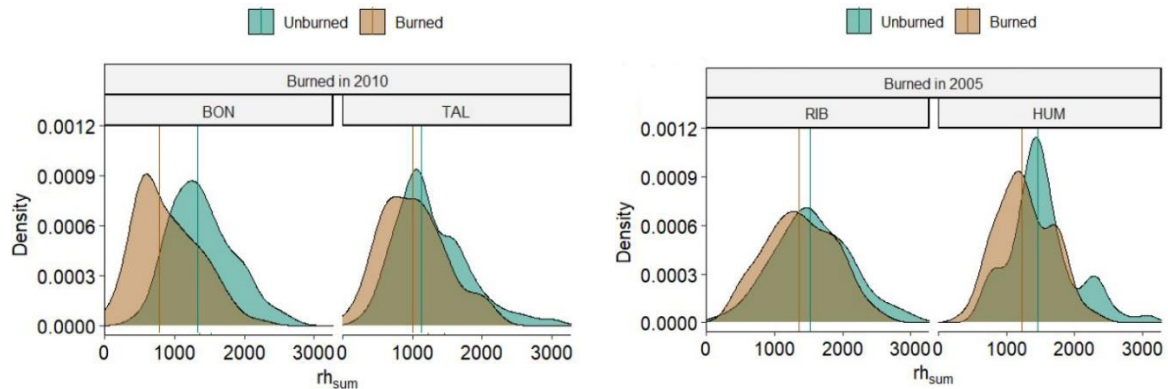
Silvério et al. (2022) examine the intensification of fire regimes in the Southern Amazon. The contemporary fire regime of southern Amazonian forests has been dominated by interactions between droughts and sources of fire ignition associated with deforestation and slash-and-burn agriculture. Until recently, wildfires have been concentrated mostly on private properties, with protected areas functioning as large-scale firebreaks along the Amazon’s agricultural frontier. However, as the climate changes, protected forests have become increasingly flammable. The authors have quantified forest degradation in the ‘Território Indígena do Xingu’ (TIX), an iconic area of 2.8 million hectares where over 6000 people from 16 different ethnic Indigenous groups live across 100 villages. Their main hypothesis was that forest degradation, defined here as areas with lower canopy cover, inside the TIX is increasing due to pervasive sources of fire ignition, more frequent extreme drought events, and changing slash-and-burn agricultural practices. Between 2001 and 2020, nearly 189 000 hectares (~7%) of the TIX became degraded by recurrent drought and fire events that were the main factors driving forest degradation, particularly in seasonally flooded forests. After three fire events, the probability of forest loss was higher in seasonally flooded areas (63%) compared to upland areas (41%). Given the same fire frequency, areas that have not suffered with extreme droughts showed a 24% lower probability of forest loss compared to areas that experienced three drought events. Distance from villages and human density had a marked effect on forest cover loss, which was generally higher in areas close to the largest villages. In one of the most culturally diverse Indigenous lands of the Amazon, in a landscape highly threatened by deforestation, our findings demonstrate that climate change may have already exceeded the conditions to which the system has adapted [179].

Figure 88: Temporal changes in percent forest cover of 'Território Indígena do Xingu' (TIX) from 2001 to 2020 (A); drought intensity, estimated based on the maximum cumulative water deficit (MCWD) based on rainfall data from the Tropical Rainfall Measuring Mission (TRMM; from 2001 to 2017) (B); percentage of TIX area burned yearly from 1985 to 2017 (C); and number of people living inside the TIX 1985–2017 (D) [179].



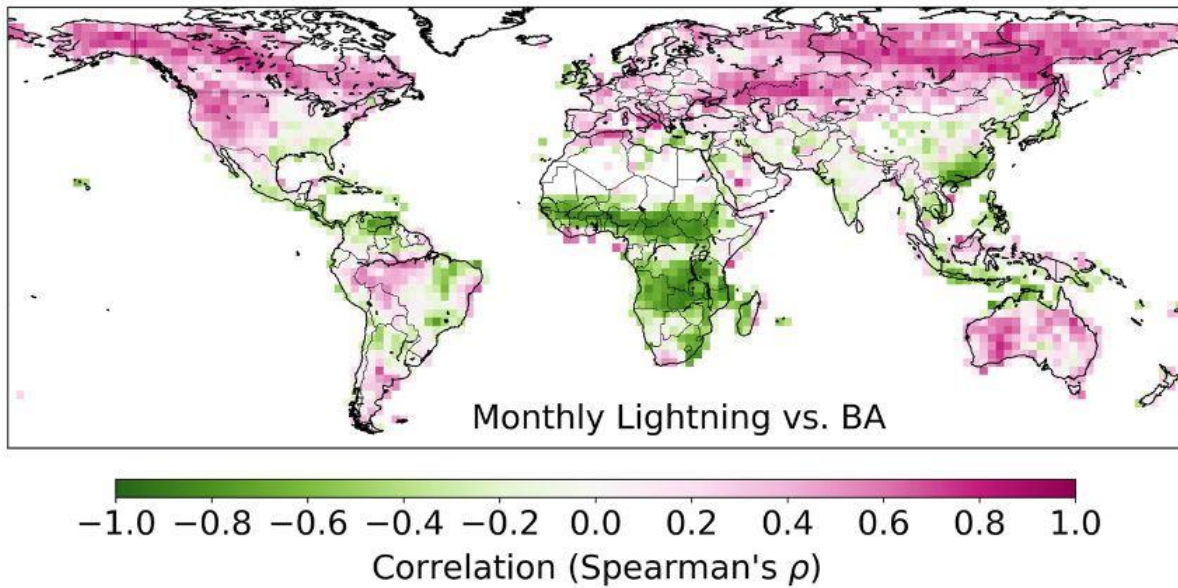
East et al. (2023) measure understory fire effects from space, and ask how the forest canopy changes in response to tropical understory fire. The ability to measure the ecological effects of understory fire in the Amazon on a landscape scale remains a frontier in remote sensing. The Global Ecosystem Dynamics Investigation's (GEDI) LiDAR data have been widely suggested as a critical new tool in this field. In this paper, the authors use the GEDI Simulator to quantify the nuanced effects of understory fire in the Amazon, and assess the ability of on-orbit GEDI data to do the same. While numerous ecological studies have used simulated GEDI data, on-orbit constraint may limit ecological inference. The authors focused on understory fire, one of the most challenging fire types to measure using remote sensing. Overall, they found mixed results for applications of on-orbit GEDI data to tropical fire. While simulated large-footprint GEDI data provide a novel look into the effects of understory fire on canopy structure, these data did not capture the intricacies of regeneration. According to the authors, they were able to detect the greatest differences in canopy metrics in the mid to lower canopy, with time-lag dynamics shifting those differences upward in the canopy with time. The analysis was also limited to areas that burned 3 to 8 years previously; they could not assess how the canopy profile would have changed directly following fire due to data constraints. However, given the relatively small effect size in terms of meter difference through canopy measurements, it is unlikely that GEDI's relative height product has the data accuracy to detect the same changes [180].

Figure 89: Density distributions for RHsum values, an indicator of fire severity, across fires between burned and unburned samples for four sites (Bonal, Talismã, Rio Branco and Humaitá) in a simulated waveform and relative height curve. Vertical lines represent median values [180].



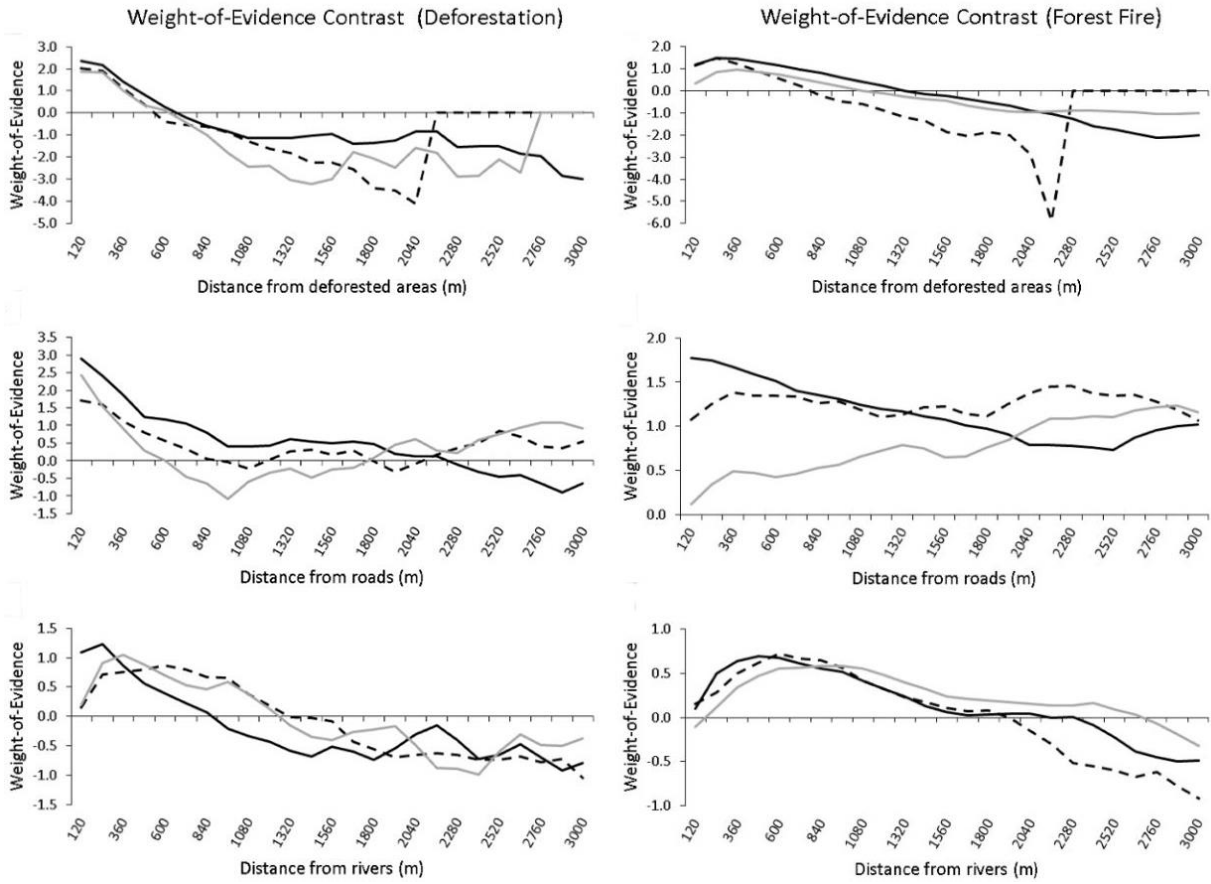
Jones et al. (2022) present a throughout and detailed overview on the global and regional trends and drivers of fire under climate change. The authors review current understanding of the impacts of climate change on fire weather (weather conditions conducive to the ignition and spread of wildfires) and the consequences for regional fire activity as mediated by a range of other bioclimatic factors (including vegetation biogeography, productivity and lightning) and human factors (including ignition, suppression, and land use). Through supplemental analyses, they present a stocktake of regional trends in fire weather and burned area (BA) during recent decades, and examine how fire activity relates to its bioclimatic and human drivers. Fire weather controls the annual timing of fires in most world regions and also drives inter-annual variability in BA in the Mediterranean, the Pacific US and high latitude forests. Increases in the frequency and extremity of fire weather have been globally pervasive due to climate change during 1979–2019, meaning that landscapes are primed to burn more frequently. Correspondingly, increases in BA of ~50% or higher have been seen in some extratropical forest ecoregions including in the Pacific US and high-latitude forests during 2001–2019, though inter-annual variability remains large in these regions. Nonetheless, other bioclimatic and human factors can override the relationship between BA and fire weather. For example, BA in savannahs relates more strongly to patterns of fuel production or to the fragmentation of naturally fire-prone landscapes by agriculture. Similarly, BA trends in tropical forests relate more strongly to deforestation rates and forest degradation than to changing fire weather. Overall, BA has reduced by 27% globally in the past two decades, due in large part to a decline in BA in African savannahs. According to climate models, the prevalence and extremity of fire weather has already emerged beyond its pre-industrial variability in the Mediterranean due to climate change, and emergence will become increasingly widespread at additional levels of warming. Moreover, several of the major wildfires experienced in recent years, including the Australian bushfires of 2019/2020, have occurred amidst fire weather conditions that were considerably more likely due to climate change. Current fire models incompletely reproduce the observed spatial patterns of BA based on their existing representations of the relationships between fire and its bioclimatic and human controls, and historical trends in BA also vary considerably across models. Advances in the observation of fire and understanding of its controlling factors are supporting the addition or optimization of a range of processes in models. Overall, climate change is exerting a pervasive upwards pressure on fire globally by increasing the frequency and intensity of fire weather, and this upwards pressure will escalate with each increment of global warming. Improvements to fire models and a better understanding of the interactions between climate, climate extremes, humans and fire are required to predict future fire activity and to mitigate against its consequences [181].

Figure 90: Spearman's correlation (ρ) between burned area (BA) and lightning activity, mapped at 2.5° resolution. Spearman's correlation between climatological monthly BA (2001–2019) and climatological monthly lightning activity in the periods 1995–2000 (extra-tropics) or 1998–2010 (tropics) [181].



Dos Reis et al. (2021) evaluate the effects of landscape and climate on spatial and temporal dynamics of forest fires and deforestation in an area near Manaus, Central Amazonas, Brazil. Forest fires and deforestation are the main threats to the Amazon forest. Extreme drought events exacerbate the impact of forest fire in the Amazon, and these drought events are predicted to become more frequent due to climate change. Fire escapes into the forest from agriculture and pasture areas. The authors assessed the potential drivers of deforestation and forest fires in the central Brazilian Amazon and show that over a period of 31 years (1985–2015) forest fires occurred only in years of extreme drought induced by El Niño (1997, 2009 and 2015). The association of forest fires with strong El Niños shows the vulnerability of forest to climate change. The areas deforested were closely associated with navigable rivers: 62% of the total deforestation from 2000 to 2018 was located within the 2 km of rivers. There was a notable increase in deforestation and forest fire during the 2015 El Niño in comparison to previous years. Only a small part of the forest that burned was deforested in the years following the wildfires: 7% (1997), 3% (2009) and 1.5% (2015). Forest close to roads, rivers and established deforestation is susceptible to deforestation and fire since these areas are attractive for agriculture and pasture. Indigenous land was shown to be important in protecting the forest, while rural settlement projects attracted both forest fire and deforestation. Of the total area in settlement projects, 40% was affected by forest fires and 17% was deforested. Rivers are particularly important for deforestation in this part of Amazonia, and efforts to protect forest along the rivers are therefore necessary. The ability to predict where deforestation and fires are most likely to occur is important for designing policies for preventative actions [182].

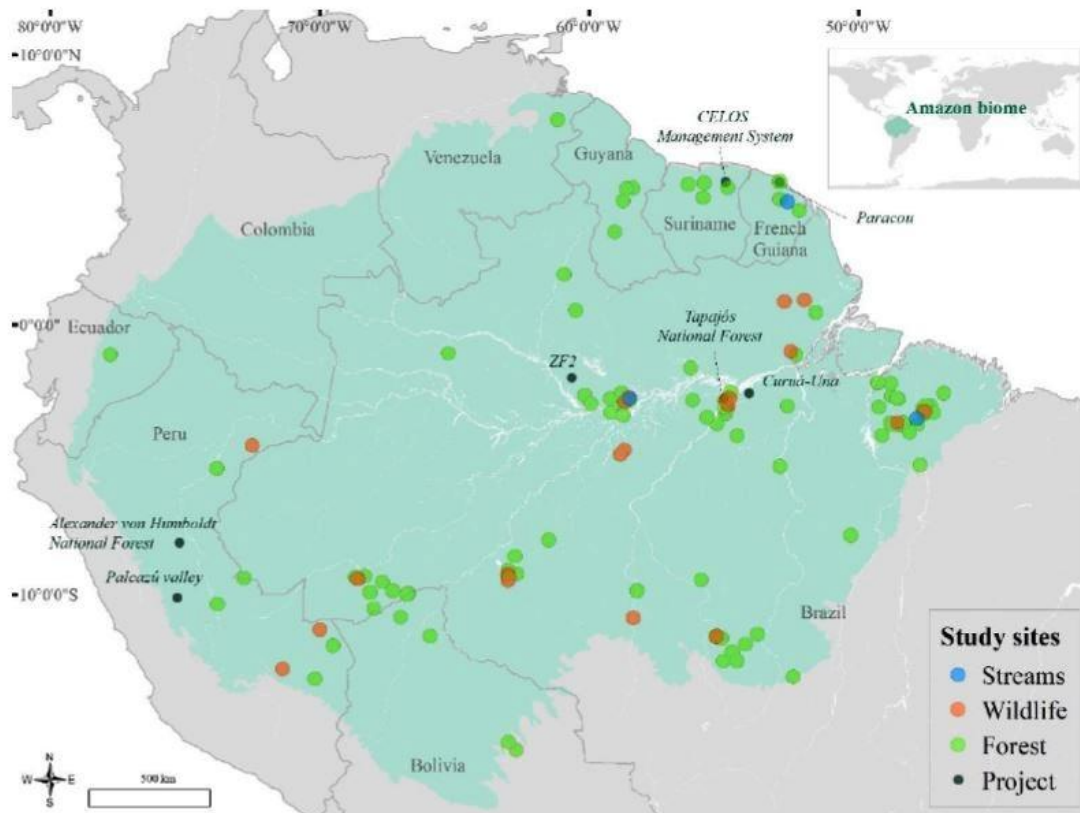
Figure 91: Weights-of-evidence contrast of variables that influence the occurrence of deforestation (left) and forest fires (right), with the variables 'distance to deforested areas' (top), 'distance to roads' (centre), and 'distance to rivers' (bottom) [182]



8.1.7 Selective logging

DeArmond et al. (2023) conduct a systematic review on logging impacts in the Amazon biome. Every year, logging in the world’s largest tropical forest, located within the Amazon biome, continues unabated. Although it is a preferred alternative to deforestation, the residual stand and site are impacted by logging. The objective of this review was to determine and assess the current state of research throughout Amazonia on the subject of logging impacts. To achieve this goal, a systematic approach was utilized to gather, assess and categorize research articles conducted in the Amazon biome over the last decade. Eligibility for inclusion of articles required demonstration of a direct impact from logging operations. A total of 121 articles were determined to meet the eligibility requirements and were included in this review. Articles were subdivided into three environmental categories: forest (n = 85), wildlife (n = 24) and streams (n = 12). The results of this review demonstrated that impacts from logging activities to the forest site were a direct result of the logging cycle (e.g., how often logging occurs) or logging intensity (e.g., how many trees are felled). The impacts to wildlife varied dependent on species, whereas impacts to streams were affected more by the logging system. Overall, research suggested that to attain sustainability and diminish the impacts from logging, a lower logging intensity of 10–15 m³ ha⁻¹ and a longer logging cycle of 40–60 years would be essential for the long-term viability of forest management in Amazonia [183].

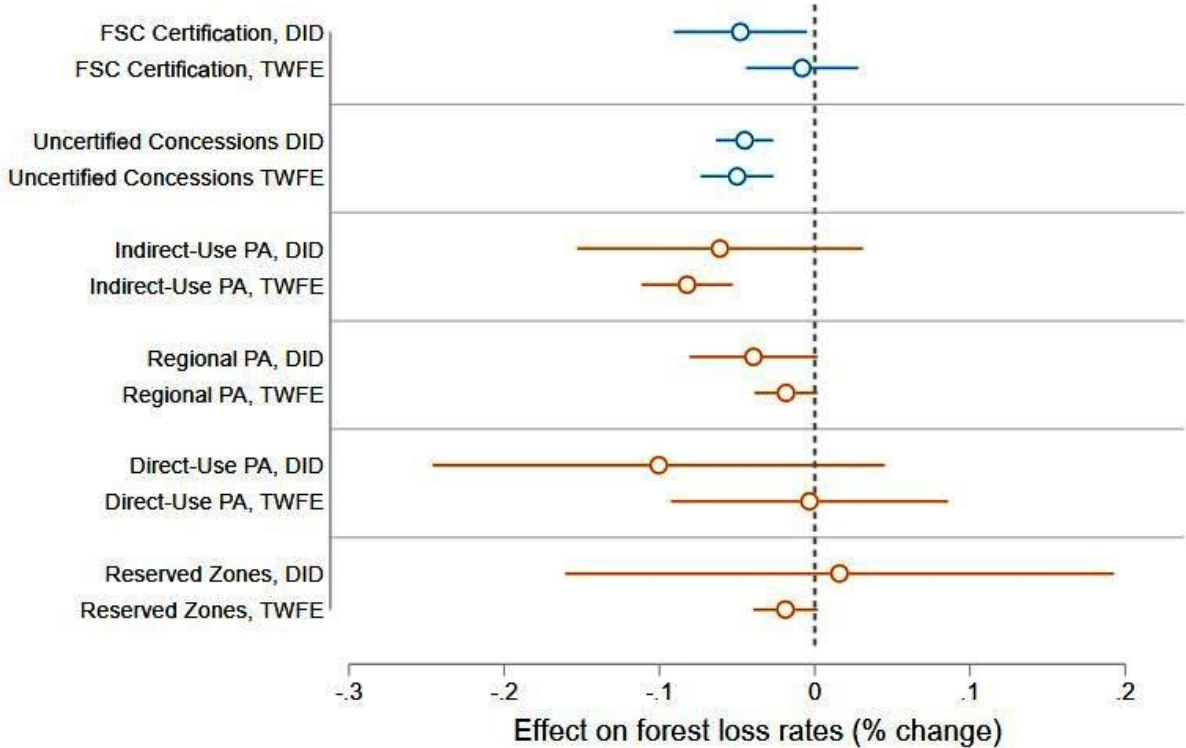
Figure 92: Locations of study sites throughout the Amazon biome included in review [183]



Forest concessions that grant logging rights to firms support economic development based on forest resources. Eco-certifications put sustainability restrictions on the operations of those concessions. For spatially detailed data, including many pre-treatment years, Rico-Straffon et al. (2023) use new difference-indifferences estimators to estimate 2002–2018 impacts upon Peruvian Amazon forests from both logging concessions and their eco-

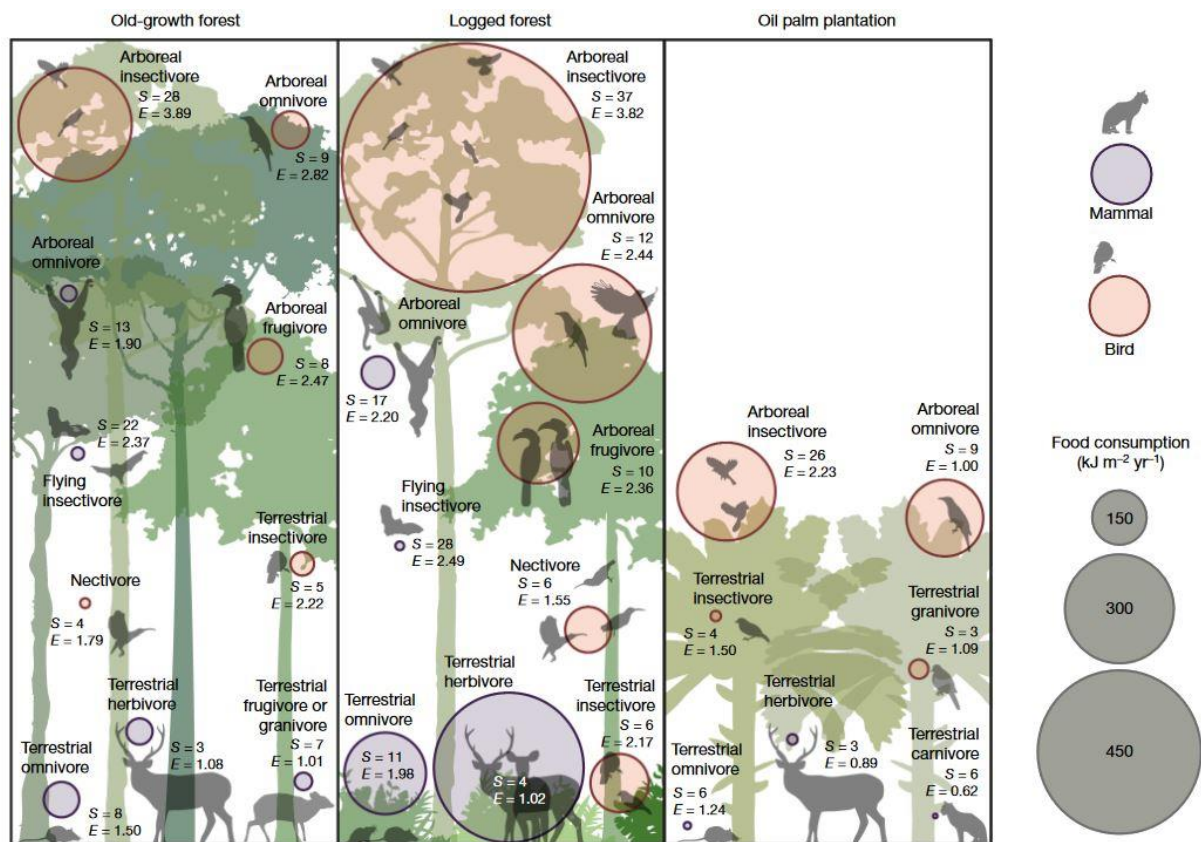
certifications. We find that the concessions - which in theory could raise or reduce forest loss - did not raise loss, if anything reducing it slightly by warding off spikes in deforestation pressure. Eco-certifications could reduce or raise forest loss, yet the authors find no significant impacts. In addition, the authors compare the forest loss impacts from different forest policies in the region [184].

Figure 93: Comparison of forest loss impacts from different forest policies in the Peruvian Amazon, comparing the forest loss impacts of FSC certification and uncertified concessions estimated in this paper with the impacts of three different types of protected areas (PAs), as well as reserved zones in the Peruvian Amazon. Indirect-Use PAs are the strictest PA type. Direct Use and Regional PAs allow some resource extraction by local communities. Reserved Zones are transitory areas that are in the process of becoming a PA, so they are the least strict since they allow more economic activities [184].



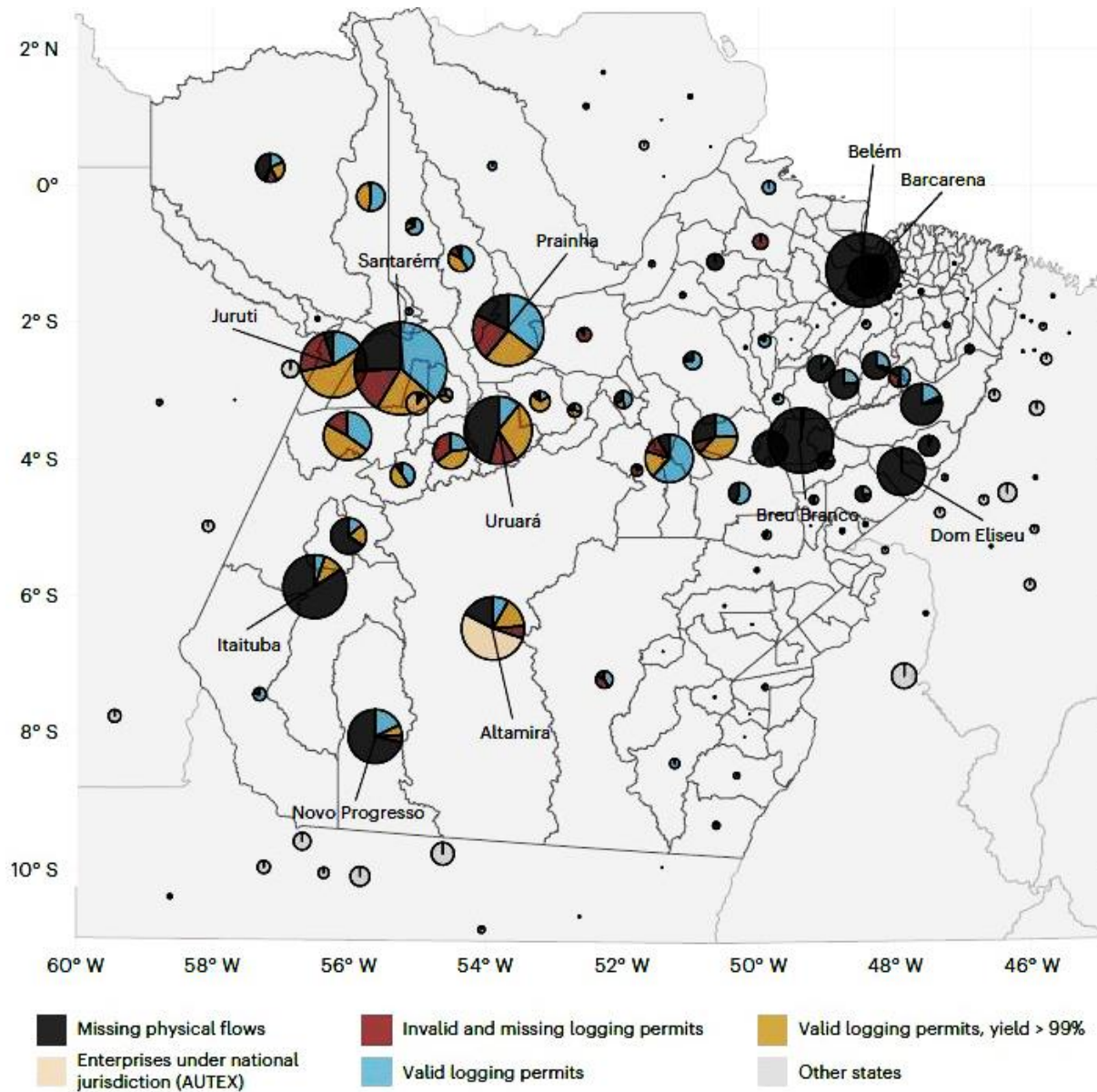
Malhi et al. (2022) look at ecosystem energetics of logged tropical forests on Sabah, Borneo (Malaysia). Old-growth tropical forests are widely recognized as being immensely important for their biodiversity and high biomass¹. Conversely, logged tropical forests are usually characterized as degraded ecosystems². However, whether logging results in a degradation in ecosystem functions is less clear: shifts in the strength and resilience of key ecosystem processes in large suites of species have rarely been assessed in an ecologically integrated and quantitative framework. Here we adopt an ecosystem energetics lens to gain new insight into the impacts of tropical forest disturbance on a key integrative aspect of ecological function: food pathways and community structure of birds and mammals. We focus on a gradient spanning old-growth and logged forests and oil palm plantations in Borneo. In logged forest there is a 2.5-fold increase in total resource consumption by both birds and mammals compared to that in old-growth forests, probably driven by greater resource accessibility and vegetation palatability. Most principal energetic pathways maintain high species diversity and redundancy, implying maintained resilience. Conversion of logged forest into oil palm plantation results in the collapse of most energetic pathways. Far from being degraded ecosystems, even heavily logged forests can be vibrant and diverse ecosystems with enhanced levels of ecological function [185].

Figure 94: Magnitude and species diversity of energetic pathways in old-growth forest, logged forest and oil palm. The size of the circles indicates the magnitude of energy flow, and the colour indicates birds or mammals. S, number of species; E, ESWI, an index of species redundancy and, therefore, resilience (high values indicate high redundancy) [185]



Franca et al (2023) quantify the timber illegality risk in the Brazilian forest frontier. Illegal logging remains widespread across the tropics, leading to extensive forest degradation and trade in illegal timber products. By adapting environmentally extended input–output modelling to timber originating from Brazilian native forests, the authors demonstrate how distinct illegality risks can be mapped and quantified at species-level across the supply chain. They focus on high-value *ipê* hardwood from the Amazon state of Pará, a leading producer of timber and contested forest frontier. Data on logging permits and state- and national-level Document of Forest Origin licenses are used to estimate illegality risks due to missing or invalid logging permits, overstated *ipê* yields or discrepancies resulting from missing inflows of legal timber. They find that less than a quarter of all *ipê* entering supply chains between 2009 and 2019 is risk-free and highlight diversified strategies for the laundering of illegal timber across geographies. While legality does not ensure sustainability, this information can be leveraged to this end by supporting improved implementation and enforcement of forest regulations [26].

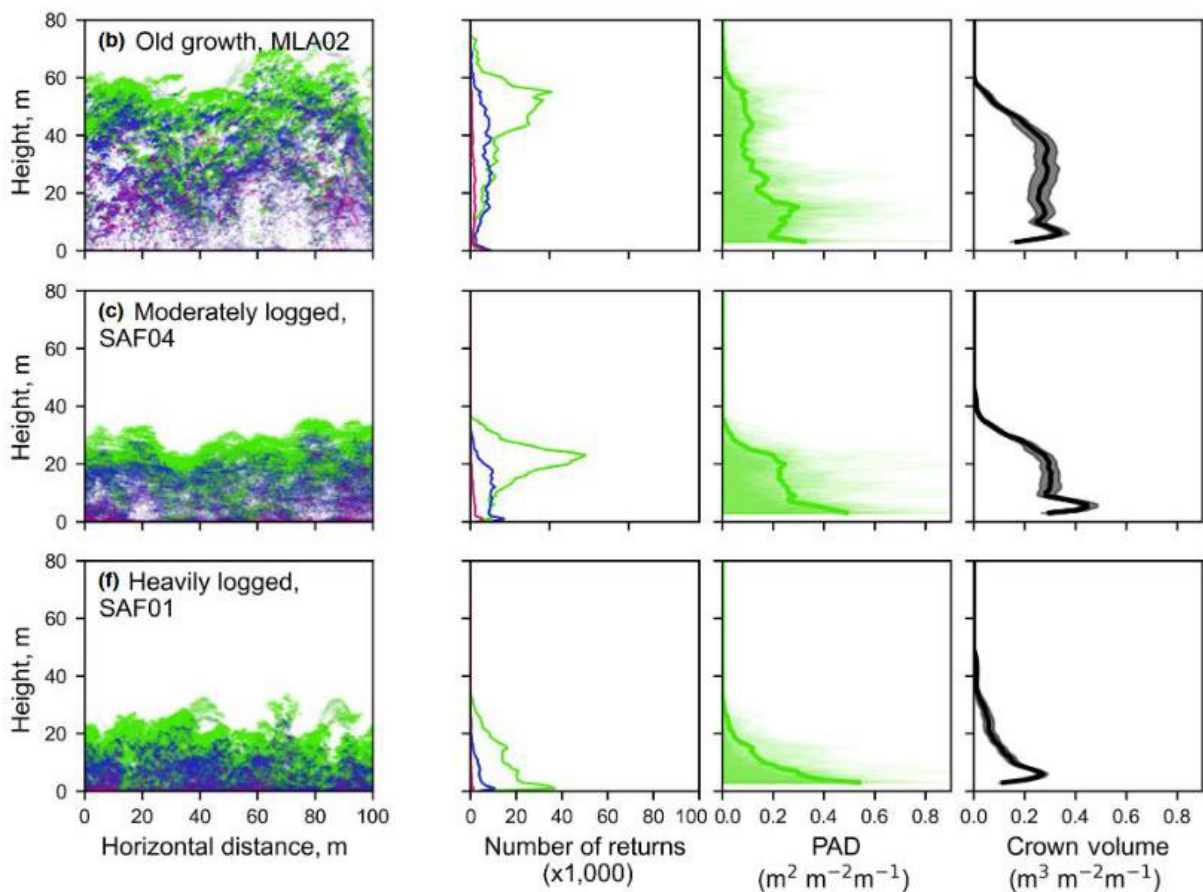
Figure 95: Ipê origins and destination according to associated illegality risks: Municipality of origin according to volume and potential illegality risk associated with timber flows [26]



Milodowski et al. (2021) examine the impact of logging on vertical canopy structure across a gradient of tropical forest degradation intensity in Borneo. Selective logging leads to changes in the three-dimensional canopy structure that have profound consequences for wildlife, microclimate and ecosystem functioning. Quantifying these structural changes is fundamental to understanding the impact of degradation, but is challenging in dense, structurally complex forest canopies. The authors exploited discrete-return airborne LiDAR surveys across a gradient of logging intensity in Sabah, Malaysian Borneo, and assessed how selective logging had affected canopy structure (Plant Area Index, PAI, and its vertical distribution within the canopy). LiDAR products compared well to independent, analogue models of canopy structure produced from detailed ground-based inventories undertaken in forest plots, demonstrating the potential for airborne LiDAR to quantify the structural impacts of forest degradation at landscape scale, even in some of the world's tallest and most structurally complex tropical forests. Plant Area Index estimates across the plot

network exhibited a strong linear relationship with stem basal area ($R^2 = 0.95$). After at least 11–14 years of recovery, PAI was $\sim 28\%$ lower in moderately logged plots and $\sim 52\%$ lower in heavily logged plots than that in old-growth forest plots. These reductions in PAI were associated with near-complete lack of trees >30 - m tall, which had not been fully compensated for by increasing plant area lower in the canopy. This structural change drives a marked reduction in the diversity of canopy environments, with the deep, dark understory conditions characteristic of old-growth forests far less prevalent in logged sites. Full canopy recovery is likely to take decades [186].

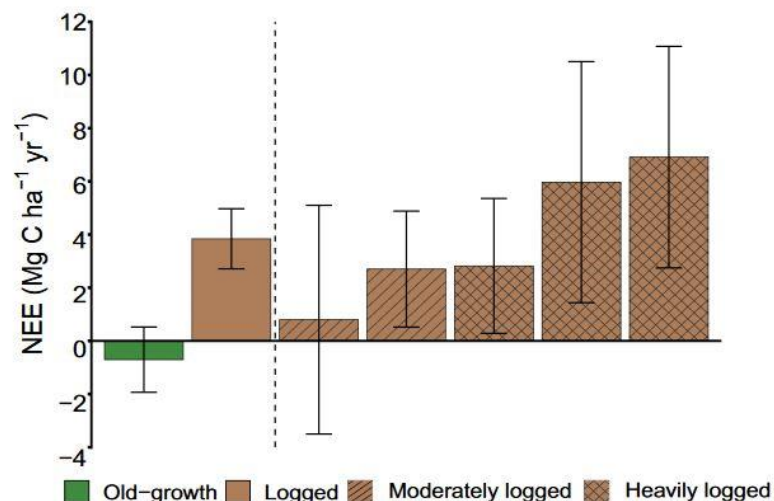
Figure 96: Point clouds and vertical canopy profiles for six of the 1ha-plots illustrating changes in vertical canopy structure across the degradation gradient. From left to right: LiDAR point cloud coloured according to return number, k (first returns - green, second returns - blue, third returns - magenta); vertical profile of LiDAR returns by return number, k ; Plant Area Density (PAD) distributions modelled from the LiDAR; crown volume profiles (mean \pm 95% confidence interval) estimated from field measurements. For the PAD profiles, thick lines represent 1ha-averages of 0.04-ha subplot profiles, subplots are plotted as semi-transparent histograms, giving an indication of structural variability [186]



Mills et al. (2023) state that tropical forests post-logging are a persistent net carbon source to the atmosphere. Logged and structurally degraded tropical forests are fast becoming one of the most prevalent land-use types throughout the tropics and are routinely assumed to be a net carbon sink because they experience rapid rates of tree regrowth. Yet this assumption is based on forest biomass inventories that record carbon stock recovery but fail to account for the simultaneous losses of carbon from soil and necromass. The authors used forest plots and an eddy covariance tower to quantify and partition net ecosystem CO_2 exchange in Malaysian Borneo, a region that is a hot spot for deforestation and forest

degradation. The data represent the complete carbon budget for tropical forests measured throughout a logging event and subsequent recovery and found that they constitute a substantial and persistent net carbon source. Consistent with existing literature, the study showed a significantly greater woody biomass gain across moderately and heavily logged forests compared with unlogged forests, but this was counteracted by much larger carbon losses from soil organic matter and deadwood in logged forests. The authors estimate an average carbon source of $1.75 \pm 0.94 \text{ Mg C ha}^{-1} \text{ yr}^{-1}$ within moderately logged plots and $5.23 \pm 1.23 \text{ Mg C ha}^{-1} \text{ yr}^{-1}$ in unsustainably logged and severely degraded plots, with emissions continuing at these rates for at least one-decade post-logging. Our data directly contradict the default assumption that recovering logged and degraded tropical forests are net carbon sinks, implying the amount of carbon being sequestered across the world's tropical forests may be considerably lower than currently estimated [187].

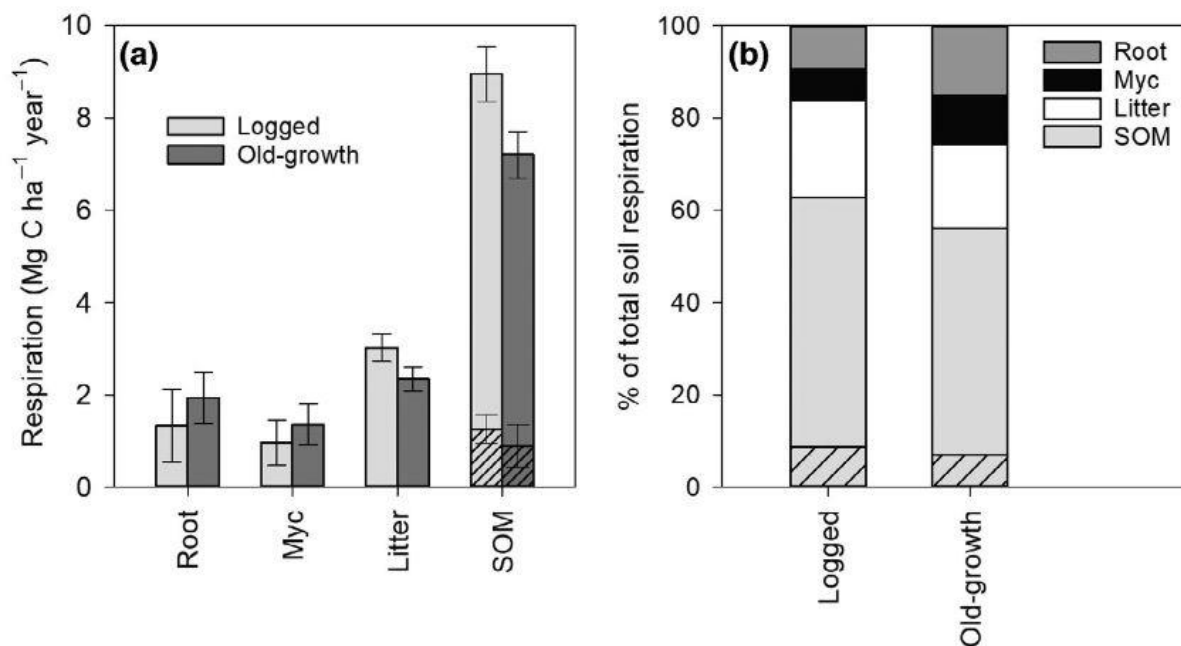
Figure 97: Net ecosystem CO₂ exchange (NEE) estimated by biometric ground-based methods. Left of the dashed line show the mean (± 1 SE) of six unlogged forest plots (green) and five logged plots (brown) with error bars representing variation across the plots. Right of the dashed line show the logged plots individually: two moderately logged plots (striped) and three heavily logged plots (hatched) with error bars representing within-plot uncertainty, estimated by propagation of SEs of the individually measured components of productivity and respiration. Positive values indicate a net source of CO₂ to the atmosphere [187]



Riutta et al. (2021) look at the effects of selective logging in tropical forests on below-ground carbon dynamics and soil respiration. Soil respiration is the largest carbon efflux from the terrestrial ecosystem to the atmosphere, and selective logging influences soil respiration via changes in abiotic (temperature, moisture) and biotic (biomass, productivity, quantity and quality of necromass inputs) drivers. Logged forests are a predominant feature of the tropical forest landscape, their area exceeding that of intact forest. We quantified both total and component (root, mycorrhiza, litter, and soil organic matter, SOM) soil respiration in logged ($n = 5$) and old-growth ($n = 6$) forest plots in Malaysian Borneo, a region which is a global hotspot for emission from forest degradation. We constructed a detailed below-ground carbon budget including organic carbon inputs into the system via litterfall and root turnover. Total soil respiration was significantly higher in logged forests than in old-growth forests (14.3 ± 0.23 and $12.7 \pm 0.60 \text{ Mg C ha}^{-1} \text{ year}^{-1}$, respectively, $p = 0.037$). This was mainly due to the higher SOM respiration in logged forests ($55 \pm 3.1\%$ of the total respiration in logged forests vs. $50 \pm 3.0\%$ in old-growth forests). In old-growth forests, annual SOM respiration was equal to the organic carbon inputs into the soil (difference between SOM respiration and inputs $0.18 \text{ Mg C ha}^{-1} \text{ year}^{-1}$, with 90% confidence intervals of -0.41 and $0.74 \text{ Mg C ha}^{-1} \text{ year}^{-1}$), indicating that the

system is in equilibrium, while in logged forests SOM respiration exceeded the inputs by $4.2 \text{ Mg C ha}^{-1} \text{ year}^{-1}$ (90% CI of 3.6 and $4.9 \text{ Mg C ha}^{-1} \text{ year}^{-1}$), indicating that the soil is losing carbon. The results contribute towards understanding the impact of logging on below-ground carbon dynamics, which is one of the key uncertainties in estimating emissions from forest degradation. The study demonstrates how significant perturbation of the below-ground carbon balance, and consequent net soil carbon emissions, can persist for decades after a logging event in tropical forests [188].

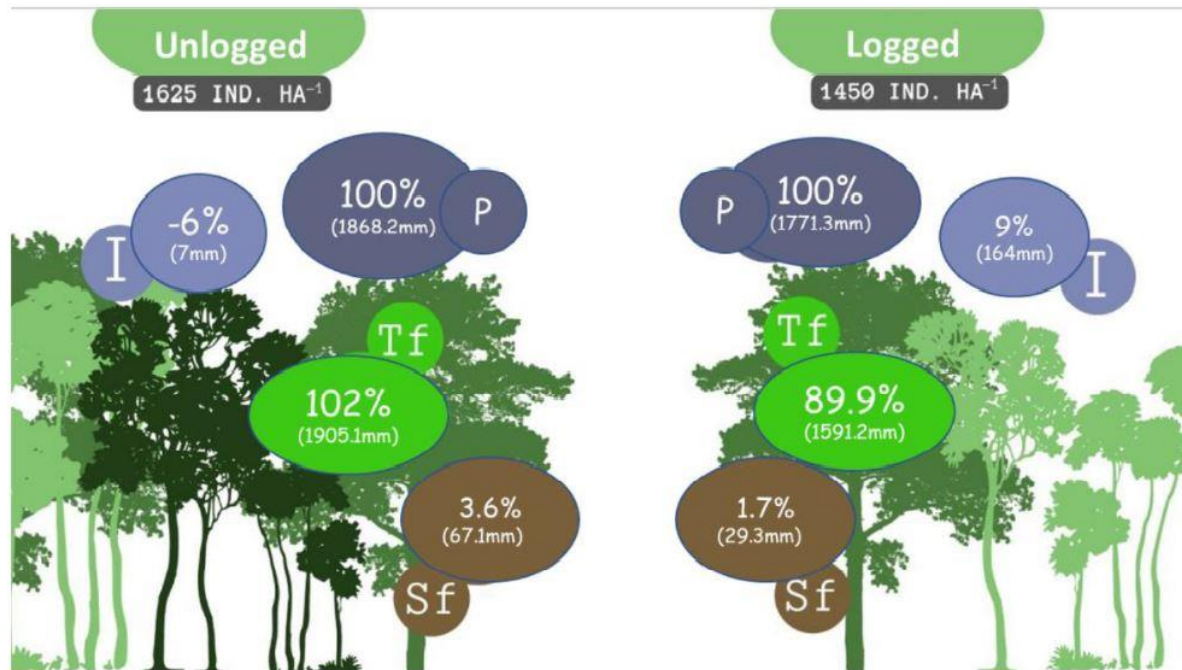
Figure 98: Soil respiration partitioned into root, mycorrhizal (Myc), litter, and soil organic matter (SOM) respiration in logged and old growth forest. (a) Mean \pm 1 SE for each respiration component by forest type (only SOM respiration significantly different, $t_{6.44} = 2.990$, $p = 0.015$) and (b) the proportional contribution of the components to total soil respiration [188]



De Lima and Tonello (2023) look at the implications of reduced impact logging for hydrological processes in the Amazon forest. To reduce environmental damage, sustainable forest management practices through low-impact exploration have been encouraged. However, studies that provide information for understanding the rainfall partitioning are incipient. This study aimed to evaluate the effects of Sustainable Forest Management on rainfall partitioning and the maintenance of forest hydrology processes in the Jamari National Forest - southwest Brazilian Amazon. We examined the throughfall, stemflow, net precipitation and interception loss variability over 13 months in both an unlogged and logged (1625 and 1450 ind ha^{-1} , respectively) Amazon Forest. Despite the higher tree density in the unlogged forest, the dendrometric attributes did not show significant differences between stands. Results indicate that throughfall exceeded rainfall on 54% and 42% of months in unlogged and logged forest, respectively. In the unlogged forest, net precipitation indicated that more water than that from rainfall reached the forest floor ($105.6\% = 102\% \text{ throughfall} + 3.6\% \text{ stemflow}$). The logged forest showed a lower amount of rainfall, with 91.0% reaching the soil floor by net precipitation ($89.8\% \text{ throughfall} + 1.7\% \text{ stemflow}$). Especially in the dry season, net precipitation was 175% higher in unlogged forest. The amount of stemflow highlighted that the unlogged forest has more stemflow than the forest subjected to reduced-logging practices, i.e., the logged forest lost $4261 \text{ L m}^{-2} \text{ BA}^{-1} \text{ y}^{-1}$ by stemflow, which is a reduction of 65%. For both stands, the total

basal area-scale stemflow yield was higher on $D <_{30}$ trees. The results reinforce that we need a better understanding of the impact of sustainable forest management on the eco-hydrology processes in the Amazon Forest, as well as their implications for rainfall partitioning, especially in the context of climate changes at the local scale [189].

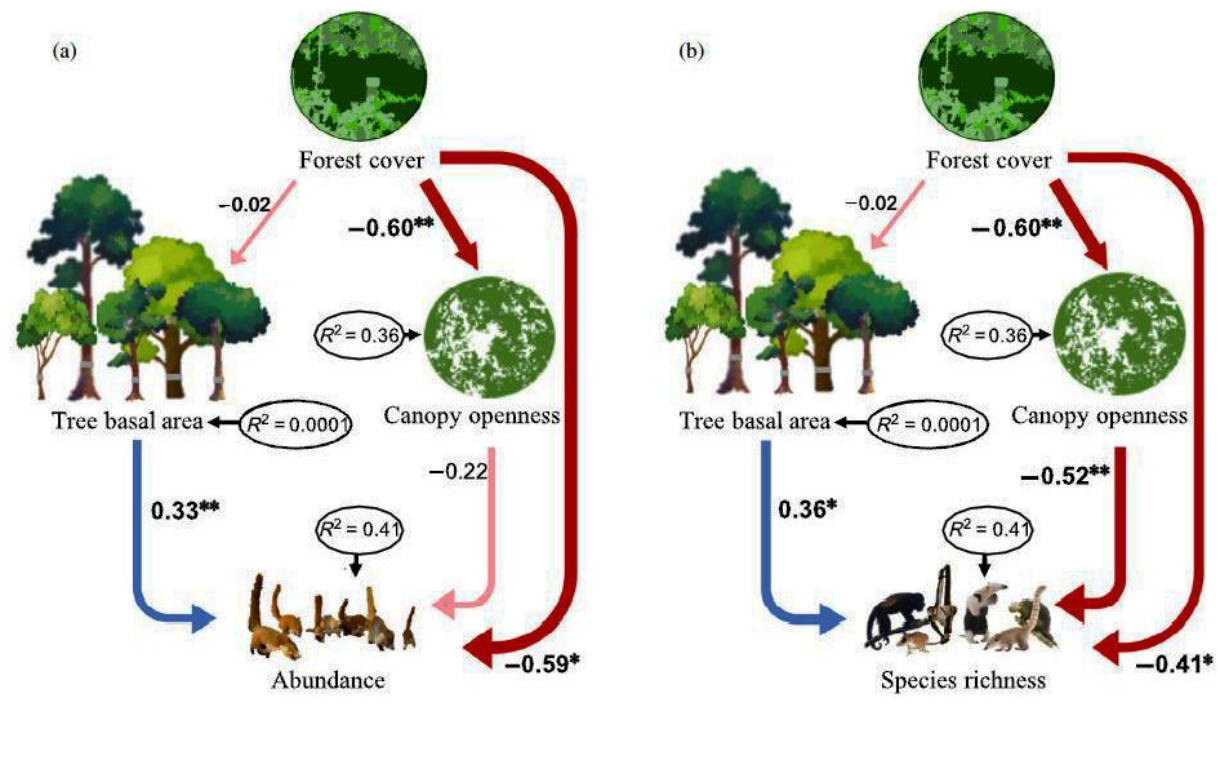
Figure 99: Rainfall partitioning of rainfall (P), throughfall (TF), stemflow (SF), interception loss (I) [% and mm] at Unlogged (UF) and Logged (LF) Amazon Forest. Jamari National Forest, Rondônia – Brazil [189].



Dionisio et al. (2022) discuss about what to do with dead trees due to natural causes or to collateral damage after a selective logging operation. Despite being in good condition and in large numbers, these trees are not harvested. In the study, the woody volume of dead trees (DBH \geq 50 cm) in logging areas was quantified. Five Annual Production Units (APUs) were inventoried, four logged in different years (2002; 2004; 2008 and 2010) and one not logged. In each area, 20 plots of 50 m \times 1000 m were monitored, totalling 100 plots of 5 ha each. Pre-logging volume, logged volume, volume lost due to mortality, volume recruited and volume gained per increment were evaluated. The dead trees had their wood classified as: without use; lumber for sawmills and wood for other purposes. The pre-logging, logged and lost through mortality volumes were, on average, 87.48 m³/ha, 27.18 m³/ha and 15.29 m³/ha, respectively. The volumes recruited and gains per increment together added up to an average of 31.04 m³/ha. The balance was negative (-11.52 m³/ha) when considering the average volume logged and lost at the end of 13 years in relation to the volume recruited and gained by increment. The output volume in the four managed areas was on average 64.5 % caused by logging and the remaining 35.5 % by post-logging mortality. The growth of remaining trees was responsible for 60 % of the input volume and the recruitment for the remaining 40 %. In the four managed areas, the average volume used was 77.7 %. The volume usable for other purposes was higher in the control area (74 %) and five years (72 %) post-logging and lowest at 13 years post-logging (36 %). For sawmills, the volume used was higher at 13 years post-logging (64 %) and lower in the control area (26 %) and five years (28 %) post-logging [190].

Cudney-Valenzuela et al. (2022) examine the effect of increased canopy openness in a Mexico rainforest, caused e.g. by deforestation and selective logging, on arboreal mammals. Using structural equation models, the authors assessed the direct and indirect effects of landscape forest loss on arboreal mammal assemblages in the Lacandona rainforest, Mexico. They placed camera traps in 100 canopy trees, and assessed the direct effect of forest cover and their indirect effects via changes in tree basal area and canopy openness on the abundance and diversity (i.e., species richness and exponential of Shannon entropy) of arboreal mammals. They found that forest loss had negative indirect effects on mammal richness through the increase of tree canopy openness. This could be related to the fact that canopy openness is usually inversely related to resource availability and canopy connectivity for arboreal mammals. Furthermore, independently of forest loss, the abundance and richness of arboreal mammals was positively related to tree basal area, which is typically higher in old-growth forests. The study's findings suggest that arboreal mammals generally prefer old-growth vegetation with relatively low canopy openness and high tree basal area. However, unexpectedly, forest loss was directly and positively related to the abundance and richness of mammals, probably due to a crowding effect, a reasonable possibility given the relatively short history (~40 years) of deforestation in the study region. Conversely, the Shannon diversity was not affected by the predictors evaluated, suggesting that rare mammals (not the common species) are the ones most affected by these changes. All in all, our findings emphasize that conservation measures ought to focus on increasing forest cover in the landscape, and preventing the loss of large trees in the remaining forest patches [191].

Figure 100: Path models of direct and indirect effects of forest cover on (a) abundance, and (b) species richness. Indirect effects of forest cover occur via two vegetation structural attributes (canopy openness and tree basal area). Significant pathways are indicated with asterisks (* $p < 0.05$; ** $p < 0.01$) to the right of the standardized path coefficients, while blue and red lines indicate positive and negative effects, respectively. Arrow thickness is scaled to illustrate the relative strength of the effects. The coefficient of determination (R^2) is shown within black ellipses for all response variables [191].



8.1.8 Mining

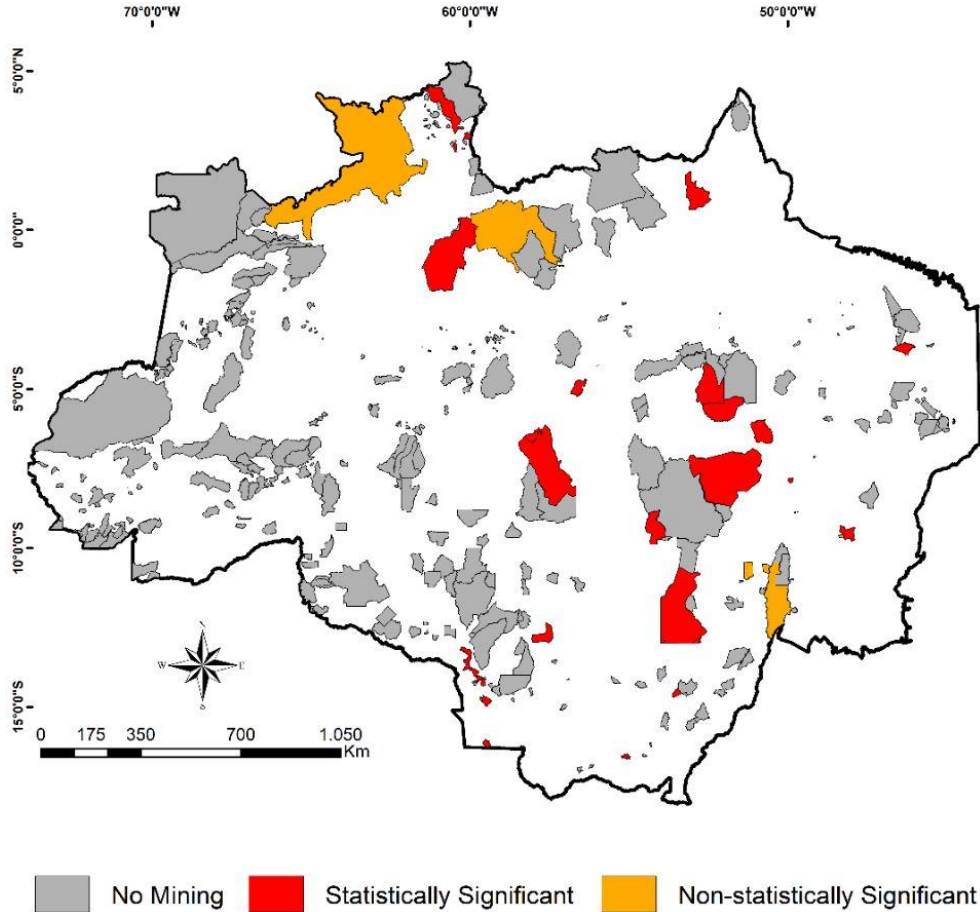
Arrifano et al. (2023) look at the synergies of mercury intoxication (caused by mining) and COVID-19. The COVID-19 pandemic affected billions of people worldwide, and exposure to toxic metals has emerged as an important risk factor for COVID-19 severity. Mercury is currently ranked as the third toxic substance of global concern for human health, and its emissions to the atmosphere have increased globally. Both COVID-19 and mercury exposure present a high prevalence in similar regions: East and Southeast Asia, South America and Sub-Saharan Africa. Since both factors represent a multi-organ threat, a possible synergism could be exacerbating health injuries. The authors discuss key aspects in mercury intoxication and SARS-CoV-2 infection, describing the similarities shared in clinical manifestations (especially neurological and cardiovascular outcomes), molecular mechanisms (with a hypothesis in the renin-angiotensin system) and genetic susceptibility (mainly by apolipoprotein E, paraoxonase 1 and glutathione family genes). Literature gaps on epidemiological data are also highlighted, considering the coincident prevalence. Furthermore, based on the most recent evidence, they justify and propose a case study of the vulnerable populations of the Brazilian Amazon. An understanding of the possible adverse synergism between these two factors is crucial and urgent for developing future strategies for reducing disparities between developed and underdeveloped/developing countries and the proper management of their vulnerable populations, particularly considering the long-term sequelae of COVID-19 [192].

Meneses et al. (2022) examine mercury contamination as a growing threat to riverine and urban communities in the Brazilian Amazon. In recent decades, widespread and uncontrolled use of mercury (Hg) in artisanal small-scale gold mining has released thousands of tons of mercury-contaminated waste in the Amazon biome, endangering the largest tropical rainforest worldwide. The authors assessed and compared blood Hg levels in individuals living in urban and riverine areas in the lower Tapajós basin and examined the association between Hg exposure and specific biochemical parameters. In total, 462 adults from eight riverine communities and one urban area were assessed. Overall, 75.6% of the participants exhibited Hg concentrations exceeding the safe limit (10 µg/L). Hg exposure was higher in the riverine population (90%) than in urban areas (57.1%). Mean Hg levels were 21.8 ± 30.9 µg/L and 50.6 µg/L in urban and riverine residents, respectively. The mean Hg level was higher in those aged 41–60 years in both urban and riparian areas, with riparian residents exhibiting a mean double that of urban residents. The highest glucose and hepatic biomarker levels were detected in the urban area, whereas the highest levels of renal biomarker occurred in the riverine population. People living in communities in the Amazon have been exposed to Hg for decades through the ingestion of mercury-contaminated fish. All the individuals analyzed, both from urban and riverine areas, who reported frequent consume of local fish, had detected Hg levels and were consequently exposed to negative health effects. High levels of this metal were found in people of all age groups, both genders, and all levels of education. However, the highest levels were registered in people who reported high daily fish consumption. This indicates that mercury exposure is not only linked to the residence location, but directly influenced by contaminated fish consumption. Santarém is far from any goldmining sites. Nevertheless, the local people assessed are exposed to different levels of Hg. Thus, exposure to mercury is not restricted to the goldmining site areas, but can occur throughout much of the river basin that is greatly impacted by the goldmining activity [193].

Mataveli et al. (2022) look at the evolution of gold mining activities from 1985 to 2020 within Indigenous Lands in the Brazilian Amazon. Conserving tropical forests is crucial for

the environment and future of our climate. Tropical rainforests worldwide, including the Brazilian Legal Amazon (BLA), offer exceptional ecosystem services. However, the disturbances that have been occurring more frequently within them are endangering their key role in tackling climate change. An alternative approach for preserving the intact forests that remain in the BLA is the delimitation of Indigenous Lands (ILs), which can, additionally, ensure the well-being of the traditional peoples inhabiting there. An increase in deforestation rates of the Lega recent years, due to the weakening of the Brazilian environmental policy, is not confined to unprotected areas but is also occurring within ILs. Under this scenario, mining, not allowed in ILs, is a growing threat in these protected areas. Thus, using the freely available MapBiomas dataset, we have quantified for the first time the total mining area within ILs of the BLA from 1985 to 2020. Such activity jumped from 7.45 km² in 1985 to 102.16 km² in 2020, an alarming increase of 1271%. Three ILs (Kayapó, Mundurukú, and Yanomami) concentrated 95% of the mining activity within ILs in 2020 and, therefore, they require closer monitoring. Most of the mining in ILs in 2020 (99.5%) was related to gold extraction. A total of 25 of the 31 ILs of the BLA where mining activity was detected in at least one of 36 years analysed (~81% of them) had a statistically significant increasing trend [194].

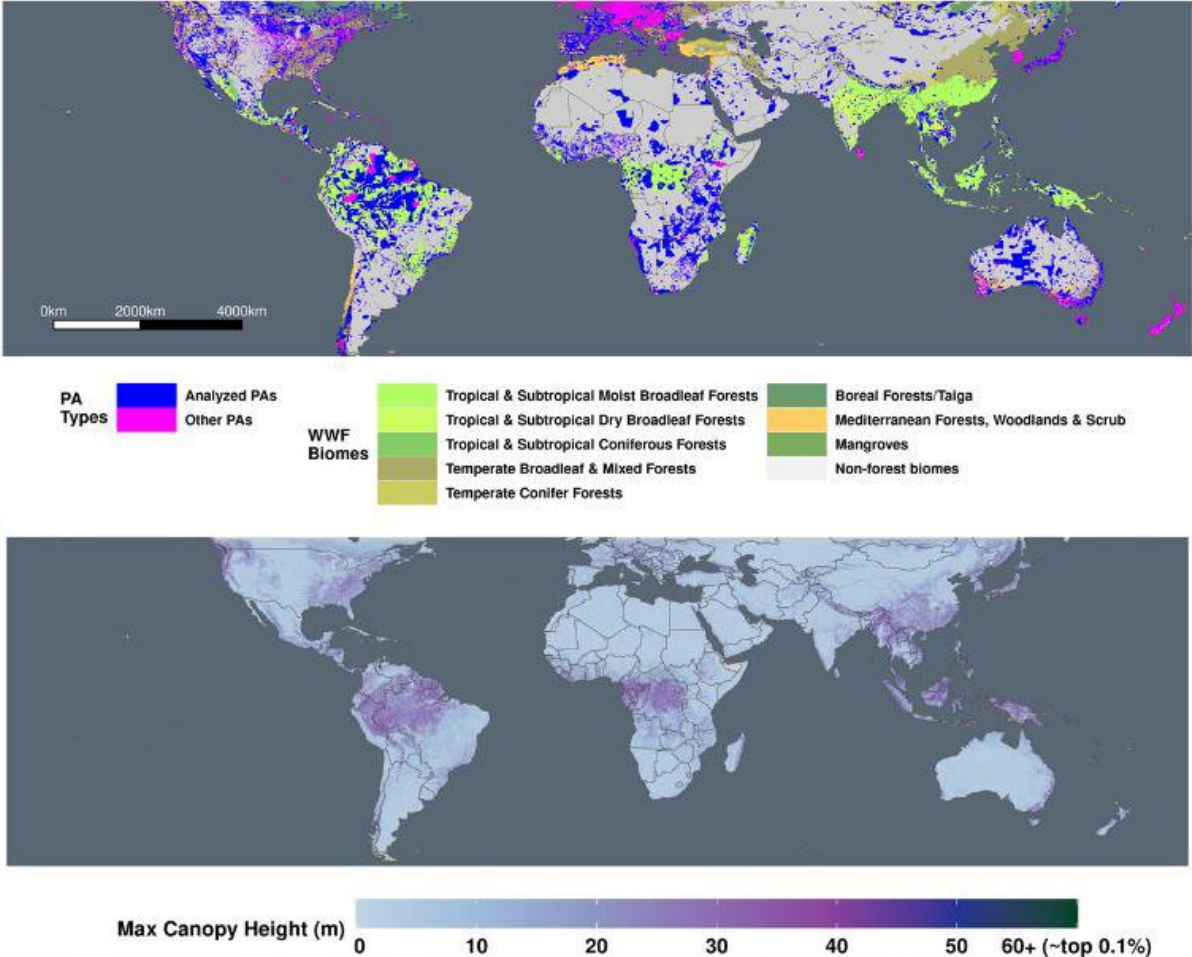
Figure 101: 4. Spatial distribution of the result obtained after applying the Mann–Kendall test to the mining activity time series of the 31 Indigenous Lands of the Brazilian Legal Amazon where mining activity was detected in at least one of 36 years analysed [194]



Duncanson et al. (2023) examine the effectiveness of global protected areas for climate change mitigation, based on data from NASA’s GEDI mission. Forests play a critical role in

stabilizing Earth’s climate. Establishing protected areas (PAs) represents one approach to forest conservation, but PAs were rarely created to mitigate climate change. The global impact of PAs on the carbon cycle has not previously been quantified due to a lack of accurate global-scale carbon stock maps. The authors used ~412 million lidar samples from NASA’s GEDI mission to estimate a total PA aboveground carbon (C) stock of 61.43 Gt (+/- 0.31), 26% of all mapped terrestrial woody C. Of this total, 9.65 +/- 0.88 Gt of additional carbon was attributed to PA status. These higher C stocks are primarily from avoided emissions from deforestation and degradation in PAs compared to unprotected forests. This total is roughly equivalent to one year of annual global fossil fuel emissions. These results underscore the importance of conservation of high biomass forests for avoiding carbon emissions and preserving future sequestration [195].

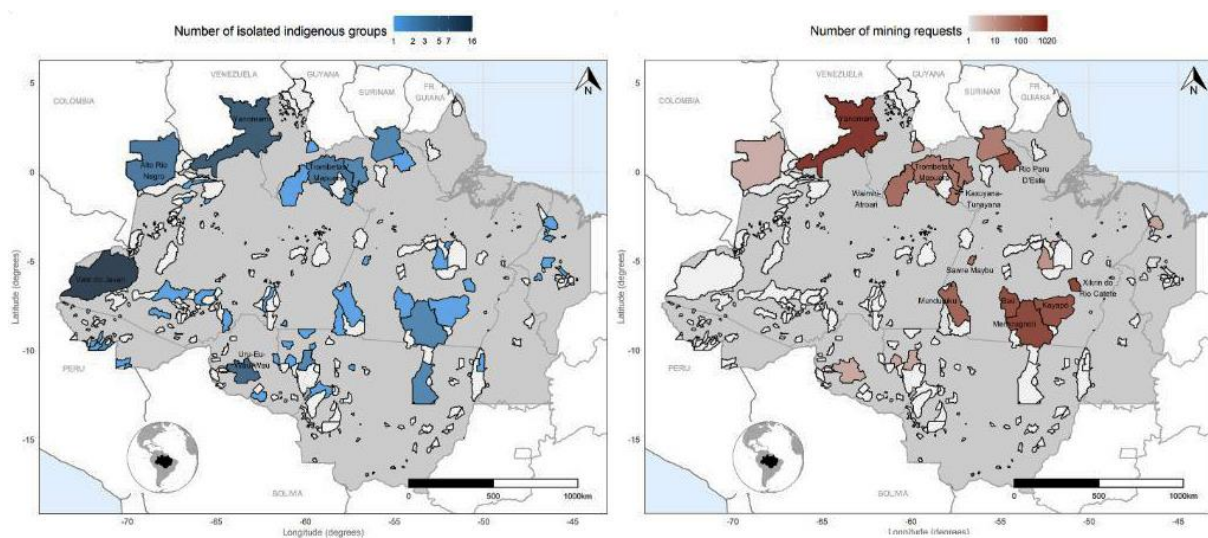
Figure 102: Global-scale vegetation 3D structure data from NASA’s GEDI mission. The GEDI-domain PAs cover a range of biomes (above), Canopy cover (below), were analysed, amongst other parameters, for all PAs and unprotected counterfactuals to establish the forest structure implications of PAs [195].



Villén-Pérez et al. (2022) look at the ‘isolated indigenous people’ and the current mining requests in their territories in the Brazilian Amazon, specifically on the background of the proposed law PL191/2020 that would legalise mining in indigenous lands. The largest concentration of isolated indigenous peoples in the world is in the Brazilian Legal Amazon. However, the right to self-isolation and the survival of these societies are at risk because powerful interests want to exploit the natural assets of their relatively untouched areas. We assess the threat imposed by mining to isolated peoples and the indigenous territories

they occupy. The authors cross data on mining requests received by the National Mining Agency with information on the distribution of isolated indigenous groups recorded by the Socio-Environmental Institute, in order to evaluate the number and aerial extent of requests for mineral prospecting and operation registered in indigenous lands with isolated groups. They analyse whether mining requests are related to the presence of isolated groups, the state of knowledge about them, and the current existence of illegal mining operations. The results indicate that, even though mining is not yet allowed in indigenous lands, mining companies are very active in the search for exploitable areas in these territories. If the PL191/2020 passes, mining operations would affect more than 10 million hectares in 25 indigenous lands in the Legal Amazon region that are home to 43 isolated groups. We found that the situation is especially worrisome for 21 isolated groups whose lands concentrate 97% of all mining requests. Mineral-rich areas overlap remote areas where more indigenous peoples persist in isolation, so that mining requests are significantly related to the presence of isolated groups. The authors show that companies are hesitant to invest in lands with well-known isolated groups that could impede the licensing process and pose reputational risks to the companies. Brazil’s mechanisms for environmental and indigenous protection have been dismantled by the current presidential administration and offer no guarantees for a safe coexistence between extractive operations and isolated peoples. Thus, the approval of bill PL191/2020 could lead to undesired contact and the extinction of a large number of unique peoples, societies and cultures [106].

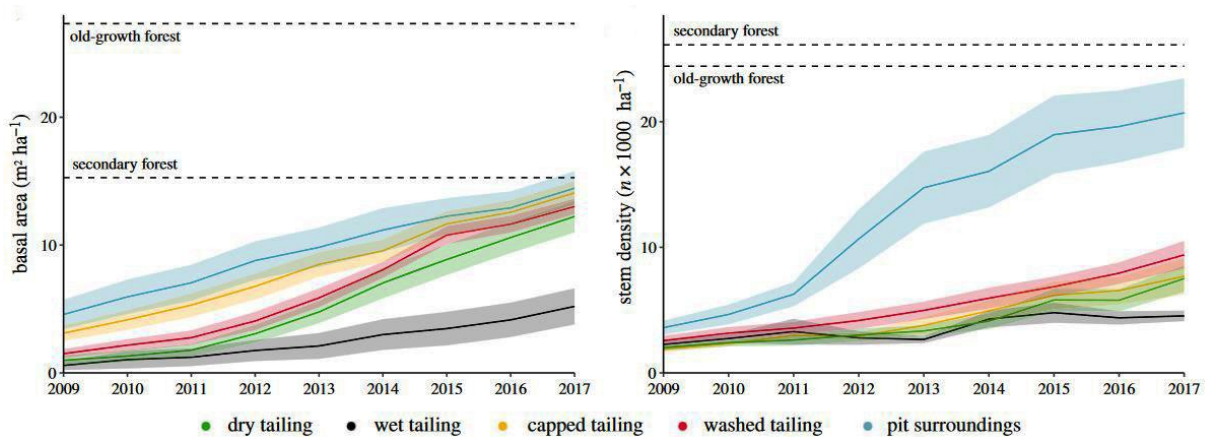
Figure 103: 4. Geographical distribution of indigenous lands in the Brazilian Legal Amazon, the number of isolated indigenous groups (A) and the number of mining requests (B). Indigenous lands with no isolated groups are in white in both maps. The Legal Amazon region is in grey. Indigenous lands with >3 isolated groups or >50 mining projects are labelled [106].



König et al. (2023) explore the factors for restoration success in former Amazonian mines. Mining contributes importantly to tropical deforestation and land degradation. To mitigate these effects, mining companies are increasingly obliged to restore abandoned mine lands, but factors driving restoration success are hardly evaluated. The authors investigate the influence of ecological factors (restoration age, soil properties and surrounding forest area) and management factors (diversity and density of planted species, mine zone) on the recovery rate of forest structure and tree diversity on 40 post-mining restoration areas in Southern Amazonia, Brazil, using a 9-year annual monitoring dataset consisting of over 25000 trees. They found that recovery of forest structure was closely associated with

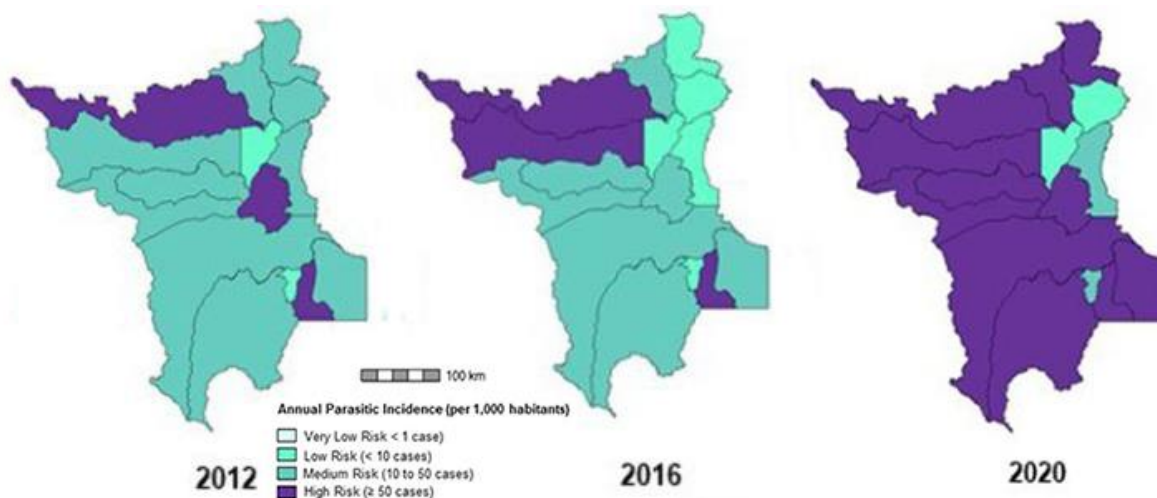
interactions between soil quality and the planted tree communities, and that tree diversity recovery was positively associated with the amount of surrounding forests. They also observed that forest structure and diversity recover more slowly in mine tailings compared to pit surroundings. The study confirms the complexity of mine land restoration but also reveals that planting design and soil improvement can increase restoration success. For resource-efficient mine restoration, the authors recommend the focusing of efforts on tailings, which are hardest to restore, and reducing efforts in pit surroundings and areas close to surrounding forest because of their potential for restoration by natural regeneration [196].

Figure 104: 4. Recovery of forest structure in restored open-pit mining areas in Brazil. The lines show the mean and the standard error in a given year and are colour-coded by mine zone. Dotted lines display average values for surveyed reference plots in secondary and old-growth forest in the immediate surroundings of the restoration areas [196].



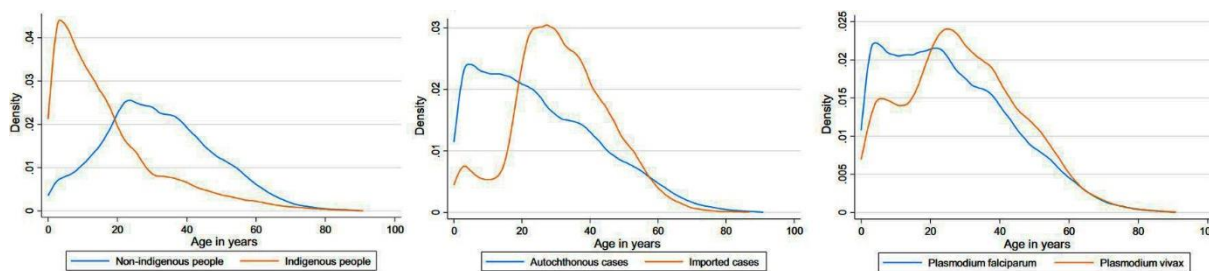
De Aguiar Barros et al. (2022) make the link between gold mining and the occurrence of malaria in indigenous territories of Roraima state, Brazil. Endemic malaria is present in all 15 municipalities of Roraima state. Knowledge of epidemiological data of specific populations can guide health policies to formulate effective strategies for integrated control of health-disease care. The study aims to ascertain when, where and who fell ill with malaria in Roraima state from 2010 to 2020. It was based on statistical secondary surveillance data through the analysis of relationships underlying numbers of cases, hospitalizations and deaths using the Malaria Epidemiological Surveillance Information System, Mortality Information System and Hospitalization Information System. From 2010 to 2020, there were 138,504 autochthonous cases, 26,158 Venezuelan imported cases, 3765 hospitalizations, and 77 deaths from malaria reported in Roraima. Annual parasitic incidence and the number of hospitalizations showed impressive changes over the period, but without significantly correlating with number of deaths. The proportion of *Plasmodium falciparum* infections had significant shifts throughout this study. Malaria prevalence in indigenous and mining areas has been increasing since 2014. The presence of miners in indigenous areas is a reality that has been contributing to the increase of malaria cases in Roraima. The need to implement health policies that also meet this contingent is reinforced [197].

Figure 105: Annual Parasitic Incidence (API) of Roraima state according to the municipality of infection, 2010 to 2020. Sources: SIVEP-MALARIA; IBGE [197]



In the same context and for the same geographic area (Roraima state in Northern Brazil), Wetzler et al. (2022) look at changing transmission dynamics among migrant, indigenous and mining populations in a malaria hotspot in Northern Brazil: 2016 to 2020. Roraima state is the primary border-crossing point between Brazil and Venezuela. The uncontrolled surge of malaria in Venezuela, coupled with mass migration of Venezuelans to neighbouring countries and the upward trend in informal mining in the state, pose a serious threat to the broader region, especially to migrant, indigenous and mining populations, jeopardizing malaria elimination efforts. The study describes changes in the epidemiological profile of malaria in Roraima state related to time, place and populations at risk from 2016 to 2020. De-identified malaria surveillance data were obtained from the Malaria Epidemiological Surveillance System from 2016 to 2020. Pearson's chi-square tested differences between imported and autochthonous cases. Multivariable logistic regression was used to identify risk factors for imported versus autochthonous cases by demographic characteristics. Odds of being an imported case were higher for *Plasmodium falciparum* cases (AOR = 2.08). However, as the number of cases from Venezuela decreased in 2020 following closure of the border, the proportion of *P. falciparum* cases increased markedly, from 6.24% in 2019 to 18.50% in 2020. Over the 5-year period, the odds of being an imported case among miners were about nine times higher than the general population (AOR = 8.99). The proportion of total malaria cases that were among indigenous people increased from 33.09% in 2016 to 54.83% in 2020. Indigenous children had a higher burden of malaria with over 40% of cases in children 0 to 9 years old, compared to 8% in non-indigenous children 0 to 9 years old. In some municipalities, place of infection differed from place of notification, with a large proportion of cases in these municipalities reporting in Boa Vista. Malaria remains a serious threat in Roraima state, especially among high-risk populations, such as miners, migrants, and indigenous people. As malaria cases have increased among indigenous people and miners, and the proportion of *P. falciparum* cases has increased, elimination efforts require understanding of these risk factors to tailor interventions appropriately. Furthermore, cross-border surveillance systems need to be urgently strengthened at formal and unofficial border points, especially since the border with Venezuela reopened in July 2021 [198].

Figure 106: Proportion of malaria cases at each age, from 2016–2020. Density plots of age distribution of cases by case type: Left: cases in indigenous and non-indigenous people, Centre: autochthonous and imported cases, Right: *P. falciparum* and *P. vivax* cases [198]

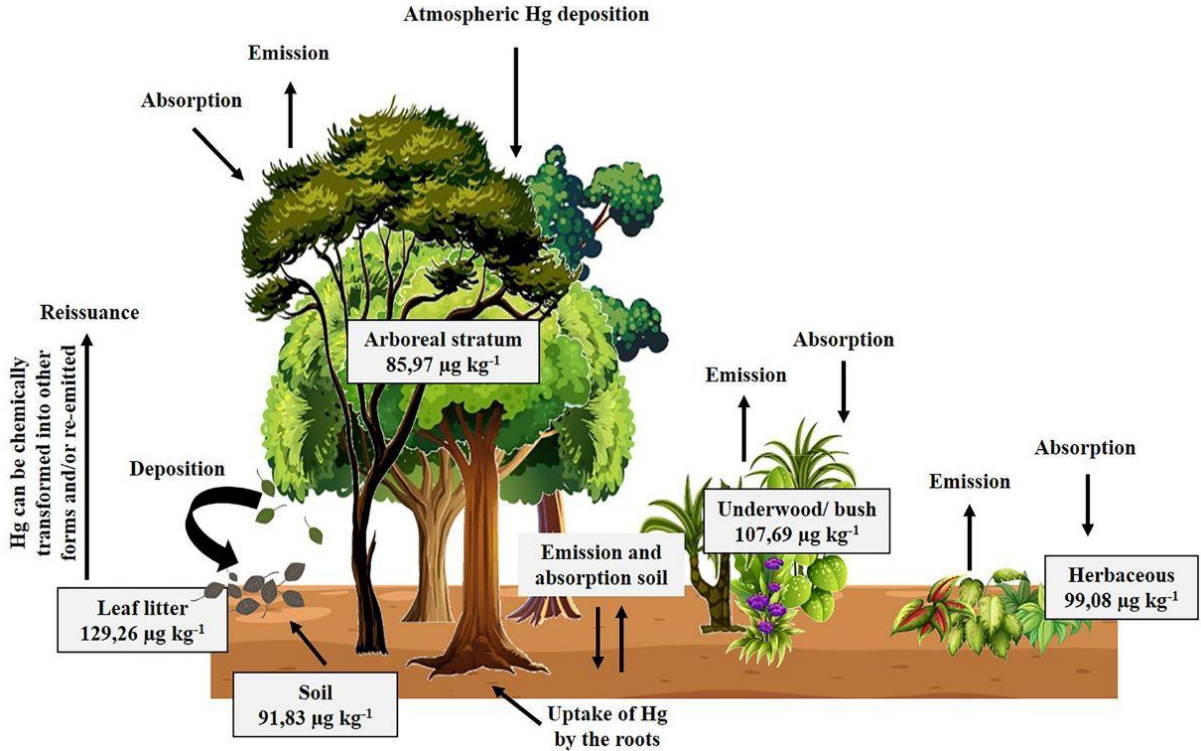


Giljum et al. (2022) carry out a pantropical assessment of deforestation caused by industrial mining. Many local- to regional-scale studies document extensive, long-lasting impacts of mining on biodiversity and ecosystem services. However, the full scope of deforestation induced by industrial mining across the tropics is yet unknown. The authors present a biome-wide assessment to show where industrial mine expansion has caused the most deforestation from 2000 to 2019. They find that 3,264 km² of forest was directly lost due to industrial mining, with 80% occurring in only four countries: Indonesia, Brazil, Ghana, and Suriname. Additionally, controlling for other non-mining determinants of deforestation, they find that mining caused indirect forest loss in two-thirds of the investigated countries. Their results illustrate significant yet unevenly distributed and often unmanaged impacts on these biodiverse ecosystems. Impact assessments and mitigation plans of industrial mining activities must address direct and indirect impacts to support conservation of the world’s tropical forests. Further, the authors revealed that industrial mining indirectly drives deforestation in the surroundings outside mining areas. Indirect deforestation effects caused by industrial mining are most considerable for Brazil and Indonesia, but these effects can be observed in more than two-thirds of the investigated countries. Against the background of rapidly increasing global demand for mineral resources, e.g., for housing and transport infrastructure (36) or green energy technologies (37), our results emphasize important yet unevenly distributed and largely unmanaged future threats to tropical forests [199].

Chaddad et al. (2022) measure the impact of mining-induced deforestation on soil surface temperature and carbon stocks through a case study using remote sensing in the Amazon rainforest. In their study, the authors assessed the evolution of deforestation in an open mine pit and its impact on surface environment (i.e., temperature and carbon stocks) using remote sensing techniques. The study was carried out on an area of 11,283.3 ha in the municipality of Marabá, Pará State, Brazil, where the “Salobo” copper mine is located. A temporal analysis was conducted, using Landsat satellite images (2005–2020). Subsequently, the Land Surface Temperature (LST) and the Normalized Difference Vegetation Index (NDVI) of the deforested area were determined. Mining-induced deforestation has expanded from 0.9 ha in 2005 to 2214 ha in 2020 with an increase in surface temperature of 10°C in the period. The temperature difference between the pit and the adjacent forest ranged from 30 to 40°C over the 15 years, while the temperature at the forest edges rose by 4°C. The correlation coefficient between exposed soil temperatures and mining deforestation was 0.66. CO₂ emissions, increasing from 0.005 Tg CO₂ in 2005 to 1.82 Tg CO₂ in 2020 due to mining deforestation [200].

Casagrande et al. (2023) carry out an accumulation analysis of atmospheric mercury in forests in a gold mining area in the southern Brazilian Amazon. The spatial distribution and dispersion of mercury (Hg) is associated with the structural conditions of the environment, primarily land use and vegetation cover. Man-made emissions of the metal from activities such as artisanal and small-scale gold mining (ASGM) can influence this distribution. Forest ecosystems are of particular importance as they constitute one of the most active environments in the biogeochemical cycle of Hg, and understanding these dynamics is essential to better understand its global cycle. The authors determined the content of Hg present in different forest strata (soil, leaf litter, herbaceous, underwood/bush, and arboreal), as well as the relationship between the presence of Hg and the landscape heterogeneity, percentage of gold mines, and ground slope. The study was carried out in tropical forest areas of the southern Brazilian Amazon. Accumulation and transport of Hg between forest strata was assessed in order to understand the influence of these forest environments on Hg accumulation in areas where ASGM occurs. They verified that there is a difference in Hg content between forest strata, indicating that atmospheric Hg is accumulated onto the arboreal stratum and transported vertically to strata below the canopy, i.e., underwood/bush and herbaceous, and subsequently accumulated in the leaf litter and transferred to the soil. Leaf litter was the stratum with the highest Hg content, characterized as a receptor for most of the Hg load from the upper strata in the forest. Therefore, it was confirmed that Hg accumulation dynamics are at play between the analysed areas due to the proximity of ASGMs in the region. This indicates that the conservation of forest areas plays an important role in the process of atmospheric Hg deposition and accumulation, acting as a mercury sink in areas close to man-made emissions [201].

Figure 107: Hg cycle in areas dominated by the Amazon Forest, with the mean Hg content of forest strata in the southern Amazon region. The main pathways of Hg movement are atmospheric deposition on the arboreal stratum and leaves falling to the forest floor [201]



Bello et al. (2023) examine the Mercury exposure in women of reproductive age in in the Madeira River basin, Rondônia State, Brazilian Amazon. The longitudinal cohort study used linear regression models to assess the effects on Hg levels of breastfeeding duration at 6 months, and of breastfeeding duration and number of new children at 2-year and 5-year. Breastfeeding duration was significantly associated with maternal Hg levels in all regression models (6 months, 2 years and 5 years) and no significant association was observed between the number of children and the change in maternal Hg levels in the 2-year and 5-year models. The study evaluated Hg levels and contributing factors among pregnant women from different communities (riverine, rural, mining and urban) in Rondônia, Amazon Region, for 5 years. A well-coordinated and designed national biomonitoring program is urgently needed to better understand the current situation of Hg levels in Brazil and the Amazon. Considering the safe reference levels of $6 \mu\text{g}\cdot\text{g}^{-1}$ for women of reproductive age, the study points to elevated Hg levels among women in Rondônia, especially among riverine and rural communities (ranging from 1.02 to $146.80 \mu\text{g}\cdot\text{g}^{-1}$). Many factors can influence the body's Hg burden, and some are especially relevant for this study: the global Hg deposition; Hg exposure due to gold mining activities in the Madeira River basin; and exposure to natural Hg present in the Amazonian soils, lixiviated to waterways due to unsustainable soil use practices. All these Hg sources contribute to fish contamination and consequently, the humans who eat them [202].

8.1.9 Hunting

Bogoni et al. (2020) inform about the extent, intensity and drivers of mammal defaunation through a continental-scale analysis across the neotropics. The neotropical mammal diversity is currently threatened by several chronic human-induced pressures. The authors compiled 1,029 contemporary mammal assemblages surveyed across the Neotropics to quantify the continental-scale extent and intensity of defaunation and understand their determinants based on environmental covariates. They calculated a local defaunation index for all assemblages—adjusted by a false-absence ratio—which was examined using structural equation models. We propose a hunting index based on socio-environmental co-variables that either intensify or inhibit hunting, which we used as an additional predictor of defaunation. Mammal defaunation intensity across the neotropics on average erased 56.5% of the local source fauna, with ungulates comprising the most ubiquitous losses. The extent of defaunation is widespread, but more incipient in hitherto relatively intact major biomes that are rapidly succumbing to encroaching deforestation frontiers. Assemblage-wide mammal body mass distribution was greatly reduced from a historical 95th-percentile of ~ 14 kg to only ~ 4 kg in modern assemblages. Defaunation and depletion of large-bodied species were primarily driven by hunting pressure and remaining habitat area. Our findings can inform guidelines to design transnational conservation policies to safeguard native vertebrates, and ensure that the “empty ecosystem” syndrome will be deterred from reaching much of the New World tropics [203].

Figure 108: Interpolation-based geographic distribution of the naïve defaunation index (DI) broken down by mammal orders across the Neotropics. Maps were pruned by the averaged limit of the distribution of any mammal species within each order via a convex-hull approach [203].

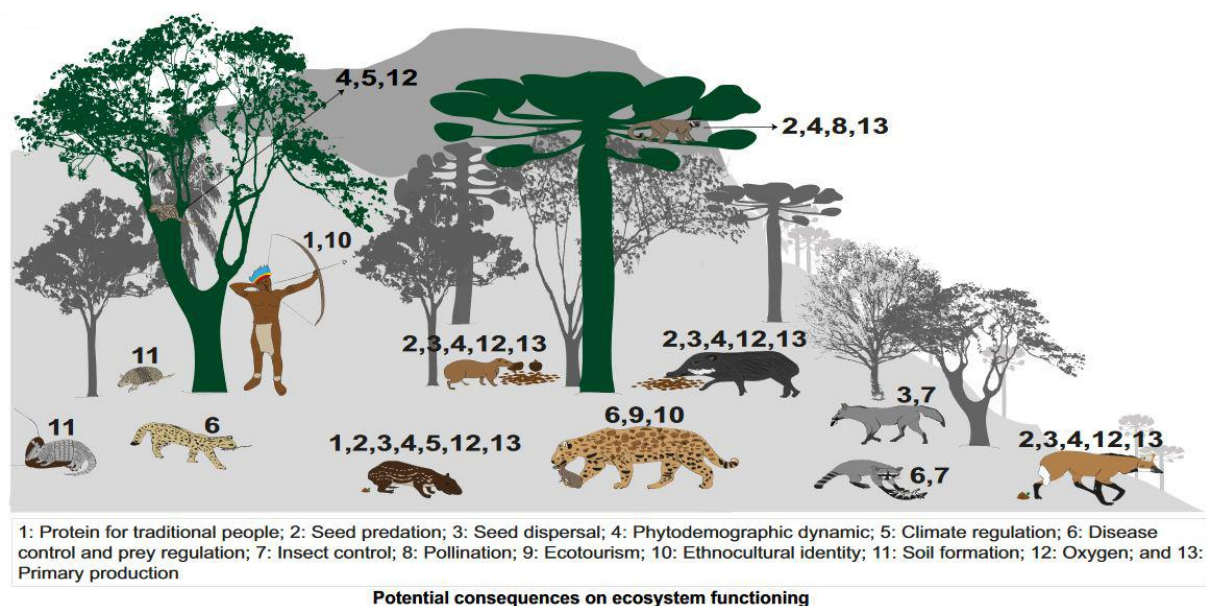


Bastos da Silva et al. (2022) look at patterns of wildlife hunting and trade by local communities in eastern Amazonian floodplains. Local people living in the Amazon rainforest rely heavily on wild meat as a source of protein and income. While the patterns and drivers of wildlife hunting and trade by local communities are well-known for upland forests, such aspects have been poorly explored in Amazonian floodplains. The study aims to describe wild meat hunting and trade patterns and assess the hunting dynamics of local communities in Amazonian floodplain areas. For this purpose, we interviewed 121 hunters in 36 communities living in white-water flooded forests in the lower Amazon River, Brazil.

Thirty taxa were cited as hunted by interviewees, who used a repertoire of 13 hunting techniques. Aquatic and semi-aquatic taxa were the most prevalent, especially *Hydrochoerus hydrochaeris*, *Cairina moschata*, and *Podocnemis unifilis*. Eight taxa were cited as traded; wild meat was sold at 2.57 ± 2.22 USD/kg, while eggs of birds and turtles were sold at 0.37 ± 0.27 USD/unit. The authors found an inverted-U relationship between the body mass and the number of citations per taxa, with species weighing between 10-40 kg presenting the highest number of citations. The hunting patterns found during the study are different from those frequently found in the literature for upland environments. Understanding these hunting and trade patterns will help develop tailored wildlife conservation and management strategies for Amazonian floodplains [204].

Bogoni et al. (2023) evaluate the lessons and prospects related to the milestone publication from Redford (1992) on 'the concept of 'the empty forest'. Based on seminal studies Redford coined the term "empty forests" to describe "defaunation" as a phenomenon of widespread vertebrate losses that is spatially decoupled from habitat loss. However, defaunation is best described as a broader concept, given that the "empty forest" syndrome *sensu Redford* refers primarily to wildlife depletion through overhunting, while defaunation *sensu lato* can be induced by multiple drivers, such as habitat loss, wildfires, wildlife disease, human-wildlife conflict, roadkill, mesopredator release, and proliferation of exotic species, all of which can act in synergy with hunting, potentially aggravating biodiversity loss. Across the Neotropics, defaunation (*sensu lato*) is widespread inducing as much as 56.5% of local extinctions in local mammal assemblages, revealing that virtually entire biomes, such as the Atlantic Forest and the Caatinga drylands, lack >70% of their large mammal fauna. These trends have led to a faunal downsizing phenomenon, whereby the size structure of mammal assemblages shrunk by an average of 71.2% compared with the pre-Columbian era. This scale of faunal depletion is mirrored by the amply cited Living Planet Report, which estimates a 68% global average decline in populations of vertebrate species between 1970 and 2016, which is particularly severe in the tropics [205].

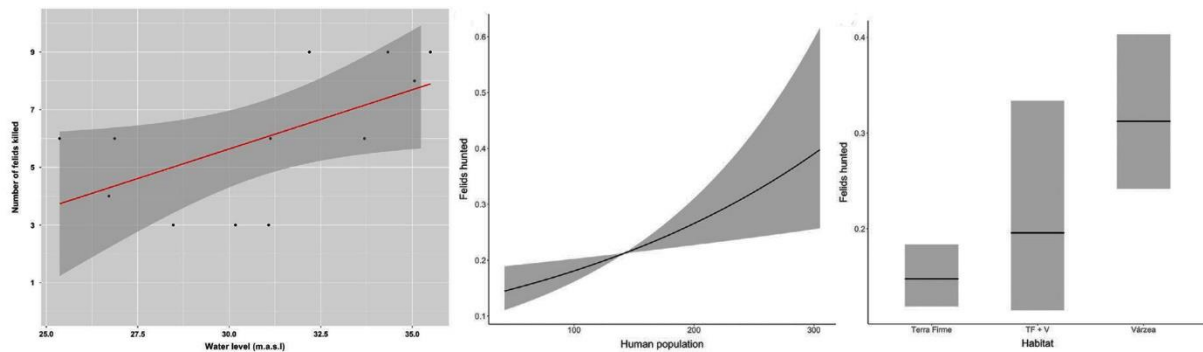
Figure 109: Schematic profile showing the most important potential consequences of defaunation on ecosystem functioning and services, here represented by Neotropical mammals [205]



Bragagnolo et al. (2019) evaluate the options related to hunting in Brazil. Most forms of hunting and keeping of wild animals in Brazil are illegal, although they remain widely practiced and are deeply culturally embedded in many regions. The drivers of such widespread noncompliance are poorly understood and evidence to support future policy decisions is generally lacking. In this paper, we seek to stimulate a critical debate on how to deal with hunting in Brazil by analysing the main factors driving non-compliance with current legislation. This is particularly timely given that several amendments to existing legislation are currently under consideration. Their analysis suggests that, while there are no simple solutions to non-compliance, a targeted suite of the following policy options could improve the monitoring, sustainability and conservation consequences of hunting in Brazil: (i) simplifying the process to become a registered subsistence hunter; (ii) expanding participation in licensing schemes; (iii) investing in pilot studies and assessing their environmental and socioeconomic impacts; (iv) expanding community-based management programmes; (v) trailing education and social marketing campaigns. These policy options are geographically and social-context specific and would be most effectively be implemented at regional or sub-regional scales [206].

Valsecchi et al. (2022) talk about community-based monitoring of wild felid hunting in Central Amazonia. Hunting is a critical issue in wild felid conservation, contributing to the decline of these species worldwide. The study presents 18 years of a community-based monitoring program, quantifying and characterizing wild felid hunting in two sustainable development reserves in Central Amazonia. The authors investigated how felid hunting was affected by the flood pulse and whether local human population size, habitat type, and total hunting events influenced felid hunting. They recorded 71 adult felids being killed, most of them in opportunistic events (88.7%), usually during hunting expeditions aimed at other game species. Four felid species were recorded in the hunts (*Panthera onca*, *Leopardus pardalis*, *Puma concolor*, and *Leopardus wiedii*) with jaguars accounting for almost half of all hunting events ($N = 35$). They found that more felid hunting events occurred during the flooded season, in more populated communities, and in *várzea* habitats. Most felids were hunted opportunistically, demonstrating the complexity of human-felid interactions. Stories of attacks on humans are widespread in the study area, which may strengthen an instinctive fear of felids, driving their persecution. The increase of hunting events during the flooded season seems to be related to a higher probability of encounters between humans and wild felids. High waters make fishing difficult, therefore, locals hunt more, entering deep into the forest through flooded habitats. Since jaguars have an arboreal lifestyle during the flooded season in *várzea* forests, they are easily spotted by locals and have less of a chance to escape since they are slower and more exposed when swimming, which increases the probability of being killed. It is generally acknowledged that involving local stakeholders in conservation projects is essential for their success. In our case, collaboration among researchers and community members was fundamental to access hunting information. We show that community-based monitoring empowers the local communities and facilitates data collection on sensitive topics [207].

Figure 110: Linear regression analysis showing the relationship between the number of felids hunted and the mean monthly water level (left), the relationship between felid hunting and human population size (centre) and habitat (right) at Amanã and Mamirauá Sustainable Development Reserves, Amazonas state, Brazil (shaded area, 95% CI) [207]

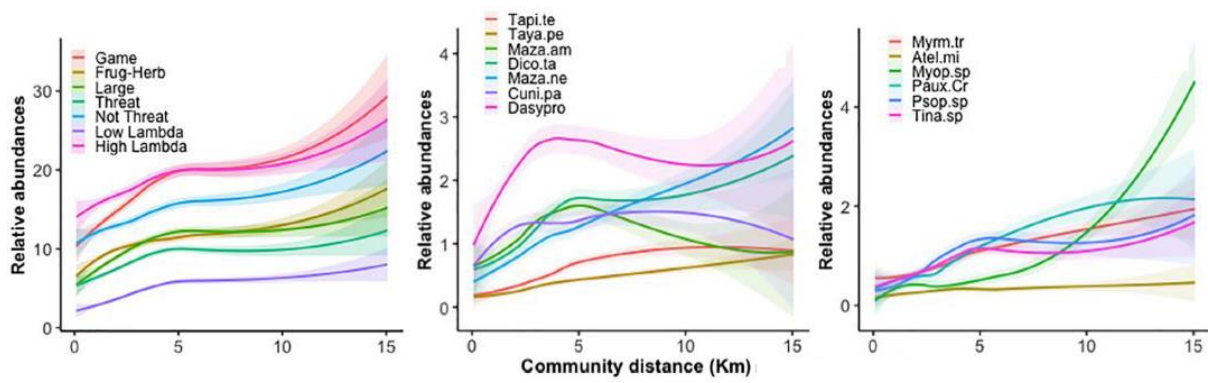


Brodie and Fragoso (2021) examine the distribution of bushmeat hunting efforts across landscapes in Guyana by testing hypotheses about human foraging. Mitigating the massive impacts of defaunation on natural ecosystems requires understanding and predicting hunting effort across the landscape. But such understanding has been hindered by the difficulty of assessing the movement patterns of hunters in thick forests and across complex terrain. The authors statistically tested hypotheses about the spatial distribution of hunting with circuit theory and structural equation models. They used a data set of >7000 known kill locations in Guyana and hunter movement models to test these methods. Comparing models with different resistance layers (i.e., different estimates of how terrain and land cover influence human movement speed) showed that rivers, on average, limited movement rather than serving as transport arteries. Moreover, far more kills occurred close to villages than in remote areas. This, combined with the lack of support for structural equation models that included latent terms for prey depletion driven by past overhunting, suggests that kill locations in this system tended to be driven by where hunters were currently foraging rather than by influences of historical harvest. These analyses are generalizable to a variety of ecosystems, species, and data types, providing a powerful way of enhancing maps and predictions of hunting effort across complex landscapes [208].

Sampaio et al. (2023) look at vertebrate population changes induced by hunting in Amazon sustainable-use areas. The purported sustainability of sustainable-use reserves (SURs) has been questioned in recent decades due to anthropogenic disturbance, including widespread game hunting. A fuller understanding of the drivers of harvest-induced game population changes in SURs is needed to inform this debate. The authors deployed 720 camera traps around 100 local communities both inside and outside nine SURs in central-western Brazilian Amazonia to generate detection records of 29 mammal and bird species. They used Royle-Nichols multi-species occupancy models to evaluate if (i) distance to and size of local communities, (ii) local human population density, (iii) distance to and size of urban areas, (iv) local level of protection, and (v) alternative availability of aquatic protein affected the (a) species richness, (b) aggregated abundance and (c) biomass, (d) mean reproductive rate of species, and (e) mean abundance of functional groups and (f) individual species. Community distance was the main determinant of wildlife declines, impacting species up to 5-km from communities, but three game species exhibited higher abundances within this distance. Other drivers, such as community size and urban neighbourhood, also contributed to species declines. Availability of alternative aquatic

protein buffered declines of only two species and local protection increased species richness and aggregate abundance. These findings can help inform evidence-based conservation strategies in tropical SURs. Their results suggest that preventing habitat loss beyond 5-km radius from communities can promote a healthy source-sink dynamic for populations of game species. Furthermore, game management measures could encourage targeting harvest-tolerant species and the protection of all game species [209].

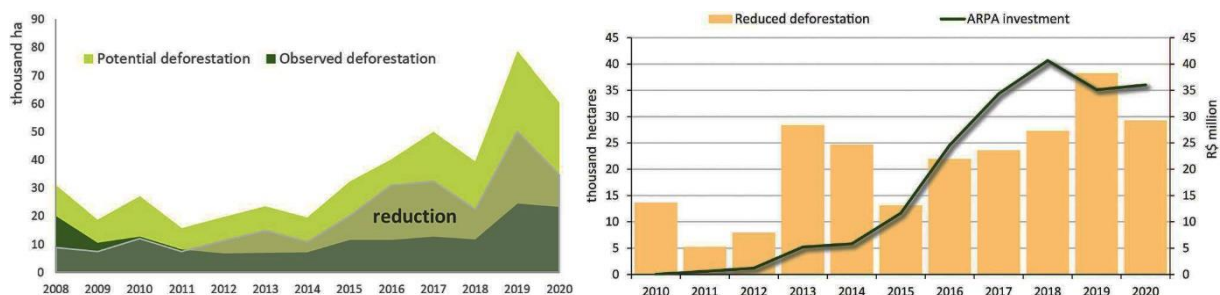
Figure 111: Relationships between distance to the nearest local community from a camera-trap station and abundance of six species groupings (E; Game; Frug-Herb [Frugivore and/or Herbivore]; Large [>15 kg]; Threat [Threatened]; Not threat [Not Threatened]; Low Lambda [$\lambda < 1.3$], and High Lambda [$\lambda > 1.3$]), and abundance of seven game species (F; tapir [Tapi.te], white-lipped peccary [Taya.pe], red brocket deer [Maza.am], collared peccary [Dico.ta], grey brocket deer [Maza.ne], paca [Cuni.pa]; and agouti [Dasypro]); and six other species (G; giant anteater [Myrm.tr], short-ear dog [Atel.mi], acouchi [Myop.sp], curassow [Paux.Cr], trumpeter [Psop.sp], and large tinamou [Tina.sp]) [209]



8.1.10 Protected Areas

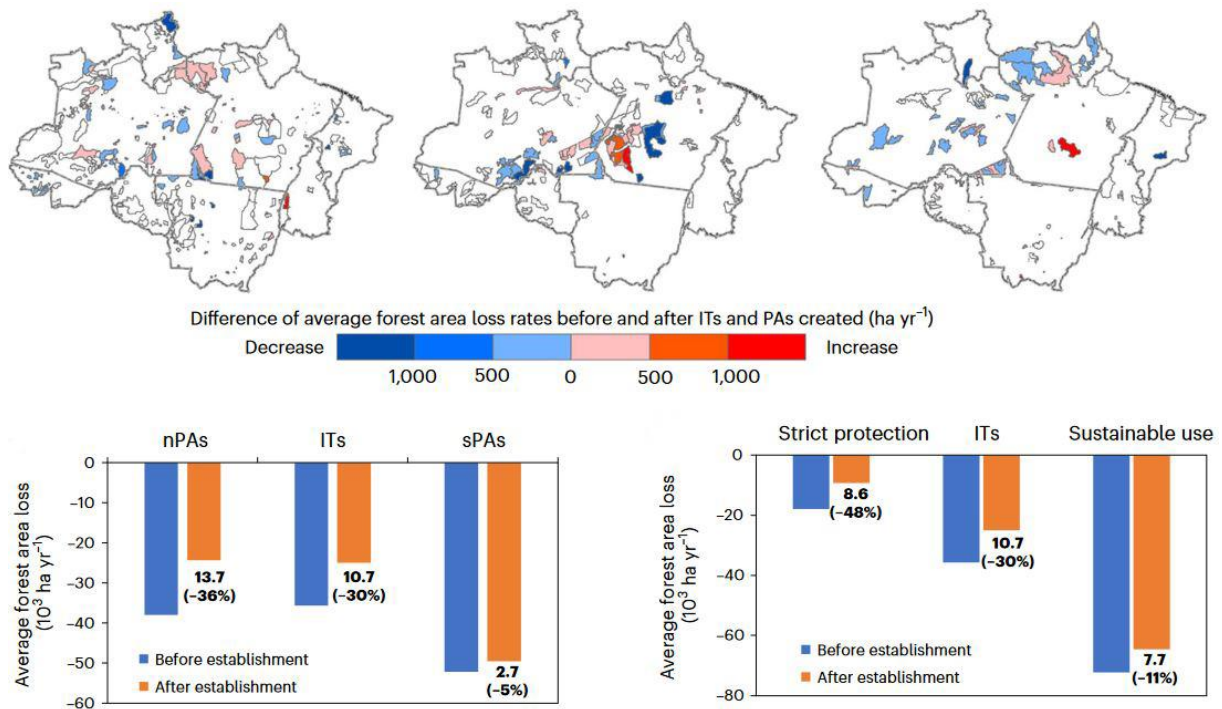
Soares-Filho et al. (2023) measure the contribution of the Amazon protected areas program to forest conservation. Established in 2002, the Amazon Protected Areas Program (ARPA) supports 120 Conservation Units (CUs) in the Brazilian Amazon, covering 62 Mha. The authors quantified the impact of ARPA support on reducing deforestation and CO₂ emissions between 2008 and 2020. They started by examining critical methodological choices, often brushed over in the impact evaluation studies on protected areas (PAs). They then applied a covariate balancing method to control for variation in covariates so as to compare differences in deforestation between Strictly Protected (SP) and Sustainable Use (SU) CUs with and without ARPA support as well as to assess the influence of ARPA investment mechanism on the differential reductions. Next, they estimated total reductions in deforestation and CO₂ emissions by using the Adjusted Odds Ratio. It was found that ARPA support accounts for additional deforestation reductions of 9 % in SP CUs and 39 % in SU CUs in relation to non-supported CUs. The effects of ARPA investment mechanism were statistically significant for both categories of CUs. CUs plus Indigenous Lands (i.e., PAs) reduced by 21 % (2.0 ± 0.3 Mha) Amazon deforestation between 2008 and 2020. Of this total, ARPA CUs accounts for 264 ± 25 thousand ha, the equivalent of 104 ± 10 Mtons of CO₂ emissions. If deforestation continues unabated, PAs will become the last citadels of the Amazon. However, protecting the Amazon only with PAs does not suffice. Additional investments in a comprehensive conservation policy mix are needed along with a monitoring and evaluation strategy to provide evidence on what works for effective and socially equitable forest conservation [210].

Figure 112: Left: Annual deforestation observed in CUs (Conservation Units) with ARPA (Amazon Protected Areas Program) support compared with the estimated potential one in case of non-protection together with associated reduction. Right: Direct investment by ARPA in supported CUs compared with their annual deforestation reductions [210].



Qin et al. (2023) look at forest conservation in indigenous territories and protected areas in the Brazilian Amazon. Conflicts between forest conservation and socio-economic development in the Brazilian Legal Amazon have persisted for years but the effects of Indigenous territory (ITs) and protected area (PAs) status on deforestation there remain unclear. To address this issue, the authors analysed time-series satellite images and qualified annual forest area in the BLA under different governance and management regimes. Between 2000 and 2021, areas classified as ITs or PAs increased to cover 52% of forested areas in the BLA while accounting for only 5% of net forest loss and 12% of gross forest loss. In the years (2003–2021) after establishment, gross forest loss fell 48% in PAs subject to 'strict protection' and 11% in PAs subject to 'sustainable use'. However, from 2018 to 2021 the percentage rate of annual gross forest loss in ITs/PAs was twice that of non-designated areas. Their findings reveal the vital role of, and substantial progress achieved by, ITs and PAs in Amazonian forest conservation as well as the dangers of recent weakening of Brazil's forest policies [211].

Figure 113: Left: The effects of ITs/PAs on annual forest area loss rates in the BLA (2001–2021). Above: Spatial distribution of the changes in annual gross forest area loss rates before and after ITs/PAs establishment by ITs (left), national PAs (centre) and state PAs (right), All ITs/PAs established before and during 2002 are white polygons. Below: changes in average annual gross forest loss rates before and after the ITs/PAs establishment by governance (national PAs, ITs and state PAs) (left) and management (strict protection and sustainable use) (right) [211].

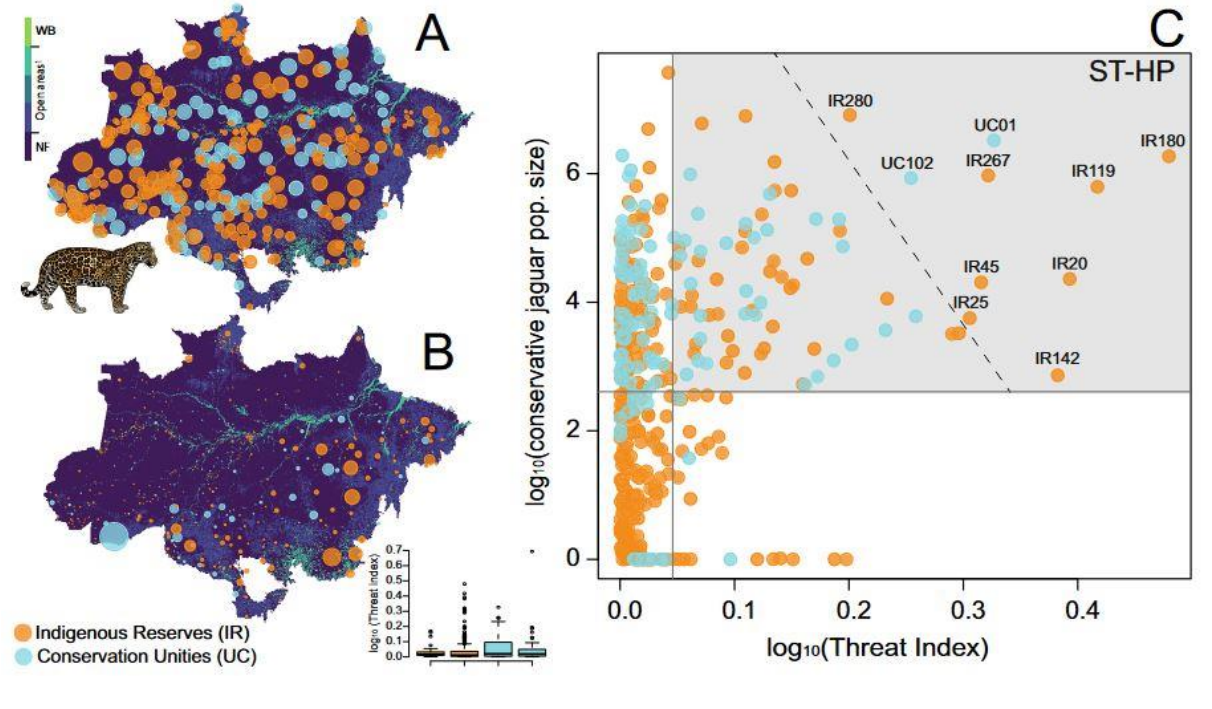


West et al. (2022) find that the Brazilian protected areas are still used to produce Brazil's cattle. Cattle production inside Brazil's protected areas (PAs), including indigenous lands, continues to contaminate Amazonian supply chains more than a decade after efforts to reform the sector were launched with the signing of the zero-deforestation cattle agreements (CAs). During 2013–2018, nearly 1.1 million cattle head were sold directly from private properties inside PAs to slaughterhouses in Mato Grosso, Pará, and Rondônia states. Another 2.2 million head were linked via indirect suppliers located in PAs. Most of these 3.3 million slaughtered head were originated in to sustainable-use areas (72%), where cattle ranching may be permitted in certain cases; however, production also occurred in strictly protected units (20%) and indigenous lands (8%), where commercial grazing activities are illegal and prohibited by the CAs. Nearly half of the PA properties linked to cattle transactions from 2013 to 2018 also had deforestation. We estimate that approximately 2.8 million cattle head from properties in PAs were sold to slaughterhouses participating in the CAs (86% of the total cattle from indirect suppliers in PAs). Controlling commercial cattle production inside of PAs is crucial to both ensure Brazil's access to international beef markets and protect critical biodiversity regions in the Amazon rainforest [212].

Bogoni et al. (2023) evaluate impending anthropogenic threats and protected area prioritization for jaguars in the Brazilian Amazon. Jaguars (*Panthera onca*) exert critical top-down control over large vertebrates across the Neotropics. Yet, this iconic species have

been declining due to multiple threats, such as habitat loss and hunting, which are rapidly increasing across the New World tropics. Based on geospatial layers, the authors extracted socio-environmental variables for 447 protected areas across the Brazilian Amazon to identify those that merit short-term high-priority efforts to maximize jaguar persistence. Data were analysed using descriptive statistics and comparisons of measures of central tendency. The results reveal that areas containing the largest jaguar densities and the largest estimated population sizes are precisely among those confronting most anthropogenic threats. Jaguars are threatened in the world’s largest tropical forest biome by deforestation associated with anthropogenic fires, and the subsequent establishment of pastures. By contrasting the highest threats with the highest jaguar population sizes in a bivariate plot, the authors provide a shortlist of the top-10 protected areas that should be prioritized for immediate jaguar conservation efforts and 74 for short-term action. Many of these are located at the deforestation frontier or in important boundaries with neighbouring countries (e.g., Peruvian, Colombian and Venezuelan Amazon). The predicament of a safe future for jaguars can only be ensured if protected areas persist and resist downgrading and downsizing due to both external anthropogenic threats and geopolitical pressures (e.g., infrastructure development and frail law enforcement) [213].

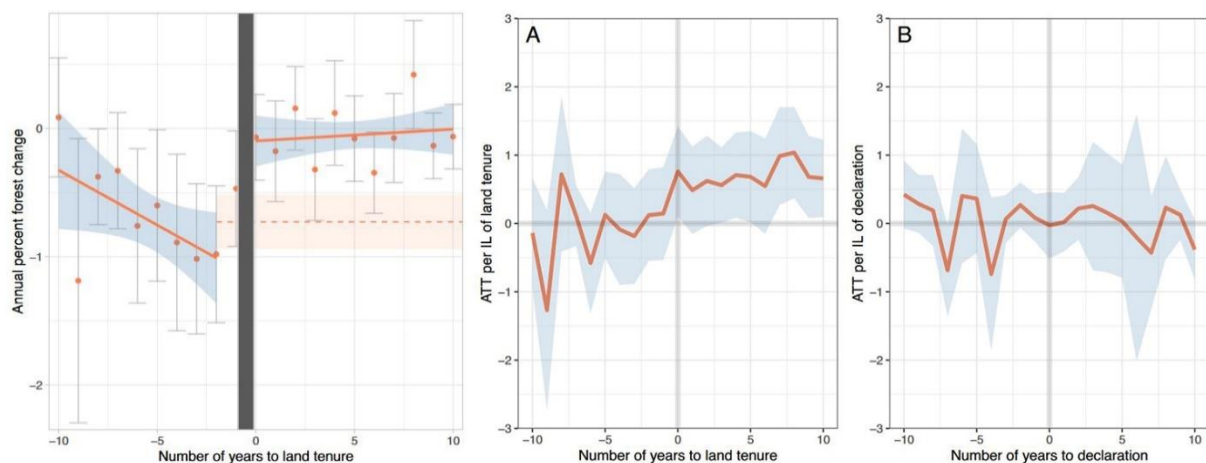
Fig. 114: Jaguar population size, threat index (TI) and prioritization diagram for jaguar conservation across the Brazilian Amazon. Distribution of jaguar population size ($\log_{10} x + 1$) inside protected areas (A), threat index (TI) and values per protected area type (B) and bivariate plot between the threat index and conservative jaguar population sizes inside 447 protected areas across the Brazilian Amazon (C). Acronyms are ST-HP: short-term high-priority quadrant (delimited by highlighted grey frame) and the respective top-ranking 10 areas that should be prioritized in each approach based on the extreme of distribution thresholds by a tangential line. We also identified additional Amazonian PAs that should be prioritized for jaguar conservation in the short to medium term according to our prioritization quadrants [213]



Benzeev et al. (2022) found a relation between the tenure formalisation of indigenous lands and improved forest outcomes in the Brazilian Atlantic Forest. A growing body of research demonstrates that tenure of Indigenous lands improves livelihoods and protects forests in addition to inherently recognizing human rights. However, the effect of tenure on environmental outcomes has scarcely been tested in regions with high development pressure, such as those with persisting forest–agriculture conflicts. The authors conduct

an event study and a difference-in-differences analysis to estimate the average treatment effect of land tenure on forest cover change for 129 Indigenous lands in the Atlantic Forest of Brazil from 1985 to 2019. They found that forest outcomes in Indigenous lands improved following tenure compared to pre-tenure and that forest outcomes improved in tenured compared to non-tenured lands. They also found that formalized tenure, rather than incomplete tenure, was necessary to improve forest outcomes. The study is the first rigorous analysis of the effect of tenure on Indigenous lands in the globally important Atlantic Forest biome and contributes to a growing body of literature on the role of rights-based approaches to conservation. The evidence presented in this study may support efforts to secure the legal rights and autonomy of Indigenous peoples [214].

Figure 115: Left: ES analysis displaying trends in forest cover change (measured by %) before and after tenure for 78 Indigenous Lands (ILs). Orange points represent binned averages of all ILs in each year in the dataset and 95% CIs (error bars) are included for each point each year. Orange lines represent the average trend and 95% CIs (blue shading) are included for the slope of the mean regression line. Right: Staggered difference-in-differences (DID) dynamic estimates of the average treatment effect of land tenure (ATT) per IL by year on forest cover change (measured by %) relative to (A) number of years to formalized tenure (the fourth and final stage of the tenure process), and (B) number of years to declaration (stage three of the tenure process). The red line represents the ATT of tenured ILs and blue shaded area represents uniform 95% CIs around the effect. The model of formalized tenure (A) shows an overall significant result of reduced deforestation and/or increased reforestation, while the model of declaration (B) does not [214]

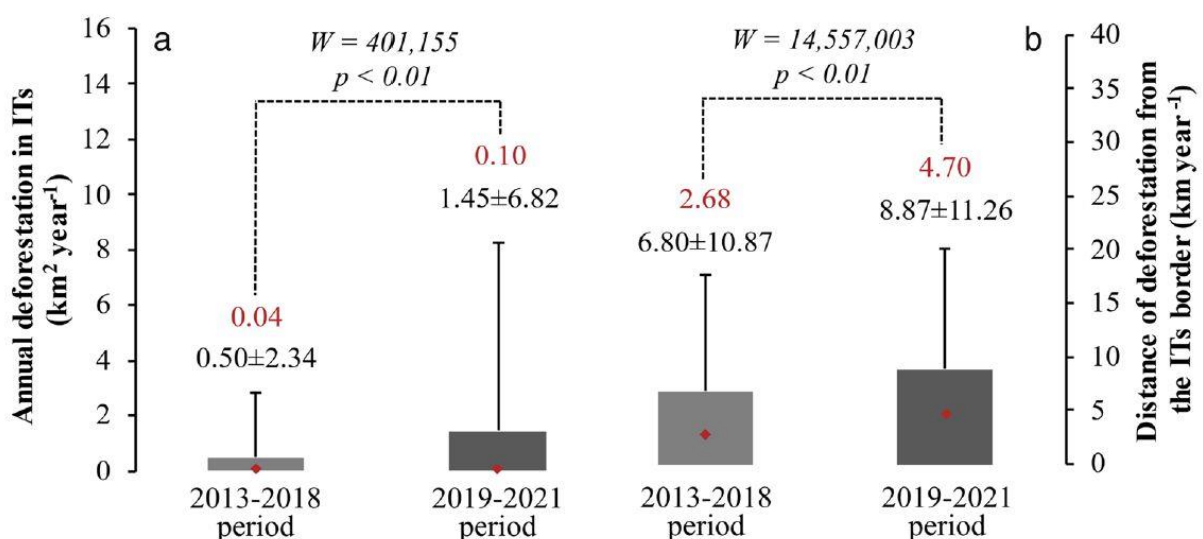


Alves et al. (2022) look at the traditional ecological knowledge maintained by local forest specialists in the face of environmental threats to Brazilian Amazonian protected areas. Environmental threats resulting in local biodiversity loss might compromise traditional peoples' livelihoods and their traditional ecological knowledge (TEK). The authors investigated how the personal characteristics of local specialists (forest experience, gender, and origin) and environmental threats (deforestation, mining, and fires) influence some components of TEK associated with forests. From 2015 to 2019, they conducted free-listing interviews with 208 specialists from 27 communities in and near 10 protected areas (PAs) in Brazilian Amazonia. They recorded forest trees and palms that the specialists mentioned as used, managed, and traded. Plant knowledge was variable, since 44% of the 795 ethnospecies were mentioned only once. Using Mixed-Effects Models, we identified that people with longer forest experience and men tended to cite more used and traded ethnospecies. Women knew more about human food, while men knew more about construction and animal food. Specialists with greater forest experience knew more about protective management and planting. Specialists living in communities influenced by mining cited fewer used ethnospecies, and those in more deforested communities cited proportionally more planting. Environmental threats had smaller effects on TEK than

personal characteristics. The components of TEK that we assessed highlight the forest's great utility and the importance of management of PAs to maintain biodiversity and traditional people's livelihoods. The communities' stocks of TEK persisted in the face of environmental threats to PAs, highlighting the resistance of traditional peoples in the face of adversities. This quantitative approach did not show the trends that are generally imagined, i.e., loss of forest TEK, but demonstrates that in order to change the Amazonian development model it is important to keep the forest standing, and that knowledge exists and resists [215].

Silva Junior et al. (2023) find that Indigenous Territories (ITs) in the Brazilian Amazon are under deforestation pressure. About 700 thousand indigenous people live in ITs in Brazil, and over half of the ITs are within the Brazilian Legal Amazon. ITs host more than one million square kilometres of rainforests that contribute to climate regulation, store carbon, and are home to unique biodiversity and sociocultural diversity of indigenous peoples. Studies showed that Brazilian Amazon ITs are efficient models for preserving forests by reducing deforestation, fires, and related carbon emissions. Considering the importance of ITs for conserving socio-environmental and cultural diversity and the recent climb in the Brazilian Amazon deforestation, the authors used official remote sensing datasets to analyse deforestation inside and outside indigenous territories within Brazil's Amazon biome during the 2013–2021 period. Deforestation has increased by 129% inside ITs since 2013, followed by an increase in illegal mining areas. In 2019–2021, deforestation was 195% higher and 30% farther from the borders towards the interior of indigenous territories than in previous years (2013–2018). Furthermore, about 59% of carbon dioxide (CO₂) emissions within ITs in 2013–2021 (96 million tons) occurred in the last three of all analysed years, revealing the magnitude of increasing deforestation to climate impacts. Therefore, curbing deforestation in indigenous territories must be a priority for the Brazilian government to secure these peoples' land rights, ensure the forests' protection and regulate the global climate [216].

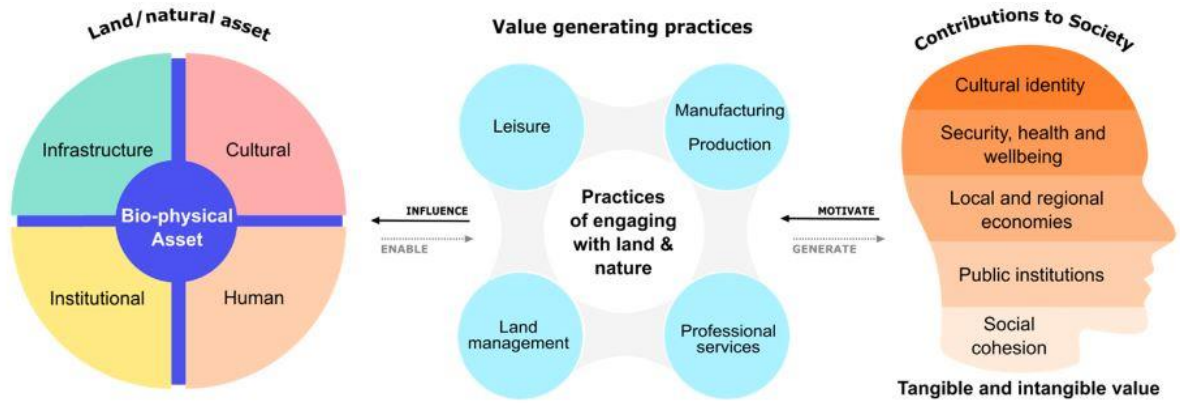
Figure 116: (a) Average deforestation within each indigenous land before (2013–2018) and during the current environmental setback intensification period (2019–2021). (b) Mean distance from deforestation polygons within indigenous lands to borders before (2013–2018) and during the current environmental setback intensification period (2019–2021). The numbers in red represent medians. The numbers after the plus/minus signal represent the standard deviation [216].



Franco-Moraes et al. (2023) look at the forest management perspective carried out by the Zo'é people in Northern Amazonia, and its implications for floristic diversity and biocultural conservation. Indigenous perspectives on forest management are grounded in traditional ecological knowledge (TEK), so that socioculture influences the ways Indigenous Peoples transform their landscapes. However, how socioculture structures Indigenous perspectives on forest management is unclear. Moreover, little is known about the influence of Indigenous landscape transformations on forest succession and floristic diversity. The authors test hypotheses from biocultural and ecological theories suggesting that: (i) key social-ecological relationships with specific taxa structure Indigenous perspectives on forest management; (ii) such relationships guide sustainable management that generates resilient forest regrowth; and (iii) this management promotes floristic diversity by acting as an intermediate disturbance. They collected information about cosmology, occupation history and management among the Zo'é, in Brazilian Amazonia. They also carried out floristic inventories in old-growth forests and in old Zo'é swidden-fallow areas to analyse forest structure and alpha- and beta-diversity along a gradient of forest successional stages. The authors show that the Zo'é perspective on forest management is structured by an ethical principle involving a social-ecological relationship with different beings, especially the spider monkey (*Ateles sp.*). This relationship generates mobility among the Zo'é that allows forest regrowth in their fallow areas, so that in 28 years, forest basal area may equal that of old-growth forests. In addition, Zo'é forest management has increased alpha- and beta-diversity by increasing species richness and diversity in intermediate secondary forests and promoting floristic turnover at the landscape-level. The study's results show that some aspects of Zo'é cosmology influence forest disturbance regimes that generate a sustainable social-ecological system, therefore being key for Zo'é well-being and local biodiversity conservation. The authors believe that Indigenous perspectives about forest management should be included in forest conservation efforts aimed at protecting Amazonian biocultural diversity, thus valuing TEK and engendering sustainable social-ecological systems [217].

Lessa et al. (2021) reveal the hidden value of protected areas. Protected areas (PAs) are the main spatial policy instrument for conserving biodiversity and have expanded dramatically in the last 30 years. This expansion has not been matched by a corresponding increase in financial investment, leaving many areas without sufficient resources for essential management actions. Moreover, in some parts of the world politicians and policy-makers are increasingly viewing PAs as an 'opportunity costs' that are holding back economic and social development. A major contributor to this perspective is that PAs are consistently undervalued, with the multiple benefits that they provide to society frequently obscured by the focus on their core missions to conserve biodiversity, protect rare species and sustain vital ecosystem processes and services. The recently proposed 'Protected Area Asset Framework' (PAAF) was designed to address these twin challenges (funding shortfalls and negative perceptions) by: i) revealing and highlighting the multiple values (tangible and intangible) that PAs generate for society, and; ii) leveraging the value-generating characteristics (assets) of PAs to attract inward investments. The authors argue that, going forward, assets-based approaches will be essential for recapitalizing and safeguarding PAs, especially in developing countries. They conclude by proposing a protocol for implementing and monitoring the PAAF [218].

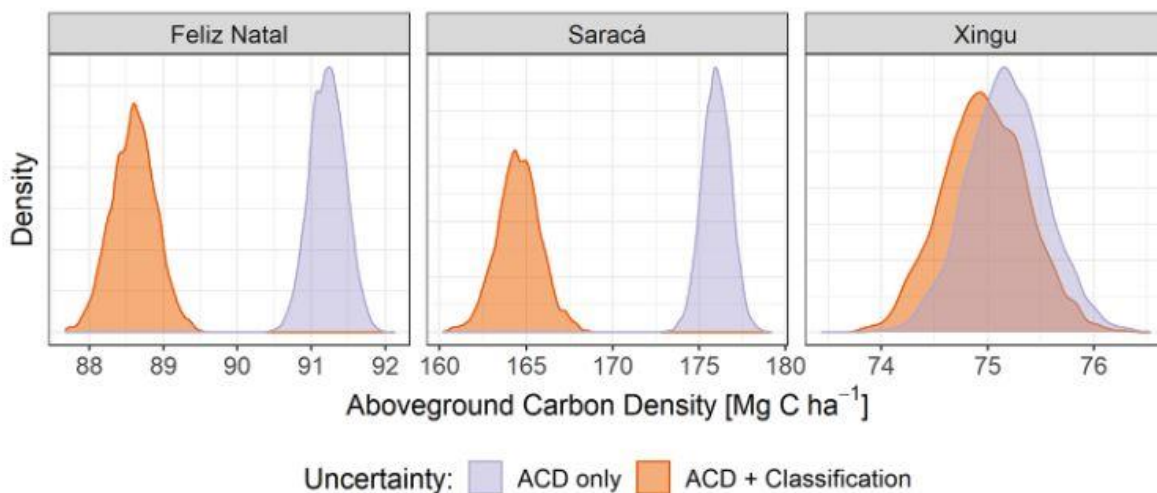
Figure 117: A schematic representation of the Protected Area Asset Framework (PAAF). Protected area assets enable and are influenced by value generating practices that generate tangible and intangible value for society [218]



8.1.11 Forest biomass and carbon

Rangel Pinagé et al. (2023) look at the effects of the mapped class of forest degradation (i.e. fire, selective logging, fragmentation) on the uncertainty of aboveground carbon estimates over three test sites in the Brazilian Amazon. Existing uncertainties on land cover classification and in biomass estimates hinder accurate attribution of carbon emissions to specific forest classes. The study used textural metrics derived from PlanetScope images to implement a probabilistic classification framework to identify intact, logged and burned forests in three Amazonian sites. The authors also estimated biomass for these forest classes using airborne lidar and compared biomass uncertainties using the lidar-derived estimates only to biomass uncertainties considering the forest degradation classification as well. Their classification approach reached overall accuracy of 0.86, with accuracy at individual sites varying from 0.69 to 0.93. Logged forests showed variable biomass changes, while burned forests showed an average carbon loss of 35%. They found that including uncertainty in forest degradation classification significantly increased uncertainty and decreased estimates of mean carbon density in two of the three test sites. The study's findings indicate that the attribution of biomass changes to forest degradation classes needs to account for the uncertainty in forest degradation classification. By combining very high-resolution images with lidar data, the authors could attribute carbon stock changes to specific pathways of forest degradation. This approach also allows quantifying uncertainties of carbon emissions associated with forest degradation through logging and fire. Both the attribution and uncertainty quantification provide critical information for national greenhouse gas inventories [219].

Figure 118: ACD (Above-ground carbon density) distributions considering uncertainties from ACD estimates only, and both ACD and forest degradation classification uncertainties [219]



Uribe et al. (2023) predict a net loss of biomass for global tropical biomes in a changing climate. Although precipitation and temperature are shifting across the tropics, their effect on biomass and carbon storage remains uncertain. The authors use empirical relationships between climate and aboveground biomass content to show that the contraction of humid regions, and expansion of those with intense dry periods, results in substantial carbon loss from the neo-tropics. Under a low emission scenario (Representative Concentration Pathway 4.5) this could cause a net reduction of aboveground live carbon of $\sim 14.4\text{--}23.9$ PgC (6.8–12%) from 1950–2100. Under a high emissions scenario (Representative Concentration Pathway 8.5) net carbon losses could double across the tropics, to $\sim 28.2\text{--}$

39.7 PgC (13.3–20.1%). The contraction of humid regions in South America accounts for ~40% of this change. Climate mitigation strategies could prevent half of the carbon losses and help maintain the natural tropical net carbon sink [220].

Figure 119: Changes in carbon in the tropics under RCP 4.5: Changes in carbon levels (in Pg) by climatic zone and by region from 1950–2099 (only three time steps labelled for readability). Bar height is the average total C in each timeframe ± the bootstrapped confidence limits [220]

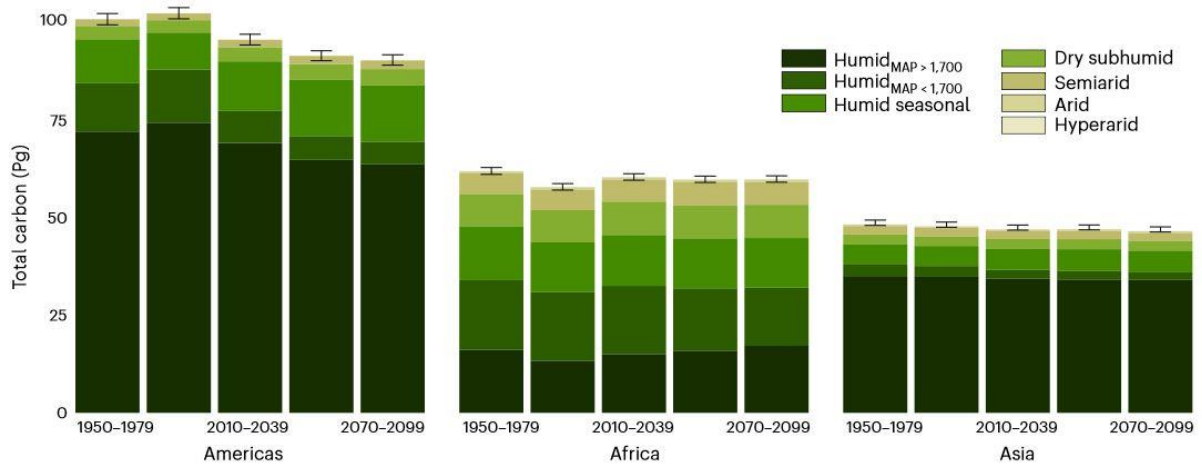
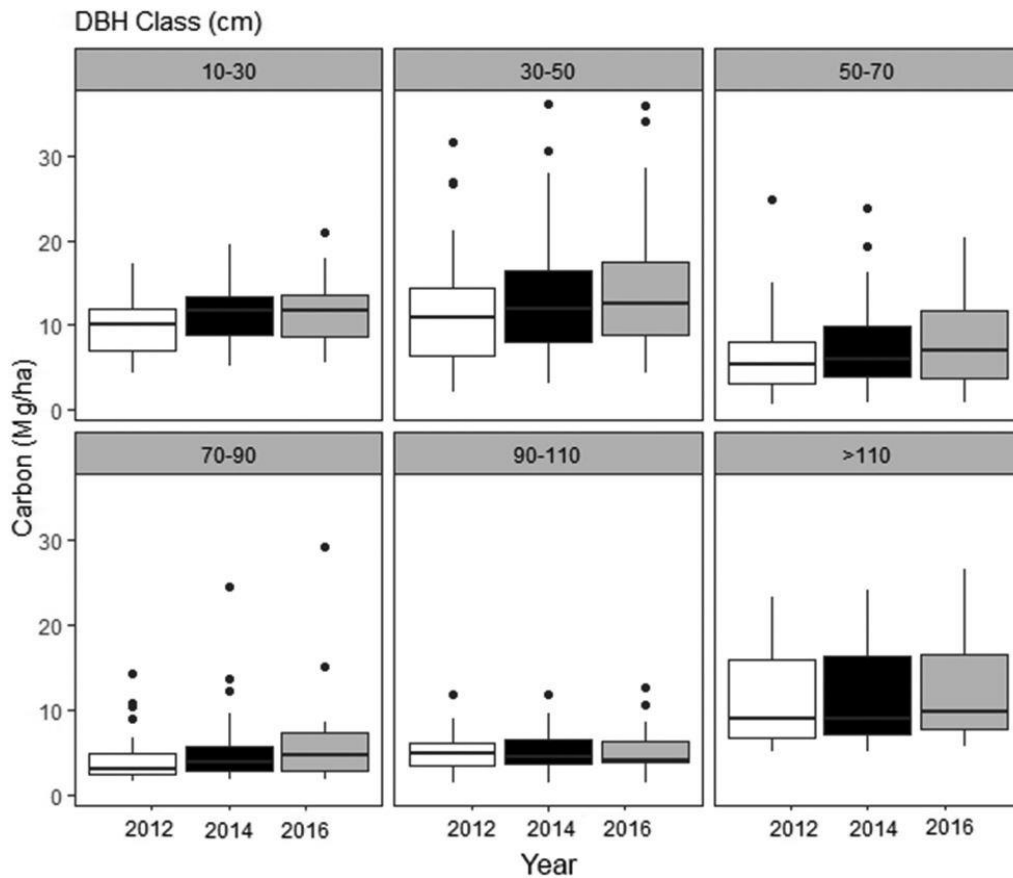


Figure 120: Boxplot (with quartiles and median) of carbon (Mg/ha) between DBH classes and years [221]

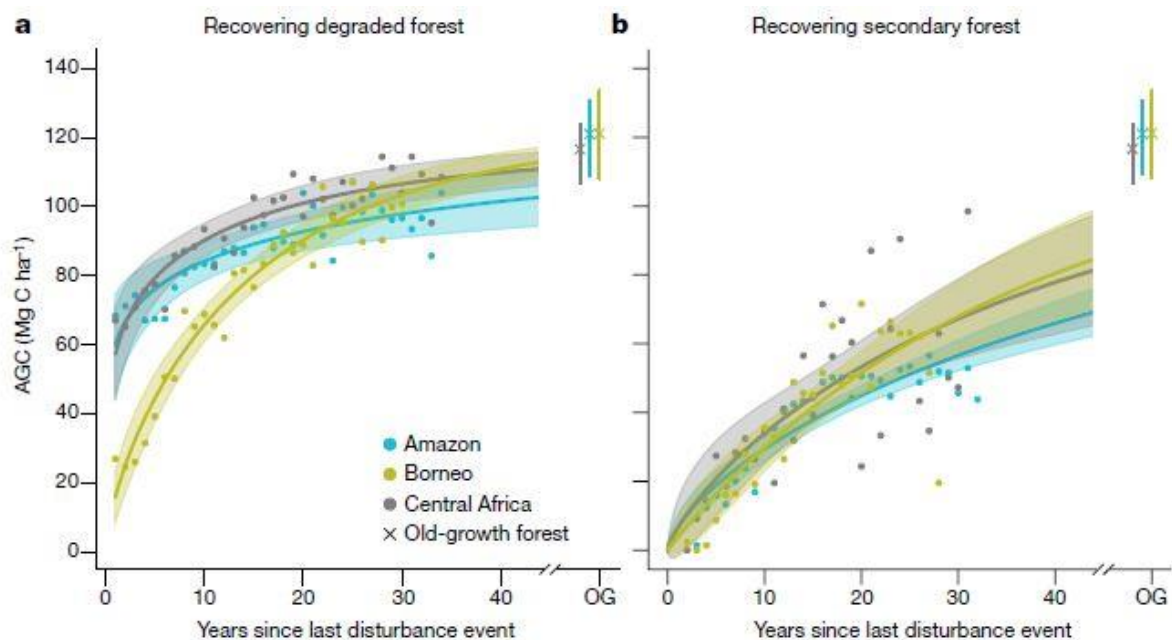


Costa et al. (2022) look at the dynamic and stock of carbon in middle Xingu forests in eastern Amazonia. The authors assessed the spatial distribution and dynamic of carbon in forest plots in the Middle Xingu. These plots are part of the vegetation monitoring area of the Belo Monte Dam. They estimated the biomass of trees with diameter at breast height (DBH) ≥ 10 cm using an allometric equation with forest inventory data in the eastern Amazonian region in the Xingu River area. They evaluated the vegetation structure and carbon stock dynamic in 2012, 2014, and 2016, and temporal effects on carbon uptake. The periodic annual increase in carbon was significantly higher between 2012 and 2014 (2.5 Mg ha^{-1}) than between 2014 and 2016 (1.84 Mg ha^{-1}). Plant biomass was highly influenced by the abundance of species with low diameters (between 10 cm and 50 cm DBH). Despite the mortality rate being higher than the recruitment in the second period (2014–2016), we found that the forest did function as a carbon sink but showing increases in carbon emissions [221].

8.1.12 Forest regrowth and restoration

Heinrich et al. (2023) analyse the carbon sink of secondary and degraded humid tropical forests. The globally important carbon sink of intact, old-growth tropical humid forests is declining because of climate change, deforestation and degradation from fire and logging. Recovering tropical secondary and degraded forests now cover about 10% of the tropical forest area, but how much carbon they accumulate remains uncertain. The authors quantify the aboveground carbon (AGC) sink of recovering forests across three main continuous tropical humid regions: the Amazon, Borneo and Central Africa. On the basis of satellite data products, their analysis encompasses the heterogeneous spatial and temporal patterns of growth in degraded and secondary forests, influenced by key environmental and anthropogenic drivers. In the first 20 years of recovery, regrowth rates in Borneo were up to 45% and 58% higher than in Central Africa and the Amazon, respectively. This is due to variables such as temperature, water deficit and disturbance regimes. They find that regrowing degraded and secondary forests accumulated 107 Tg C year⁻¹ (90–130 Tg C year⁻¹) between 1984 and 2018, counterbalancing 26% (21–34%) of carbon emissions from humid tropical forest loss during the same period. Protecting old-growth forests is therefore a priority. Furthermore, we estimate that conserving recovering degraded and secondary forests can have a feasible future carbon sink potential of 53 Tg C year⁻¹ (44–62 Tg C year⁻¹) across the main tropical regions studied [222].

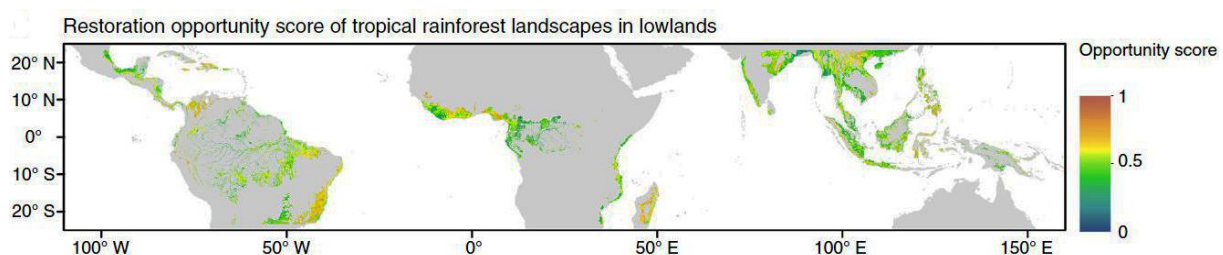
Figure 121: Modelled AGC accumulation with YSLD in different tropical regions. AGC is shown in degraded forests (a) and secondary forests (b) in the Amazon, Borneo and Central Africa tropical humid forest regions. Points denote the median AGC value calculated for each YSLD, fitted lines are based on a nonlinear model. Shading denotes the 95% confidence interval of the nonlinear model. Crosses denote the median AGC of old-growth (OG) forests in the respective regions and associated 95% confidence interval from the Monte Carlo simulation [222]



Edwards et al. (2021) look at upscaling tropical restoration to deliver environmental benefits and socially equitable outcomes. The UN Decade on Ecosystem Restoration offers immense potential to return hundreds of millions of hectares of degraded tropical landscapes to functioning ecosystems. Well-designed restoration can tackle multiple Sustainable Development Goals, driving synergistic benefits for biodiversity, ecosystem

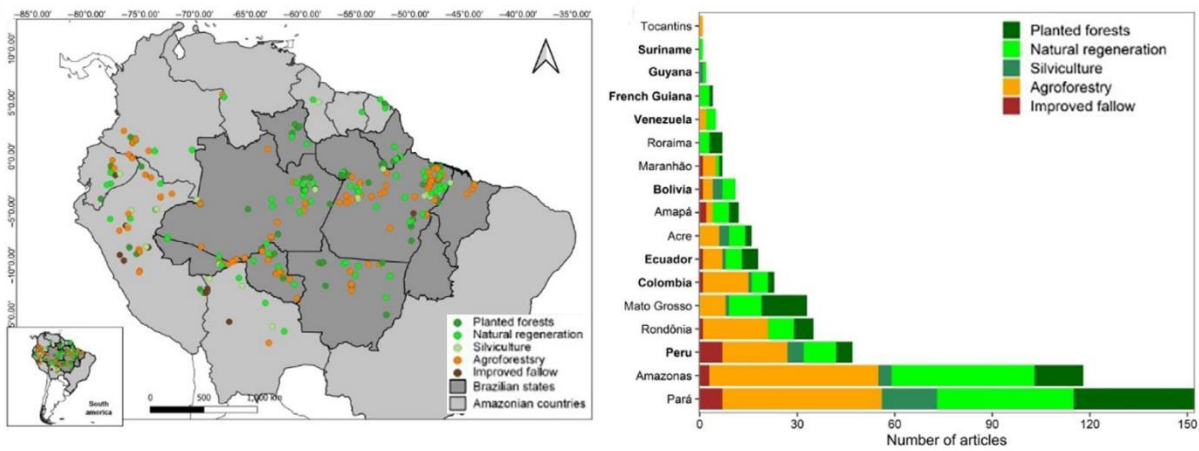
services, agricultural and timber production, and local livelihoods at large spatial scales. To deliver on this potential, restoration efforts must recognize and reduce trade-offs among objectives, and minimize competition with food production and conservation of native ecosystems. Restoration initiatives also need to confront core environmental challenges of climate change and inappropriate planting in savanna biomes, be robustly funded over the long term, and address issues of poor governance, inadequate land tenure, and sociocultural disparities in benefits and costs. Tackling these issues using the landscape approach is vital to realizing the potential for restoration to break the cycle of land degradation and poverty, and deliver on its core environmental and social promises. Restoration of terrestrial vegetation, from tree-dominated to sparsely wooded savanna habitats, offers multiple potential benefits across the tropics. It also offers benefits in open wetlands and mangroves, but the authors concentrate on terrestrial ecosystems as the primary restoration frontiers. Across the diversity of restoration actions — spanning logged forest recovery, regeneration of abandoned farmland, plantation development, and on-farm restoration—environmental and social outcomes and challenges vary considerably, including across regions [223].

Figure 122: Restoration opportunity score in lowland moist tropical forest, indicating that restoration hotspots (i.e. clusters of red cells with a normalised score >0.8) exist across the tropics. Higher scores denote areas where appropriate restoration may maximise benefits (biodiversity conservation, climate change mitigation, climate adaptation, and water security) while increasing the likelihood of effective implementation and long-term sustainability (low land opportunity cost, lower deforestation rates in surrounding area, and higher likelihood of biodiversity recovery) [223]



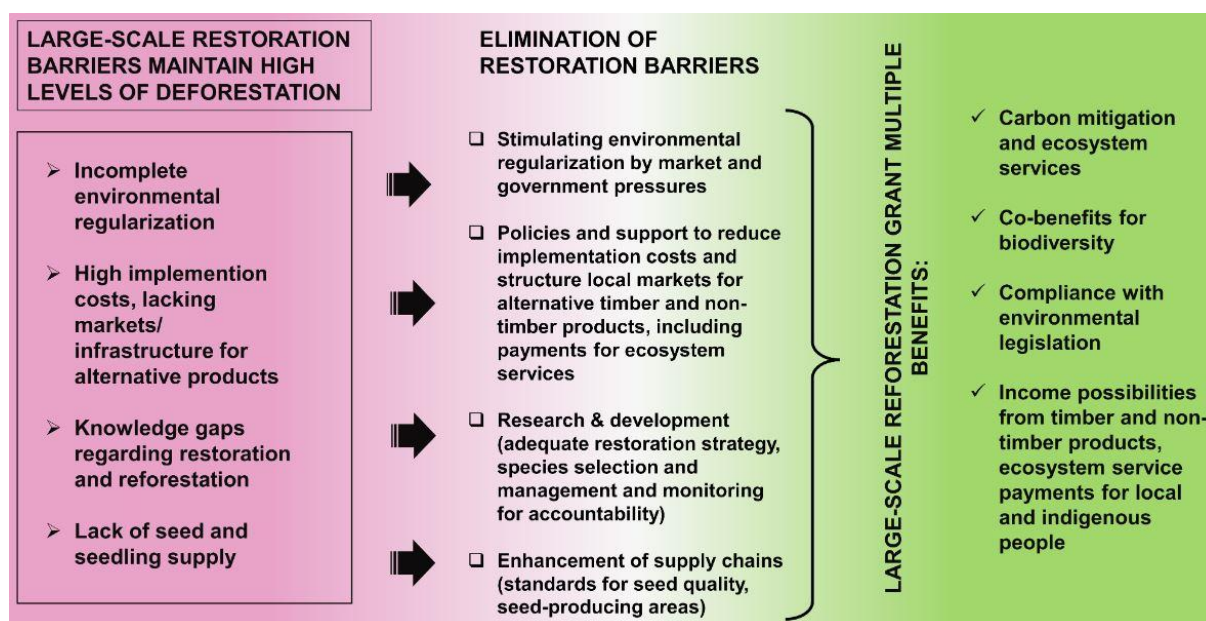
Da Silva et al. (2023), in a review article, examine the potential for forest landscape restoration in the Amazon with a view on the state of the art of restoration strategies. Forest landscape restoration (FLR) is the intentional intervention in the forest landscape to recover biological diversity and ecosystem functions, improving human well-being in altered landscapes. The general objective of the study was to understand the state of the art of research that potentially contributes to FLR practices in the Amazon. The authors carried out a comprehensive literature review using the Web of Science platform, considering papers published between 2000 and 2020 to understand the state of knowledge on restoration strategies that support FLR in the nine Amazonian countries and the nine states of the Brazilian Amazon. They selected 362 articles that met their inclusion criteria after analysing 1,205 articles. They found that Brazil, followed by Peru, Colombia, and Ecuador, has the largest number of published articles on FLR. Agroforestry (37.88%) and natural regeneration (30.35%) were the most common FLR strategies across all countries and Brazilian states. Most studies investigated ecological functioning (33%), vegetation structure (31%), and tree diversity (15.5%). Forest restoration strategies (forest plantation, natural regeneration, or silviculture) are reported in most studies (57.23%), in comparison to restoration strategies of agricultural lands (agroforestry systems or improved fallow; 42.77%). They found an increase in publications describing restoration strategies over time in the Amazon, especially from 2012 onwards, with a peak in 2018. According to the authors, future studies in the Amazon region should address socioeconomic issues and expand the geographic scope within the Amazon, as well as the FLR strategies and the ecosystem attributes investigated [224].

Figure 123: Left: Spatial distribution of restoration strategies in the countries of the Amazon biome and in the Brazilian states of the Amazon (bold lines). Different colours represent the different restoration strategies implemented in the region. Right: Number of articles describing restoration strategies in the Amazon biome in horizontal bars [224].



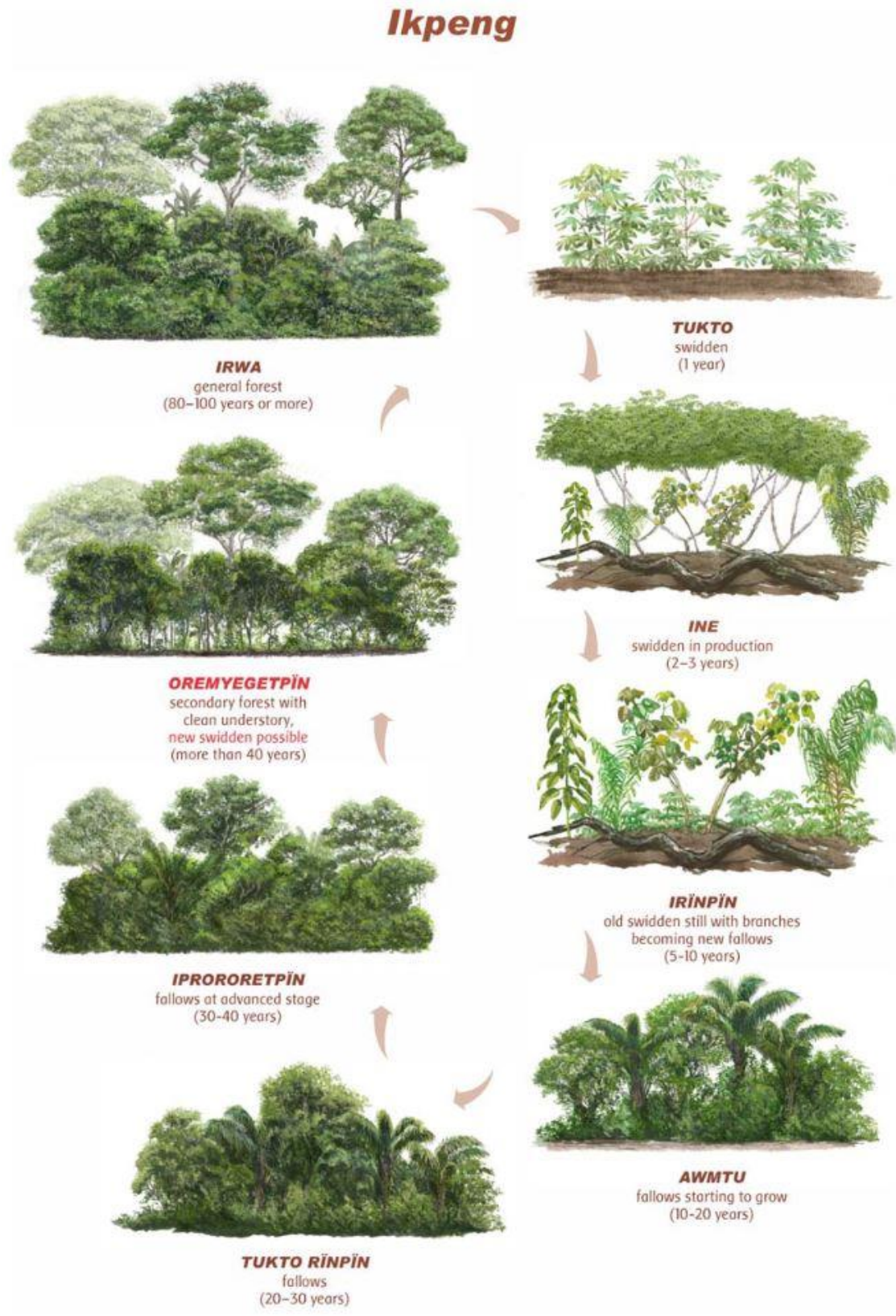
Gastauer et al. (2020) look at the opportunities and constraints of large-scale forest restoration in the Brazilian Amazon. The scientific community claims that for Amazonia 4.0, i.e. an emerging bio-economy valuing biodiversity by aggregating new technologies and possibilities such as cyber-physical systems, internet of things, communication networks and artificial intelligence with the socio-environmental resources of the Amazon region, large-scale forest restoration is required to prevent the world's largest tropical forest from collapsing. The forest landscape restoration concept extends beyond pure ecological restoration, i.e., the restitution of biodiversity and ecosystem structure and functioning to original, old-growth forest levels, to include agroforestry systems, tree plantations and further initiatives to reconstitute the forest canopy aiming to link ecological needs to enhance biodiversity and ecosystem services with the economic demands of local communities and land owners. Although carbon sequestration is often the primary driver of contemporary forest restoration, further co-benefits emerge for air purification, water management, biodiversity and income possibilities, especially when native species are used. Monitoring is necessary to evaluate the success of forest restoration activities, especially when regenerating forests are used to achieve corporate carbon neutrality or fulfil national or international environmental commitments. A range of indicators, such as the amount and monetary value of sequestered carbon, the number of created jobs, realized trainings, costs related to implementation and net gains of incomes and subsistence, are available to measure socioeconomic restoration outcomes. Environmental assessments necessary to measure the success of ecological restoration efforts should include the evaluation of the vegetation structure, biodiversity measures and ecological processes such as the return of productivity, nutrient cycling, and water management. Despite the recognition of this potential, large-scale restoration initiatives are still challenged by knowledge gaps, insufficient supplies of seeds and seedlings, a lack of incentives, and socioeconomic constraints such as high implementation costs and competition with less sustainable forms of land use. To realize the potential related to large-scale forest restoration in the Brazilian Amazon, it is thus necessary to establish and enhance the entire restoration value chain, ranging from the availability of seeds and seedlings to the processing and commercialization of timber and non-timber products [225].

Figure 124: The elimination of restoration barriers enables society to take advantage of multiple benefits resulting from reduced deforestation rates and increasing forest cover [225].



Saraiva et al. (2020) look at public policies and economic conditions of forest regeneration in the Brazilian Amazon. Secondary vegetation is the land use that has increased the most in the Brazilian Amazon in recent years. Approximately 49% of the increase in the total area since the mid-2000s was due to forest regeneration. In this context, the present study aimed to evaluate how environmental policies and economic conditions have influenced forest regeneration in the Amazon biome. The study is based on the Forest Transition theory, which is associated to a long-term phenomenon in which a decline in primary forest area is followed by forest regeneration. The authors used panel data procedures to estimate several models to assess sources of forest regeneration. The results indicate that variables associated to secondary forest change are the value and intensity of fines, rural credit, agricultural share of GDP, and agricultural and extractive prices. We conclude that public policies that impose fines to combat illegal deforestation favoured an increase in forest regeneration, which was an environmentally positive spillover effect as these policies may promote second forest regeneration as well as decreases in deforestation. Overall, the study's results suggest that both economic drivers (rural credit, agricultural prices, and agricultural share of GDP) and public policies (e.g., command and control enforcement actions applied by IBAMA, represented here by fine number and intensity) were associated with the level of secondary vegetation in the Brazilian Amazon. First, fine value and fine number intensity applied by IBAMA might have played a major role in increasing the proportion of secondary vegetation in the Brazilian Amazon. This reflects a positive spillover effect of national command and control policies, which might not only lead to a decrease in deforestation, but also to an increase in secondary forest. Even though the authors did not detect a leakage from deforestation to secondary variation in the Brazilian Amazon biome, they believe that an assessment of a leakage effect of command and control policies applied in the Amazon on nearby biomes could broaden the notion of the net effect on national environmental performance. Other Brazilian biomes have weaker conservation policies and show increasing deforestation rates, and such a broad analysis could improve our understanding of the determinants of primary and secondary vegetation deforestation on the national level [226].

Figure 125: Illustration of Ikpeng cassava (*Manihot esculenta Crantz*) shifting cultivation cycle in non-anthropogenic soils (nADE). When the fallow reaches the OREMYEGETPİN phase (in red), soils and vegetation are considered as recovered and a new cycle may start [227]



Schmidt et al. (2021) examine how indigenous knowledge and forest succession management can contribute to the reforestation of degraded areas. The indigenous systems of agricultural and forest management in the Amazon are characterized by a deep knowledge of ecological processes, biodiversity, and the use and management of fire. The influence of these systems on the distribution of biodiversity includes semi-domesticated and domesticated species and landscapes, which have led to extensive anthropogenic or cultural forests. However, in many places, the livelihoods of indigenous peoples are being transformed by the intensification of agriculture and social, ecological, and economic changes, putting at risk the sustainability of production systems and food security and sovereignty of these peoples. In the last years, in the Xingu Indigenous Territory (XIT), the food production systems and the form of occupation of territories have changed, affecting the recovery of secondary forests, which now demand a too long period. The increase in the number and frequency of fires has aggravated this situation, due to a drier climate that has become predominant in the region. Changes in climate are attributed to deforestation in the neighboring municipalities, especially in the headwaters of the Xingu river basin. The study was conducted among the Kawaiwete (Tupi-Guarani) and the Ikpeng (CaribArara) peoples in the XIT, in the state of Mato Grosso, Brazil. The main objective was to develop alternative techniques of forest management based on indigenous and scientific knowledge more adapted to the new livelihood contexts, aiming to favour forest regeneration in areas dominated by shifting cultivation. We sought to answer the following questions: (I) How do forests regenerate during the fallow period? (II) How can local management improve forest regeneration? (III) Are there indicator species for secondary succession, soil recovery, and vulnerability to fires? (IV) Is the increase in the number of fires affecting the sustainability of the shifting cultivation systems? Our results show that some local practices based on indigenous knowledge have the potential to facilitate natural regeneration, such as choosing forest areas that have been recovered for agricultural use, limiting the number of cultivation cycles, protecting and selecting of individual trees during cultivation period, and attracting seed dispersers. Assisted natural regeneration strategies grounded on indigenous knowledge are promising ways to restore degraded lands of the XIT [227].

Chen et al. (2023) characterise aboveground biomass and tree cover of regrowing forests in all Brazilian biomes with multi-source remote sensing data. Characterization of regrowing forests is vital for understanding forest dynamics to assess the impacts on carbon stocks and to support sustainable forest management. Although remote sensing is a key tool for understanding and monitoring forest dynamics, the use of exclusively remotely sensed data to explore the effects of different variables on regrowing forests across all biomes in Brazil has rarely been investigated. The authors analysed how environmental and human factors affect regrowing forests. Based on Brazil's secondary forest age map, 3060 locations disturbed between 1984 and 2018 were sampled, interpreted and analysed in different biomes. They interpreted the time since disturbance for the sampled pixels in Google Earth Engine. Elevation, slope, climatic water deficit (CWD), the total Nitrogen of soil, cation exchange capacity (CEC) of soil, surrounding tree cover, distance to roads, distance to settlements and fire frequency were analysed in their importance for predicting aboveground biomass (AGB) and tree cover derived from global forest aboveground biomass map and tree cover map, respectively. Results show that time since disturbance interpreted from satellite time series is the most important predictor for characterizing AGB and tree cover of regrowing forests. AGB increased with increasing time since disturbance, surrounding tree cover, soil total N, slope, distance to roads, and distance to settlements and decreased with larger fire frequency, CWD and CEC of soil. Tree cover increased with larger time since disturbance, soil total N, surrounding tree cover, distance to roads, distance to settlements, slope and decreased with increasing elevation and CWD. These results emphasize the importance of remotely sensing products as key opportunities to improve the characterization of forest regrowth and to reduce data

gaps and uncertainties related to forest carbon sink estimation. The results provide a better understanding of regional forest dynamics, toward developing and assessing effective forest-related restoration and climatic mitigation strategies [228].

Figure 126: 3D scatter plots of all the 3060 sampled regrowing forest points and the regression planes of the fixed effects while modelling AGB and tree cover with time since disturbance and surrounding tree cover. Left: AGB (non-scaled data), right: tree cover (non-scaled data) [228].

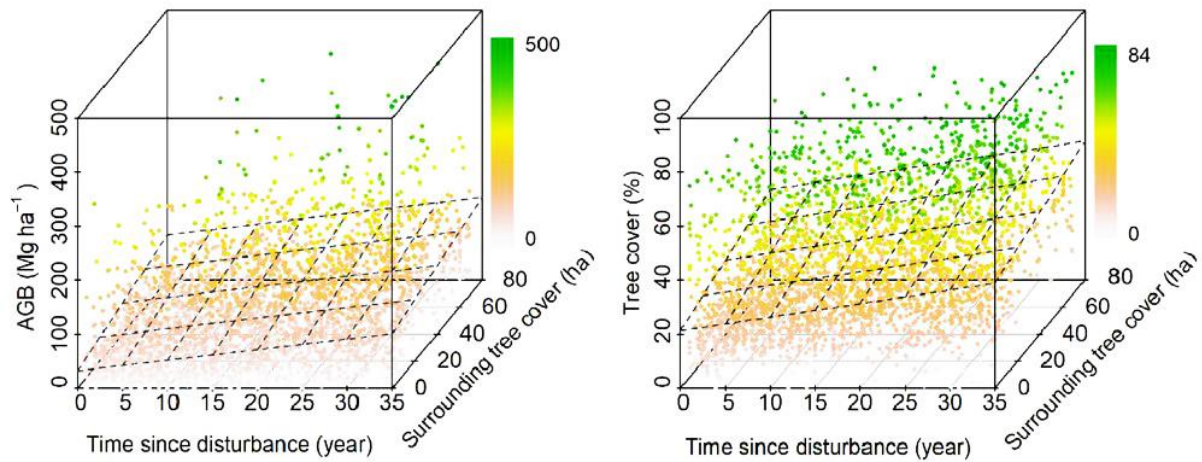
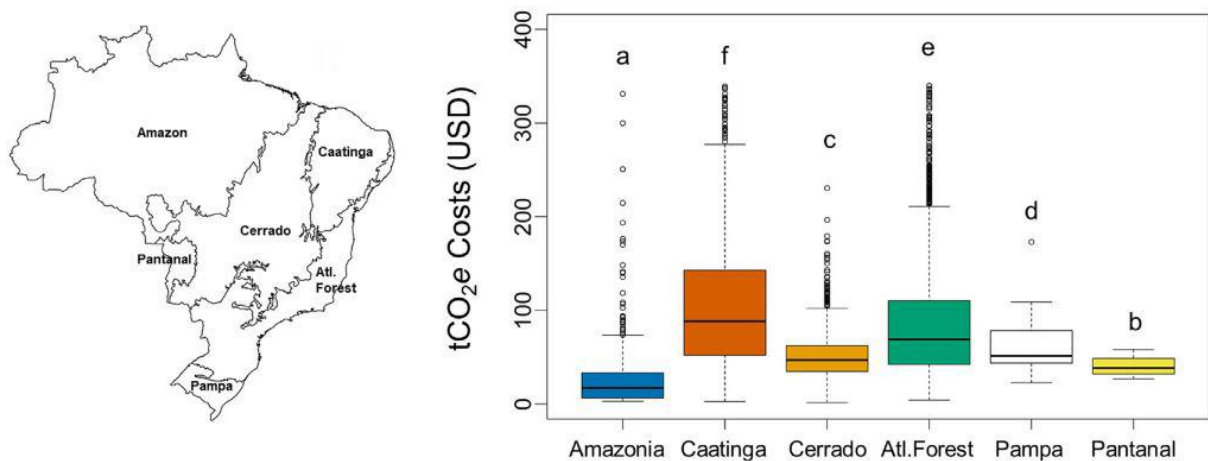


Figure 127: Left: The physical limits of the six ecoregions (Amazonia, Atlantic Forest, Cerrado, Caatinga, Pantanal and Pampa) defined by the Brazilian Institute of Geography and Statistics (IBGE). Right: Distribution of restoration costs for each ecoregion. Each sample unit corresponds to one municipality within each region. The box limits represent the first and third quartiles, with the middle line representing the median. The whiskers represent the minimum and maximum values, excluding the outliers, represented by the empty circles [229]



Barros et al. (2023) look at the costs of forest restoration for carbon sequestration across Brazil's biomes. Brazil has been highlighted as a vital part of global climate agreements because, whilst ongoing land-use change causes it to be the world's fifth biggest greenhouse gas emitting country, it also has one of the greatest potentials to implement ecosystem restoration. Global carbon markets provide the opportunity of a financially viable way to implement restoration projects at scale. However, except for rainforests, the restoration potential of many major tropical biomes is not widely recognised, with the result that carbon sequestration potential may be squandered. The authors synthesize data on

land availability, land degradation status, restoration costs, area of native vegetation remaining, carbon storage potential and carbon market prices for 5475 municipalities across Brazil's major biomes, including the savannas and tropical dry forests. Using a modelling analysis, they determine how fast restoration could be implemented across these biomes within existing carbon markets. The authors argue that even with a sole focus on carbon, also other tropical biomes must be restored, as well as rainforests, to effectively increase benefits. The inclusion of dry forests and savannas doubles the area which could be restored in a financially viable manner, increasing the potential CO₂e sequestered >40% above that offered by rainforests alone. Importantly, we show that in the short-term avoiding emissions through conservation will be necessary for Brazil to achieve its 2030 climate goal, because it can sequester 1.5 to 4.3 Pg of CO₂e by 2030, relative to 0.127 Pg CO₂e from restoration. However, in the longer term, restoration across all biomes in Brazil could draw down between 3.9 and 9.8 Pg of CO₂e from the atmosphere by 2050 and 2080 [229].

References

1. Beuchle, R.; Achard, F.; Bourgoïn, C.; Vancutsem, C.; Eva, H.D.; Follador, M. Deforestation and Forest Degradation in the Amazon: Status and Trends up to Year 2020; *Publications Office of the European Union*: Luxembourg, **2021**; p. 77.
2. Beuchle, R.; Achard, F.; Bourgoïn, C.; Vancutsem, C. Deforestation and Forest Degradation in the Amazon: Status and Trends up to Year 2021; *Publications Office of the European Union*: Luxembourg, **2022**; p. 97.
3. Vásquez-Grandón, A.; Donoso, P.; Gerding, V. Forest Degradation: When Is a Forest Degraded? *Forests* **2018**, *9*, 726, doi:10.3390/f9110726.
4. Vancutsem, C.; Achard, F.; Pekel, J.-F.; Vieilledent, G.; Carboni, S.; Simonetti, D.; Gallego, J.; Aragão, L.E.O.C.; Nasi, R. Long-Term (1990–2019) Monitoring of Forest Cover Changes in the Humid Tropics. *Sci. Adv.* **2021**, *7*, eabe1603, doi:10.1126/sciadv.abe1603.
5. Lovejoy, T.E.; Nobre, C. Amazon Tipping Point. *Sci. Adv.* **2018**, *4*, eaat2340, doi:10.1126/sciadv.aat2340.
6. Duku, C.; Hein, L. Assessing the Impacts of Past and Ongoing Deforestation on Rainfall Patterns in South America. *Glob. Change Biol.* **2023**, doi:10.1111/gcb.16856.
7. Curado, L.F.A.; de Paulo, S.R.; de Paulo, I.J.C.; de Oliveira Maionchi, D.; da Silva, H.J.A.; de Oliveira Costa, R.; da Silva, I.M.C.B.; Marques, J.B.; de Souza Lima, A.M.; Rodrigues, T.R. Trends and Patterns of Daily Maximum, Minimum and Mean Temperature in Brazil from 2000 to 2020. *Climate* **2023**, *11*, 168, doi:10.3390/cli11080168.
8. Valadão, L.V.; da Fonseca, I.R.; Cicerelli, R.E.; de Almeida, T.; Garnier, J.; Sano, E.E. Temporal Dynamics of the Hydropower Water Reservoirs of the Tocantins–Araguaia Basin, Brazil, Based on Remote Sensing and Hydrometeorological Station Datasets. *water* **2023**, *15*, 1684, doi:10.3390/w15091684.
9. Ritchie, P.D.L.; Parry, I.; Clarke, J.J.; Huntingford, C.; Cox, P.M. Increases in the Temperature Seasonal Cycle Indicate Long-Term Drying Trends in Amazonia. *Commun. Earth Environ.* **2022**, *3*, 199, doi:10.1038/s43247-022-00528-0.
10. Maeda, E.E.; Abera, T.A.; Siljander, M.; Aragão, L.E.O.C.; Moura, Y.M. de; Heiskanen, J. Large-Scale Commodity Agriculture Exacerbates the Climatic Impacts of Amazonian Deforestation. *Proc. Natl. Acad. Sci.* **2021**, *118*, e2023787118, doi:10.1073/pnas.2023787118.
11. Gatti, L.V.; Basso, L.S.; Miller, J.B.; Gloor, M.; Gatti Domingues, L.; Cassol, H.L.G.; Tejada, G.; Aragão, L.E.O.C.; Nobre, C.; Peters, W.; et al. Amazonia as a Carbon Source Linked to Deforestation and Climate Change. *Nature* **2021**, *595*, 388–393, doi:10.1038/s41586-021-03629-6.
12. Zalles, V.; Hansen, M.C.; Potapov, P.V.; Stehman, S.V.; Tyukavina, A.; Pickens, A.; Song, X.-P.; Adusei, B.; Okpa, C.; Aguilar, R.; et al. Near Doubling of Brazil's Intensive Row Crop Area since 2000. *Proc. Natl. Acad. Sci.* **2019**, *116*, 428–435, doi:10.1073/pnas.1810301115.
13. Murillo- Sandoval, P.J.; Kilbride, J.; Tellman, E.; Wrathall, D.; Van Den Hoek, J.; Kennedy, R.E. The Post- conflict Expansion of Coca Farming and Illicit Cattle Ranching in Colombia. *Sci. Rep.* **2023**, *13*, doi:10.1038/s41598-023-28918-0.

14. Skidmore, M.E.; Moffette, F.; Rausch, L.; Christie, M.; Munger, J.; Gibbs, H.K. Cattle Ranchers and Deforestation in the Brazilian Amazon: Production, Location, and Policies. *Glob. Environ. Change* **2021**, *68*, 102280, doi:10.1016/j.gloenvcha.2021.102280.
15. Brito, B.; Barreto, P.; Brandão, A.; Baima, S.; Gomes, P.H. Stimulus for Land Grabbing and Deforestation in the Brazilian Amazon. *Environ. Res. Lett.* **2019**, *14*, 064018, doi:10.1088/1748-9326/ab1e24.
16. Carrero, G.C.; Walker, R.T.; Simmons, C.S.; Fearnside, P.M. Land Grabbing in the Brazilian Amazon: Stealing Public Land with Government Approval. *Land Use Policy* **2022**, *120*, 106133, doi:10.1016/j.landusepol.2022.106133.
17. Silveira, M.V.F.; Silva- Junior, C.H.L.; Anderson, L.O.; Aragão, L.E.O.C. Amazon Fires in the 21st Century: The Year of 2020 in Evidence. *Glob. Ecol. Biogeogr.* **2022**, *31*, 2026–2040, doi:10.1111/geb.13577.
18. Cremers, L., Kolen, J., Theije, M. de, Eds. Small-Scale Gold Mining in the Amazon: The Cases of Bolivia, Brazil, Colombia, Peru, and Suriname; Cuadernos del CEDLA; Centre for Latin American Studies and Documentation: Amsterdam, The Netherlands, **2013**; ISBN 978-90-70280-18-5.
19. Dezécache, C.; Faure, E.; Gond, V.; Salles, J.-M.; Vieilledent, G.; Hérault, B. Gold-Rush in a Forested El Dorado: Deforestation Leakages and the Need for Regional Cooperation. *Environ. Res. Lett.* **2017**, *12*, 034013, doi:10.1088/1748-9326/aa6082.
20. Mestanza-Ramón, C.; Jiménez-Oyola, S.; Montoya, A.V.G.; Vizúete, D.D.C.; D’Orío, G.; Cedeño-Laje, J.; Straface, S. Assessment of Hg Pollution in Stream Waters and Human Health Risk in Areas Impacted by Mining Activities in the Ecuadorian Amazon. *Environ. Geochem. Health* **2023**, doi:10.1007/s10653-023-01597-6.
21. Sonter, L.J.; Herrera, D.; Barrett, D.J.; Galford, G.L.; Moran, C.J.; Soares-Filho, B.S. Mining Drives Extensive Deforestation in the Brazilian Amazon. *Nat. Commun.* **2017**, *8*, 1013, doi:10.1038/s41467-017-00557-w.
22. Malca, U.F.G.; Dunin-Borkowski, A.S.; Bustamante, N.F.; Reaño, M.J.M.; Armas, J.M.G. Alluvial Gold Mining, Conflicts, and State Intervention in Peru’s Southern Amazonia. *Extr. Ind. Soc.* **2023**, *13*, 101219, doi:10.1016/j.exis.2023.101219.
23. Ouboter, P.E. Review of Mercury Pollution in Suriname. *Acad. J. Suriname* **2015**, *6*, 531–543.
24. Scammacca, O.; Gunzburger, Y.; Mehdizadeh, R. Gold Mining in French Guiana: A Multi-Criteria Classification of Mining Projects for Risk Assessment at the Territorial Scale. *Extr. Ind. Soc.* **2021**, *8*, 32–43, doi:10.1016/j.exis.2020.06.020.
25. Condé, T.M.; Higuchi, N.; Lima, A.J.N. Illegal Selective Logging and Forest Fires in the Northern Brazilian Amazon. *Forests* **2019**, *10*, 61, doi:10.3390/f10010061.
26. Franca, C.S.S.; Persson, U.M.; Carvalho, T.; Lentini, M. Quantifying Timber Illegality Risk in the Brazilian Forest Frontier. *Nat. Sustain.* **2023**, doi:10.1038/s41893-023-01189-3.
27. Sist, P.; Piponiot, C.; Kanashiro, M.; Pena-Claros, M.; Putz, F.E.; Schulze, M.; Verissimo, A.; Vidal, E. Sustainability of Brazilian Forest Concessions. *For. Ecol. Manag.* **2021**, *496*, 119440, doi:10.1016/j.foreco.2021.119440.
28. DeArmond, D.; Emmert, F.; Pinto, A.C.M.; Lima, A.J.N.; Higuchi, N. A Systematic Review of Logging Impacts in the Amazon Biome. *Forests* **2023**, *14*, 81, doi:10.3390/f14010081.

29. Lapola, D.M.; Pinho, P.; Barlow, J.; Aragão, L.E.O.C.; Berenguer, E.; Carmenta, R.; Liddy, H.M.; Seixas, H.; Silva, C.V.J.; Silva-Junior, C.H.L.; et al. The Drivers and Impacts of Amazon Forest Degradation. *Science* **2023**, *379*, eabp8622, doi:10.1126/science.abp8622.
30. Brancalion, P.H.S.; de Almeida, D.R.A.; Vidal, E.; Molin, P.G.; Sontag, V.E.; Souza, S.E.X.F.; Schulze, M.D. Fake Legal Logging in the Brazilian Amazon. *Sci. Adv.* **2018**, *4*, eaat1192, doi:10.1126/sciadv.aat1192.
31. UNODC. The Nexus between Drugs and Crimes That Affect the Environment and Convergent Crime in the Amazon Basin, Contemporary Issues on Drugs - part 4; *United Nations Office on Drugs and Crime*: Vienna, **2023**; p. 59.
32. Deutsch, S.; Fletcher, R. The 'Bolsonaro Bridge': Violence, Visibility, and the 2019 Amazon Fires. *Environ. Sci. Policy* **2022**, *132*, 60–68, doi:10.1016/j.envsci.2022.02.012.
33. Human Rights Watch. Rainforest Mafias: How Violence and Impunity Fuel Deforestation in Brazil's Amazon; *Human Rights Watch*: New York, USA, **2019**; p. 170.
34. Fearnside, P.M. The Outlook for Brazil's New Presidential Administration. *Trends Ecol. Evol.* **2023**, S016953472300006X, doi:10.1016/j.tree.2023.01.002.
35. Eva, H.; Huber, O.; Achard, F.; Balslev, H.; Beck, S.; Behling, H.; Belward, A.; Beuchle, R.; Cleef, A.; Colchester, M.; et al. A Proposal for Defining the Geographical Boundaries of Amazonia; Eva, Hugh.D., Huber, O., Eds.; EUR 21808 EN, *Publications Office of the European Union*: Luxembourg, **2005**; p. 53.
36. Lima, T.A.; Beuchle, R.; Langner, A.; Grecchi, R.C.; Griess, V.C.; Achard, F. Comparing Sentinel-2 MSI and Landsat 8 OLI Imagery for Monitoring Selective Logging in the Brazilian Amazon. *Remote Sens.* **2019**, *11*, 961, doi:10.3390/rs11080961.
37. Grecchi, R.C.; Beuchle, R.; Shimabukuro, Y.E.; Aragão, L.E.O.C.; Arai, E.; Simonetti, D.; Achard, F. An Integrated Remote Sensing and GIS Approach for Monitoring Areas Affected by Selective Logging: A Case Study in Northern Mato Grosso, Brazilian Amazon. *Int. J. Appl. Earth Obs. Geoinformation* **2017**, *61*, 70–80, doi:10.1016/j.jag.2017.05.001.
38. Lima, T.A.; Beuchle, R.; Griess, V.C.; Verhegghen, A.; Vogt, P. Spatial Patterns of Logging-Related Disturbance Events: A Multi-Scale Analysis on Forest Management Units Located in the Brazilian Amazon. *Landsc. Ecol.* **2020**, *35*, 2083–2100, doi:10.1007/s10980-020-01080-y.
39. Velasco Gomez, M.D.; Beuchle, R.; Shimabukuro, Y.; Grecchi, R.; Simonetti, D.; Eva, H.D.; Achard, F. A Long-Term Perspective on Deforestation Rates in the Brazilian Amazon. *ISPRS - Int. Arch. Photogramm. Remote Sens. Spat. Inf. Sci.* **2015**, *XL-7/W3*, 539–544, doi:10.5194/isprsarchives-XL-7-W3-539-2015.
40. Diniz, C.G.; Souza, A.A. de A.; Santos, D.C.; Dias, M.C.; Luz, N.C. da; Moraes, D.R.V. de; Maia, J.S.A.; Gomes, A.R.; Narvaes, I. da S.; Valeriano, D.M.; et al. DETER-B: The New Amazon Near Real-Time Deforestation Detection System. *IEEE J. Sel. Top. Appl. Earth Obs. Remote Sens.* **2015**, *8*, 3619–3628, doi:10.1109/JSTARS.2015.2437075.
41. De Maria, M.; Robinson, E.; Kangile, J.R.; Kadigi, R.M.; Dreoni, I.; Couto, M.; Howai, N.; Peci, J.; Fiennes, S. Global Soybean Trade – The Geopolitics of a Bean; *UN Environment Programme World Conservation Monitoring Centre (UNEP-WCMC)*, **2020**; p. 56.
42. Brito, T.; Fragoso, R.; Santos, L.; Martins, J.A.; Fernandes Silva, A.A.; Aranha, J. Life Cycle Assessment for Soybean Supply Chain: A Case Study of State of Pará, Brazil. *Agronomy* **2023**, *13*, 1648, doi:10.3390/agronomy13061648.

43. Martinelli, L.; Batistella, M.; Silva, R.; Moran, E. Soy Expansion and Socioeconomic Development in Municipalities of Brazil. *Land* **2017**, *6*, 62, doi:10.3390/land6030062.
44. Simoes, A.J.G.; Hidalgo, C.A. The Economic Complexity Observatory: An Analytical Tool for Understanding the Dynamics of Economic Development. In: *Proceedings of the 17th AAAI Conference on Scalable Integration of Analytics and Visualization, AAAIWS'11-17*; AAAI Press: Palo Alto, CA, USA, **2011**; p. 39–42.
45. Jia, F.; Peng, S.; Green, J.; Koh, L.; Chen, X. Soybean Supply Chain Management and Sustainability: A Systematic Literature Review. *J. Clean. Prod.* **2020**, *255*, 120254, doi:10.1016/j.jclepro.2020.120254.
46. Greenpeace. Eating up the Amazon; *Greenpeace USA*: Washington D.C., **2006**; p. 64.
47. Wedeux, B.; Schulmeister-Oldenhove, A. Stepping Up? The Continuing Impact of EU Consumption on Nature Worldwide; *World Wildlife Fund WWF*, **2021**; p. 33.
48. Pendrill, F.; Persson, U.M.; Godar, J.; Kastner, T. Deforestation Displaced: Trade in Forest-Risk Commodities and the Prospects for a Global Forest Transition. *Environ. Res. Lett.* **2019**, *14*, 055003, doi:10.1088/1748-9326/ab0d41.
49. IDH Sustainable Trade Initiative. European Soy Monitor; Insights on European Uptake of Responsible, Deforestation, and Conversion-Free Soy in 2020; *IDH Sustainable Trade Initiative*: Utrecht, the Netherlands, **2022**; p. 67.
50. Lourençoni, T.; da Silva Junior, C.A.; Lima, M.; Teodoro, P.E.; Pelissari, T.D.; dos Santos, R.G.; Teodoro, L.P.R.; Luz, I.M.; Rossi, F.S. Advance of Soy Commodity in the Southern Amazonia with Deforestation via PRODES and ImazonGeo: A Moratorium-Based Approach. *Sci. Rep.* **2021**, *11*, 21792, doi:10.1038/s41598-021-01350-y.
51. Fehlenberg, V.; Baumann, M.; Gasparri, N.I.; Piquer-Rodriguez, M.; Gaviera-Pizarro, G.; Kuemmerle, T. The Role of Soybean Production as an Underlying Driver of Deforestation in the South American Chaco. *Glob. Environ. Change* **2017**, *45*, 24–34, doi:10.1016/j.gloenvcha.2017.05.001.
52. Henderson, J.; Godar, J.; Frey, G.P.; Börner, J.; Gardner, T. The Paraguayan Chaco at a Crossroads: Drivers of an Emerging Soybean Frontier. *Reg. Environ. Change* **2021**, *21*, 72, doi:10.1007/s10113-021-01804-z.
53. Finer, M.; Ariñez, A. Soy Deforestation in the Bolivian Amazon; *MAAP, Monitoring of the Andean Amazon Project*, **2023**; p. 5.
54. Søndergaard, N., de Sá, C.D., Barros-Platiau, A.F., Eds. Sustainability Challenges of Brazilian Agriculture: Governance, Inclusion, and Innovation; Environment & Policy; *Springer International Publishing*: Cham, **2023**; Vol. 64; ISBN 978-3-031-29852-3.
55. Gavioli, E.A. Explanations for the Rise of Soybean in Brazil. In: A Comprehensive Survey of International Soybean Research - Genetics, Physiology, Agronomy and Nitrogen Relationships; Board, J., Ed.; *InTech: IntechOpen Limited*, UK, **2013**; p. 26, ISBN 978-953-51-0876-4.
56. zu Ermgassen, E.K.H.J.; Godar, J.; Lathuillière, M.J.; Löfgren, P.; Gardner, T.; Vasconcelos, A.; Meyfroidt, P. The Origin, Supply Chain, and Deforestation Risk of Brazil's Beef Exports. *Proc. Natl. Acad. Sci.* **2020**, *117*, 31770–31779, doi:10.1073/pnas.2003270117.
57. Souza, C.M.; Azevedo, T. MapBiomas General "Handbook"; *Mapbiomas*, **2017**; p. 24.
58. Song, X.-P.; Hansen, M.C.; Potapov, P.; Adusei, B. Massive Soybean Expansion in South America since 2000 and Implications for Conservation. *Nat. Sustain.* **2021**, *4*, 784–792, doi:10.1038/s41893-021-00729-z.

59. Garrett, R.D.; Lambin, E.F.; Naylor, R.L. Land Institutions and Supply Chain Configurations as Determinants of Soybean Planted Area and Yields in Brazil. *Land Use Policy* **2013**, *31*, 385–396, doi:10.1016/j.landusepol.2012.08.002.
60. Rudorff, B.; Risso, J.; Baldi, C.; Aguiar, D.; Salgado, M.; Perrut, J.; Oliveira, L.; Virtuoso, M.; Cabral, G.; Rosa, O.; et al. Geospatial Analysis of Soy Expansion, Associated Land Use and Land Cover Change, and Agricultural Suitability in the Brazilian Amazon Biome - 2000 to 2017; *Agrosatélite Ltd.*: Florianópolis, Santa Catarina, Brazil, **2018**; p. 40.
61. Fearnside, P.M. Soybean Cultivation as a Threat to the Environment in Brazil. *Environ. Conserv.* **2001**, *28*, 23–38, doi:10.1017/S0376892901000030.
62. de Avila, A.M.H.; Boucas Farias, J.R.; Silveira, H.; Gustavo, F. Climatic Restrictions for Maximizing Soybean Yields. In: A Comprehensive Survey of International Soybean Research - Genetics, Physiology, Agronomy and Nitrogen Relationships; Board, J., Ed.; *InTech: IntechOpen Limited*, UK, **2013**; p. 11, ISBN 978-953-51-0876-4.
63. Rausch, L.L.; Gibbs, H.K. The Low Opportunity Costs of the Amazon Soy Moratorium. *Front. For. Glob. Change* **2021**, *4*, 621685, doi:10.3389/ffgc.2021.621685.
64. Aragão, R.B. de A.; Bastos Lima, M.G.; Burns, G.L.; Ross, H. To Clear or Not to Clear: Unpacking Soy Farmers' Decision-Making on Deforestation in Brazil's Cerrado. *Front. Sustain. Food Syst.* **2022**, *6*, 942207, doi:10.3389/fsufs.2022.942207.
65. Soterroni, A.C.; Ramos, F.M.; Mosnier, A.; Fargione, J.; Andrade, P.R.; Baumgarten, L.; Pirker, J.; Obersteiner, M.; Kraxner, F.; Câmara, G.; et al. Expanding the Soy Moratorium to Brazil's Cerrado. *Sci. Adv.* **2019**, *5*, eaav7336, doi:10.1126/sciadv.aav7336.
66. Caetano, J.M.; Tessarolo, G.; de Oliveira, G.; Souza, K. da S. e; Diniz-Filho, J.A.F.; Nabout, J.C. Geographical Patterns in Climate and Agricultural Technology Drive Soybean Productivity in Brazil. *PLOS ONE* **2018**, *13*, e0191273, doi:10.1371/journal.pone.0191273.
67. Trase. SEI-PCS Brazil Soy v2.6 Supply Chain Map: Data Sources and Methods; *Trase*, **2022**; p. 31.
68. Macedo, M.N.; DeFries, R.S.; Morton, D.C.; Stickler, C.M.; Galford, G.L.; Shimabukuro, Y.E. Decoupling of Deforestation and Soy Production in the Southern Amazon during the Late 2000s. *Proc. Natl. Acad. Sci.* **2012**, *109*, 1341–1346, doi:10.1073/pnas.1111374109.
69. Richards, P.D.; Walker, R.T.; Arima, E.Y. Spatially Complex Land Change: The Indirect Effect of Brazil's Agricultural Sector on Land Use in Amazonia. *Glob. Environ. Change* **2014**, *29*, 1–9, doi:10.1016/j.gloenvcha.2014.06.011.
70. Pendrill, F.; Gardner, T.A.; Meyfroidt, P.; Persson, U.M.; Adams, J.; Azevedo, T.; Bastos Lima, M.G.; Baumann, M.; Curtis, P.G.; De Sy, V.; et al. Disentangling the Numbers behind Agriculture-Driven Tropical Deforestation. *Science* **2022**, *377*, eabm9267, doi:10.1126/science.abm9267.
71. Miranda, J.; Börner, J.; Kalkuhl, M.; Soares-Filho, B. Land Speculation and Conservation Policy Leakage in Brazil. *Environ. Res. Lett.* **2019**, *14*, 045006, doi:10.1088/1748-9326/ab003a.
72. Costa, W.; Soares-Filho, B.; Nobrega, R. Can the Brazilian National Logistics Plan Induce Port Competitiveness by Reshaping the Port Service Areas? *Sustainability* **2022**, *14*, 14567, doi:10.3390/su142114567.
73. Costa, W.; Davis, J.; Ribeiro, A.; Soares Filho, B.S. Amazônia do futuro: o que esperar dos impactos socioambientais da Ferrogrão?; *Federal University of Minas Gerais: Belo Horizonte*, **2020**; p. 9.

74. Bragança, A.; Araújo, R.; Assunção, J. Measuring the Indirect Effects of Transportation Infrastructure in the Amazon; *Climate Policy Initiative*: Rio de Janeiro, **2020**; p. 9.
75. Ferrante, L.; Andrade, M.B.T.; Fearnside, P.M. Land Grabbing on Brazil's Highway BR-319 as a Spearhead for Amazonian Deforestation. *Land Use Policy* **2021**, *108*, 105559, doi:10.1016/j.landusepol.2021.105559.
76. Lima, M.; Santana, D.C.; Junior, I.C.M.; Costa, P.M.C. da; Oliveira, P.P.G. de; Azevedo, R.P. de; Silva, R. de S.; Marinho, U. de F.; Silva, V. da; Souza, J.A.A. de; et al. The "New Transamazonian Highway": BR-319 and Its Current Environmental Degradation. *Sustainability* **2022**, *14*, 823, doi:10.3390/su14020823.
77. Santos, J.L.; Yanai, A.M.; Graça, P.M.L.A.; Correia, F.W.S.; Fearnside, P.M. Amazon Deforestation: Simulated Impact of Brazil's Proposed BR-319 Highway Project. *Environ. Monit. Assess.* **2023**, *195*, 22, doi:10.1007/s10661-023-11820-7.
78. Fearnside, P.M. Brazil's Cuiabá - Santarém (BR-163) Highway: The Environmental Cost of Paving a Soybean Corridor Through the Amazon. *Environ. Manage.* **2007**, *39*, 601–614, doi:10.1007/s00267-006-0149-2.
79. zu Ermgassen, E.K.H.J.; Ayre, B.; Godar, J.; Bastos Lima, M.G.; Bauch, S.; Garrett, R.; Green, J.; Lathuilière, M.J.; Löfgren, P.; MacFarquhar, C.; et al. Using Supply Chain Data to Monitor Zero Deforestation Commitments: An Assessment of Progress in the Brazilian Soy Sector. *Environ. Res. Lett.* **2020**, *15*, 035003, doi:10.1088/1748-9326/ab6497.
80. Nepstad, D.; McGrath, D.; Stickler, C.; Alencar, A.; Azevedo, A.; Swette, B.; Bezerra, T.; DiGiano, M.; Shimada, J.; Seroa da Motta, R.; et al. Slowing Amazon Deforestation through Public Policy and Interventions in Beef and Soy Supply Chains. *Science* **2014**, *344*, 1118–1123, doi:10.1126/science.1248525.
81. Heilmayr, R.; Rausch, L.L.; Munger, J.; Gibbs, H.K. Brazil's Amazon Soy Moratorium Reduced Deforestation. *Nat. Food* **2020**, *1*, 801–810, doi:10.1038/s43016-020-00194-5.
82. Gollnow, F.; Hissa, L. de B.V.; Rufin, P.; Lakes, T. Property-Level Direct and Indirect Deforestation for Soybean Production in the Amazon Region of Mato Grosso, Brazil. *Land Use Policy* **2018**, *78*, 377–385, doi:10.1016/j.landusepol.2018.07.010.
83. Moffette, F.; Gibbs, H.K. Agricultural Displacement and Deforestation Leakage in the Brazilian Legal Amazon. *Land Econ.* **2021**, *97*, 155–179, doi:10.3368/wple.97.1.040219-0045R.
84. Valdiones, A.P.; Silgueiro, V.; Carvalho, R.; Bernasconi, P.; Vasconcelos, A. Soy and Illegal Deforestation: The State of the Art and Guidelines for an Expanded Monitoring Program Protocol in Mato Grosso; *Instituto Centro da Vida: Alta Floresta, Brazil*, **2022**; p. 9.
85. Ferrante, L.; Fearnside, P.M. Brazil's Political Upset Threatens Amazonia. *Science* **2021**, *371*, 898–898, doi:10.1126/science.abg9786.
86. Fernandes, S.; Fernandes, G.W.; Fearnside, P.M. Viewpoint: Sovereignty and Reversing Brazil's History of Amazon Destruction. *Land Use Policy* **2023**, *133*, 106868, doi:10.1016/j.landusepol.2023.106868.
87. BNDS. Amazon Fund - Annual Report 2022; *Brazilian Development Bank*: Rio de Janeiro, RJ, Brazil, **2023**; p. 230.
88. Carvalho, W.D.; Mustin, K.; Hilário, R.R.; Vasconcelos, I.M.; Eilers, V.; Fearnside, P.M. Deforestation Control in the Brazilian Amazon: A Conservation Struggle Being Lost as Agreements and Regulations Are Subverted and Bypassed. *Perspect. Ecol. Conserv.* **2019**, *17*, 122–130, doi:10.1016/j.pecon.2019.06.002.

89. Coelho-Junior, M.G.; Valdiones, A.P.; Shimbo, J.Z.; Silgueiro, V.; Rosa, M.; Marques, C.D.L.; Oliveira, M.; Araújo, S.; Azevedo, T. Unmasking the Impunity of Illegal Deforestation in the Brazilian Amazon: A Call for Enforcement and Accountability. *Environ. Res. Lett.* **2022**, *17*, 041001, doi:10.1088/1748-9326/ac5193.
90. Bonilla, O.; Capiberibe, A. From 'Flocking for Rights' to the Politics of Death: Indigenous Struggle and Indigenous Policy in Brazil (1980–2020). *Port. Stud.* **2021**, *37*, 102–119.
91. Barbosa, L.G.; Alves, M.A.S.; Grelle, C.E.V. Actions against Sustainability: Dismantling of the Environmental Policies in Brazil. *Land Use Policy* **2021**, *104*, 105384, doi:10.1016/j.landusepol.2021.105384.
92. Dutra da Silva, M.; Fearnside, P.M. Brazil: Environment under Attack. *Environ. Conserv.* **2022**, *49*, 203–205, doi:10.1017/S0376892922000364.
93. Abessa, D.; Famá, A.; Buruaem, L. The Systematic Dismantling of Brazilian Environmental Laws Risks Losses on All Fronts. *Nat. Ecol. Evol.* **2019**, *3*, 510–511, doi:10.1038/s41559-019-0855-9.
94. Bonelli, F.; Fernandes, A.S.A.; Cavalcante, P.L.C. The Active Dismantling of Environmental Policy in Brazil: Paralysis and Setbacks of the Deforestation Inspection and Control. *Sustain. Debate* **2023**, *14*, 58–80, doi:10.18472/SustDeb.v14n1.2023.44277.
95. Coates, R.; Sandroni, L. Protected Truths: Neoextractivism, Conservation, and the Rise of Posttruth Politics in Brazil. *Ann. Am. Assoc. Geogr.* **2023**, 1–20, doi:10.1080/24694452.2023.2209627.
96. Kuschnig, N.; Vashold, L.; C Soterroni, A.; Obersteiner, M. Eroding Resilience of Deforestation Interventions—Evidence from Brazil's Lost Decade. *Environ. Res. Lett.* **2023**, *18*, 074039, doi:10.1088/1748-9326/acdf7.
97. Chaves, M.E.D.; Sanches, I.D.; Adami, M. Brazil Needs Juridical Security to Recover Agri-Environmental Epistemic Sovereignty. *Land Use Policy* **2023**, *132*, 106809, doi:10.1016/j.landusepol.2023.106809.
98. Jakimow, B.; Baumann, M.; Salomão, C.; Bendini, H.; Hostert, P. Deforestation and Agricultural Fires in South-West Pará, Brazil, under Political Changes from 2014 to 2020. *J. Land Use Sci.* **2023**, *18*, 176–195, doi:10.1080/1747423X.2023.2195420.
99. Milhorange, C. Policy Dismantling and Democratic Regression in Brazil under Bolsonaro: Coalition Politics, Ideas, and Underlying Discourses. *Rev. Policy Res.* **2022**, *39*, 752–770, doi:10.1111/ropr.12502.
100. Gatti, L.V.; Cunha, C.L.; Marani, L.; Cassol, H.L.G.; Messias, C.G.; Arai, E.; Denning, A.S.; Soler, L.S.; Almeida, C.; Setzer, A.; et al. Increased Amazon Carbon Emissions Mainly from Decline in Law Enforcement. *Nature* **2023**, doi:10.1038/s41586-023-06390-0.
101. Da Luz Scherf, E.; Viana da Silva, M.V. Brazil's Yanomami Health Disaster: Addressing the Public Health Emergency Requires Advancing Criminal Accountability. *Front. Public Health* **2023**, *11*, 1166167, doi:10.3389/fpubh.2023.1166167.
102. Watts, J. Health Emergency over Brazil's Yanomami People. *The Lancet* **2023**, *401*, 631, doi:10.1016/S0140-6736(23)00384-7.
103. Mueller, B. Property Rights and Violence in Indigenous Land in Brazil. *SSRN Electron. J.* **2020**, doi:10.2139/ssrn.3581185.
104. Mondardo, M. In Defense of Indigenous Territories in Brazil: Rights, Demarcations and Land Retake. *Geosp* **2022**, *26*, e-176224.

105. da Silva Ribeiro, R.; Vicente, R.E.; Arrolho, S.; Fearnside, P.M. Amazon Deforestation Restrictions Likely to Be Circumvented. *ERDE* **2022**, 216–217, doi:10.12854/erde-2022-621.
106. Villén-Pérez, S.; Anaya-Valenzuela, L.; Conrado da Cruz, D.; Fearnside, P.M. Mining Threatens Isolated Indigenous Peoples in the Brazilian Amazon. *Glob. Environ. Change* **2022**, 72, 102398, doi:10.1016/j.gloenvcha.2021.102398.
107. Moutinho, P.; Azevedo-Ramos, C. Untitled Public Forestlands Threat Amazon Conservation. *Nat. Commun.* **2023**, 14, 1152, doi:10.1038/s41467-023-36427-x.
108. Korting, M.S.; Lima, D.A.; Filho, J.S. Brazilian Agricultural Frontier: Land Grabbing, Land Policy, and Conflicts. *IDS Bull.* **2023**, 54, 73–88, doi:10.19088/1968-2023.106.
109. Azevedo-Ramos, C.; Moutinho, P.; Arruda, V.L. da S.; Stabile, M.C.C.; Alencar, A.; Castro, I.; Ribeiro, J.P. Lawless Land in No Man's Land: The Undesignated Public Forests in the Brazilian Amazon. *Land Use Policy* **2020**, 99, 104863, doi:10.1016/j.landusepol.2020.104863.
110. Pignati, W.A.; Soares, M.R.; Lara, S.S. de; Lima, F.A.N. de S. e; Fava, N.R.; Barbosa, J.R.; Corrêa, M.L.M. Exposição aos agrotóxicos, condições de saúde autorreferidas e Vigilância Popular em Saúde de municípios mato-grossenses. *Saúde Em Debate* **2022**, 46, 45–61, doi:10.1590/0103-11042022e203.
111. Nasralla Neto, E.; Lacaz, F.A. de C.; Pignati, W.A. Health Surveillance and Agribusiness: The Impact of Pesticides on Health and the Environment. *Danger Ahead! Ciênc. Saúde Coletiva* **2014**, 19, 4709–4718, doi:10.1590/1413-812320141912.03172013.
112. Ferrante, L. Bills Undermine Brazil's Environmental Goals. *Science* **2023**, 381, 490–491, doi:10.1126/science.adi9196.
113. Botelho, J.; Costa, S.C.P.; Ribeiro, J.G.; Souza, C.M. Mapping Roads in the Brazilian Amazon with Artificial Intelligence and Sentinel-2. *Remote Sens.* **2022**, 14, 3625, doi:10.3390/rs14153625.
114. Costa, W.; Davis, J.; de Oliveira, A.R.; Fernandes, F.; Rajão, R.; Filho, B.S.S. Ferrogrão Railroad with a Freight Terminal in Matupá Will Split in Half the Indigenous Lands of Xingu; *Federal University of Minas Gerais: Belo Horizonte*, **2021**; p. 8.
115. Araújo, R.; Assunção, J.; Bragança, A. Os impactos ambientais da Ferrogrão: Uma avaliação ex-ante dos riscos de desmatamento; *PUC / Climate Policy Initiative: Rio de Janeiro*, **2020**; p. 9.
116. Simmons, C.S.; Famolare, L.; Macedo, M.N.; Walker, R.T.; Coe, M.T.; Scheffers, B.; Arima, E.; Munoz-Carpena, R.; Valle, D.; Fraisse, C.; et al. Science in Support of Amazonian Conservation in the 21st Century: The Case of Brazil. *Biotropica* **2018**, 50, 850–858, doi:10.1111/btp.12610.
117. Vilela, T.; Malky Harb, A.; Bruner, A.; Laísa da Silva Arruda, V.; Ribeiro, V.; Auxiliadora Costa Alencar, A.; Julissa Escobedo Grandez, A.; Rojas, A.; Laina, A.; Botero, R. A Better Amazon Road Network for People and the Environment. *Proc. Natl. Acad. Sci.* **2020**, 117, 7095–7102, doi:10.1073/pnas.1910853117.
118. Rangel, L.H.; Miotto, T. Violência Contra os Povos Indígenas no Brasil - Dados de 2022; *Conselho Missionário Indigenista: Brasília*, **2023**; p. 285.
119. Pérez, J.O. Brazil's Foreign Policy and Security under Lula and Bolsonaro: Hierarchy, Racialization, and Diplomacy. *Secur. Stud.* **2023**, 1–27, doi:10.1080/09636412.2023.2230447.
120. Peres, C.A.; Campos-Silva, J.; Ritter, C.D. Environmental Policy at a Critical Junction in the Brazilian Amazon. *Trends Ecol. Evol.* **2023**, 38, 113–116, doi:10.1016/j.tree.2022.11.011.

121. de Carvalho, I.S. Governar para não entregar - uma agenda de Segurança Multidimensional para a Amazônia brasileira; Segurança Climática; *Instituto Igarapé*: Rio de Janeiro, **2022**; p. 36.
122. Machado Vilani, R.; Ferrante, L.; Fearnside, P.M. The First Acts of Brazil's New President: Lula's New Amazon Institutionalality. *Environ. Conserv.* **2023**, *50*, 148–151, doi:10.1017/S0376892923000139.
123. Luiz, C.H.P.; Steinke, V.A. Recent Environmental Legislation in Brazil and the Impact on Cerrado Deforestation Rates. *Sustainability* **2022**, *14*, 8096, doi:10.3390/su14138096.
124. Fernandes, G.W.; Roque, F. de O.; Fernandes, S.; Grelle, C.E. de V.; Ochoa-Quintero, J.M.; Toma, T.S.P.; Vilela, E.F.; Fearnside, P.M. Brazil's Democracy and Sustainable Agendas: A Nexus in Urgent Need of Strengthening. *Perspect. Ecol. Conserv.* **2023**, S253006442300038X, doi:10.1016/j.pecon.2023.06.001.
125. Fearnside, P.M. The Outlook for Brazil's New Presidential Administration. *Trends Ecol. Evol.* **2023**, *38*, 387–388, doi:10.1016/j.tree.2023.01.002.
126. Colussi, J.; Schnitkey, G. Investments in Brazilian Grain Transportation Shrink U.S. Logistical Advantage. *Farmdoc Dly.* **2022**, *12*, 5.
127. Rodrigues, M. Oil from the Amazon? Drilling Plan for River Mouth Prompts Alarm. *Nature* **2023**, *619*, 680–681, doi:10.1038/d41586-023-02187-3.
128. Freitas, C.E.; de Almeida Mereles, M.; Pereira, D.V.; Siqueira-Souza, F.; Hurd, L.; Kahn, J.; Morais, G.; Sousa, R.G.C. Death by a Thousand Cuts: Small Local Dams Can Produce Large Regional Impacts in the Brazilian Legal Amazon. *Environ. Sci. Policy* **2022**, *136*, 447–452, doi:10.1016/j.envsci.2022.07.013.
129. Lees, A.C.; Peres, C.A.; Fearnside, P.M.; Schneider, M.; Zuanon, J.A.S. Hydropower and the Future of Amazonian Biodiversity. *Biodivers. Conserv.* **2016**, *25*, 451–466, doi:10.1007/s10531-016-1072-3.
130. Fearnside, P.M. Amazon Environmental Services: Why Brazil's Highway BR-319 Is so Damaging. *Ambio* **2022**, *51*, 1367–1370, doi:10.1007/s13280-022-01718-y.
131. Finer, M.; Babbitt, B.; Novoa, S.; Ferrarese, F.; Pappalardo, S.E.; Marchi, M.D.; Saucedo, M.; Kumar, A. Future of Oil and Gas Development in the Western Amazon. *Environ. Res. Lett.* **2015**, *10*, 024003, doi:10.1088/1748-9326/10/2/024003.
132. Santos e Silva, F.C.N. Is Exploration in the Brazilian Amazon the Best Energy Solution? Case Study in the Cajuhiri Indigenous Land Crossed. *Rev. Gest. E Secr.* **2023**, *14*, 13127–13144, doi:10.7769/gesec.v14i8.2437.
133. Masek, J.G.; Wulder, M.A.; Markham, B.; McCorkel, J.; Crawford, C.J.; Storey, J.; Jenstrom, D.T. Landsat 9: Empowering Open Science and Applications through Continuity. *Remote Sens. Environ.* **2020**, *248*, 111968, doi:10.1016/j.rse.2020.111968.
134. Flores-Anderson, A.I.; Cardille, J.; Azad, K.; Cherrington, E.; Zhang, Y.; Wilson, S. Spatial and Temporal Availability of Cloud-Free Optical Observations in the Tropics to Monitor Deforestation. *Sci. Data* **2023**, *10*, 550, doi:10.1038/s41597-023-02439-x.
135. Beuchle, R.; Eva, H.D.; Stibig, H.-J.; Bodart, C.; Brink, A.; Mayaux, P.; Johansson, D.; Achard, F.; Belward, A. A Satellite Data Set for Tropical Forest Area Change Assessment. *Int. J. Remote Sens.* **2011**, *32*, 7009–7031, doi:10.1080/01431161.2011.611186.
136. Roebroek, C.T.J.; Duveller, G.; Seneviratne, S.I.; Davin, E.L.; Cescatti, A. Releasing Global Forests from Human Management: How Much More Carbon Could Be Stored? *Science* **2023**, *380*, 749–753, doi:10.1126/science.add5878.

137. de Lima, R.B.; Görgens, E.B.; da Silva, D.A.S.; de Oliveira, C.P.; Batista, A.P.B.; Caraciolo Ferreira, R.L.; Costa, F.R.C.; Ferreira de Lima, R.A.; da Silva Aparício, P.; de Abreu, J.C.; et al. Giants of the Amazon: How Does Environmental Variation Drive the Diversity Patterns of Large Trees? *Glob. Change Biol.* **2023**, gcb.16821, doi:10.1111/gcb.16821.
138. Nascimento, M.N.; Heijink, B.M.; Bush, M.B.; Gosling, W.D.; McMichael, C.N.H. Early to Mid-Holocene Human Activity Exerted Gradual Influences on Amazonian Forest Vegetation. *Philos. Trans. R. Soc. B Biol. Sci.* **2022**, 377, 20200498, doi:10.1098/rstb.2020.0498.
139. Carvalho, R.L.; Resende, A.F.; Barlow, J.; França, F.M.; Moura, M.R.; Maciel, R.; Alves-Martins, F.; Shutt, J.; Nunes, C.A.; Elias, F.; et al. Pervasive Gaps in Amazonian Ecological Research. *Curr. Biol.* **2023**, S0960982223008631, doi:10.1016/j.cub.2023.06.077.
140. Delaroche, M.; Le Tourneau, F.-M.; Daugeard, M. How Vegetation Classification and Mapping May Influence Conservation: The Example of Brazil's Native Vegetation Protection Law. *Land Use Policy* **2022**, 122, 106380, doi:10.1016/j.landusepol.2022.106380.
141. Maracahipes-Santos, L.; Silvério, D.V.; Maracahipes, L.; Macedo, M.N.; Lenza, E.; Jankowski, K.J.; Wong, M. Intraspecific Trait Variability Facilitates Tree Species Persistence along Riparian Forest Edges in Southern Amazonia. *Sci. Rep.* **2023**, 13, 12, doi:10.1038/s41598-023-39510-x.
142. Zhang, Z.; Cescatti, A.; Wang, Y.-P.; Gentine, P.; Xiao, J.; Guanter, L.; Huete, A.R.; Wu, J.; Chen, J.M.; Ju, W.; et al. Large Diurnal Compensatory Effects Mitigate the Response of Amazonian Forests to Atmospheric Warming and Drying. *Sci. Adv.* **2023**, 9, eabq4974, doi:10.1126/sciadv.abq4974.
143. Pohl, M.J.; Lehnert, L.W.; Thies, B.; Seeger, K.; Berdugo, M.B.; Gradstein, S.R.; Bader, M.Y.; Bendix, J. Valleys Are a Potential Refuge for the Amazon Lowland Forest in the Face of Increased Risk of Drought. *Commun. Earth Environ.* **2023**, 4, 198, doi:10.1038/s43247-023-00867-6.
144. Basso, L.S.; Wilson, C.; Chipperfield, M.P.; Tejada, G.; Cassol, H.L.G.; Arai, E.; Williams, M.; Smallman, T.L.; Peters, W.; Naus, S.; et al. Atmospheric CO₂ Inversion Reveals the Amazon as a Minor Carbon Source Caused by Fire Emissions, with Forest Uptake Offsetting about Half of These Emissions. *Atmospheric Chem. Phys.* **2023**, 23, 9685–9723, doi:10.5194/acp-23-9685-2023.
145. Tavares, J.V.; Oliveira, R.S.; Mencuccini, M.; Signori-Müller, C.; Pereira, L.; Diniz, F.C.; Gilpin, M.; Marca Zevallos, M.J.; Salas Yupayccana, C.A.; Acosta, M.; et al. Basin-Wide Variation in Tree Hydraulic Safety Margins Predicts the Carbon Balance of Amazon Forests. *Nature* **2023**, doi:10.1038/s41586-023-05971-3.
146. Albert, J.S.; Carnaval, A.C.; Flantua, S.G.A.; Lohmann, L.G.; Ribas, C.C.; Riff, D.; Carrillo, J.D.; Fan, Y.; Figueiredo, J.J.P.; Guayasamin, J.M.; et al. Human Impacts Outpace Natural Processes in the Amazon. *Science* **2023**, 379, eabo5003, doi:10.1126/science.abo5003.
147. Xu, X.; Zhang, X.; Riley, W.J.; Xue, Y.; Nobre, C.A.; Lovejoy, T.E.; Jia, G. Deforestation Triggering Irreversible Transition in Amazon Hydrological Cycle. *Environ. Res. Lett.* **2022**, 17, 034037, doi:10.1088/1748-9326/ac4c1d.
148. Fawcett, D.; Sitch, S.; Ciais, P.; Wigneron, J.P.; Silva-Junior, C.H.L.; Heinrich, V.; Vancutsem, C.; Achard, F.; Bastos, A.; Yang, H.; et al. Declining Amazon Biomass Due to Deforestation and Subsequent Degradation Losses Exceeding Gains. *Glob. Change Biol.* **2023**, 29, 1106–1118, doi:10.1111/gcb.16513.

149. Engels, A.; Marotzke, J.; Gresse, E.G.; López-Rivera, A.; Pagnone, A.; Wilkens, J. Hamburg Climate Futures Outlook: The Plausibility of a 1.5°C Limit to Global Warming - Social Drivers and Physical Processes; *Universität Hamburg*: Hamburg, **2023**; p. 234.
150. Harris, N.L.; Gibbs, D.A.; Baccini, A.; Birdsey, R.A.; de Bruin, S.; Farina, M.; Fatoyinbo, L.; Hansen, M.C.; Herold, M.; Houghton, R.A.; et al. Global Maps of Twenty-First Century Forest Carbon Fluxes. *Nat. Clim. Change* **2021**, *11*, 234–240, doi:10.1038/s41558-020-00976-6.
151. Venturini, A.M.; Gontijo, J.B.; Mandro, J.A.; Berenguer, E.; Peay, K.G.; Tsai, S.M.; Bohannon, B.J.M. Soil Microbes under Threat in the Amazon Rainforest. *Trends Ecol. Evol.* **2023**, S0169534723001118, doi:10.1016/j.tree.2023.04.014.
152. Fagundes, H.O.; Fleischmann, A.S.; Fan, F.M.; Paiva, R.C.D.; Buarque, D.C.; Siqueira, V.A.; Collischonn, W.; Borelli, P. Human-Induced Changes in South American River Sediment Fluxes From 1984 to 2019. *Water Resour. Res.* **2022**, *59*, doi:10.1029/2023WR034519.
153. Ellwanger, J.H.; Fearnside, P.M.; Ziliotto, M.; Valverde-Villegas, J.M.; Veiga, A.B.G.D.; Vieira, G.F.; Bach, E.; Cardoso, J.C.; Müller, N.F.D.; Lopes, G.; et al. Synthesizing the Connections between Environmental Disturbances and Zoonotic Spillover. *An. Acad. Bras. Ciênc.* **2022**, *94*, e20211530, doi:10.1590/0001-376520220211530.
154. Reygadas, Y.; Spera, S.A.; Salisbury, D.S. Effects of Deforestation and Forest Degradation on Ecosystem Service Indicators across the Southwestern Amazon. *Ecol. Indic.* **2023**, *147*, 109996, doi:10.1016/j.ecolind.2023.109996.
155. Rorato, A.C.; Dal'Asta, A.P.; Lana, R.M. Trajetorias: A Dataset Environmental, Epidemiological, and Economic Indicators for the Brazilian Amazon. *Sci. Data* **2023**, *10*, 1–15, doi:10.1038/s41597-023-01962-1.
156. Requena Suarez, D.; Rozendaal, D.M.A.; De Sy, V.; Decuyper, M.; Málaga, N.; Durán Montesinos, P.; Arana Olivos, A.; De la Cruz Paiva, R.; Martius, C.; Herold, M. Forest Disturbance and Recovery in Peruvian Amazonia. *Glob. Change Biol.* **2023**, gcb.16695, doi:10.1111/gcb.16695.
157. Butt, E.W.; Conibear, L.; Smith, C.; Baker, J.C.A.; Rigby, R.; Knotte, C.; Spracklen, D.V. Achieving Brazil's Deforestation Target Will Reduce Fire and Deliver Air Quality and Public Health Benefits. *Earths Future* **2022**, *10*, doi:10.1029/2022EF003048.
158. Smith, C.; Baker, J.C.A.; Spracklen, D.V. Tropical Deforestation Causes Large Reductions in Observed Precipitation. *Nature* **2023**, doi:10.1038/s41586-022-05690-1.
159. Pacheco, A.; Meyer, C. Land Tenure Drives Brazil's Deforestation Rates across Socio-Environmental Contexts. *Nat. Commun.* **2022**, *13*, 5759, doi:10.1038/s41467-022-33398-3.
160. Marin, F.R.; Zanon, A.J.; Monzon, J.P.; Andrade, J.F.; Silva, E.H.F.M.; Richter, G.L.; Antolin, L.A.S.; Ribeiro, B.S.M.R.; Ribas, G.G.; Battisti, R.; et al. Protecting the Amazon Forest and Reducing Global Warming via Agricultural Intensification. *Nat. Sustain.* **2022**, *5*, 1018–1026, doi:10.1038/s41893-022-00968-8.
161. Gollnow, F.; Cammelli, F.; Carlson, K.M.; Garrett, R.D. Gaps in Adoption and Implementation Limit the Current and Potential Effectiveness of Zero-Deforestation Supply Chain Policies for Soy. *Environ. Res. Lett.* **2022**, *17*, 114003, doi:10.1088/1748-9326/ac97f6.
162. Pires, M.M.; Benchimol, M.; Cruz, L.R.; Peres, C.A. Terrestrial Food Web Complexity in Amazonian Forests Decays with Habitat Loss. *Curr. Biol.* **2023**, *33*, 389–396.e3, doi:10.1016/j.cub.2022.11.066.

163. de Oliveira, G.L.; Viana-Junior, A.B.; Trindade, P.H.S.; dos Santos, I.R.; de Almeida-Maués, P.C.R.; Carvalho, F.G.; Silva, D.P.; Wiig, Ø.; Sena, L.; Mendes-Oliveira, A.C. Wild Canids and the Ecological Traps Facing the Climate Change and Deforestation in the Amazon Forest. *Ecol. Evol.* **2023**, *13*, e10150, doi:10.1002/ece3.10150.
164. Faria, A.P.J.; Ligeiro, R.; Calvão, L.B.; Giam, X.; Leibold, M.A.; Juen, L. Land Use Types Determine Environmental Heterogeneity and Aquatic Insect Diversity in Amazonian Streams. *Hydrobiologia* **2023**, doi:10.1007/s10750-023-05190-x.
165. Nunes, M.H.; Camargo, J.L.C.; Vincent, G.; Calders, K.; Oliveira, R.S.; Huete, A.; Mendes de Moura, Y.; Nelson, B.; Smith, M.N.; Stark, S.C.; et al. Forest Fragmentation Impacts the Seasonality of Amazonian Evergreen Canopies. *Nat. Commun.* **2022**, *13*, 917, doi:10.1038/s41467-022-28490-7.
166. Smith, M.N.; Stark, S.C.; Taylor, T.C.; Schietti, J.; de Almeida, D.R.A.; Aragón, S.; Torralvo, K.; Lima, A.P.; de Oliveira, G.; de Assis, R.L.; et al. Diverse Anthropogenic Disturbances Shift Amazon Forests along a Structural Spectrum. *Front. Ecol. Environ.* **2023**, *21*, 24–32, doi:10.1002/fee.2590.
167. Pillay, R.; Watson, J.E.M.; Hansen, A.J.; Jantz, P.A.; Aragon-Osejo, J.; Armenteras, D.; Atkinson, S.C.; Burns, P.; Ervin, J.; Goetz, S.J.; et al. Humid Tropical Vertebrates Are at Lower Risk of Extinction and Population Decline in Forests with Higher Structural Integrity. *Nat. Ecol. Evol.* **2022**, *6*, 1840–1849, doi:10.1038/s41559-022-01915-8.
168. Mancini, G.; Benítez-López, A.; Di Marco, M.; Pacifici, M.; Rondinini, C.; Santini, L. Synergistic Effects of Habitat Fragmentation and Hunting on the Extinction Risk of Neotropical Primates. *Biodivers. Conserv.* **2023**, doi:10.1007/s10531-023-02623-w.
169. Armenteras, D.; González-Delgado, T.M.; González-Trujillo, J.D.; Meza-Elizalde, M.C. Local Stakeholder Perceptions of Forest Degradation: Keys to Sustainable Tropical Forest Management. *Ambio* **2022**, doi:10.1007/s13280-022-01797-x.
170. Feng, Y.; Negrón-Juárez, R.I.; Romps, D.M.; Chambers, J.Q. Amazon Windthrow Disturbances Are Likely to Increase with Storm Frequency under Global Warming. *Nat. Commun.* **2023**, *14*, 101, doi:10.1038/s41467-022-35570-1.
171. Zhu, L.; Li, W.; Ciais, P.; He, J.; Cescatti, A.; Santoro, M.; Tanaka, K.; Cartus, O.; Zhao, Z.; Xu, Y.; et al. Comparable Biophysical and Biogeochemical Feedbacks on Warming from Tropical Moist Forest Degradation. *Nat. Geosci.* **2023**, doi:10.1038/s41561-023-01137-y.
172. Hughes, L.J.; Massam, M.R.; Morton, O.; Edwards, F.A.; Scheffers, B.R.; Edwards, D.P. Global Hotspots of Traded Phylogenetic and Functional Diversity. *Nature* **2023**, doi:10.1038/s41586-023-06371-3.
173. Willmer, J.N.G.; Püttker, T.; Prevedello, J.A. Global Impacts of Edge Effects on Species Richness. *Biol. Conserv.* **2022**, *272*, 109654, doi:10.1016/j.biocon.2022.109654.
174. Püttker, T.; Crouzeilles, R.; Almeida-Gomes, M.; Schmoeller, M.; Maurenza, D.; Alves-Pinto, H.; Pardini, R.; Vieira, M.V.; Banks-Leite, C.; Fonseca, C.R.; et al. Indirect Effects of Habitat Loss via Habitat Fragmentation: A Cross-Taxa Analysis of Forest-Dependent Species. *Biol. Conserv.* **2020**, *241*, 108368, doi:10.1016/j.biocon.2019.108368.
175. Rosan, T.M.; Sitch, S.; Mercado, L.M.; Heinrich, V.; Friedlingstein, P.; Aragão, L.E.O.C. Fragmentation-Driven Divergent Trends in Burned Area in Amazonia and Cerrado. *Front. For. Glob. Change* **2022**, *5*, 801408, doi:10.3389/ffgc.2022.801408.
176. Balch, J.K.; Abatzoglou, J.T.; Joseph, M.B.; Koontz, M.J.; Mahood, A.L.; McGlinchy, J.; Cattau, M.E.; Williams, A.P. Warming Weakens the Night-Time Barrier to Global Fire. *Nature* **2022**, *602*, 442–448, doi:10.1038/s41586-021-04325-1.

177. Cano, I.M.; Shevliakova, E.; Malyshev, S.; John, J.G.; Yu, Y.; Smith, B.; Pacala, S.W. Abrupt Loss and Uncertain Recovery from Fires of Amazon Forests under Low Climate Mitigation Scenarios. *Proc. Natl. Acad. Sci.* **2022**, *119*, e2203200119, doi:10.1073/pnas.2203200119.
178. Drüke, M.; Sakschewski, B.; von Bloh, W.; Billing, M.; Lucht, W.; Thonicke, K. Fire May Prevent Future Amazon Forest Recovery after Large-Scale Deforestation. *Commun. Earth Environ.* **2023**, *4*, 248, doi:10.1038/s43247-023-00911-5.
179. Silvério, D.V.; Oliveira, R.S.; Flores, B.M.; Brando, P.M.; Almada, H.K.; Furtado, M.T.; Moreira, F.G.; Heckenberger, M.; Ono, K.Y.; Macedo, M.N. Intensification of Fire Regimes and Forest Loss in the Território Indígena Do Xingu. *Environ. Res. Lett.* **2022**, *17*, 045012, doi:10.1088/1748-9326/ac5713.
180. East, A.; Hansen, A.; Armenteras, D.; Jantz, P.; Roberts, D.W. Measuring Understory Fire Effects from Space: Canopy Change in Response to Tropical Understory Fire and What This Means for Applications of GEDI to Tropical Forest Fire. *Remote Sens.* **2023**, *15*, 696, doi:10.3390/rs15030696.
181. Jones, M.W.; Abatzoglou, J.T.; Veraverbeke, S.; Andela, N.; Lasslop, G.; Forkel, M.; Smith, A.J.P.; Burton, C.; Betts, R.A.; van der Werf, G.R.; et al. Global and Regional Trends and Drivers of Fire Under Climate Change. *Rev. Geophys.* **2022**, *60*, doi:10.1029/2020RG000726.
182. dos Reis, M.; Graça, P.M.L. de A.; Yanai, A.M.; Ramos, C.J.P.; Fearnside, P.M. Forest Fires and Deforestation in the Central Amazon: Effects of Landscape and Climate on Spatial and Temporal Dynamics. *J. Environ. Manage.* **2021**, *288*, 112310, doi:10.1016/j.jenvman.2021.112310.
183. DeArmond, D.; Emmert, F.; Pinto, A.C.M.; Lima, A.J.N.; Higuchi, N. A Systematic Review of Logging Impacts in the Amazon Biome. *Forests* **2023**, *14*, 81, doi:10.3390/f14010081.
184. Rico-Straffon, J.; Wang, Z.; Panlasigui, S.; Loucks, C.J.; Swenson, J.; Pfaff, A. Forest Concessions and Eco-Certifications in the Peruvian Amazon: Deforestation Impacts of Logging Rights and Logging Restrictions. *J. Environ. Econ. Manag.* **2023**, *118*, 102780, doi:10.1016/j.jeem.2022.102780.
185. Malhi, Y.; Riutta, T.; Wearn, O.R.; Deere, N.J.; Mitchell, S.L.; Bernard, H.; Majalap, N.; Nilus, R.; Davies, Z.G.; Ewers, R.M.; et al. Logged Tropical Forests Have Amplified and Diverse Ecosystem Energetics. *Nature* **2022**, *612*, 707–713, doi:10.1038/s41586-022-05523-1.
186. Milodowski, D.T.; Coomes, D.A.; Swinfield, T.; Jucker, T.; Riutta, T.; Malhi, Y.; Svátek, M.; Kvasnica, J.; Burslem, D.F.R.P.; Ewers, R.M.; et al. The Impact of Logging on Vertical Canopy Structure across a Gradient of Tropical Forest Degradation Intensity in Borneo. *J. Appl. Ecol.* **2021**, *58*, 1764–1775, doi:10.1111/1365-2664.13895.
187. Mills, M.B.; Malhi, Y.; Ewers, R.M.; Kho, L.K.; Teh, Y.A.; Both, S.; Burslem, D.F.R.P.; Majalap, N.; Nilus, R.; Huaraca Huasco, W.; et al. Tropical Forests Post-Logging Are a Persistent Net Carbon Source to the Atmosphere. *Proc. Natl. Acad. Sci.* **2023**, *120*, e2214462120, doi:10.1073/pnas.2214462120.
188. Riutta, T.; Kho, L.K.; Teh, Y.A.; Ewers, R.; Majalap, N.; Malhi, Y. Major and Persistent Shifts in Below-ground Carbon Dynamics and Soil Respiration Following Logging in Tropical Forests. *Glob. Change Biol.* **2021**, *27*, 2225–2240, doi:10.1111/gcb.15522.
189. de Lima, J.A.; Tonello, K.C. Rainfall Partitioning in Amazon Forest: Implications of Reduced Impact Logging for Hydrological Processes. *Agric. For. Meteorol.* **2023**, *337*, 109505, doi:10.1016/j.agrformet.2023.109505.

190. Dionisio, L.F.S.; Vaz, M.M.; de Carvalho, J.O.P.; Lopes, J. do C.A. Volume of Commercial Timber Found Dead in Managed Amazonian Natural Forests: Is It Possible to Take Advantage? *For. Ecol. Manag.* **2022**, *521*, 120441, doi:10.1016/j.foreco.2022.120441.
191. Cudney-Valenzuela, S.J.; Arroyo-Rodríguez, V.; Morante-Filho, J.C.; Toledo-Aceves, T.; Andresen, E. Tropical Forest Loss Impoverishes Arboreal Mammal Assemblages by Increasing Tree Canopy Openness. *Ecol. Appl.* **2023**, *33*, doi:10.1002/eap.2744.
192. Arrifano, G. de P.; Augusto-Oliveira, M.; Lopes-Araújo, A.; Santos-Sacramento, L.; Macchi, B.M.; Nascimento, J.L.M. do; Crespo-Lopez, M.E. Global Human Threat: The Potential Synergism between Mercury Intoxication and COVID-19. *Int. J. Environ. Res. Public Health* **2023**, *20*, 4207, doi:10.3390/ijerph20054207.
193. Meneses, H. do N. de M.; Oliveira-da-Costa, M.; Basta, P.C.; Morais, C.G.; Pereira, R.J.B.; de Souza, S.M.S.; Hacon, S. de S. Mercury Contamination: A Growing Threat to Riverine and Urban Communities in the Brazilian Amazon. *Int. J. Environ. Res. Public Health* **2022**, *19*, 2816, doi:10.3390/ijerph19052816.
194. Mataveli, G.; Chaves, M.; Guerrero, J.; Escobar-Silva, E.V.; Conceição, K.; de Oliveira, G. Mining Is a Growing Threat within Indigenous Lands of the Brazilian Amazon. *Remote Sens.* **2022**, *14*, 4092, doi:10.3390/rs14164092.
195. Duncanson, L.; Liang, M.; Leitold, V.; Armston, J.; Krishna Moorthy, S.M.; Dubayah, R.; Costedoat, S.; Enquist, B.J.; Fatoyinbo, L.; Goetz, S.J.; et al. The Effectiveness of Global Protected Areas for Climate Change Mitigation. *Nat. Commun.* **2023**, *14*, 2908, doi:10.1038/s41467-023-38073-9.
196. König, L.A.; Medina-Vega, J.A.; Longo, R.M.; Zuidema, P.A.; Jakovac, C.C. Restoration Success in Former Amazonian Mines Is Driven by Soil Amendment and Forest Proximity. *Philos. Trans. R. Soc. B Biol. Sci.* **2023**, *378*, 20210086, doi:10.1098/rstb.2021.0086.
197. de Aguiar Barros, J.; Granja, F.; Pequeno, P.; Marchesini, P.; Ferreira da Cruz, M. de F. Gold Miners Augment Malaria Transmission in Indigenous Territories of Roraima State, Brazil. *Malar. J.* **2022**, *21*, 358, doi:10.1186/s12936-022-04381-6.
198. Wetzler, E.A.; Marchesini, P.; Villegas, L.; Canavati, S. Changing Transmission Dynamics among Migrant, Indigenous and Mining Populations in a Malaria Hotspot in Northern Brazil: 2016 to 2020. *Malar. J.* **2022**, *21*, 127, doi:10.1186/s12936-022-04141-6.
199. Giljum, S.; Maus, V.; Kuschig, N.; Luckeneder, S.; Tost, M.; Sonter, L.J.; Bebbington, A.J. A Pantropical Assessment of Deforestation Caused by Industrial Mining. *Proc. Natl. Acad. Sci.* **2022**, *119*, e2118273119, doi:10.1073/pnas.2118273119.
200. Chaddad, F.; Mello, F.A.O.; Tayebi, M.; Safanelli, J.L.; Campos, L.R.; Amorim, M.T.A.; Barbosa de Sousa, G.P.; Ferreira, T.O.; Ruiz, F.; Perlatti, F.; et al. Impact of Mining-Induced Deforestation on Soil Surface Temperature and Carbon Stocks: A Case Study Using Remote Sensing in the Amazon Rainforest. *J. South Am. Earth Sci.* **2022**, *119*, 103983, doi:10.1016/j.jsames.2022.103983.
201. Casagrande, G.C.R.; Dambros, J.; de Andrade, E.A.; Martello, F.; Sobral-Souza, T.; Moreno, M.I.C.; Battirolo, L.D.; de Andrade, R.L.T. Atmospheric Mercury in Forests: Accumulation Analysis in a Gold Mining Area in the Southern Amazon, Brazil. *Environ. Monit. Assess.* **2023**, *195*, doi:10.1007/s10661-023-11063-6.
202. Bello, T.C.S.; Buralli, R.J.; Cunha, M.P.L.; Dórea, J.G.; Diaz-Quijano, F.A.; Guimarães, J.R.D.; Marques, R.C. Mercury Exposure in Women of Reproductive Age in Rondônia State, Amazon Region, Brazil. *Int. J. Environ. Res. Public Health* **2023**, *20*, 5225, doi:10.3390/ijerph20065225.

203. Bogoni, J.A.; Peres, C.A.; Ferraz, K.M.P.M.B. Extent, Intensity and Drivers of Mammal Defaunation: A Continental-scale Analysis across the Neotropics. *Sci. Rep.* **2020**, *10*, 14750, doi:10.1038/s41598-020-72010-w.
204. Bastos da Silva, A.; E. R. Pereyra, P.; R. El Bizri, H.; M. S. Souto, W.; S. L. Barboza, R. Patterns of Wildlife Hunting and Trade by Local Communities in Eastern Amazonian Floodplains. *Ethnobiol. Conserv.* **2022**, doi:10.15451/ec2022-07-11.16-1-19.
205. Bogoni, J.A.; Percequillo, A.R.; Ferraz, K.M.P.M.B.; Peres, C.A. The Empty Forest Three Decades Later: Lessons and Prospects. *Biotropica* **2023**, *55*, 13–18, doi:10.1111/btp.13188.
206. Bragagnolo, C.; Gama, G.M.; Vieira, F.A.S.; Campos-Silva, J.V.; Bernard, E.; Malhado, A.C.M.; Correia, R.A.; Jepson, P.; de Carvalho, S.H.C.; Efe, M.A.; et al. Hunting in Brazil: What Are the Options? *Perspect. Ecol. Conserv.* **2019**, *17*, 71–79, doi:10.1016/j.pecon.2019.03.001.
207. Valsecchi, J.; Monteiro, M.C.M.; Alvarenga, G.C.; Lemos, L.P.; Ramalho, E.E. Community-Based Monitoring of Wild Felid Hunting in Central Amazonia. *Anim. Conserv.* **2022**, *10*, doi:doi:10.1111/acv.12811.
208. Brodie, J.F.; Fragoso, J.M.V. Understanding the Distribution of Bushmeat Hunting Effort across Landscapes by Testing Hypotheses about Human Foraging. *Conserv. Biol.* **2021**, *35*, 1009–1018, doi:10.1111/cobi.13612.
209. Sampaio, R.; Morato, R.G.; Royle, A.; Abrahams, M.I.; Peres, C.A.; Chiarello, A.G. Vertebrate Population Changes Induced by Hunting in Amazonian Sustainable-Use Protected Areas. *Biol. Conserv.* **2023**, *284*, 110206, doi:10.1016/j.biocon.2023.110206.
210. Soares-Filho, B.S.; Oliveira, U.; Ferreira, M.N.; Marques, F.F.C.; de Oliveira, A.R.; Silva, F.R.; Börner, J. Contribution of the Amazon Protected Areas Program to Forest Conservation. *Biol. Conserv.* **2023**, *279*, 109928, doi:10.1016/j.biocon.2023.109928.
211. Qin, Y.; Xiao, X.; Liu, F.; de Sa e Silva, F.; Shimabukuro, Y.; Arai, E.; Fearnside, P.M. Forest Conservation in Indigenous Territories and Protected Areas in the Brazilian Amazon. *Nat. Sustain.* **2023**, doi:10.1038/s41893-022-01018-z.
212. West, T.A.P.; Rausch, L.; Munger, J.; Gibbs, H.K. Protected Areas Still Used to Produce Brazil's Cattle. *Conserv. Lett.* **2022**, *15*, doi:10.1111/conl.12916.
213. Bogoni, J.A.; Boron, V.; Peres, C.A.; Coelho, M.E.M.S.; Morato, R.G.; Oliveira-da-Costa, M. Impending Anthropogenic Threats and Protected Area Prioritization for Jaguars in the Brazilian Amazon. *Commun. Biol.* **2023**, *6*, 132, doi:10.1038/s42003-023-04490-1.
214. Benzeev, R.; Zhang, S.; Rauber, M.A.; Vance, E.A.; Newton, P. Formalizing Tenure of Indigenous Lands Improved Forest Outcomes in the Atlantic Forest of Brazil. *PNAS Nexus* **2023**, *2*, pgac287, doi:10.1093/pnasnexus/pgac287.
215. Alves, R.P.; Levis, C.; Bertin, V.M.; Ferreira, M.J.; Cassino, M.F.; Pequeno, P.A.C.L.; Schietti, J.; Clement, C.R. Local Forest Specialists Maintain Traditional Ecological Knowledge in the Face of Environmental Threats to Brazilian Amazonian Protected Areas. *Front. For. Glob. Change* **2022**, *5*, 1028129, doi:10.3389/ffgc.2022.1028129.
216. Silva-Junior, C.H.L.; Silva, F.B.; Arisi, B.M.; Mataveli, G.; Pessôa, A.C.M.; Carvalho, N.S.; Reis, J.B.C.; Júnior, A.R.S.; Ribeiro, F.D.; Siqueira-Gay, J.; et al. Brazilian Amazon Indigenous Territories under Deforestation Pressure. *Sci. Rep.* **2023**, *13*, 5851, doi:10.1038/s41598-023-32746-7.

217. Franco-Moraes, J.; Braga, L.V.; Clement, C.R. The Zo'é Perspective on What Scientists Call "Forest Management" and Its Implications for Floristic Diversity and Biocultural Conservation. *Ecol. Soc.* **2023**, *28*, doi:10.5751/ES-13711-280137.
218. Lessa, T.; Jepson, P.; Bragagnolo, C.; Campos-Silva, J.V.; Barros, E.; Gomes, F.; Pinheiro, B.R.; Fé, T.P.M.; Malhado, A.C.M.; Ladle, R.J. Revealing the Hidden Value of Protected Areas. *Land Use Policy* **2021**, *111*, 105733, doi:10.1016/j.landusepol.2021.105733.
219. Rangel Pinagé, E.; Keller, M.; Peck, C.P.; Longo, M.; Duffy, P.; Csillik, O. Effects of Forest Degradation Classification on the Uncertainty of Aboveground Carbon Estimates in the Amazon. *Carbon Balance Manag.* **2023**, *18*, 2, doi:10.1186/s13021-023-00221-5.
220. Uribe, M. del R.; Coe, M.T.; Castanho, A.D.A.; Macedo, M.N.; Valle, D.; Brando, P.M. Net Loss of Biomass Predicted for Tropical Biomes in a Changing Climate. *Nat. Clim. Change* **2023**, doi:10.1038/s41558-023-01600-z.
221. Costa, J.F.; Hernández Ruz, E.J.; Galdino Alves Dos Santos, G. Carbon Stock and Dynamic in the Middle Xingu Forests at Eastern Amazonia. *Neotropical Biodivers.* **2022**, *8*, 371–380, doi:10.1080/23766808.2022.2148438.
222. Heinrich, V.H.A.; Vancutsem, C.; Dalagnol, R.; Rosan, T.M.; Fawcett, D.; Silva-Junior, C.H.L.; Cassol, H.L.G.; Achard, F.; Jucker, T.; Silva, C.A.; et al. The Carbon Sink of Secondary and Degraded Humid Tropical Forests. *Nature* **2023**, *615*, 436–442, doi:10.1038/s41586-022-05679-w.
223. Edwards, D.P.; Cerullo, G.R.; Chomba, S.; Worthington, T.A.; Balmford, A.P.; Chazdon, R.L.; Harrison, R.D. Upscaling Tropical Restoration to Deliver Environmental Benefits and Socially Equitable Outcomes. *Curr. Biol.* **2021**, *31*, R1326–R1341, doi:10.1016/j.cub.2021.08.058.
224. da Silva, C.M.; Elias, F.; do Nascimento, R.O.; Ferreira, J. The Potential for Forest Landscape Restoration in the Amazon: State of the Art of Restoration Strategies. *Restor. Ecol.* **2023**, e13955, doi:10.1111/rec.13955.
225. Gastauer, M.; Cavalcante, R.B.L.; Caldeira, C.F.; Nunes, S. de S. Structural Hurdles to Large-Scale Forest Restoration in the Brazilian Amazon. *Front. Ecol. Evol.* **2020**, *8*, 593557, doi:10.3389/fevo.2020.593557.
226. Saraiva, M.B.; Ferreira, M.D.P.; da Cunha, D.A.; Daniel, L.P.; Homma, A.K.O.; Pires, G.F. Forest Regeneration in the Brazilian Amazon: Public Policies and Economic Conditions. *J. Clean. Prod.* **2020**, *269*, 122424, doi:10.1016/j.jclepro.2020.122424.
227. Schmidt, M.V.C.; Ikpeng, Y.U.; Kayabi, T.; Sanches, R.A.; Ono, K.Y.; Adams, C. Indigenous Knowledge and Forest Succession Management in the Brazilian Amazon: Contributions to Reforestation of Degraded Areas. *Front. For. Glob. Change* **2021**, *4*, 605925, doi:10.3389/ffgc.2021.605925.
228. Chen, N.; Tsendbazar, N.; Requena Suarez, D.; Verbesselt, J.; Herold, M. Characterizing Aboveground Biomass and Tree Cover of Regrowing Forests in Brazil Using Multi-source Remote Sensing Data. *Remote Sens. Ecol. Conserv.* **2023**, rse2.328, doi:10.1002/rse2.328.
229. Barros, F. de V.; Lewis, K.; Robertson, A.D.; Pennington, R.T.; Hill, T.C.; Matthews, C.; Lira-Martins, D.; Mazzochini, G.G.; Oliveira, R.S.; Rowland, L. Cost-Effective Restoration for Carbon Sequestration across Brazil's Biomes. *Sci. Total Environ.* **2023**, *876*, 162600, doi:10.1016/j.scitotenv.2023.162600.

List of abbreviations and definitions

AGB	Aboveground Biomass
ASGM	Artisanal Small-scale Gold Mining
BLA	Brazilian Legal Amazon
CI	Confidence Interval
CL	Conventional Selective Logging
COVID-19	Corona Virus Disease 2019
CURU	Conservation Unit of Restricted Use
CUSU	Conservation Unit of Sustainable Use
DETER	Brazilian alert system for deforestation and forest degradation in the Amazonas biome
ES	Ecosystem Services
ESA	European Space Agency
FCC	Forest Cover Change
FUNAI	Brazilian National Foundation for Indigenous People
GFC	Global Forest Change
GWIS	Global Wildfire Information System
IBAMA	Brazilian National Institute for Environment and Renewable Natural Resources
IIRSA	Initiative to Integrate the Regional Infrastructure of South America
IL	Indigenous Lands
IMAZON	Institute of the People and the Environment of the Amazon
INPE	Brazilian National Space Research Institute
IO	Independent Organisation
IT	Indigenous Territories
IUCN	International Union for Conservation of Nature
JRC	Joint Research Centre of the European Commission
NDC	Nationally Determined Contribution
NGO	Non-Governmental Organisation
NPP	Net Primary Production
OGD	Old-Growth Deforestation
PA	Protected Areas
PFR	Precision Forest Restoration
PL	Brazilian Law Proposal
PEC	Brazilian Constitutional Amendment
PRODES	Brazilian program for monitoring deforestation in the Amazonas and Cerrado biomes

SAD	IMAZON's Deforestation Alert System
SFM	Sustainable Forest Management
SFR	Secondary Forest Regrowth
TLS	Terrestrial Laser-Scanning
TMF	Tropical Moist Forest Project at the JRC
USGS	United States Geological Survey
UN	United Nations
ZD	Zoonotic Disease

List of figures

Figure 1. Subset of JRC-TMF humid forest disturbances statistics for the Pan-Amazon for the past five years. The stars (2020-2022) indicate that the distribution of the two classes within the yearly overall forest disturbances is an “educated guess” 9

Figure 2. Forest disturbances in the Pan-Amazon humid forest from 2000-2022. The geographic basis are the areas of “Amazonia sensu stricto” and “Guiana”, according to Eva and Huber [35]. GFC statistics appear as grey dashed line.10

Figure 3. Distribution of accumulated JRC-TMF forest disturbances during period 2020-2022, i.e. the sum of deforestation and forest degradation (above an area of 30 km²) within 50 km X 50 km grid cells in the Pan-Amazon humid forest (red circles). The Country borders are shown as black lines, major roads as grey lines. Background: TMF forest cover change map, status 1990. Image width ca. 4,000 km.....11

Figure 4. Examples of accumulated (2020-2022) JRC-TMF forest disturbances within two 50km X 50km grid cells in the Pan-Amazon humid forest. The borders of the 50 km X 50 km grid cells are shown in white. Left: new deforestation frontier in Southern Amazonas State (near the Rondônia State border) – all red and brown areas were deforested between 2020 and 2022. Right: Bolivian forest destroyed by a large fire in 2022 (brown area)12

Figure 5. Disturbed humid forest area (deforestation and forest degradation) during years 2020, 2021 and 2022 for Amazon countries, according to JRC-TMF data12

Figure 6. Percentage of disturbed forest area (deforestation and forest degradation) during years 2020, 2021 and 2022 in relation to remaining intact moist forests for Amazon countries, according to JRC-TMF data.....13

Figure 7. Deforested area between 1990 and 2019 in the Amazon region (i.e. Amazonia sensu stricto and Guiana, according to Eva & Huber, 2005) within 50 km X 50 km grid cells, with colours indicating the 5-year period of peak deforestation. Deforestation areas lower than 200 km² within a single grid cell are not displayed.13

Figure 8. 50 km X 50 km grid cell with JRC-TMF data in Central Rondônia, with 67% forest cover in 1990 (left panel, with deforested areas before 1990 in white) due to ‘early deforestation’ in the 1970s and 1980s. By 2019, a further 83% of the forest standing in 1990 were deforested (right panel, with deforested areas during period 1990-2019 in orange).14

Figure 9. Accumulated forest degradation (not followed by deforestation) during period 1990-2019, caused by selective logging, fire or natural events with subsequent forest recovery, areas per 50 km X 50 km grid cell (see Figure 11 for examples A and B).....15

Figure 10. Two examples of accumulated degraded forest over period 1990-2019, i.e. areas that are still forests in 2019 after a disturbance in the previous three decades. Left panel: Large burned forest area (989 km²) in Rondônia State, where forest fires happened near ‘fishbone-type’ secondary roads. Right panel: 1000 km² of burned forest near the city of Santarém (Pará State). Map width: 50 km, grid cell borders in white....16

Figure 11. Percentage of average yearly forest degradation areas (i.e. mainly selective logging, forest fires and natural events) versus area of average yearly forest disturbances (i.e. deforestation and forest degradation) for Amazon countries and regions.....16

Figure 12. Forest disturbances in the Bolivian humid forest from 2000 to 2022, according to JRC-TMF. Tree cover loss estimates from GFC appear as grey dashed line. 17

Figure 13. Forest disturbances in the Brazilian humid forest from 2000 to 2022, according to JRC-TMF. Tree cover loss estimates from GFC appear as grey dashed line. 18

Figure 14. Forest disturbances in Colombian humid forest from 2000 to 2022, according to JRC-TMF. Tree cover loss estimates from GFC appear as grey dashed line.19

Figure 15. Forest disturbances in Ecuadorian humid forest from 2000 to 2022, according to JRC-TMF. Tree cover loss estimates from GFC appear as grey dashed line.	20
Figure 16. Forest disturbances in the Guiana Shield’s humid forest from 2000 to 2022, according to JRC-TMF. Tree cover loss estimates from GFC appear as grey dashed line.	21
Figure 17. Forest disturbances in Peruvian humid forest from 2000 to 2022, according to JRC-TMF. Tree cover loss estimates from GFC appear as grey dashed line.	22
Figure 18. Forest disturbances in Venezuelan humid forest from 2000 to 2022, according to JRC-TMF. Tree cover loss estimates from GFC appear as grey dashed line.	23
Figure 19. Annual deforestation and forest degradation in the BLA from 2000 to 2022, according to JRC-TMF data. Deforestation appears in red, forest degradation appears in orange. For comparison, INPE-PRODES and GFC deforestation estimates appear as blue and grey dashed lines, respectively.	24
Figure 20. GWIS weekly cumulative burnt areas for the Brazilian Legal Amazon for year 2021 (left panel) and 2022 (right panel).....	25
Figure 21. Yearly consolidated deforestation estimates (‘reference years’, i.e. August to July) for the Brazilian Legal Amazon reported by INPE-PRODES.....	26
Figure 22. Yearly consolidated deforestation estimates (‘reference years’, i.e. August to July) for the Brazilian Cerrado biome reported by INPE-PRODES.....	27
Figure 23. INPE-DETER yearly aggregation of deforestation near-real-time alerts (blue bars) and INPE-PRODES official consolidated deforestation estimates (red bars) from 2015/16 – 2022/23 (August-July) for the BLA	28
Figure 24. Difference between ‘reference year’ (August-July) and ‘calendar year’ (January-December) accumulation of INPE-DETER monthly deforestation alerts.	28
Figure 25. left: INPE-DETER forest degradation alerts for the BLA, right: INPE-DETER forest fire alerts for the BLA (forest fire being a sub-class of the forest degradation alerts)	29
Figure 26. left: monthly statistics of INPE-DETER deforestation alerts 2023 for the BLA (January – October), right: INPE-DETER accumulated deforestation alerts for the BLA (January – October).....	30
Figure 27. DETER deforestation alerts for the Brazilian Legal Amazon (red line) of the January-June period, and the increase of law enforcement and legal action of IBAMA in 2023	30
Figure 28. Monthly deforestation alerts from January – December 2022 (left), according to INPE-DETER and IMAZON-SAD, with accumulated monthly deforestation alerts of both systems (right)	31
Figure 29. Monthly deforestation alerts (left) from the period January – September for year 2022 and 2023, according to INPE-DETER and IMAZON-SAD, with monthly accumulated monthly deforestation alerts of both systems (right).	32
Figure 30. Soy exports from Brazil and the Brazilian Amazon towards the EU and deforestation exposure (calculation based on TRASE data)	35
Figure 31. Soy exports and deforestation exposure in the Brazilian Amazon. Calculation based on (calculation based on TRASE data). “Other” does not include domestic consumption.	35
Figure 32. Increase of the soy production area in the Brazilian Amazon	36
Figure 33. Soy expansion in the Brazilian Amazon biome (<i>Amazonia sensu stricto</i> by Eva et al., 2005), soy production area (top panel) and period of maximum expansion (bottom panel) for 50 km X 50 km grid cells, based on JRC-TMF and MapBiomias data	37

Figure 34. Deforestation in the Brazilian Amazon from 1990 to 2021 due to soy plantation within five years (red bars), soy plantation at least five years after the deforestation event (yellow bars), and permanent pasture (green bars). The dotted blue line marks the cut-off date of the Soy Moratorium. The chart is based on JRC-TMF and MapBiomias data.....	39
Figure 35. Soybean expansion in the Brazilian Amazon categorised in terms of time lag between the forest conversion and soybean plantation.....	40
Figure 36. Relationship between the areas converted to soybean and average time lags between deforestation and soy planting within 50 km X 50 km size grid cells. Main existing grain transport network to the ports of international trade and new infrastructure projects (roads, train lines) are overlaid (road lines taken from https://www.openstreetmap.org/).....	41
Figure 37. Area of deforestation leading to soy fields vs average time lag between deforestation and soybean expansion within 50 km X 50 km grid cells (with trend line).	41
Figure 38. Top Panel: Landsat image from 2010, bottom panel: time lags (years) between deforestation and soybean expansion at the landscape-level (lon: -56.4 / lat: -12). Since 2010, the land cover patterns are unchanged, image width ca. 16 km	42
Figure 39. End of the asphalt (in 2019) of the BR-319 highway Manaus – Porto Velho, ca. 200 km southwest of Manaus (picture by Google Street View)	50
Figure 40: Comparison of mapped forest disturbance area 2022 (Pan-Amazon) with Landsat 9 and Landsat7/8 imagery	53
Figure 41: Comparison of forest disturbance mapping with Landsat Collection-1 vs. Collection-2, based on the JRC-TMF forest cover change mapping during year 2021 for the Pan-Amazon.....	54
Figure 42: Comparison between Landsat-based TMF map (top right panel) and new hybrid Landsat - Sentinel-2 map (bottom right panel), with additional deforestation area mapped (displayed in white) due to additional availability of cloud-free Sentinel-2 imagery. Dates of last cloud-free observation 2022 of Landsat 8 (top left panel) and S2 (bottom left panel) are indicated on satellite images. Image width: ca. 5 km	55
Figure 43: Comparison between Landsat-based TMF map (left panel) and the hybrid Landsat – Sentinel-2 map (right panel), with more detection of selective logging (light brown) and smaller rivers (blue) due to higher spatial resolution of Sentinel-2 imagery. Image width: ca. 700 m	56
Figure 44: Average number of valid observations (VOs) per pixel for 250 km x 250 km grid cells in the Amazon region. Left: Landsat 7/8/9, right: Sentinel-2	57
Figure 45: Moist forest disturbances 2022 mapped with a hybrid approach (Landsat, Sentinel-2), compared to the mapped forest disturbances with Landsat only. Surplus of the hybrid map is indicated as percentage	57
Figure 46: Additional carbon storage potential. (A) Additional carbon storage potential (CSP) in the hypothetical scenario in which all forests would resettle in their natural equilibrium if all direct human management was removed from them. The CSP is calculated from the difference between biomass carrying capacity and the expected biomass (the biomass that would occur under local conditions with the given natural disturbance regime and average intensity of human intervention). (B) National statistics of additional CSP for countries where absolute values exceed 0.7 Pg biomass [136].	58
Figure 47: Fisher's alpha-diversity distribution for large trees (dbh ≥ 70 cm) and diversity distribution considering all trees (dbh ≥ 10 cm) estimated by the RF model for the Brazilian Amazon [137].	59
Figure 48. Map of the distributions of the earliest dated evidence of human occupation (based on lake sediment (circles), soil charcoal (squares) and archaeological records	

(triangles) plotted in 2000-year time bins from before 10 000 cal yr BP until present (here only the earliest and most recent time bins are shown). Phytolith soil records from archaeological sites are shown as archaeological sites (triangles). Circle colours indicate the proxy used by the original author to indicate the onset of humans, and symbols in grey indicate sites where the earliest evidence of human occupation happened on an earlier panel. Black line represents the Amazonia *sensu stricto* boundary [138].....60

Figure 49 The map represents the average research probability across all organism groups and habitat types, i.e. aquatic, wetlands and uplands research probabilities [139].61

Figure 50: Mean functional traits of riparian forest tree communities in forested catchments (Forest) and cropland catchments (Cropland) in southern Amazonia, Querência-MT, Brazil. Hmax = maximum tree height; BT = bark thickness; SSD = stem-specific density; LA = leaf area; LT = leaf thickness, SLA = specific leaf area [141]62

Figure 51: Diurnal patterns of solar-induced chlorophyll fluorescence (SIF, $\text{mW} \cdot \text{m}^{-2} \cdot \text{nm}^{-1}$) and evapotranspiration (ET, $\text{W} \cdot \text{m}^{-2}$) in Amazonian forests throughout 2015–2020 at 2-hour intervals: 7:00 to 9:00, 9:00 to 11:00, 11:00 to 13:00, 13:00 to 15:00, and 15:00 to 17:00. The mean and SD are shown in the bottom right of each panel. The spatial resolution is $1^\circ \times 1^\circ$ [142].63

Figure 52: Left: Location of three typical sites with two convex and one concave landforms. Convex: Amazon Tall Tower Observatory ATTO with 13% long-term FLS-frequency and Station 1 with 32% long-term FLS-frequency, concave: Station 2 with 50% long-term FLS-frequency. Right: Idealised cross section illustrating at which topographic position the threshold between TLCF (tropical lowland cloud forests) and non-TLCF conditions is expected to be reached [143].....64

Figure 53: Annual mean carbon fluxes for the Amazon: : posterior total flux with the Amazon vertical profile observations in the inversion (black bars) and posterior fire fluxes using MOPITT carbon monoxide observations in the inversion (red bars). Annual cumulative water deficit (blue line), annual mean temperature (pink line), annual mean shortwave solar radiation downward flux (all sky; black line) and annual total burned area (brown line) [144].....65

Figure 54: Hydraulic trait variation across and within Amazon forest sites, left: Xylem water potential at which 50% of the conductance is lost (ψ_{50}), right: hydraulic trait variation within forests with intermediate dry season length (DSL), subsetted according to Amazon region (central eastern Amazon: TAP, CAX and MAN; western Amazon: FEC and TAM). [145].....66

Figure 55: Temporal and spatial scales of anthropogenic and natural processes in the Earth system. Data for 55 cases, with references in Table 1. Circles and triangles indicate anthropogenic and natural processes, respectively; red and blue symbols indicate processes from South America and globally, respectively. All regressions are power functions represented as linear curves on a log-log plot [146].....67

Figure 56: Lower atmosphere warmed as a function of forest loss. Temperature change (ΔT_a , °C) profiles from 1000 to 300 hpa during 2000–2019 in relative to 1980–1999 for tropical rainforest climate zones during the dry, transition and wet seasons. The blue '+' indicates the level below which forest loss positively contributed to the warming. Black dots indicate ΔT is statistically significant for the category of forest loss at a pressure level [147].....68

Figure 57: Relative changes (%) in rainfall magnitude as a result of the conversion of tree cover outside protected areas in the Amazon biome (green boundary) to pasture (left); and all tree cover in the biome to pasture (right) [6].69

Figure 58: Trends in AGC and the associated forest cover fractions. (a) AGC trends (2011–2019) over the Amazon biome. Grid-cells where trends are significant are indicated with cross-hatches and cells where reliable data were not available are omitted

(e.g. flooded areas and regional anomalies). (b) Mean land cover fractions in 2018 averaged over grid-cells showing significant positive (gain) and negative (loss) trends. Displayed are the proportions of old-growth, degraded (edge and non-edge), secondary forest and non-forest area. Edge degradation includes forest within 120 m distance from human-made forest edges. The net change in forest area fraction relative to 2011 is also indicated (~ 0 for gain cells, -0.03 or 4% reduction for loss cells) [148].....69

Figure 59: Net annual GhG flux. For display purposes, maps have been resampled from the 30-m observation scale to a 0.04° geographic grid. Values in the legend reflect the average annual GhG flux from all forest dynamics occurring within a grid cell, including emissions from all observed disturbances and removals from both forest regrowth after disturbance as well as removals occurring in undisturbed forests [150].70

Figure 60: Impacts of forest-to-pasture conversion in the Brazilian Amazon: Three typical Amazonian upland landscapes (left to right): primary forest, pasture (the most common anthropogenic land use of the region), and secondary forest (originating from abandoned deforested areas). Pasture establishment (through vegetation clearing and burning) alters above-ground biodiversity and releases large emissions of greenhouse gases (GHGs), while primary forests are sinks of carbon dioxide (CO_2) and methane (CH_4). Secondary forests sequester carbon, but in the short term, total GHG emissions from deforestation cannot be entirely offset by secondary forest growth. For the situation below ground, these processes are even less well understood. Forest-to-pasture conversion impacts soil properties, microbial communities, and their ecosystem services, leading to a CH_4 sink-to-source shift from soils due to changes in the number of CH_4 -producing and -consuming microorganisms. However, it is still unclear whether soil microbial communities from secondary forests and their roles, including CH_4 regulation, can be completely recovered [151].71

Figure 61: Temporal changes in sediment fluxes in South American rivers between 1984 and 2019. Maps show the QST and their changes (%) considering the isolated effect of land use and land cover changes (LULCC). The map on the left shows QST values for the baseline period (1984-1992). The other maps present the sediment flow changes compared with the baseline period. Numbers in red indicate the average sediment delivery from South America (SA) to the oceans in each period. Percentage values indicate the increase or decrease of sediment delivery compared with the previous period [152].72

Figure 62: Deforestation and other anthropogenic pressures on Amazon Forest are closely connected activities. These pressures facilitate spillover events, the emergence of pathogens and the spread of infectious diseases, affecting populations living inside and outside the Amazon region [153].....73

Figure 63: Data distribution of a) the annual ET totals, b) the average of the monthly ET totals, c) the annual LST averages, d) the average of the monthly LST averages over areas classified as intact forest, degradation, and deforestation in the entire study area [154].74

Figure 64: The Trajetorias dataset indicators are computed for two periods for each municipality, as shown in the diagram. The reference point of each period is the date of agrarian census, from which the rural techno-productive trajectory is computed. The database harmonizes epidemiological, environmental and economic indicators [155]75

Figure 65: Road density obtained with the U-Net road model. A comparison of the U-Net model (2020) and the Amazon Road Dataset (ARD, 2016) is shown in the image panels: (a) the BR-319 highway with unconnected segments by the U-Net road model (black line) and ARD showing the full connected length; (b) the fishbone road pattern of the Trans-Amazonia highway main road (BR-230) and perpendicular ones; (c) a typical road pattern of selective logging; (d,e) a geometric road pattern in agriculture lands [113]. .76

Figure 66: Number of forest inventory plots per disturbance intensity Δ NDMI (left) and time since disturbance event (centre), aboveground biomass of disturbed and undisturbed forest (right) [156]	77
Figure 67: Permutation importance across all years (2003–2020) representing the importance of features for fire count prediction. Boxes show quartiles of the calculated permutation importance across individual years the median of which showing 50th percentile. Calculated permutation importance is taken as an average combination of neural network (NN) and XGBoost (XGB). Model (NN and XGB) prediction sensitivity showing annual change in total fires across the BAB as a function of incremental changes in surface temperature (+0.1 K to +1K), precipitation (–1% to –10%) and deforestation (+1% to +50%) calculated as an average across all years (2003–2020) [157].	78
Figure 68: Impact of projected future forest loss on annual mean precipitation. Left: mean projected forest cover loss over 2015–2100 under Shared Socioeconomic Pathway 3–Representative Concentration Pathway 4.5 for the tropics, Amazon, Congo and SEA. Right: Impact of projected forest cover loss on precipitation (P; ± 1 standard error from the mean) [158].....	78
Figure 69: Effects of alternative land-tenure regimes (here: private lands) on forest-to-agriculture conversion rates in Brazil. Circles indicate average effects sizes estimated using regression analysis (using matched parcels) at different spatial-temporal scales, compared to two alternative counterfactuals. Labelled effect sizes (larger circles) report effects across Brazil over the period 1985–2018. Effects to the left of the zero line indicate a decrease in average parcel-level deforestation rate (to the right: increase) [159].	79
Figure 70: Trends in soybean area and yield in main producing areas in Brazil. A: percentage of soybean expansion occurring in each biome, while the total increase in soybean area in each period is shown next to the pie charts. B: annual rate of yield improvement for each region during 2007–2019, with shadow bands representing the 95% confidence intervals estimated for the fitted linear regression models. Values indicate the annual rate of yield improvement in each region and for Brazil. C: Contribution of cropland expansion and yield improvement to soybean production increase in each region. The size of the pie chart in each region is proportional to the share of national soybean production [160].	80
Figure 71: A conceptual framework describing hypothetical and empirical land change patterns arising from different drivers of illicit land use activities. (1) Hypothetical patterns depend on historical institutional processes: (A) The War on Drugs and perverse incentives for coca substitution promote coca stabilization within PAs; (B) agrarian policies, such as the Integrated National Program for the Substitution of Illicitly Used Crops (PNIS), that promote cattle as a strategy less "illicit" than coca farming promote conversion from coca to cattle; (C) peace accord policies that enhanced land speculation for cattle ranching. (2) While drivers are not mutually exclusive, places outside the agricultural frontier (PAs and deeper regions of the Amazon) provide incentives for illicit activities that lead to consolidating coca and cattle to obtain rent and guaranteed economic returns for small farmers. (3) Coca and cattle lands produce diverse land-use patterns in the observed Landsat time-series (NIR, SWIR1, Red—false color combination). The areas reported refer to the mean and standard deviation area of change during the 34-year study period in the Amazon [13].	82
Figure 72: Structure of predator-prey networks (A–F) Variation in different structural descriptors of predator-prey networks as a function of forest area within surveyed forest sites. Circles represent the mean and error bars the standard deviation for the metrics computed for each of 100 potential networks generated per site. The colour gradient follows forest area, and the three darkest circles represent mainland forest sites. Curves represent the model with highest fit [162]	83
Figure 73: Predictions of climatic niche distributions for the three species of wild Amazon canids (<i>Atelocynus microtis</i> , <i>Cerdocyon thous</i> , and <i>Speothos venaticus</i>) in South	

America, based on a mean ensemble considering the best Jaccard values for each modelling method. Current — Areas of occurrence considering the current climate suitability for the species; Future — Climate niche projections for 2060 for each species; Loss of Climate Niche—Areas that will lose climate suitability for the species in the future [163].

84

Figure 74: A: Box plot of the EPT α -diversity in the natural contiguous forest (NCF), forest fragment (FF), conventional logging (CL), reduced-impact logging (RIL), plantation of primary oil palm (PPP), plantation of secondary oil palm (PSP), and livestock farming (LIV). The horizontal line represents the median; the box represents the interquartile range (IQR), and the whiskers represent values up to $\pm 1.5 \times$ IQR from the 75th and 25th percentiles, respectively. B: Relationship between α -diversity and % of riffle habitats. The gray color represents the confidence interval of 0.95 for the linear model [164]85

Figure 75: Projections of 2019–2050 resulting combined carbon losses of Amazon forest degradation concerning the main proximate drivers (extreme drought, edge effects, fire occurrence and timber extraction) under climate and deforestation governance (GOV), left and business-as-usual (BAU) scenarios, right. Inset charts show resulting carbon emissions in the 2019–2050 period resulting from deforestation (DFT) and degradation (DGR). The share of C emissions per driver is shown in the DGR bar (purple = edge effect, pink = drought, cyan = fire and green = logging). Black map areas denote deforestation in the 2019–2050 period, whereas gray areas depict deforestation prior to 2019 [29].....86

Figure 76: Predicted relative Plant area index (PAI, %) time-series. Forest phenology acquired using a Terrestrial Laser Scanner (TLS) within the Biological Dynamics of Forest Fragments Project (BDFFP) was vertically stratified, with the understory (<15 m aboveground) and upper canopy (≥ 15 m aboveground) presenting different trajectories of growth during the dry season. However, the vegetation structure and phenology were both significantly altered by edge effects up to 40 m from the forest fragment margins. The shaded areas represent 95% confidence intervals based on uncertainty in those parameter estimates [165].87

Figure 77: Structural impact of different disturbance types on (a) key structural metrics that are (b) summarized as the mean rank order impact, from least impacted (drought and fragmentation) to most impacted (burned *igapó*), across all 11 focal metrics included in the HCPC. Structural impacts of burned *igapó* closely align with the structural differences between the savanna versus mature forest contrast (outgroup, black). In (a), impact is quantified as the difference in each structural metric relative to the control forest (disturbed minus control), standardized by the standard deviation (SD); bars show means of transect sections and error bars indicate 95% CIs; grey vertical lines at zero indicate no change relative to the control. Disturbance types are separated into forest type where the latter has an important effect (fire in *terra firme* versus *igapó* forests). Structural metrics are as follows: mean canopy height, maximum canopy height, surface rugosity, ERR, gap fraction, LAI, LAHV, LAWH, and height of 50% incident light [166]. .88

Figure 78: The relative importance of forest integrity, structural condition and forest cover on the odds of mammals, birds, reptiles and amphibians being threatened and having declining population trends. Forest integrity tended to be associated with a beneficial effect on biodiversity (lower odds of species being threatened and having declining population trends), relative to forest cover [167].89

Figure 79: Interaction between area of habitat and threat variables. The plots show the response of one variable at two fixed values of the interacting variable, corresponding to its 5th percentile (green) and 95th percentile (purple). The shaded areas represent the 95% confidence intervals of the responses calculated across the responses of the ten imputed datasets. Different slopes in the two curves represent the interaction between 89

Figure 80: Mean values of stakeholders' perceptions of the importance of forest degradation. The purple dots correspond to the means. The central horizontal bars are

the medians. The lower and upper limits of the box are the first and third quartiles. C-coal; F-fire; G-grazing; IS-invasive species; P_NTFF-persistent extraction for domestic use of NTFP, PC-persistent cutting, S_NTFF-selective extraction for domestic use of NTFP, SC-selective cutting, WC-wood for commercial use, WD-wood for domestic use [169]...90

Figure 81: The spatial pattern of windthrows and mean afternoon convective available potential energy (CAPE). Left: 1012 Windthrow events identified manually using Landsat 8 images; green colour in the background represents forested area. Right: Contour lines of windthrow density (counts per 10,000 km²) over the mean afternoon CAPE at 0.25° resolution [170]91

Figure 82: ΔLST (Land Surface Temperature) of forest degradation estimated from different satellite data. ΔLST is calculated as the LST of each land cover type minus the LST of paired interior forests. a–c: Kernel density distributions of ΔLST for Landsat daytime (a), MODIS daytime (b) and MODIS night time (c). Coloured dashed lines and numbers show the weighted mean values. d: Biophysical ΔLST averaged over all tropical land areas from different satellite data. Dots and error bars represent the mean values and one standard deviation of all 0.25° grid cells in the tropics [171]92

Figure 83: Boxplot with the average (2002–2018) normalized burned area (BA) fraction by each FAD category for Amazonia and Cerrado biomes; (B) Scatterplot showing the relationship between the normalized BA fraction and FAD for Amazonia, points highlighted in green were used in the boxplot (>75th percentile) for each category, grey points are the lower 75th percentile and the red line shows the fitted loess regression considering all the grid-cells; (C) Scatterplot showing the relationship between the normalized BA fraction and FAD for Cerrado, points highlighted in orange were used in the boxplot (>75th percentile) for each category, grey points are values <75th percentile and the red line shows the fitted LOESS regression considering all the grid-cells [175]..95

Figure 84: Large portions of the globe experience night-time fires. The map shows the percentage of 2003–2020 active fire detections (n = 80,190,449) that occurred at night, from MODIS Fire Information for Resource Management System (FIRMS) data aggregated to 1° resolution. The displayed pixel values are thresholded at 60% detection; less than 1% of the mapped land area had more than 60% of fire detections at night [176].96

Figure 85: Projected trends in total tree biomass in the Neo-tropics based on GFDL-ESM4.1 global simulations under CMIP6 emission scenarios SSP1-2.6 (optimistic future pathway) and SSP5-8.5 (pessimistic future pathway). Each line corresponds to the dynamics of natural tropical forests in an individual grid cell location (i.e., tiles that were unaffected by changes in land use). Trajectories showing a decrease in total biomass are highlighted with a purple hue. Flames along the abscissa indicate years with high carbon emissions due to fires. *Right:* Distribution (as probability density function) of tree biomass by the end of the simulation for grid cell locations showing increasing or decreasing trends [177].97

Figure 86: Left: Time series of biomass recovery. Without fire (dashed line for 450 ppm and blue area for other CO₂ concentrations), biomass nearly fully recovers under 284, 450, and 750 ppm, respectively, but only 80% under 1200 ppm. Fire (solid line for 450 ppm and red area for other CO₂ concentrations) inhibits full biomass recovery, with only 20% (at 1200 ppm), 40% (at 284 ppm), and 50% (at 450 ppm and 750 ppm) of biomass recovered after 250 years. Right: Bar plot showing final relative biomass under different atmospheric CO₂ concentration forcing (mean of the last 10 years of the recovery phase). Biomass is normalized to its corresponding control simulation experiment (same atmospheric CO₂ concentration) [178].98

Figure 87: Left: Permutation importance across all years (2003–2020) representing the importance of features for fire count prediction. Boxes show quartiles of the calculated permutation importance across individual years the median of which showing 50th percentile. Calculated permutation importance is taken as an average combination of neural network (NN) and XGBoost (XGB). Right: Model (NN and XGB) prediction

sensitivity showing annual change in total fires across the BAB as a function of incremental changes in surface temperature (+0.1 K to +1K), precipitation (−1% to −10%) and deforestation (+1% to +50%) calculated as an average across all years (2003–2020) [157].....99

Figure 88: Temporal changes in percent forest cover of 'Território Indígena do Xingu' (TIX) from 2001 to 2020 (A); drought intensity, estimated based on the maximum cumulative water deficit (MCWD) based on rainfall data from the Tropical Rainfall Measuring Mission (TRMM; from 2001 to 2017) (B); percentage of TIX area burned yearly from 1985 to 2017 (C); and number of people living inside the TIX 1985–2017 (D) [179]..... 100

Figure 89: Density distributions for RHsum values, an indicator of fire severity, across fires between burned and unburned samples for four sites (Bonal, Talismã, Rio Branco and Humaitá) in a simulated waveform and relative height curve. Vertical lines represent median values [180]..... 101

Figure 90: Spearman's correlation (ρ) between burned area (BA) and lightning activity, mapped at 2.5° resolution. Spearman's correlation between climatological monthly BA (2001–2019) and climatological monthly lightning activity in the periods 1995–2000 (extra-tropics) or 1998–2010 (tropics) [181]. 102

Figure 91: Weights-of-evidence contrast of variables that influence the occurrence of deforestation (left) and forest fires (right), with the variables 'distance to deforested areas' (top), 'distance to roads' (centre), and 'distance to rivers' (bottom) [182]..... 103

Figure 92: Locations of study sites throughout the Amazon biome included in review [183] 104

Figure 93: Comparison of forest loss impacts from different forest policies in the Peruvian Amazon, comparing the forest loss impacts of FSC certification and uncertified concessions estimated in this paper with the impacts of three different types of protected areas (PAs), as well as reserved zones in the Peruvian Amazon. Indirect-Use PAs are the strictest PA type. Direct Use and Regional PAs allow some resource extraction by local communities. Reserved Zones are transitory areas that are in the process of becoming a PA, so they are the least strict since they allow more economic activities [184]..... 105

Figure 94: Magnitude and species diversity of energetic pathways in old-growth forest, logged forest and oil palm. The size of the circles indicates the magnitude of energy flow, and the colour indicates birds or mammals. S, number of species; E, ESWI, an index of species redundancy and, therefore, resilience (high values indicate high redundancy) [185] 106

Figure 95: Ipê origins and destination according to associated illegality risks: Municipality of origin according to volume and potential illegality risk associated with timber flows [26]..... 107

Figure 96: Point clouds and vertical canopy profiles for six of the 1ha-plots illustrating changes in vertical canopy structure across the degradation gradient. From left to right: LiDAR point cloud coloured according to return number, k (first returns - green, second returns - blue, third returns - magenta); vertical profile of LiDAR returns by return number, k; Plant Area Density (PAD) distributions modelled from the LiDAR; crown volume profiles (mean \pm 95% confidence interval) estimated from field measurements. For the PAD profiles, thick lines represent 1ha-averages of 0.04-ha subplot profiles, subplots are plotted as semi-transparent histograms, giving an indication of structural variability [186] 108

Figure 97: Net ecosystem CO₂ exchange (NEE) estimated by biometric ground-based methods. Left of the dashed line show the mean (\pm 1 SE) of six unlogged forest plots (green) and five logged plots (brown) with error bars representing variation across the plots. Right of the dashed line show the logged plots individually: two moderately logged plots (striped) and three heavily logged plots (hatched) with error bars representing

within-plot uncertainty, estimated by propagation of SEs of the individually measured components of productivity and respiration. Positive values indicate a net source of CO₂ to the atmosphere [187] 109

Figure 98: Soil respiration partitioned into root, mycorrhizal (Myc), litter, and soil organic matter (SOM) respiration in logged and old growth forest. (a) Mean ± 1 SE for each respiration component by forest type (only SOM respiration significantly different, $t_{6.44} = 2.990$, $p = 0.015$) and (b) the proportional contribution of the components to total soil respiration [188] 110

Figure 99: Rainfall partitioning of rainfall (P), throughfall (TF), stemflow (SF), interception loss (I) [% and mm] at Unlogged (UF) and Logged (LF) Amazon Forest. Jamari National Forest, Rondônia – Brazil [189]. 111

Figure 100: Path models of direct and indirect effects of forest cover on (a) abundance, and (b) species richness. Indirect effects of forest cover occur via two vegetation structural attributes (canopy openness and tree basal area). Significant pathways are indicated with asterisks (* $p < 0.05$; ** $p < 0.01$) to the right of the standardized path coefficients, while blue and red lines indicate positive and negative effects, respectively. Arrow thickness is scaled to illustrate the relative strength of the effects. The coefficient of determination (R^2) is shown within black ellipses for all response variables [191]. .. 112

Figure 101: 4. Spatial distribution of the result obtained after applying the Mann–Kendall test to the mining activity time series of the 31 Indigenous Lands of the Brazilian Legal Amazon where mining activity was detected in at least one of 36 years analysed [194] 114

Figure 102: Global-scale vegetation 3D structure data from NASA’s GEDI mission. The GEDI-domain PAs cover a range of biomes (above), Canopy cover (below), were analysed, amongst other parameters, for all PAs and unprotected counterfactuals to establish the forest structure implications of PAs [195]. 115

Figure 103: 4. Geographical distribution of indigenous lands in the Brazilian Legal Amazon, the number of isolated indigenous groups (A) and the number of mining requests (B). Indigenous lands with no isolated groups are in white in both maps. The Legal Amazon region is in grey. Indigenous lands with >3 isolated groups or >50 mining projects are labelled [106]..... 116

Figure 104: 4. Recovery of forest structure in restored open-pit mining areas in Brazil. The lines show the mean and the standard error in a given year and are colour-coded by mine zone. Dotted lines display average values for surveyed reference plots in secondary and old-growth forest in the immediate surroundings of the restoration areas [196]. .. 117

Figure 105: Annual Parasitic Incidence (API) of Roraima state according to the municipality of infection, 2010 to 2020. Sources: SIVEP-MALARIA; IBGE [197] 118

Figure 106: Proportion of malaria cases at each age, from 2016–2020. Density plots of age distribution of cases by case type: Left: cases in indigenous and non-indigenous people, Centre: autochthonous and imported cases, Right: *P. falciparum* and *P. vivax* cases [198] 119

Figure 107: Hg cycle in areas dominated by the Amazon Forest, with the mean Hg content of forest strata in the southern Amazon region. The main pathways of Hg movement are atmospheric deposition on the arboreal stratum and leaves falling to the forest floor [201]..... 120

Figure 108: Interpolation-based geographic distribution of the naïve defaunation index (DI) broken down by mammal orders across the Neotropics. Maps were pruned by the averaged limit of the distribution of any mammal species within each order via a convex-hull approach [203]. 122

Figure 109: Schematic profile showing the most important potential consequences of defaunation on ecosystem functioning and services, here represented by Neotropical mammals [205] 123

Figure 110: Linear regression analysis showing the relationship between the number of felids hunted and the mean monthly water level (left), the relationship between felid hunting and human population size (centre) and habitat (right) at Amanã and Mamirauá Sustainable Development Reserves, Amazonas state, Brazil (shaded area, 95% CI) [207] 125

Figure 111: Relationships between distance to the nearest local community from a camera-trap station and abundance of six species groupings (E; Game; Frug-Herb [Frugivore and/or Herbivore]; Large [>15 kg]; Threat [Threatened]; Not threat [Not Threatened]; Low Lambda [$\lambda < 1.3$], and High Lambda [$\lambda > 1.3$]), and abundance of seven game species (F; tapir [Tapi.te], white-lipped peccary [Taya.pe], red brocket deer [Maza.am], collared peccary [Dico.ta], grey brocket deer [Maza.ne], paca [Cuni.pa]; and agouti [Dasypro]); and six other species (G; giant anteater [Myrm.tr], short-ear dog [Atel.mi], acouchi [Myop.sp], curassow [Paux.Cr], trumpeter [Psop.sp], and large tinamou [Tina.sp]) [209] 126

Figure 112: Left: Annual deforestation observed in CUs (Conservation Units) with ARPA (Amazon Protected Areas Program) support compared with the estimated potential one in case of non-protection together with associated reduction. Right: Direct investment by ARPA in supported CUs compared with their annual deforestation reductions [210]. ... 127

Figure 113: Left: The effects of ITs/PAs on annual forest area loss rates in the BLA (2001–2021). Above: Spatial distribution of the changes in annual gross forest area loss rates before and after ITs/PAs establishment by ITs (left), national PAs (centre) and state PAs (right), All ITs/PAs established before and during 2002 are white polygons. Below: changes in average annual gross forest loss rates before and after the ITs/PAs establishment by governance (national PAs, ITs and state PAs) (left) and management (strict protection and sustainable use) (right) [211]..... 128

Fig. 114: Jaguar population size, threat index (TI) and prioritization diagram for jaguar conservation across the Brazilian Amazon. Distribution of jaguar population size ($\log_{10} x + 1$) inside protected areas (A), threat index (TI) and values per protected area type (B) and bivariate plot between the threat index and conservative jaguar population sizes inside 447 protected areas across the Brazilian Amazon (C). Acronyms are ST-HP: short-term high-priority quadrant (delimited by highlighted grey frame) and the respective top-ranking 10 areas that should be prioritized in each approach based on the extreme of distribution thresholds by a tangential line. We also identified additional Amazonian PAs that should be prioritized for jaguar conservation in the short to medium term according to our prioritization quadrants [213] 129

Figure 115: Left: ES analysis displaying trends in forest cover change (measured by %) before and after tenure for 78 Indigenous Lands (ILs). Orange points represent binned averages of all ILs in each year in the dataset and 95% CIs (error bars) are included for each point each year. Orange lines represent the average trend and 95% CIs (blue shading) are included for the slope of the mean regression line. Right: Staggered difference-in-differences (DID) dynamic estimates of the average treatment effect of land tenure (ATT) per IL by year on forest cover change (measured by %) relative to (A) number of years to formalized tenure (the fourth and final stage of the tenure process), and (B) number of years to declaration (stage three of the tenure process). The red line represents the ATT of tenured ILs and blue shaded area represents uniform 95% CIs around the effect. The model of formalized tenure (A) shows an overall significant result of reduced deforestation and/or increased reforestation, while the model of declaration (B) does not [214] 130

Figure 116: (a) Average deforestation within each indigenous land before (2013–2018) and during the current environmental setback intensification period (2019–2021). (b) Mean distance from deforestation polygons within indigenous lands to borders before

(2013–2018) and during the current environmental setback intensification period (2019–2021). The numbers in red represent medians. The numbers after the plus/minus signal represent the standard deviation [216]. 131

Figure 117: A schematic representation of the Protected Area Asset Framework (PAAF). Protected area assets enable and are influenced by value generating practices that generate tangible and intangible value for society [218] 133

Figure 118: ACD (Above-ground carbon density) distributions considering uncertainties from ACD estimates only, and both ACD and forest degradation classification uncertainties [219] 134

Figure 119: Changes in carbon in the tropics under RCP 4.5: Changes in carbon levels (in Pg) by climatic zone and by region from 1950–2099 (only three time steps labelled for readability). Bar height is the average total C in each timeframe ± the bootstrapped confidence limits [220] 135

Figure 120: Boxplot (with quartiles and median) of carbon (Mg/ha) between DBH classes and years [221] 135

Figure 121: Modelled AGC accumulation with YSLD in different tropical regions. AGC is shown in degraded forests (a) and secondary forests (b) in the Amazon, Borneo and Central Africa tropical humid forest regions. Points denote the median AGC value calculated for each YSLD, fitted lines are based on a nonlinear model. Shading denotes the 95% confidence interval of the nonlinear model. Crosses denote the median AGC of old-growth (OG) forests in the respective regions and associated 95% confidence interval from the Monte Carlo simulation [222] 137

Figure 122: Restoration opportunity score in lowland moist tropical forest, indicating that restoration hotspots (i.e. clusters of red cells with a normalised score >0.8) exist across the tropics. Higher scores denote areas where appropriate restoration may maximise benefits (biodiversity conservation, climate change mitigation, climate adaptation, and water security) while increasing the likelihood of effective implementation and long-term sustainability (low land opportunity cost, lower deforestation rates in surrounding area, and higher likelihood of biodiversity recovery) [223] 138

Figure 123: Left: Spatial distribution of restoration strategies in the countries of the Amazon biome and in the Brazilian states of the Amazon (bold lines). Different colours represent the different restoration strategies implemented in the region. Right: Number of articles describing restoration strategies in the Amazon biome in horizontal bars [224]. 139

Figure 124: The elimination of restoration barriers enables society to take advantage of multiple benefits resulting from reduced deforestation rates and increasing forest cover [225]. 140

Figure 125: Illustration of Ikpeng cassava (*Manihot esculenta Crantz*) shifting cultivation cycle in non-anthropogenic soils (nADE). When the fallow reaches the OREMYEGETPİN phase (in red), soils and vegetation are considered as recovered and a new cycle may start [227] 141

Figure 126: 3D scatter plots of all the 3060 sampled regrowing forest points and the regression planes of the fixed effects while modelling AGB and tree cover with time since disturbance and surrounding tree cover. Left: AGB (non-scaled data), right: tree cover (non-scaled data) [228]. 143

Figure 127: Left: The physical limits of the six ecoregions (Amazonia, Atlantic Forest, Cerrado, Caatinga, Pantanal and Pampa) defined by the Brazilian Institute of Geography and Statistics (IBGE). Right: Distribution of restoration costs for each ecoregion. Each sample unit corresponds to one municipality within each region. The box limits represent the first and third quartiles, with the middle line representing the median. The whiskers

represent the minimum and maximum values, excluding the outliers, represented by the empty circles [229].....143

GETTING IN TOUCH WITH THE EU

In person

All over the European Union there are hundreds of Europe Direct centres. You can find the address of the centre nearest you online (european-union.europa.eu/contact-eu/meet-us_en).

On the phone or in writing

Europe Direct is a service that answers your questions about the European Union. You can contact this service:

- by freephone: 00 800 6 7 8 9 10 11 (certain operators may charge for these calls),
- at the following standard number: +32 22999696,
- via the following form: european-union.europa.eu/contact-eu/write-us_en.

FINDING INFORMATION ABOUT THE EU

Online

Information about the European Union in all the official languages of the EU is available on the Europa website (european-union.europa.eu).

EU publications

You can view or order EU publications at op.europa.eu/en/publications. Multiple copies of free publications can be obtained by contacting Europe Direct or your local documentation centre (european-union.europa.eu/contact-eu/meet-us_en).

EU law and related documents

For access to legal information from the EU, including all EU law since 1951 in all the official language versions, go to EUR-Lex (eur-lex.europa.eu).

Open data from the EU

The portal data.europa.eu provides access to open datasets from the EU institutions, bodies and agencies. These can be downloaded and reused for free, for both commercial and non-commercial purposes. The portal also provides access to a wealth of datasets from European countries.

Science for policy

The Joint Research Centre (JRC) provides independent, evidence-based knowledge and science, supporting EU policies to positively impact society



EU Science Hub

joint-research-centre.ec.europa.eu



@EU_ScienceHub



EU Science Hub - Joint Research Centre



EU Science, Research and Innovation



EU Science Hub



@eu_science



Publications Office
of the European Union